Peripapillary retinal nerve fibre layer thickness in individuals with epilepsy exposed to vigabatrin

Lisa Michelle Clayton

A thesis for submission to UCL for the degree of Doctor of Philosophy

Declaration

I, Lisa Michelle Clayton confirm that the work presented in this thesis is my own. All of the work is original and where information has been derived from other sources, I confirm that this has been indicated. Dr Claudia Catarino provided some of the clinical phenotype data, particularly with reference to epilepsy phenotype and syndrome. Dr Krishna Chinthapalli provided data regarding drug resistant epilepsy. Dr Gavin Winston analysed a subset of the visual field reports.

Signed:

21st August 2011

Abstract

Background: The antiepileptic drug vigabatrin (VGB) is associated with the development of visual field loss in around 50% of exposed individuals. The mechanisms of VGB retinotoxicity are unknown, and there is continued debate as to the best methods of assessing visual function in VGB-exposed individuals, particularly in those unable to perform perimetry.

Methods: 204 VGB-exposed individuals, 90 non-exposed individuals with epilepsy and 90 healthy controls participated. Individuals underwent visual field testing using Goldmann kinetic perimetry and peripapillary retinal nerve fibre layer (ppRNFL) imaging using optical coherence tomography (OCT).

Results: A retrospective analysis of the evolution of vigabatrin associated visual field loss (VAVFL) in individuals continuing VGB showed progression of VAVFL in all individuals over a ten-year period.

More VGB-exposed individuals were able to perform OCT compared to perimetry. Measures of ppRNFL thickness were found to be highly repeatable in this population. There was a strong correlation between ppRNFL thickness and visual field size suggesting that irreversible VAVFL may be related to loss of retinal ganglion cells (RGCs). Duration of VGB exposure, maximum daily VGB dose, male gender and the presence of a homonymous visual field defect were associated with ppRNFL thinning.

The pattern of ppRNFL thinning suggested that ppRNFL loss progresses with increasing VGB exposure. Subtle ppRNFL thinning may occur in discrete areas after exposure to small amounts of VGB, whilst other ppRNFL areas appear to be resistant to large cumulative VGB exposure.

The ppRNFL was significantly thinner in non-exposed individuals with epilepsy compared to healthy controls. Factors that may be associated with ppRNFL thinning included the presence of learning disability, MTLE with HS and longer duration of epilepsy.

Conclusions: ppRNFL imaging using OCT provides a useful tool to assess VGB-exposed individuals, and can provide an accurate estimate of the extent of VAVFL in the absence of a reliable direct measure of the visual field. Understanding patterns of ppRNFL thinning associated with cumulative VGB-exposure may aid in the early detection of VGB toxicity. Pathophysiological mechanisms of VAVFL are unknown; however, pathology of RGC apparatus is evidently implicated.

Table of Contents

List of Tables

List of figures

List of Abbreviations

ACTH	Adrenocorticotrophic hormone
AED	Antiepileptic drug
CBZ	Carbamazepine
CI	Confidence interval
CLB	Clobazam
CLN	Clonazepam
Cl^-	Chloride
ELM	External limiting membrane
EOG	Electrooculogram
ERG	Electroretinogram
ETS	Ethosuximide
FDA	Food and Drug Administration
FBM	Felbamate
GABA	γ-aminobutyric acid
GABA-T	GABA-transaminase
GBP	Gabapentin
GFAP	Glial fibrillary acidic protein
GKP	Goldmann kinetic perimetry
HVFA	Humphrey Visual Field Analyser
Inf	Inferior
ICC	Intraclass correlation coefficient
IMO	Intramyelinic oedema
INL	Inner nuclear layer
IPL	Inner plexiform layer
IN	Inferior-nasal
IT	Inferior-temporal

LAC	Lacosamide
LEV	Levetiracetam
mf-ERG	Multifocal electroretinogram
MRD	Mean radial degrees
Na^+	Sodium
Nas	Nasal
NI	Nasal-inferior
NS	Nasal-superior
OCT	Optical coherence tomography
ONH	Optic nerve head
ONL	Outer nuclear layer
OP	Oscillatory potential
OPL	Outer plexiform layer
OXC	Oxcarbazepine
PERG	Pattern electroretinogram
PB	Phenobarbital
PHT	Phenytoin
PGB	Pregabalin
PMD	Primidone
ppRNFL	Peripapillary retinal nerve fibre layer
RGC	Retinal ganglion cell
RNFL	Retinal nerve fibre layer
RPE	Retinal pigment epithelium
Sup	Superior
SD-OCT	Spectral-domain optical coherence tomography
SN	Superior-nasal
ST	Superior-temporal
TD-OCT	Time-domain optical coherence tomography

Temp	Temporal
TGB	Tiagabine
TI	Temporal-inferior
TLE	Temporal lobe epilepsy
TPM	Topiramate
TS	Temporal-superior
TSC	Tuberous sclerosis complex
TSNIT	Temporal-superior-nasal-inferior-temporal
UK	United Kingdom
VAVFL	Vigabatrin associated visual field loss
VEP	Visual evoked potential
VGB	Vigabatrin
VPA	Valproate
ZNS	Zonisamide

Glossary of commonly used terms

VGB-exposed	Includes all individuals who have any history of exposure to VGB. Includes both individuals currently receiving VGB and individuals previously exposed to VGB.
Non-exposed	Includes individuals with epilepsy who have nerve been exposed to vigabatrin
Healthy controls	Includes individuals who have never been diagnosed with epilepsy and have never been exposed to any antiepileptic drug.
ppRNFL and RNFL	Please note that ppRNFL refers specifically to the retinal nerve fibre layer immediately surrounding the ONH. RNFL refers in general to the whole retinal nerve fibre layer throughout the retina, or in focal retinal areas as specified in the text.
TD-OCT and SD-OCT	Unless otherwise stated, discussion of TD-OCT refers to (Stratus OCT software version 4.0, Carl Zeiss Meditec, Inc., Dublin, CA, USA) discussion of SD-OCT refers to (Cirrus HD-OCT software version 5.0, Carl Zeiss Meditec, Inc., Dublin, CA, USA).

Acknowledgements

There are many people who have made this work possible and to whom I owe thanks.

Firstly, to my supervisor Professor Sanjay Sisodiya. Thank you for believing in me from the beginning, and for giving me an opportunity to work with you. I have learnt so much in the last three years, and I am indebted to you for your endless support, wisdom, and patience. I am eternally grateful for your inspiration and encouragement.

Thank you to Mr James Acheson for allowing me to disrupt your clinic for three years so that I could learn techniques and see patients, for always having time for my questions, and for your continuous enthusiasm in stimulating my interest in neuro-ophthalmology.

Thank you to Professor Sander for your critical support, advice and knowledge in all aspects of my work.

I am grateful to all of the patients and control subjects who took time to be a part of this work, and to the epilepsy consultants at the National Hospital for Neurology and Neurosurgery and at the National Society for Epilepsy for their time and efforts in recruiting patients.

Thank you to my friends for putting up with me being a terrible friend during the last year of writing, and to my fellow researchers in the Epilepsy Department, for your words of encouragement and support.

To my Mum, Dad, Sister, Nans and Grandads who have continually supported me and (most importantly) fed me during the thesis writing process, and long before. Tania, "thesis Lisa" is finally gone! I love you all very much.

And finally to Simon, who is as much a part of this thesis as I am, and without whom I would never have finished.

'I can do all things through him who strengthens me' Philippians 4.13

Chapter 1 Introduction

1.1 γ-aminobutyric acid

In the late 1950's it was discovered that γ-aminobutyric acid (GABA) was the major inhibitory neurotransmitter in the central nervous system (CNS) (1-3). GABA is synthesized in presynaptic GABAergic axon terminals from intracellular glutamate in a reaction that is dependent on the enzyme glutamic acid decarboxylase (GAD). After synthesis, GABA is loaded into vesicles and released from nerve terminals during membrane depolarization via calcium-dependent exocytosis. The effects of GABA are mediated both pre- and post-synaptically through ionotropic $GABA_A$ and $GABA_C$ receptors and metabotropic $GABA_B$ receptors. Termination of GABA signaling is achieved by active transport of GABA from the synaptic cleft into the pre-synaptic nerve terminal or surrounding glial cells through high affinity Na^+- and Cl^- -dependent GABA-transporters (GAT) in the plasma membrane. Within the neuron or glial cell, GABA is metabolized in a reaction catalyzed by the mitochondrial enzyme GABA-transaminase (GABA-T) (1) (Figure 1.1). The end product of this metabolic process is glutamate. In GABAergic neurons that contain GAD, glutamate is metabolized again to form GABA. In glial cells GAD is not present, and glutamate is converted to glutamine (via glutamine synthetase) which diffuses from glial cells into neighboring neurons where it is again converted to glutamate (Figure 1.1).

Figure 1.1 Normal GABA metabolism

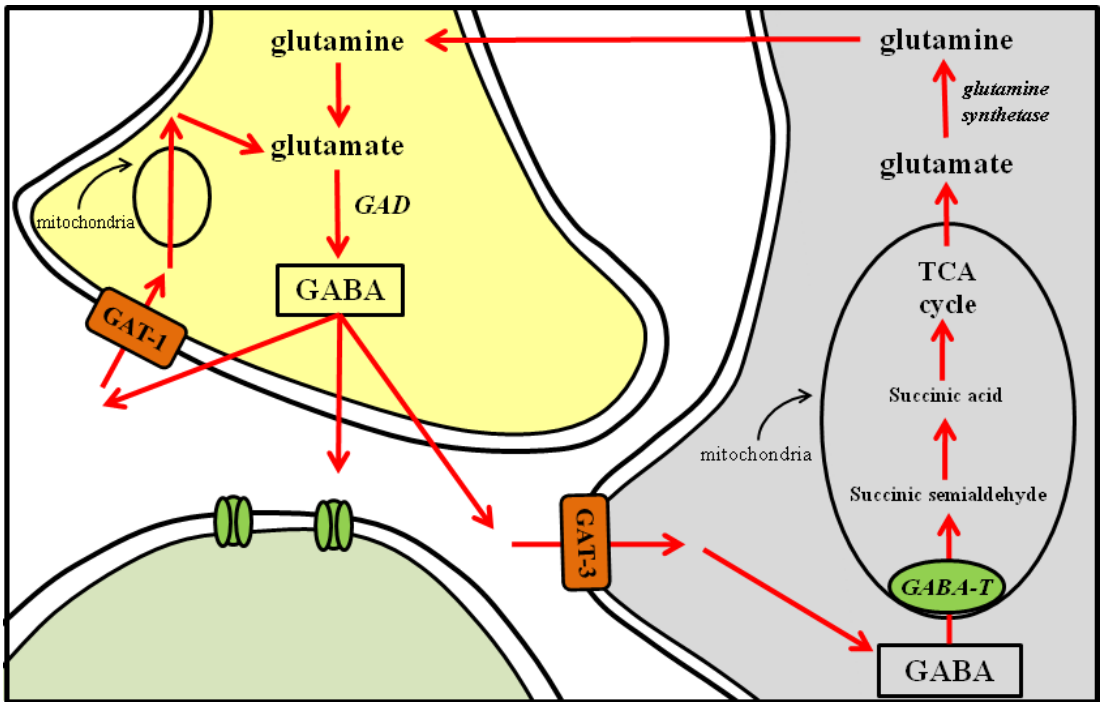

Figure 1.1 legend: yellow cell = GABAergic neurone; Grey cell = Glial cell; Green cell = post-synaptic neurone; GAD = glutamic acid decarboxylase; GABA = γ-aminobutyric acid; TCA = tricarboxylic acid cycle; GABA-T = GABA transaminase; GAT-1 = GABA-transporter 1; GAT-3 = GABA-transporter 3

1.1.1 The search for GABAergic antiepileptic drugs

The identification of GABA as the major inhibitory neurotransmitter in the CNS led to much attention directed toward this molecule and its role in neurological disease. Soon compounds aimed at targeting processes within CNS GABAergic systems were sought as potential therapies for diseases in which impairment of GABA-mediated inhibition was suggested as a pathological mechanism (2;3), including epilepsy (3) in which an imbalance of excitatory and inhibitory neurotransmission is implicated (4). Several inhibitors of GABA-T, the metabolising enzyme of GABA were synthesised and some were found to have anticonvulsant properties (5). However, many of these compounds

were hampered by toxicity, lack of specificity for GABA-T, low potency and inability to penetrate the blood brain barrier (2;5;6).

1.2 Vigabatrin: a designer antiepileptic drug

The first of the GABA-T inhibitors found to have a suitably potent (7;8) and specific (8;9) biological action for potential clinical use (10) was 4-amino-5-hexenoic acid (vigabatrin, (also γ-vinyl-GABA)). A structural analogue of GABA (Figure 1.2), vigabatrin (VGB) was designed specifically to increase CNS GABA through irreversible inhibition of GABA-T, and represented the first attempt at mechanism-based antiepileptic drug development (11) and became the first "designer" antiepileptic drug (AED) available for clinical use (12).

Figure 1.2 Chemical structure of GABA and VGB

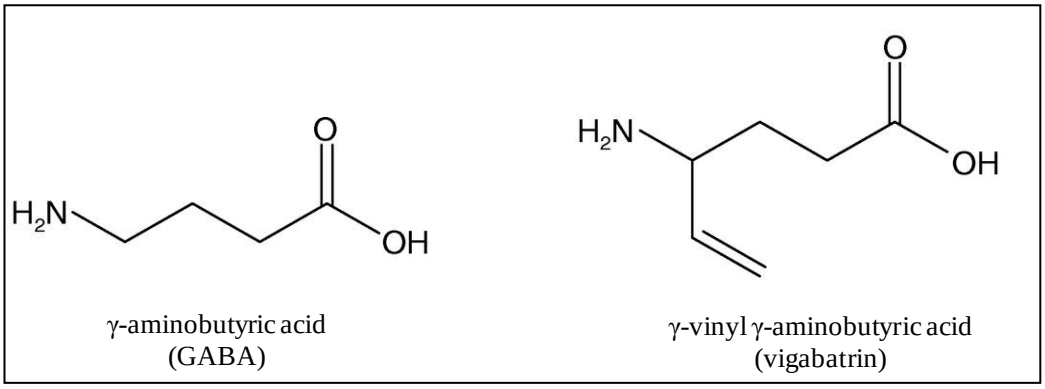

γ-aminobutyric acid (GABA)

γ-vinyl γ-aminobutyric acid (vigabatrin)

Figure 1.2 legend: VGB was designed as a structural analogue to GABA with a vinyl appendage. VGB = vigabatrin; GABA = γ-aminobutyric acid. Figure taken from (13)

1.2.1 Vigabatrin: mechanism of action

Studies in mice and rats showed that when administered peripherally (per oral, intra-peritoneal, intra-venous), VGB concentration increases in a dose-dependent manner in the CNS[1] (10;14;15) and produces a rapid dose-dependent inhibition of brain GABA-T activity (10;15-18) . In the mitochondria, GABA-T metabolises GABA, thus inhibition of this enzyme by VGB results in increased total brain concentrations of GABA (9;10;15-19). The distribution of increased GABA was found to include both increased intracellular GABA levels (nerve terminal and glial cell) (20) and increased extracellular GABA as detected in the CSF (21).

In rats exposed to a single dose of VGB, whole brain GABA-T activity decreases rapidly, reaching 20% of control activity within 4 hours of dosing which was maintained for at least 48 hours (10). Concurrently, whole brain GABA concentrations rapidly increase also peaking at around four hours post-dosing, at concentrations around five-times the baseline GABA levels. The pharmacological effects of VGB are determined by the half life of GABA-T which is longer than that of VGB (10;22). As new GABA-T is synthesised GABA-T activity slowly begins to increase, and GABA levels subsequently decrease. By five days post-dosing GABA-T activity is still reduced, and GABA concentrations were just returning to baseline levels (10).

In pre-treated rats VGB has also been shown to increase both resting and potassium-evoked GABA release from cortical slices (14;23;24). The GABA release recorded after pre-treatment with VGB was highly calcium–dependent and thus is likely to represent neuronal (as opposed to glial) GABA release (24). In addition, a reduction in GABA uptake after VGB exposure has also been reported (16;23;25). The mechanisms

[1] cerebellum, pons, hippocampus, frontal cortex, dorsal cortex and retina (Sills 2001); cortex, spinal cord and retina (Neal 1990); whole brain (Jeung 1990)

of GABA uptake inhibition by VGB are unknown, but have been suggested to represent competitive inhibition between GABA and VGB for uptake via one of the GATs (16;25). Alternatively, once GABA has accumulated in the Müller cell, such an intracellular GABA accumulation will impair the efficiency of the GABA uptake into Müller cells due to a decrease in the transmembrane driving force (26).

Decreased GAD activity after VGB exposure has also been reported in some studies (10;14;16;18), although to a lesser extent than that of GABA-T (10). VGB may have a direct inhibitory effect on GAD activity (10;18). Alternatively, inhibition of GAD activity may be due to a negative feedback loop resulting from high GABA levels (9;14;18;27;28). Decreases in brain glutamine after VGB exposure have also been reported (18) which could result from direct inhibition of glutamine synthetase by VGB (18). Alternatively, the decreased GABA metabolism resulting from inhibition of GABA-T by VGB may result in decreased production of glutamate and thus less glutamate availability for metabolism by glutamine synthetase to glutamine.

In humans, oral VGB intake was associated with a dose-dependent increase in cerebrospinal fluid GABA (22;29-32) and brain GABA concentrations (33).

1.2.2 Antiepileptic properties in animals

VGB has shown to protect against seizures in several animal seizure models including audiogenic seizures (9), chemically-induced seizures (20;34), photic-induced seizures (35) and amygdala-kindled seizures (36).

1.2.3 VGB for drug-resistant partial seizures

The anticonvulsant properties of VGB observed in rodents (9;20;34), and non-human primates (35), alongside the finding that exposure to VGB results in a dose-dependent

increase in CSF GABA in humans (22;29-32) suggested a potential for antiepileptic drug use in individuals with epilepsy (37).

Early single-blind, placebo-controlled studies in individuals with drug-resistant epilepsy showed that VGB decreased seizure frequency (32;38;39) and severity (32) when used as add-on therapy. Subsequent double-blind, placebo-control trials confirmed this, reporting that around 50% of individuals with drug-resistant epilepsy had a more than 50% reduction in seizure frequency after VGB add-on therapy (37;40-43), around 20% of individuals had a more than 75% reduction in seizure frequency (37;40;42). More recent, larger studies have further confirmed these findings in individuals with drug-resistant complex partial seizures (44-46). A recent systematic review of randomised, double-blind, placebo-controlled trials of VGB for drug-resistant partial epilepsy concluded that VGB is effective in reducing seizure frequency in this group of individuals (47).

1.2.4 VGB for infantile spasms

Infantile spasms is a devastating childhood epilepsy syndrome characterised by spasms, characteristic EEG abnormalities (hypsarrhythmia), psychomotor delay and poor long-term prognosis. Seizures associated with infantile spasms are usually refractory to treatment with conventional AEDs (48;49), and currently adrenocorticotropic hormone and VGB are first-line therapies (50). In 1991 Chiron et al. (51) reported that cessation of spasms was achieved in 43% of children with drug-resistant infantile spasms after receiving VGB add-on therapy. Subsequent studies have reported the effectiveness of VGB as first-line monotherapy in infantile spasms (52-59), particularly in infantile spasms secondary to tuberous sclerosis complex (TSC) (55;60;61) where cessation of spasms is achieved in up to 100% of children (60). A recent meta-analysis of treatment of infantile spasms found that there is no clear evidence as to which treatment is optimal

for infantile spasms; however, VGB may be the superior treatment in infantile spasms secondary to TSC (48).

1.3 Vigabatrin tolerability and adverse effects

Double-blind, placebo-controlled trials found VGB to be an effective and well tolerated drug (37;46) with few significant drug interactions (46). Adverse effects in adults were generally mild and included drowsiness (37;41-43;45;47), dizziness (47) and mood changes (37;41;47;62) (particularly depression (47)). These tended to improve with careful titration and continued VGB use (37). In children adverse effects were also mild and included sedation, irritability and insomnia (55;60;61). However, the trials were typically of short duration, the longest follow-up being 36 weeks (46).

1.3.1 Intramyelinic oedema

In VGB-exposed animals microscopic vacuolation resulting from separation of the outer layers of the myelin sheaths were reported (63). The lesions, referred to as "intramyelinic oedema" (IMO), were limited to discrete myelinated tracts, with no evidence of structural change to the cell bodies or axons (64) and reverse on cessation of treatment (65). IMO was seen in VGB-exposed mice (64;65), rats (63;65) and dogs (63;65). In monkeys, there was no conclusive evidence to suggest that IMO occurred after VGB exposure (63;65). Similarly, in studies of post mortem and surgical brain tissue from VGB-exposed adults, no evidence of intamyelinic oedema was detected (65-69). However, IMO has recently been described in a post mortem specimen from a VGB-exposed infant with quadriplegic cerebral palsy and infantile spasms (70).

In VGB-exposed dogs, IMO was found to be prominent in the optic tracts and was associated with increased latencies of the visual evoked potentials (71). In preclinical (72;73) and early clinical (74) studies of VGB-exposed individuals with epilepsy, visual evoked potentials were assessed to monitor individuals for early damage involving the visual pathways. Studies demonstrated normal VEP after up to 3.5 years of VGB exposure (72-74) suggesting that in humans VGB is not associated with visual pathway IMO (75).

1.3.2 Psychosis

Early clinical trials with VGB found behavioural disturbances to be the most common adverse effect (62). Behavioural adverse effects of VGB included agitation, irritability, confusion, hyperactivity and depression (62). In a small number of individuals VGB exposure was associated with the development of psychotic episodes (76;77). However, these episodes tended to respond well to careful titration, reduced VGB dose or treatment with antipsychotic drugs (76) and resolved after discontinuation of therapy (77).

1.3.3 Vigabatrin associated visual field loss

In 1997 Eke et al. reported three cases of symptomatic visual-field constriction in individuals with two to three years of VGB exposure that could not be explained by any opthalmological or neurological insult (78). Several authors suggested that the visual field defect could result as a consequence of the epilepsy, rather than a toxic effect of VGB (79-81). In addition, the individuals reported by Eke et al. (78) had all been exposed to several AEDs that could also have contributed to the visual impairment. However, in the ensuing year numerous authors reported individual cases and case series of vigabatrin-associated visual field loss (VAVFL) (79;82-85).

1.4 Prevalence of VAVFL

After the initial case report from Eke et al. (78), several authors reported individual cases and case series of visual field constriction associated with VGB exposure (79;82-85). At this time, the manufacturers of VGB, Hoechst Marion Roussel, reported that since the introduction of VGB in 1989 they had received "rare" reports of visual field defects associated with VGB use, with a frequency of less than 0.1% (86), and an overall incidence estimated to be 14.5/10,000 patients with epilepsy per year (84). Many of the initial statistics were based upon sporadic reports from symptomatic individuals and questionnaires of visual symptoms (82;87). However, it was suggested early on that VAVFL may be asymptomatic and may be more common than initially suggested by these studies (85;88-90). Subsequent studies have estimated the prevalence of VAVFL to be between 17 and 92% in adults, and between 6 and 65% in children (Table 1.1). Recently, a systematic review of observational studies investigating the prevalence of VAVFL was published (91). The review identified 32 studies which met the inclusion criteria, and found that the proportion of VGB-exposed individuals described as having "visual field loss" was 45%. The proportion of individuals specifically described as showing VAVFL was 31%. When separated into studies of adults and studies of children, the combined random effects estimate for the estimated mean proportion of vigabatrin-exposed individuals with field loss was 52% and 34% for adults and children, respectively (91).

Table 1.1 Summary of studies reporting the prevalence of VAVFL in VGB-exposed adults and children

Reference	Prevalence (%)	Number of individuals	Perimetric method	Mean cumulative VGB exposure (kg) [range]	Mean duration VGB exposure (months) [range]
Wild 2009 (92)	34%	301	BOTH	2.5	44
Sergott 2010 (93)	72%	258	GKP	-	-
Hardus 2000 (94)	17%	118	Peritest Static	-	-
Newman 2002 (95)	20%∞	100	GKP	4.0 [0.17-17.5]	61
Malmgren 2001 (96)	19%	99	GKP	[0.3- >7]	[1-152]
Wild 1999 (97)	29%	99	BOTH	4.1	49
Nicolson 2002 (98)	*43%*	*98*	*HVFA*	-	-
Kinirons 2006 (99)	53 %	93	GKP	5.4	86
Nousiainen 2001(100)	40 %	60	GKP	[0.42-18.7]	[7-168]
Daneshvar 1999 (101)	29%	41	HVFA [a, b]	-	39
Tseng 2006 (102)	79%	34	HVFA [a]	3.7	46
McDonagh 2003 (103)	59%	32	HVFA [c]	5.9	84
Kalviainen 1999 (104)	41%	32	GKP	-	69
Krauss 2003 (105)	53%	32	GKP	-	47
Miller 1999 (106)	50 %	32	BOTH	-	52
Conway 2008 (107)	18%	31	HVFA[a]	>1	>24
Schmitz 2002 (108)	45%	29	GKP	-	[4-71]
van der Torren 2002 (109)	69 %	29	BOTH	3.0	55
Fledelius 2003 (110)	92%	26	GKP	-	102
Lawden 1999 (81)	39 %	25	HVFA [a,b,c,d,e]	[0.6-10.3]	50
Paul 2001 (111)	41%	22	BOTH	-	>24
Besch 2002(112)	*90%*	*20*	*GKP*	*[0.06-65]*	*2-96*
Manuchehri 2000 (113)	67%	20	HVFA [c]	2.9	59
Arndt 1999 (114)	58%	19	HVFA	-	12
Hui 2008 (115)	56%	18	HVFA [a]	-	24
Midelfart 2000 (116)	83%	18	HVFA [c]	-	-

Moreno 2005 (117)	89%	18	HVFA[c]	-	44
Toggweiler 2001 (118)	60 %	15	GKP	3.1	47
Ardagil 2010 (119)	29 %	12	HVFA [a]	3.3	78
Ponjavic 2001(120)	58%	12	GKP	-	[24-120]
Jensen 2002 (121)	30%	10	GKP	-	79
Paediatric studies					
Vanhatalo 2002 (122)	19%	91	GKP	2.1	40
Wild 2009 (92)	20%	85	BOTH	1.3	37
You 2006 (123)	22%	67	HVFA[a]	22.8mg/kg	50
Werth 2006 (124)	27%	30	Non-commercial arc perimetry	-	46
Agrawal 2009 (125)	29%	28	White sphere kinetic perimetry	-	-
Gross-Tsur 2000 (126)	65%	17	BOTH	43mg/kg	36
Gaily 2009 (127)	6%	16	GKP	0.66	24
Ascaso 2003 (128)	20%	15	HVFA [a]	-	42
Wohlrab 1999 (129)	42%	12	GKP	-	26
Iannetti 2000 (130)	33%	12	BOTH	-	-
Spencer 2003 (131)	36%	11	HVFA[a]	-	[3-108]

VAVFL = vigabatrin associated visual field loss; VGB = vigabatrin; GKP = Goldmann kinetic perimetry; HVFA = Humphrey visual field analyzer; Studies are listed in order of the number of VGB-exposed individuals who were examined using perimetry.

Italic – cases were recruited as "suspected VAVFL" or "those in whom analysis of the visual field should be considered"

[a] HVFA 30-2 program

[b] HVFA 60-4 program

[c] HVFA full field 120-point program

[d] HVFA 24-2 program

[e] HVFA 30/60-2 program

The large range in reported prevalence of VAVFL could be due to a number of factors including non-blinded assessments, ascertainment bias and small sample sizes (12). Different studies have used different perimetric techniques to assess the visual field, including both manual kinetic and automated static techniques which could influence the reported prevalence of VAVFL (12;93;132;133). This was investigated in a recent systematic review which found no effect of perimetric assessment method on the reported prevalence of VAVFL (91). However, the review only examined the difference between using "static" or "kinetic" techniques and did not account for different programmes or testing strategies used. For example, in studies using automated static perimetry (mainly the Humphrey Visual Field Analyzer (HVFA)), different visual field assessment programmes have been employed between studies which examine the visual field out to varying eccentricities. For example, the 120-point programme examines the visual field out to 60^{o} eccentricity in all meridians, compared to the 30-2 programme which only examines out to 28^{o} eccentricity. Individuals with mild peripheral VAVFL may not be identified using a programme which assesses only the central visual field (97;101;106;122). Similarly, in studies using manual-kinetic perimetry (mainly Goldmann Kinetic Perimetry (GKP)), the use of various testing stimuli (i.e. plotting various isopters) between studies may also lead to differences in the reported prevalence (91).

Differences in demographic, clinical and therapeutic factors between the populations included in the studies may also contribute to the differences in reported prevalence of VAVFL. For example, studies in which the individuals have a high cumulative VGB exposure or long duration of VGB exposure may be expected to report a higher prevalence of VAVFL (91). Other yet unidentified risk factors for VAVFL may differ between study cohorts and could influence the prevalence of VAVFL.

The criteria used to define VAVFL differ between studies, even those using the same perimetric technique. Differences in the criteria used to define "normal" and "abnormal" visual fields could result in differences in the prevalence recorded between studies (93). In a large study by Sergott using GKP, 72% of VGB-exposed individuals had visual field defects (93), compared to a similar-sized study by Wild et al. who found that only 34% of VGB-exposed individuals had VAVFL (92). In the study by Wild et al. each visual-field test result was evaluated by a single investigator who semi-qualitatively classified each visual field as "normal" or "VAVFL" based on available criteria (97). In the study by Sergott et al. the extent of the visual field in the temporal meridian was determined based on the largest available isopter (V4e or IV4e). Visual fields that extended to less than 80^{o} in the temporal meridian were considered abnormal (93). In the study by Sergott et al. 55% of individuals with epilepsy with no history of exposure to VGB (non-exposed) showed abnormal visual fields, whereas in the study by Wild et al. only 1% of non-exposed individuals showed a visual field that was classified as showing VAVFL according to the criteria used (92).

The effect of using different criteria for defining an abnormal visual field on the reported prevalence of VAVFL was highlighted by Vanhatalo et al. In their study different "limits for normality" were applied to visual field data from 91 VGB-exposed children illustrating that changing the criteria for normality may result in substantial differences in the reported prevalence of VAVFL (Table 1.2) (122).

Table 1.2 The effect of changing the criteria for normality of the visual field on the prevalence of VAVFL (taken from (122))

Limit for normality in the temporal meridian (degrees)	Number of individuals (normal:abnormal)	Prevalence of VAVFL
$\geq 80^{o}$	41:50	54.9%
$\geq 70^{o}$	74:17	23%
$\geq 60^{o}$	84:7	8.3%
$\geq 50^{o}$	90:1	1.1%

The proportion of individuals included in a study by Vanhatalo et al. with visual fields classified as "abnormal" when the limits for normality are set at different degrees in temporal meridian (taken from (122))

VAVFL = vigabatrin associated visual field loss

1.5 Characteristics of VAVFL

The characteristics of vigabatrin-associated visual field loss (VAVFL) were first explored systematically by Wild et al. who observed the severity, type and location of visual field defects in VGB-exposed individuals (97). Using static threshold perimetry of the central 30^{o} of the visual field (HVFA 30-2 program) a unique pattern of visual field loss was described as showing "localised bilateral nasal loss, extending in an annulus over the horizontal midline, with a relative sparing of the temporal field". The visual field defect was found to be steeply bordered and absolute, that is, at the edge of the remaining, intact visual field the sensitivity to light fell from normal to absolute loss of light sensitivity suddenly and rapidly (81;94;134). In individuals examined using Goldmann kinetic perimetry, the visual field (examined beyond 30^{o} eccentricity) was found to be concentrically constricted, with a more profound nasal than temporal

constriction. In the most severe cases the visual field loss manifested as a bilateral, symmetric, concentric constriction within 30^{o} eccentricity. In the same study, a population of individuals with epilepsy not exposed to VGB (non-exposed) were also examined using perimetry. Visual field defects were found in seven individuals, all of which could be attributed to known retinal or cortical pathology. None of the non-exposed individuals manifested a pattern of visual field loss with characteristics of that seen in the VGB-exposed individuals (97).

Ensuing studies and clinical experience confirm that the characteristics of VAVFL are of a peripheral (101;104;106;116), concentric (94;101;104) contraction of the visual field affecting both eyes (94;97;101;104;106;134;135) symmetrically (81;97;101;104;107;109;134;136).

Several groups have described VAVFL as showing more extensive involvement of the nasal visual field than the temporal visual field (81;97;126). However, this characteristic of VAVFL is contentious (106;137;138). An overestimation of the degree of involvement of the nasal visual field in individuals with VAVFL may be due to the perimetric technique used (137). The normal monocular visual field extends to around 60^{o} nasally and 100^{o} temporally. Many of the automated perimetric techniques used do not examine the full extent of the visual field. For example, the commonly used 30-2 program of the HVFA examines the monocular visual field out to 28^{o} eccentricity in all meridians. A concentric contraction of the visual field (i.e. by an equal amount in all meridians) of around 30^{o} may show as a mild nasal visual field defect in an individual assessed using this technique, but would not be detected in the temporal field (137). Where studies have compared the percentage constriction in each hemifield in individuals with VAVFL, either the temporal hemifield shows more constriction than

the nasal hemifield (106) or there was no difference found in the degree of constriction between hemifields (94;110).

1.5.1 The severity of VAVFL

The severity of VAVFL varies widely (12;96;97;106), with some individuals showing very mild loss of the far periphery of the visual field (94;96;116) whist others develop a very severe constriction extending to involve the central 30^{o} of the visual field (96;101;109;139) (Figure 1.3). In most individuals with VAVFL the defect is mild to moderate with few individuals showing severe defects. In a large study of 119 adults and children with VAVFL, 52% were classified as showing mild VAVFL, 35% as moderate and 13% as severe (92).

Figure 1.3 The characteristics and severity of VAVFL

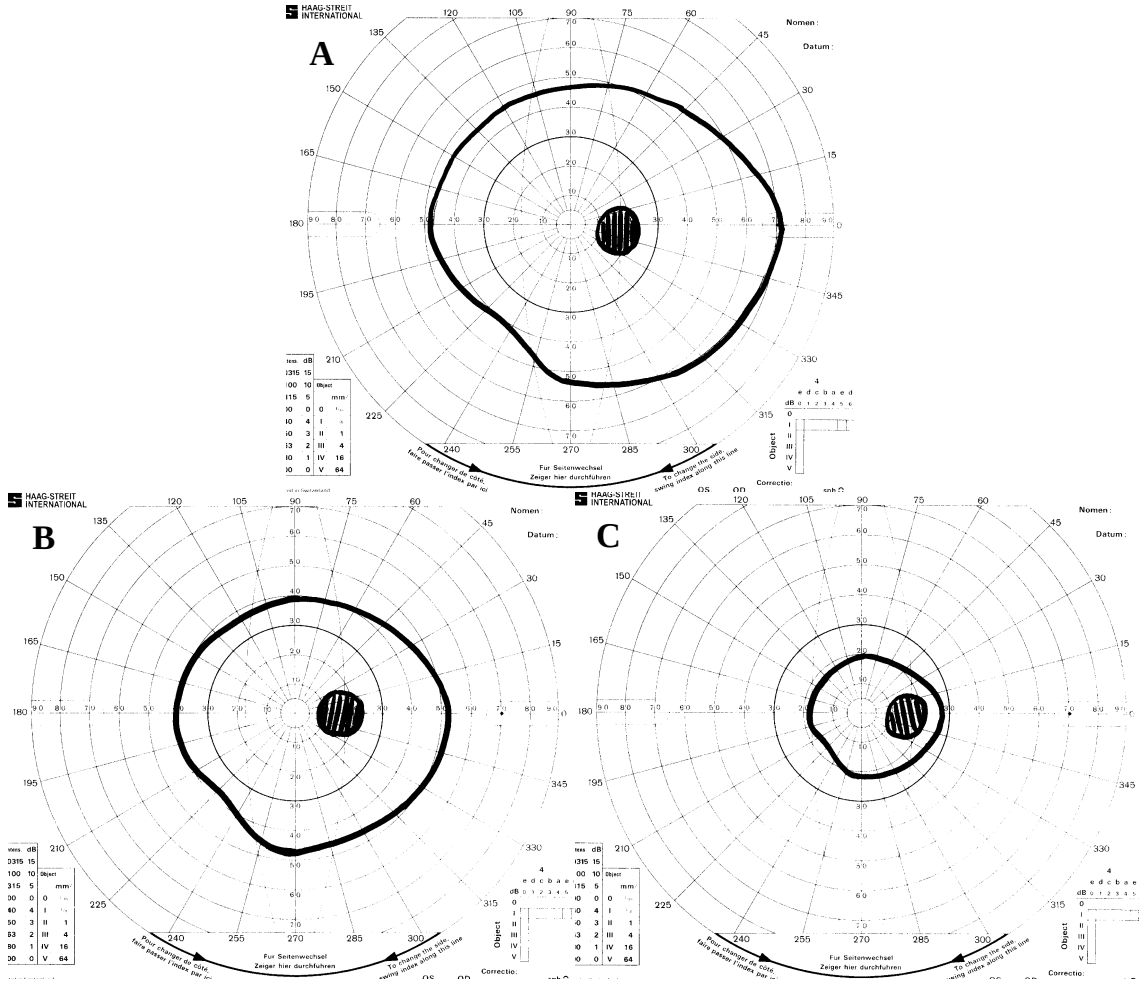

Figure 1.3 legend: VAVFL is well characterised as a concentric peripheral constriction of the visual field. A normal visual field plotted with the I4e isopter using Goldmann Kinetic perimetry is shown **(A)**. The severity of VAVFL ranges from mild **(B)** to severe **(C)**.

1.6 The evolution of VAVFL

1.6.1 Time to onset of VAVFL

The time to onset of VAVFL after starting VGB has been difficult to establish as most studies have been cross sectional and individuals included have been receiving VGB for variable periods before entry into the study. Very few prospective studies of VAVFL have been carried out, and even in these studies the time of VAVFL detection may not

be the time of VAVFL onset due to the asymptomatic and possibly insidious nature of the visual field loss (140).

In an unpublished clinical trial of VGB reported by the FDA, 25 VGB-exposed individuals were prospectively assessed for VAVFL at three monthly intervals (141). 7/25 individuals developed VAVFL within the follow-up period (median duration of follow-up was 500 days). One individual developed VAVFL after two months of VGB exposure and five individuals developed VAVFL after around one year of exposure (141).

In a prospective study of the use of VGB for treatment of cocaine and metamphetamine abuse, visual field testing was performed at baseline and at one, four and eight weeks during VGB exposure. In the 18 individuals who completed the study, no changes were seen in the visual field compared to baseline. However, the duration of VGB exposure and the cumulative VGB exposure were relatively short (eight weeks and 137 grams, respectively) compared to the treatment strategies used in individuals with epilepsy (142).

Schmitz et al. performed visual field testing in 29 individuals before exposure to VGB, and again 34-120 months after initiation of VGB (108). At the follow-up examination 13/29 (45%) had developed VAVFL. Of the individuals who had developed VAVFL, the duration of VGB exposure ranged from 9 - 71 months. However, because individuals had not undergone repeated visual field assessments during the VGB exposure period, the time of onset of VAVFL after VGB exposure could not be determined.

In cross-sectional studies, VAVFL has frequently been detected in individuals within around one year of VGB exposure (96;99;112;138;143). Abnormalities of the ERG

have also been reported to occur within six months after VGB exposure (105;144). It is not known whether these abnormalities relate to the development of VAVFL, or are associated with the direct effects of VGB on retinal physiology as healthy individuals exposed to a one-off dose of VGB develop ERG abnormalities despite maintaining normal visual fields (145).

The onset of symptoms of visual field constriction (e.g. "bumping into things") has been reported to occur from 6 – 75 months after starting VGB therapy (78;79;82;101;143;146). The onset of symptoms suggests that the visual field constriction is likely to be severe, and encroaching on central vision (97). In these individuals it is possible that a degree of mild VAVFL may have been present before the onset of symptoms, and thus the development of symptomatic VAVFL may not provide an accurate estimate of the time of onset of VAVFL.

1.6.2 The development of VAVFL

The nature of the onset of VAVFL is unknown. The asymptomatic characteristics of VAVFL suggest that the development of visual field constriction is slowly progressive, allowing adaptive processes to take place to compensate for impaired peripheral vision (81;92;97;112). In addition, the range in severity of VAVFL from mild and asymptomatic to severe constriction suggest that VGB toxicity may be slowly progressive, with individuals with varying degrees of VAVFL at varying stages of progression (147). Conversely, in some VGB-exposed individuals, significant changes in the visual field occur within short time periods, suggesting that VAVFL onset may occur rapidly in some cases (139;143). Analysis of serial visual field assessments over a ten-year period in an individual on VGB therapy showed a significant deterioration in visual field size between assessments carried out one year apart (139). Similarly, in an unpublished prospective study of VGB-exposed individuals assessed using perimetry at

three-monthly intervals, VAVFL was first detected as a moderate degree of constriction within 20-30^{o} of fixation in three individuals (141). As the individuals included in the study were assessed at three-monthly intervals, this demonstrated that in these cases moderate VAVFL developed rapidly within the three month period between visual field examinations (141).

The nature of onset of VAVFL will be difficult to determine (140). VAVFL is largely asymptomatic and few individuals who are able to perform reliable perimetry are newly started on VGB, meaning that good prospective data are unlikely to become available (99). In addition, inferences about the nature of VAVFL onset may be influenced by the frequency of perimetric examinations undertaken. From the available studies it is difficult to determine the nature of VAVFL onset and it is possible that the onset of VAVFL may differ between individuals, showing either a slowly progressive or rapidly progressive onset (Figure 1.4) (141).

Figure 1.4 The nature of the onset of VAVFL (adapted from (141))

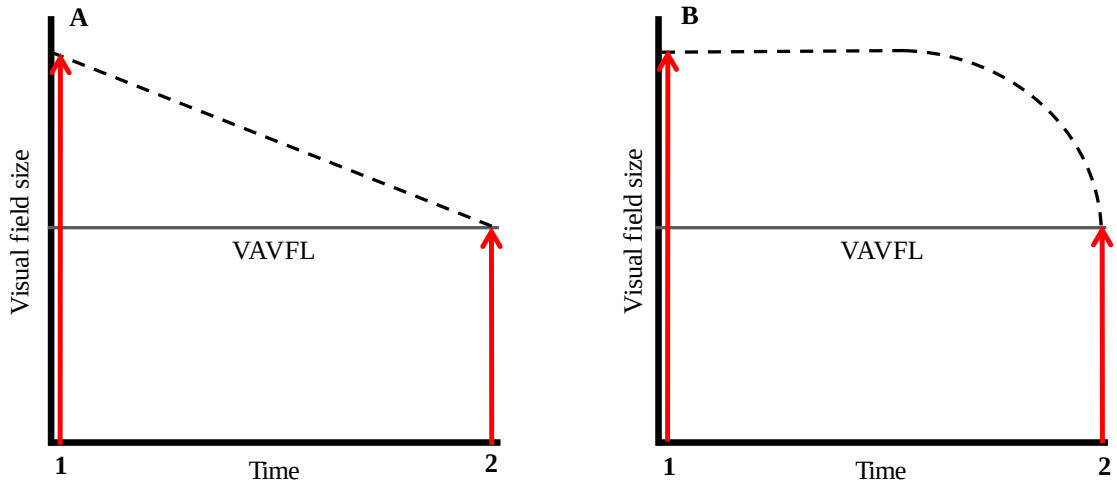

Figure 1.4 legend: Visual field assessments taken at Time 1 (red arrow) reveal normal visual fields. Repeat assessment at Time 2 (red arrow) show that VAVFL has developed.

However, the nature of onset of VAVFL between this period is unknown (black dashed line). VAVFL may develop in a slowly progressive pattern occurring over a protracted time period **(A)** (black dashed line). Alternatively VAVFL may have a sudden and rapid onset, occurring over a short time period **(B)** (black dashed line).

1.6.3 The progression of VAVFL

It is generally accepted that once established, VAVFL is stable and does not progress with continued VGB exposure (111). Follow-up studies of individuals who continue VGB therapy have shown no progression of VAVFL over time (81;100;111;148-150) (See Table 3.1). In addition, several studies have shown that the risk and severity of VAVFL does not increase with increasing VGB exposure (see 1.7.1)

However, other studies have shown an association between increasing VGB exposure and increased risk of VAVFL (see 1.7.1). In addition, progression of VAVFL with continued VGB use has been reported in some studies (81;139;151;152) (Table 3.1).

Overall, studies of the evolution of VAVFL in individuals continuing VGB therapy have typically followed patients for less than four years (Table 3.1). Only one case report has assessed the evolution of the visual field with continued VGB therapy over a longer period (139). In this report, rapid, severe VAVFL developed after ten years of VGB exposure, suggesting that VAVFL can progress in some individuals after many years of VGB use (139).

1.6.4 The irreversibility of VAVFL

The irreversible nature of VAVFL has been suggested since the initial case series reported by Eke et al. (78). Subsequent follow-up studies have confirmed that in most individuals VAVFL is irreversible after VGB withdrawal (Table 1.3).

Table 1.3 Summary of follow-up studies investigating the effect of VGB withdrawal on visual field size.

Reference	Number of individuals	Follow-up after VGB withdrawal (months)	Overall finding
Nousiaien 2001 (100)	29	4 - 38	No change#
Newman 2002 (95)	21	6- 18	No change#
Hardus 2000 (152)	16	24[b]	No change
Johnson 2000 (153)	13	3 - 11	No change
Schmidt 2002 (149)	11	12 - 24	No change
Lawden 1999 (81)	10	Not stated	No change#
Kjellstrom 2008 (154)	8	48 - 72	No change
Fledelius 2003 (110)	8	Not stated	Improvement
Vanhatalo 2001 (155)*	7	Not stated	Improvement
Hardus 2003 (151)	6	37 – 47	No change
Eke 1997 (78)	2	12, 48	No change
Krakow 2000 (156)	2	6, 1	Improvement
Wong 1997 (82)	1	48	No change
Giordano 2000 (157)*	1	9	Improvement
Versino 1999 (158)*	1	10	Improvement

*Paediatric studies

#Some individuals included in the study did show an improvement in the visual field, although overall the authors concluded that there was no change in the visual field size after VGB withdrawal.

Some cases of reversibility of VAVFL have been reported, particularly in children (155;157;158) and rarely in adults (81;95;100;110;156). Young age has been suggested as a favourable factor for reversal of VAVFL (157) due to more efficient retinal repair mechanisms (158) and neural plasticity (155) in childhood. However, it is still unknown whether rare cases of reversibility of VAVFL reflect true improvement in visual function after VGB withdrawal or whether they are a product of the limitations of perimetry in the assessment of some individuals. A learning effect in repeat perimetry is well recognised (159;160) and the apparent reversal of VAVFL after VGB withdrawal may be related to improved performance and familiarly with the task (81). In particular, children often show a progressive improvement of the visual field over subsequent test sessions related to the learning effect (122), which could explain the more frequent reports of VAVFL reversibility in paediatric studies. For example, in one child, progressive improvement of the visual field was seen alongside progressive improvement in the reliability of the visual-field assessment (157). Similarly, in an individual with a reported improvement in VAVFL after VGB withdrawal (158), the illustrated visual field taken whilst on VGB showed a "clover-leaf" pattern which is typical of functional visual impairment, or concentration and fatigue-related artefact (152;161). Vanhatalo et al. reported a case series of seven children who showed improvement of the visual field after VGB withdrawal (155). In the analysis to determine the change in visual field size the "worse visual field" whilst on VGB was chosen to compare against the latest visual field after VGB withdrawal (155). Several factors may have contributed to the integrity of the "worse visual field" that were not related to VGB exposure, including poor task performance, impaired attention and concentration and fatigue. Use of the "worse visual field" in the analysis may have led to an overestimation of the improvement in visual field size after VGB withdrawal.

It is possible that there are both reversible and irreversible effects of VGB on visual function. In most individuals VAVFL does not improve even many years after VGB withdrawal. In agreement with this a post mortem examination of an individual with VAVFL concluded that the degree of cell loss from the retina and optic nerve would suggest that the damage to the visual pathway was irreversible (162). On the other hand, some features of VAVFL might be transient and related to the physiological effects of VGB. Various retinal electrophysiological abnormalities that are seen during VGB exposure return to normal after VGB withdrawal, further suggesting that aspects of visual dysfunction related to VGB exposure may be reversible.

1.7 Risk factors for VAVFL

1.7.1 Cumulative VGB exposure and duration of VGB exposure

The relationship between increasing VGB exposure and the development of VAVFL is controversial and studies have shown conflicting findings. Increasing cumulative VGB exposure (81;96;113;122;137;163), duration of VGB exposure (81;92;94;96;108;118;126;137;164), maximum daily VGB dose (107) and mean daily VGB dose (92;109;137) have been associated with increased risk of VAVFL in some studies (Table 5.7). However, other studies have reported no effect of cumulative VGB exposure (95;97-100;104;109;124;164), duration of VGB exposure (95;97;99;100;109;122;124;128;135), maximum daily VGB dose (99;102;108) or mean daily VGB dose (124;126;128;165) on risk of VAVFL (Table 5.7).

Recently, a large, multicentre study of VAVFL in 386 VGB-exposed adults and children identified increasing duration of VGB therapy, and increasing mean daily dose

of VGB, to be risk factors for VAVFL (92). It appears that there is likely to be an association between increasing VGB exposure and increasing risk of VAVFL. But it is clear that there is not a simple dose-related toxic effect (12). Some individuals develop significant VAVFL after relatively small cumulative VGB exposure and short periods of VGB exposure; conversely, other individuals maintain normal vision despite receiving high doses of VGB for many years (96;98;122). Multiple clinical, therapeutic and demographic factors may contribute to an individual's risk of developing VAVFL. It has been suggested that VAVFL may represent an idiosyncratic adverse drug reaction (12;95;99) where susceptible individuals will develop VAVFL irrespective of the dose or duration of VGB exposure, possibly dependent on genetic variability (166).

1.7.2 Male sex

In a large multicentre study of 386 VGB-exposed individuals male sex was found to be a risk factor for VAVFL (92). This is in agreement with previous findings (92;94;95;97;98;103;137) (Table 1.4). In some studies males were found to be more than two times as likely to develop VAVFL compared to females (92;97;140). In addition, certain abnormalities of the electroretinogram were found to be more prevalent in VGB-exposed males compared to females (167). Conversely, other studies have found no increased risk of VAVFL associated with male sex (100;104;122;135) (Table 1.4). Differences in findings between studies may relate to the approach to analysis of the data. Studies that have reported no association between sex and risk of VAVFL have not controlled for the amount of VGB exposure (e.g. cumulative VGB exposure, duration of VGB exposure) between groups (Table 1.4). As this variable is likely to be associated with risk of VAVFL (see above) it is important to control for it in any statistical exploration of other risk factors.

No theories for the mechanisms of increased susceptibility to VAVFL in males have been suggested, although Newman et al. proposed that this finding may indicate a genetic susceptibility to VGB toxicity (95).

Table 1.4 Summary of studies exploring an association between male sex and VAVFL

Reference	Number of participants	Male gender a risk factor	Control for VGB exposure
Wild 2009 (92)	386	Yes	Yes
Hardus 2000 (94)	118	Yes	No
Newman 2002 (95)	100	Yes	Yes*
Wild 1999 (97)	99	Yes	Yes
Nicolson 2002 (98)	98	Yes	No
Hardus 2001 (137)	92	Yes#	Yes
Vanhatalo 2002 (122)	91	No	No
Nousiainen 2001 (100)	60	No	No
Durbin 2009 (167)**	42	Yes	No
Kalviainen 1999 (104)	32	No	No
McDonagh 2003 (103)	32	Yes	No

*No significant difference was found between males and females in terms of cumulative VGB exposure (independent samples T-test).

#only found when quantifying visual fields using the surface method but no difference was found between males and females when visual fields were quantified using the Esterman method.

**Visual fields were not assessed. VGB retinotoxicity was defined as a reduction in the 30Hz flicker amplitude of the electroretinogram compared to amplitudes measured before VGB therapy.

1.7.3 Other risk factors

Increased risk of VAVFL has also been associated with increasing age (108) and co-medication with valproate (108;114;164). However, most demographic, clinical and therapeutic factors have shown no association with increased risk of VAVFL, including; exposure to other AEDs (94;97;137), number of other AEDs exposed to (108;112), age (97;112;122;135), epilepsy syndrome (104;113), duration of epilepsy (94;112), temporal lobe lesions (94), history of status (94) or poor cognitive performance (122).

1.7.4 Genetic predisposition

Genetic variation may play a role in the development of VAVFL (95;98;99;104;168). In a study by Kinirons et al. three candidate genes were found to be associated with increased risk of VAVFL including a gene encoding GABAb receptor (GABRR1/2) and two genes encoding GABA-transporters (GAT1/3 and GAT2). However, no significant association was found on replication of the study by the same authors in a second independent cohort (168). Whilst the initial genetic association found in the study probably represents a false positive result, a real association between the gene variants detected in the study, or indeed other variants, cannot be ruled out. The study may have been underpowered to detect variants of small effect; in addition findings may have been confounded by variability in the visual field measurement (168).

Genetic variation in the mitochondrial enzyme ornithine δ-aminotransferase has also been suggested as a possible source of inter-individual susceptibility to VAVFL (169;170). Individuals with a deficiency of ornithine δ-aminotransferase in the rare

inherited metabolic disease gyrate atrophy of the choroid and retina (gyrate atrophy), develop peripheral visual field loss that was suggested to be similar to that seen in individuals with VAVFL (170). VGB is a weak inhibitor of ornithine δ-aminotransferase (171) and may lead to accumulation of ornithine resulting in a mild form of gyrate atrophy (172). Allelic variability in the gene encoding ornithine δ-aminotransferase may modulate its vulnerability to inhibition by VGB, and thus the vulnerability of the retina to VGB-induced toxicity (170). A recent study showed that individuals with VAVFL and a history of VGB exposure had reduced ornithine δ-aminotransferase activity compared to individuals with a history of VGB exposure with normal visual fields. The authors concluded that individuals with congenitally decreased ornithine δ-aminotransferase activity may have increased risk of VAVFL during VGB exposure (172). However, the same study found no difference in ornithine δ-aminotransferase activity between individuals currently exposed to VGB with VAVFL and those with normal visual fields. In addition, sequencing of the ornithine δ-aminotransferase gene in 17 VGB-exposed individuals did not reveal any clinically significant mutations (169). A common intronic polymorphism was identified, but it was not associated with VAVFL (169).

1.8 Symptoms and quality of life in individuals with VAVFL

1.8.1 Symptoms of VAVFL

The delay in recognition of VAVFL (first reported in 1997) after VGB was licensed (in 1989 in the UK) was probably largely due to the asymptomatic nature of VAVFL (12). The initial reports of VAVFL by Eke et al. (78) and others (79;82) were in symptomatic individuals. Soon thereafter, it was reported that asymptomatic visual field defects may also occur with VGB exposure (85;88-90). In the first study to screen VGB-exposed individuals with no visual complaints, 11/15 showed VAVFL (173) demonstrating that VAVFL was likely to be largely asymptomatic (173). Later studies confirmed that in most individuals (approximately 90% (12)) VAVFL is asymptomatic (81;93;94;96;98;101;104;106;112;121;137). The peripheral characteristics of VAVFL with preserved central vision and normal visual acuity and colour vision account for individuals being largely asymptomatic. In addition, the development of and progression of VAVFL may be slow enough to establish adaptation processes such as using compensatory gaze movements to explore the visual field (81;92;97;112).

The first reports of VAVFL from Eke et al. (78) described symptomatic individuals with complaints of "tunnel vision" and "bumping into objects" associated with the development of visual field loss. Subsequent studies have also reported some VGB-exposed individuals with these symptoms (81;101;103;104;114). Occasionally symptoms were reported spontaneously, but more often individuals only reported symptoms of visual field constriction on direct questioning (104;108). Symptoms of VAVFL appear not to occur until the defect encroaches on the central visual field (97). In reports of symptomatic VAVFL, the visual field constriction typically encroaches on the central 30^{o} (78;104;146). Using a questionnaire of visual symptoms and disability,

the number of complaints experienced by an individual correlated with decreasing visual field size (93;174). In a larger study no correlation was found between the presence of visual symptoms and disability and the presence of VAVFL (92). The questionnaires used in each study were not specifically developed for the assessment of individuals with VAVFL. In the study which reported no association between visual field size and visual disability measures, the questionnaire used was one which was developed for individuals with retinitis pigmentosa and Usher syndrome (92). It is possible that the questionnaire was not specific or sensitive enough to detect the impact of VAVFL on visual disability (92)

In some individuals with VAVFL, symptoms of blurred vision (81;103;104;114), photopsia (81;104) and phosphenes (81) were also reported. However, VGB-exposed individuals with normal visual fields also reported these symptoms (104), suggesting that they may not be directly related to the mechanisms leading to VAVFL. In addition, several AEDs are associated with visual side effects including blurred vision, phosphenes and photopsia (175;176); thus these symptoms may have been related to concomitant treatment with other AEDs and not directly related to VGB exposure.

1.8.2 Quality of life in individuals with VAVFL

Moderate to severe impairment in performing "daily tasks" which involve reading, writing and orientation and mobility occurred in individuals with a visual field area of smaller than 2000 degrees^2 (equivalent to a 50^o diameter of the Goldmann II4e isopter (177).

In most individuals with VAVFL, visual field loss is mild and asymptomatic and does not affect quality of life or impair ability to perform everyday tasks (93;97). However, using a questionnaire of visual complaints, individuals with VAVFL were found to have

more subjective impairments in tasks associated with visual field defects (e.g. difficulties in seeing a car in time when crossing the road) compared to individuals without VAVFL (174). Furthermore, VAVFL may be severe in some individuals, limiting their ability to perform a number of activities of daily living (97;106;178). Individuals with severe VAVFL may not meet the visual field standards required by the DVLA for driving eligibility (179) despite having good seizure control (180).

1.9 Clinical features of VAVFL

1.9.1 Visual acuity

Visual acuity is normal in the majority of studies of VGB-exposed individuals with VAVFL and with normal visual fields (78;94;96;101;104;111;112;114-116;120-122;128;164;181). Occasional reports of reduced visual acuity with VGB exposure have arisen (81;106;113;114;138); this may due to co-existing ocular pathology in some cases and not related to VGB exposure (138;182). In a prospective study of individuals receiving eight weeks of VGB therapy for cocaine and metamphetamine abuse, no change in visual acuity over the eight week assessment period was observed (142).

1.9.2 Colour vision

Most studies have found that VGB-exposed individuals with VAVFL exhibit normal colour vision (81;101;112;138;183). Even in individuals with severe symptomatic visual field loss, colour vision can remain intact (101;139;146). However, in some VGB-exposed individuals colour vision impairment has been reported (113;184-186). One study of individuals receiving VGB monotherapy showed impaired colour discrimination in 32% of VGB-exposed individuals (184). In addition, healthy individuals showed an impairment of colour vision after a one-off dose of 2000mg of

VGB (187;188). The colour vision defects that have been reported with VGB exposure have been mainly in the tritanoptic axis (detected using the Farnsworth-Munsell 100 hue test) (176;184;186;188) and are suggested to be consistent with enhanced retinal GABAergic inhibition and relate to the physiological effects of VGB rather than retinotoxic mechanisms (187;188). In individuals currently taking VGB the number of misread plates on the Ishihara charts ranged from 0-13 (out of a possible 15) and ranged from 0-1 in individuals previously exposed to VGB (113), further suggesting that abnormalities with colour perception may be related to physiological effects of current VGB exposure as opposed to retinotoxic effects related to the mechanisms of VAVFL. Conversely, other studies have shown diffuse, generalised colour vision impairment, suggesting that VGB induces toxic damage in all chromatic pathways (176;185).

Exposure to other AEDs including carbamazepine (184;187;189;190), valproate (189;191), topiramate (186), tiagabine (192) and phenytoin (193) is also associated with impairments of colour vision (for a review see (176)), making it difficult to distinguish physiological effects of AEDs on visual perception from those mechanisms that might be related to neurotoxic effects (176).

1.9.3 Contrast sensitivity

Measures of contrast sensitivity examine the minimal contrast required to detect a difference between the luminance of an object from the luminance of its surroundings. Abnormal contrast sensitivity has been described in some VGB-exposed individuals (167;181;185), which was found to be related to the presence of VAVFL (181), but not to abnormal electrophysiological measures (167). Conversely, other studies have found normal contrast sensitivity in VGB-exposed individuals (150). A single dose of VGB had no effect on contrast sensitivity in healthy individuals (194). Furthermore,

abnormal contrast sensitivity detected in individuals treated with carbamazepine improved after six months add-on therapy with VGB (195).

1.9.4 Ophthalmoscopic features

Assessment of the fundus through direct examination, slit-lamp biomicroscopy and using fundus photography, reveals that in most individuals with VAVFL, the fundus is normal (78;94;95;97;101;104;106;112;116;120;121;128;130;147;148;164;196). Even in individuals with severe VAVFL (i.e. visual field less than 20^{o} eccentricity), the fundus can be normal (139;146). Rare abnormalities that have been described in some VGB-exposed individuals include narrowing of the retinal arteries (97;105;106;121;138), epiretinal membrane formation (105;106), abnormal retinal pigmentation (105;106;197), "maculopathy" (79) and peripheral retinal pigment epithelium disturbance (97). These findings may be incidental and not related to VGB toxicity and VAVFL (182). More commonly described abnormalities include changes in the retinal nerve fibre layer (RNFL) and optic disc. Atrophy of the peripheral RNFL (147;183;198), optic disc pallor or optic atrophy (78;81;82;97;101;105;112;120;147;183) have been described in several studies, and may be associated with the severity of VAVFL (147).

1.10 Electrophysiological features of VAVFL

1.10.1 Retinal electrodiagnostic techniques

Many studies have been carried out using electrodiagnostic techniques in VGB-exposed individuals to explore abnormalities in the visual pathways that may be associated with VGB toxicity and the development of VAVFL. The most commonly used techniques include the recording of visual evoked potentials (VEP), the electro-oculogram (EOG),

the full-field electroretinogram (ERG), the pattern electroretinogram (PERG) and the multifocal electroretinogram (mf-ERG). Using these techniques can aid in the localisation of visual system abnormalities to particular pathways and cell types (Table 1.5).

Table 1.5 Electrodiagnostic techniques used to explore various visual pathway structures and cell types (adapted from (199)).

Visual pathway structure	Electrodiagnostic technique
Retinal pigment epithelium	EOG
Photoreceptors	
Rod photoreceptors	ERG a-wave (scotopic)
Cone photoreceptors	ERG a-wave (photopic)
	30Hz flicker ERG
Middle/inner retina	ERG and PERG (P50 component)
Bipolar cells	ERG b-wave
Müller cells	ERG b-wave
Amacrine cells	ERG oscillatory potentials
Retinal ganglion cells	PERG (N95 component)
Optic tract, radiation and cortex	VEP

EOG = electrooculogram; ERG = electroretinogram; PERG = pattern electroretinogram; VEP = visual evoked potentials

1.10.1.1 Visual evoked potentials

The visual evoked potential (VEP) is the electrophysiological response of the visual cortex evoked by a visual stimulus (either a flash or pattern-reversal stimulus). Recording of the VEP allows assessment of the integrity and function of the intracranial visual pathways including the optic nerve, chiasm and retrochiasmal function, and will be abnormal in disease involving any of these pathways (200). Due to cortical magnification of central vision in the visual cortex the VEP is dominated by responses elicited from activity of the central retina (201).

1.10.1.2 The electro-oculogram

The electro-oculogram provides information about the integrity and function of the retinal pigment epithelium (RPE) and outer retina (202;203). The EOG is based on recording changes in the standing potential (the potential between the front and the back of the eye), under successive periods of light and dark adaption (202). Changes in the standing potential are mainly derived from differences in ion permeability across the basal RPE membrane during light and dark adaptation (202). Under dark adaptation the amplitude of the standing potential decreases. A subsequent light stimulus leads to an initial fall in the standing potential, followed by an increase in amplitude (202). By comparing the maximum amplitude achieved during light adaptation, to the minimum amplitude during dark adaptation, the EOG ratio, or Arden ratio, is determined (202). In diseases affecting the RPE or RPE-photoreceptor complex the ratio between the light and dark peak (the Arden ratio) decreases (199).

1.10.1.3 The full-field electroretinogram

The ERG is a technique that provides information about the mass retinal electrical response elicited by a visual stimulus. After a visual stimulus a chain of biochemical and electrical activity occurs through the retina; the resulting electrical potentials that

reflect these events are conducted thorough the ocular media and can be recorded using electrode at the cornea. The resulting ERG waveform reflects a summation of the activity of all of these electrical processes (199) (Figure 1.5). By using various visual stimuli and by adapting the eye to different light conditions, the contribution of particular retinal sub-structures to the ERG waveform can be elicited and can provide information as to the retinal localization of any visual impairment. Under light-adapted (photopic) conditions, cone pathway contributions to the ERG waveform can be determined. Under dark-adapted (scotopic) conditions rod pathways are explored (199). Abnormalities of the ERG include changes in the normal amplitude or temporal aspects of each component of the ERG waveform (i.e. the a-wave, b-wave and oscillatory potentials), and reflect pathology in various retinal sub-structures.

Figure 1.5 The normal ERG wave form

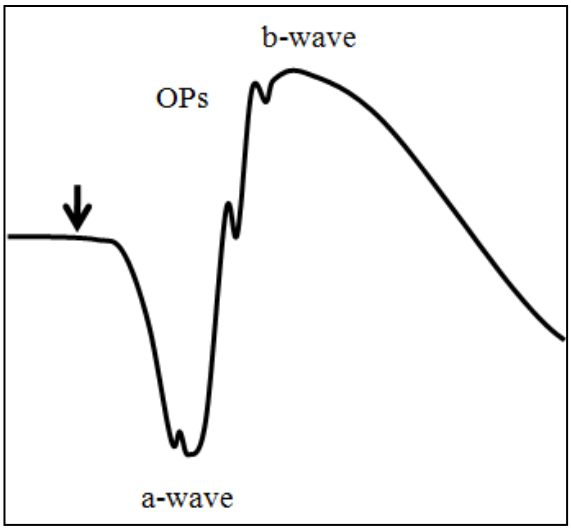

Figure 1.5 legend: Example of a normal ERG waveform elicited by a single flash light stimulus. The black arrow indicates the stimulus onset. The waveform consists of the early negative a-wave followed by a positive b-wave. Under certain conditions oscillatory potentials can be recorded on the ascending arm of the b-wave

The a-wave

The a-wave (Figure 1.5) is the early cornea-negative component of the ERG and is generated by the rod and cone photoreceptors (204).

The b-wave

The b-wave (Figure 1.5) reflects the depolarization of Müller cells in response to a light-induced increase in the potassium levels in the inner retina probably following the depolarization of ON-bipolar cells, and thus reflects both bipolar and Müller cell function (205;206).

Oscillatory potentials

Low amplitude rapid oscillations are present on the ascending arm of the b-wave (Figure 1.5). These oscillatory potentials (OPs) can be isolated from the ERG using certain recording procedures (207) and reflect synaptic activity of amacrine cells (206).

30Hz flicker response

Presentation of a flickering stimulus (of 30Hz) to elicit a retinal response allows cone pathway function to be assessed independently of rod pathway function. Cone photoreceptors and post-receptoral cone pathway cells including ON- and OFF-bipolar cells contribute to the formation of the 30Hz flicker response (208).

Pattern ERG

The PERG is the retinal potential that is evoked in response to presentation of a high-contrast patterned stimulus (typically stripes or a checkerboard) (209;210). The PERG waveform consists of a positive peak at around 50ms after stimulation (P50 component) and a negative trough at around 95ms (N95). The PERG allows assessment of macular

function and in particular macular RGC function (reflected predominantly in the N95 component) (200;209;211).

Multifocal ERG

Whilst the ERG reflects a summation of the activity of electrical processes throughout the whole retina, the multifocal ERG (mf-ERG) provides a topographic measure of retinal electrophysiological activity within the central 60^{o} (200;212). Using an array of hexagonal elements which flicker in a pseudo-random sequence, localized ERG responses are recorded from the macular and paramacular retinal areas (212). In addition, a newer technique, the wide-field mf-ERG, enables the assessment of localized ERG responses from the central (up to 60^{o}) and peripheral ($60 – 90^{o}$) retina.

1.10.2 Electrophysiology in VGB-exposed: Introduction

Electrophysiological abnormalities associated with VAVFL were reported in the first descriptions of VAVFL by Eke et al. In the individuals tested, the ERG showed reduced OP amplitudes, and the Arden ratio of the EOG was reduced in one individual (78). Ensuing case reports confirmed that ERG and EOG changes were present in some individuals with VAVFL, including reduced OP amplitudes reduces a- and b-wave amplitudes of the photopic and scotopic ERG (79;82;138). Others found normal electrodiagnostics in individuals with VAVFL (83) and when the individuals with VAVFL reported by Eke et al. were re-examined after VGB withdrawal, the EOG and ERG abnormalities had returned to normal, despite the persistence of the VAVFL (80). Furthermore, the same ERG abnormalities were reported in VGB-exposed individuals with normal visual fields (138;213), suggesting that the ERG and EOG changes may be related to the physiological effect of VGB-induced increased GABA concentrations in

the retina, rather than related to the pathological processes associated with VAVFL (97;127;145;214).

Ensuing studies of the electrophysiological correlates of VAVFL have provided little clarity. Often studies have shown conflicting results. Even within studies, individuals who have comparable visual fields can show markedly different ERG findings (101;104;120;150). Some of the variability in findings between studies and between individuals may be explained by the following factors, and should be taken into consideration in the interpretation of findings.

1.10.2.1 Electrodiagnostic techniques and standards

The International Society of Clinical Electrophysiology have published standards for electrodiagnostic assessment including ffERG (207), EOG (202), VEP (201), PERG (215) and mf-ERG (212) to reduce the variability in results between centres . Whilst most studies acknowledged that these standards were met for all electrodiagnostic testing , others have not stated if these standards were met (144;196), or have used non-standard recording conditions (101;135) which could account for some of the variation in findings between studies (153).

1.10.2.2 Control groups

For all electrophysiological procedures, normative data are established by each individual facility; thus the normal ranges used usually vary between laboratories (200;207). Whilst some studies of VGB-exposed individuals have compared ERG findings to normative data based on healthy controls (120;154), other studies have used non-exposed individuals with epilepsy, often matched for exposure to other AEDs, as a control population (103;106).

For example in VGB-exposed children assessed using ERG, abnormalities of the 30Hz flicker were defined arbitrarily as a response less than 56 µV. When this definition of abnormality was used one out of four children with VAVFL showed a reduced 30Hz flicker amplitude, yielding a sensitivity of 25%. However, when the normal cut-off for healthy adults was used (below 70 µV) three out of four children with VAVFL showed abnormal responses, yielding a sensitivity of 75% (131).

1.10.2.3 Other AEDs

Most VGB-exposed individuals included in the ERG studies are receiving polytherapy with a range of other AEDs. Only three studies have examined individuals on VGB monotherapy (128;216;217). The possible effect of other AEDs on the ERG must be considered when interpreting ERG studies. Several AEDs have been associated with abnormalities of retinal electrophysiology in humans (175) including the ERG (carbamazepine (218)), VEP (sodium valproate (219), carbamazepine (187;219) and phenytoin (220)) and the EOG (lamotrigine (221)). In addition, several studies have described abnormal ERG findings involving both the rod and cone pathways in individuals with epilepsy, with no history of VGB exposure, receiving a variety of AEDs, (103;121;165;196). The effect that multiple AEDs in various combinations may have in the ERG is unknown.

1.10.2.4 Cohorts studied

Separating the physiological effects of VGB exposure (and concurrent AED exposure), from the pathological changes in retinal electrophysiology has proved difficult. Studies have often been small; the largest have included less than 40 VGB-exposed subjects, and have typically integrated heterogeneous cohorts including individuals both on and off-VGB; with VAVFL and normal visual fields; and receiving a variety of other AEDs. Recognizing electrodiagnostic features that are present in discrete sub-groups within

each study cohort (e.g. “current VGB exposure with VAVFL” or “current VGB exposure with normal visual fields”), may help to distinguish the physiological changes related to VGB from those associated with pathology. This review of the literature on the electrodiagnostic features of VGB exposure and VAVFL has attempted to do this. However, it is important to note that the sub-group populations discussed are often small.

1.10.3 VEPs in VGB-exposed individuals

In agreement with preclinical studies of VGB-exposed individuals (74), most studies have found normal VEPs in individuals with VAVFL (78;81;97;101;106;126;134;138;146;183). Some studies have reported reduced amplitude (106) or prolonged latency of the P100 component (101;106;126;138;197) of the VEP, which has typically been associated with the presence of moderate to severe VAVFL extending to involve the central visual field (101). However, increased latencies of the P100 component of the VEP have also been found in individuals with epilepsy with no exposure to VGB (72) and are suggested to be due underlying neurological insult, seizure activity or exposure to other AEDs and may not be related to VGB exposure or VAVFL (72;197). In addition, abnormal VEPs were not found to be associated with the presence of VAVFL or ERG abnormalities in one study of VGB-exposed individuals (106).

The normal VEP in most VGB-exposed individuals suggests that the lesion associated with the development of VAVFL is unlikely to be in the anterior visual pathway or visual cortex (74;97). However, the VEP is dominated by responses elicited from activity of the central visual field (201), which is typically normal in individuals with

VAVFL. Pathological involvement of projections in the visual pathway and visual cortex subserving the retinal periphery may not result in an abnormal VEP if the central projections remain intact.

1.10.4 The EOG in VGB-exposed individuals

1.10.4.1 The EOG in individuals currently exposed to VGB

In individuals currently exposed to VGB the Arden ratio has been show to be reduced in those with VAVFL (78;81;101;112;114;134;135;165) and in individuals with normal visual fields (81;114;135), with no relationship seen between the severity of the VAVFL and the Arden ratio (114). The reduction in the Arden ratio was found to be present in individuals on VGB monotherapy and in individuals receiving other AEDs alongside their VGB therapy (216). In addition, compared to individuals previously exposed to VGB, the Arden index was significantly lower in those currently exposed to VGB (165). Conversely, in some individuals currently exposed to VGB, with normal visual fields and with VAVFL, the Arden ratio is normal (101;112;134;216).

Increasing cumulative VGB exposure (109) and maximum daily VGB dose (164) have been shown to correlated with abnormalities of the Arden ratio, suggesting that there may be a dose-related effect of VGB on the RPE electrophysiology.

1.10.4.2 The EOG in individuals after VGB withdrawal

The Arden ratio was found to be normal in the majority of individuals after VGB withdrawal, (with VAVFL and with normal visual fields) (81;134;216). However, in some individuals previously exposed to VGB with VAVFL the Arden ratio was reduced (134;151).

In a number of studies of VGB-exposed individuals, EOGs were recorded before and several months after discontinuing vigabatrin. In all patients, the EOG Arden ratio increased substantially on discontinuation, becoming normal in some individuals (81;135;150).

1.10.4.3 Summary of EOG in VGB-exposed individuals

Abnormalities of the Arden ratio appear to be related to current VGB exposure regardless of the presence of VAVFL (134;165). After VGB withdrawal there is recovery of the Arden ratio, even though the VAVFL persists. This suggests that abnormalities of the EOG are not directly related to pathological process leading to VAVFL but more likely represent a physiological effect of increased retinal GABA levels on normal RPE function (81;135;216).

1.10.5 The ERG oscillatory potentials in VGB-exposed individuals

1.10.5.1 Finding in individuals on-VGB with VAVFL

One of the most consistently reported ERG abnormalities in individuals with VAVFL has been reduced OP amplitudes. In four studies, reduced OP amplitudes were found in all individuals examined (78;112;138;146). However, it is important to note these reports include case reports, case series and observations of subgroups of individuals from larger VGB-exposed cohorts, and together these studies only constitute 24 individuals. Kalviainen found reduced OP amplitudes in 3/3 individuals with severe VAVFL currently receiving VGB, but only 6/10 individuals with mild VAVFL (104), suggesting that abnormalities of OP amplitude might reflect the severity of the VAVFL. In agreement with this Besch found that although all individuals with VAVFL and

current VGB therapy had subnormal OP amplitudes, the degree of abnormality was associated with the severity of the VAVFL (112).

In contradiction to these reports, Daneshvar found normal OPs in 10/10 individuals with VAVFL currently receiving VGB (101). This discrepancy in findings could have been related to differences in VGB exposure between the cohorts studied. The duration of VGB exposure was lowest in the individuals studied by Daneshvar et al. (9 – 75 months) (101), compared to those included in two of the larger studies by Kalviainen et al. (29 – 119 months) (104), and Besch et al. (12 – 96 months) (112). Furthermore, it may have related to differences in the recording techniques used between studies, as the ERG recordings by Daneshvar et al. did not comply with ISCEV standards (153), or differences in the methods used to measure the OP amplitudes (101). However, in agreement with the findings by Daneshvar, others have found normal OP amplitudes in some individuals with VAVFL and current VGB therapy (83;104;114).

1.10.5.2 Findings in individuals on-VGB with normal visual fields

Several studies of individuals currently taking VGB have found reduced OP in individuals with normal visual fields (105;114;121;153). In healthy individuals with normal visual fields exposure to a one-off dose of VGB did not alter the OPs (145), suggesting that the abnormal OPs reported in some VGB-exposed individuals is unlikely to reflect an acute effect of VGB-associated increases in retinal GABA on amacrine cell physiology.

1.10.5.3 Findings in individuals after VGB withdrawal

Individuals with VAVFL and decreased OP amplitudes during VGB exposure showed no improvement in either measure after VGB withdrawal (153;154). However, in another study, three VGB-exposed individuals with normal visual fields showed a substantial improvement in the OP amplitude after VGB withdrawal, two individuals

returning to normal levels (153). Similarly, the OP amplitudes were found to be subnormal in 17/17 children whilst receiving VGB. After VGB withdrawal, the OP amplitudes showed some improvement in 12/17 although the amplitudes remained at subnormal levels in most children (222).

In a study by Harding et al. ERGs were compared between individuals with severe VAVFL currently exposed to VGB and those with severe VAVFL previously exposed to VGB. The implicit time of the OP was delayed in individuals currently taking VGB compared to those previously taking VGB, suggesting that this abnormality of the ERG is related to current VGB exposure rather than irreversible VAVFL (165).

1.10.5.4 Summary of oscillatory potentials

OP amplitudes appear to be one of the more sensitive electophysiologcial techniques to identify individuals with VAVFL. However, some individuals with VAVFL may have normal OPs and some individuals with normal visual fields have reduced OP amplitudes. Furthermore, OP may improve after VGB withdrawal, particularly if the visual fields are normal.

It is possible that in VGB-exposed individuals, abnormal OP amplitudes reflect both physiological effects of increased retinal GABA on amacrine cell physiology (153), and pathological changes to amacrine cell function, which manifest as reversible and irreversible changes in the ERG OPs, respectively.

1.10.6 The ERG a-wave in VGB-exposed individuals

1.10.6.1 Finding in individuals with VAVFL currently taking VGB

In individuals with VAVFL currently receiving VGB the photopic and scotopic a-wave implicit times (78;81;101;106;138) and amplitudes (78;81;101;106) were normal. Normal a-waves were also found in individuals on current VGB monotherapy, but the visual field was not examined in these individuals (216). Conversely, in other studies of individuals with severe VAVFL the photopic and scotopic a-wave amplitudes were decreased (104) and the photopic a-wave implicit time was delayed (112;138).

1.10.6.2 Findings in individuals after VGB withdrawal

In individuals with VAVFL previously exposed to VGB the photopic a-wave amplitude was reduced compared to individuals with VAVFL currently receiving VGB (136;151). The reduction in the a-wave in the previously exposed individuals was suggested to be related to current exposure to other AEDs including carbamazapine (136;151) which decreases the photopic a-b wave amplitude (218).

In individuals with severe VAVFL and previous VGB exposure the scotopic a-wave latency was normal. In individuals with severe VAVFL and current VGB exposure it was delayed, suggesting that this measure reflects current VGB exposure and is not related to irreversible VAVFL (223).

1.10.6.3 Summary of a-wave

In most individuals with VAVFL, ERG a-waves are normal. Any abnormalities in the a-wave in VGB-exposed individuals may be related to current VGB exposure and not to pathological mechanisms associated with VAVFL (223). Photoreceptor pathology is therefore unlikely to be a prominent feature of VGB toxicity and is probably not implicated in the mechanisms associated with VAVFL.

1.10.7 The ERG b-wave in VGB-exposed individuals

1.10.7.1 Findings in healthy individuals

In healthy individuals receiving a one-off dose of VGB (1000mg or 2000mg) the group mean latency of the photopic ERG b-wave was significantly increased compared to pre-dose recordings although visual fields were unchanged compared to baseline (145).

1.10.7.2 Findings in individuals on VGB monotherapy

In a study of nine adults on VGB monotherapy, the amplitude of the ERG b-wave was decreased in 2/9 individuals under photopic conditions and in 3/9 individuals under scotopic conditions, (216). The visual fields were not examined and so the relationship between these changes and VAVFL could not be determined.

In a study of children receiving VGB monotherapy, the ERG was performed prior to starting VGB and then repeated at frequent intervals over 18 months of VGB exposure. At the earliest follow-up (around six months after initiation of VGB therapy), the photopic ERG b-wave amplitude was increased compared to baseline, which was subsequently followed by a progressive decrease over time to subnormal amplitudes. Again, the visual fields were not assessed in this study owing to the age and cognitive impairment of the children included in the cohort (217).

1.10.7.3 Finding in individuals with VAVFL currently taking VGB

The amplitude of the ERG b-wave was found to be reduced in individuals with VAVFL on current VGB therapy, under both photopic (104;120;138) and scotopic conditions (101;104;150;154;196). Equally, however, the b-wave was normal in some individuals with VAVFL and current VGB exposure under both photopic (78;101;104;120;146) and scotopic (78;101;104;112;138;146;150) conditions. Even within the same study where

techniques are standardised across subjects, some individuals with VAVFL can show b-wave abnormalities where others have normal findings (101;104;120;150).

This difference in findings between studies may be related to differences in co-medication with other AEDs. The amplitude of the photopic b-wave was found to be reduced in individuals with epilepsy not-exposed to VGB which may have been related to treatment with carbamazepine (165) or other AEDs (223) which reduce the photopic b-wave amplitude (218). Different combinations of AEDs could have a unique effect on the retinal electrophysiology and account for some of the differences seen between individuals and between studies. In opposition to this, some, but not all, individuals receiving VGB monotherapy were found to have decreased photopic and scotopic b-wave amplitudes, however, the visual field status of these subjects was not known (216).

In individuals with VAVFL currently receiving VGB the implicit times of photopic b-wave has been reported as normal (101;112;150;216) and delayed (112;150). The scotopic b-wave implicit time was normal (101;216).

1.10.7.4 Finding in individuals currently taking VGB with normal visual fields

Reduced amplitude of the photopic (109;121;138) and scotopic (109;121) b-wave have been reported in individuals with normal visual fields. Normal scotopic (136;138;196) and photopic (136) b-waves have also be reported.

1.10.7.5 Findings in individuals after VGB withdrawal

Reductions of the photopic (150;151;153;154;222) and scotopic (151;153;154) b-wave amplitudes recorded whilst on VGB did not improve after VGB withdrawal. In addition the photopic b-wave implicit time was delayed and did not improve after VGB

withdrawal (150). However others have found that the scotopic b-wave amplitude increased after VGB withdrawal (to normal levels in some individuals) (150).

In some studies the scotopic and photopic b-wave amplitudes were decreased in individuals previously exposed to VGB compared to individuals currently exposed to VGB (136). The authors suggested that this may be related to the current therapy with carbamazepine in the group previously exposed to VGB, which decreases the amplitude of the ERG (218). This finding is in agreement with other studies which have found the b-wave amplitude to increase when currently exposed to VGB (218;224). In children the b-wave was found to increase after VGB therapy was initiated compared to that recorded before VGB was started (217;222).

The conflicting findings regarding the effect of VGB on the b-wave of the ERG may be related to the opposing effects of GABA on $GABA_A$ and $GABA_C$ receptors (106) which are found on the axon terminals of bipolar cells (225). In isolated rat retina, suppression of $GABA_A$ receptors using the $GABA_A$ receptor antagonist bicuculline led to an increase in the b-wave amplitude, whilst suppression of $GABA_C$ receptors, with $GABA_C$ receptor antagonist 3-aminopropylphosponic acid, led to a decrease in b-wave amplitude (226). $GABA_A$ receptors located on bipolar cells appear to act to decrease the light evoked response of these cells, whereas $GABA_C$ receptors appear to enhance the response from bipolar cells (226). Differences in the effect of VGB on the b-wave of the ERG seen between studies and between individuals may be related to variation in the relative activity of GABA at each of the receptor subtypes. $GABA_C$ receptors have a higher affinity for GABA than $GABA_A$ receptors (227). Therefore, the increased ERG b-wave seen early after exposure to VGB may result from activity at $GABA_C$ receptors. After chronic VGB exposure, and persistently elevated GABA, pathological

or long term physiological changes in bipolar cells may occur, resulting in a decrease in the ERG b-wave.

1.10.7.6 Summary b-wave

An abnormal reduction of the photopic and scotopic ERG b-wave is associated with VGB exposure and VAVFL and does not improve in most individuals after VGB withdrawal. However, the effect of VGB on the b-wave is complex, and probably includes an early physiological component associated with increased activity at bipolar cell $GABA_C$ receptors (and a resulting increase in the ERG b-wave amplitude), followed by a later irreversible pathological component which could involve both bipolar and Müller cell function.

1.10.8 The 30Hz flicker in VGB-exposed individuals

1.10.8.1 Finding in individuals with VAVFL currently taking VGB

A reduction of the 30Hz flicker amplitude has been suggested as a sensitive and specific marker for VAVFL reflecting VGB-associated dysfunction in the cone pathway (165). In individuals with VAVFL currently exposed to VGB a decrease in the amplitude of the 30Hz flicker response has been reported (101;120;134;153;154;165;196). However, it is also normal in some individuals (101;114;146). A delayed implicit time of the 30Hz flicker response has been reported in some individuals with VAVFL (165;196). In a study by Harding et al. the amplitude of the 30Hz flicker correlated with the severity of VAVFL, and was associated with the presence of VAVFL regardless of current or previous VGB exposure (165).

Although ERG abnormalities have been reported in both cone and rod pathways, many studies have reported that the cone system is affected to a greater extent (103;106;138;165).

The apparent preferential susceptibility of the cone system to VGB toxicity might be explained by differences in GABA receptor expression between rod bipolar and cone bipolar cells (106). Both $GABA_C$ and $GABA_A$ receptors are found on bipolar cell axon terminals (225). The distribution of $GABA_A$ and $GABA_C$ receptors differs for each bipolar-cell type with rod bipolar cells having the highest ratio of $GABA_C$ to $GABA_A$ receptors compared to cone ON-bipolar and OFF-bipolar cells (228). In addition the effect of activity differs between the receptor subtypes; $GABA_A$ receptors appear to act to decrease the light evoked response of bipolar cells (thus decreasing the ERG b-wave), whereas $GABA_C$ receptors appear to enhance the response from bipolar cells (and increase the ERG b-wave) (226). After VGB exposure high retinal GABA levels would inhibit the response of cone bipolar-cells through activity at $GABA_A$ receptors, impairing cone pathway output. Conversely, activity at $GABA_B$ receptors on rod bipolar cells would lead to enhanced activity through the rod pathway. Overall this manifests as the cone ERG (photopic and 30Hz flicker responses) showing preferential susceptibility to VGB toxicity (106).

1.10.8.2 Findings in individuals currently taking VGB with normal visual fields

A reduced 30Hz flicker amplitude was found in individuals with normal visual fields (153;196) which persisted after VGB withdrawal suggesting that it is not a drug-related effect (153). Conversely Ardnt et al. found the amplitude to be normal in 2/2 individuals with normal visual fields (114). A delayed implicit time of the 30Hz flicker response was also found in individuals with normal visual fields (153).

1.10.8.3 Findings in individuals after VGB withdrawal

A decreased amplitude of the 30Hz flicker response did not improve up to six years after VGB withdrawal (154;222). Similarly Johnson et al. examined the ERG in thirteen individuals whilst receiving VGB, and again after VGB withdrawal. Whilst on VGB, individuals showed decreased amplitudes and delayed implicit times of the 30Hz flicker response, which did not improve after VGB withdrawal (153)

1.10.8.4 Summary 30Hz flicker

A reduction of the 30Hz flicker amplitude has been suggested as a sensitive and specific marker for the presence and severity of VAVFL (165), and does not improve after VGB withdrawal. However, it may be normal in some individuals with VAVFL, and reduced in some individuals with normal visual fields. Cone pathway function is evidently impaired in individuals with VAVFL. The reported predominant cone pathway dysfunction associated with VGB exposure may reflect physiological differences in GABA receptor expression between rod and cone bipolar cells.

1.10.9 The Pattern ERG in VGB-exposed individuals

In eight individuals with severe VAVFL (within 15^{o} eccentricity), PERG latencies and amplitudes of the P50 and N95 components were within normal limits (134). In agreement, a report of one individual with VAVFL currently receiving VGB the PERG was normal when the central visual field was stimulated (i.e. according to the ISCEV guidelines for PERG recording (215)). Conversely, when part of the pattern stimulus was presented in an area of VAVFL the N95 component was reduced (146). These findings suggest that whilst macular RGC function is normal in individuals with VAVFL, peripheral RGC function may be impaired.

1.10.10 Multifocal ERG in VGB-exposed individuals

Several studies have used mf-ERG to assess the distribution of electrophysiological abnormalities across the retina. Harding et al. found that in eight individuals with severe VAVFL there was a "reasonable correlation" between the pattern of mf-ERG abnormalities and the pattern of VAVFL (134). However, in some individuals the focal ERG abnormalities were more diffuse, and did not appear to be related to areas of VAVFL (134). In agreement, other studies found diffuse mf-ERG abnormalities across the retina which were not related to areas of VAVFL (81;153) or even the presence of VAVFL, as some individuals with normal visual fields also showed mf-ERG abnormalities (120;153).

Using wide-field mf-ERG, McDonagh et al. found that individuals with VAVFL had significantly reduced ERG amplitudes in the central ($<60^{o}$) and peripheral ($60^{o} – 90^{o}$) retina, and delayed implicit times in the periphery, compared to VGB-exposed individuals with normal visual fields (103). The difference between the central and peripheral implicit times was thought to represent a marker for VAVFL, identifying all individuals with VAVFL and only 2/13 VGB-exposed individuals with normal visual fields. The authors suggested that although diffuse physiological abnormalities related to VGB exposure (and exposure to other AEDs) may be present, certain features of the wide-field mf-ERG may be specific to VAVFL and indicative of peripheral retinal dysfunction (103).

1.10.11 Relationship between ERG abnormalities and VAVFL

Although all ERG measures have been associated with VAVFL in various studies, including decreased OP amplitudes (103;112;135) and increased implicit time of the OP (109;150); decreased 30Hz flicker amplitude (103;106;134) and increased implicit time of the 30Hz flicker (134); decreased amplitude of the photopic

(105;106;109;135;150;151) and scotopic (109;135;150;151) b-wave; and an increased implicit time of the photopic a-wave (151), non have consistently shown to be associated with the presence of or severity of VAVFL (229).

1.11 VGB, GABA and the retina

The mechanisms of VGB toxicity and VAVFL are unknown. However, the normal VEPs reported in most VGB-exposed individuals alongside the abnormal ERG findings suggest that the pathological insult associated with the development of VAVFL is unlikely to be in the optic tract or visual cortex and suggest a retinal origin of VGB toxicity (74;81;97;104;134;154;180). In addition, concentric visual field loss is most commonly associated with retinal disease (81) and pathology involving the optic nerve typically involves loss of visual acuity and colour vision, which are rarely seen in individuals with VAVFL (81).

1.11.1 Normal retinal anatomy

The retina is a thin, multilayered sheet of neural tissue lining the inner, posterior aspect of the globe. The basic organisation of the retinal layers include three layers of cell bodies (inner nuclear layer (INL), outer nuclear layer (ONL) and ganglion cell layer (GCL)) separated by two synaptic layers (inner plexiform layer (IPL) and the outer plexiform layer (OPL)). The outer most surface of the retina is the retinal pigment epithelium (RPE) which abuts Bruch's membrane, the choroid and the sclera. The rod and cone photoreceptor cell bodies comprise the INL. In the IPL rod and cone photoreceptors make synapses with horizontal cells and their respective bipolar cells, the cell bodies of which lie in the INL along with the cell bodies of amacrine cells.

Bipolar cells make synapses with amacrine cells and retinal ganglion cells (RGC) dendrites in the IPL. The RGC bodies lie in the innermost nuclear layer, the GCL, and project their axons in the retinal nerve fibre layer (RNFL) towards the optic nerve head (ONH) where they will exit the globe as the optic nerve. The RNFL also contains displaced amacrine cells, astrocytes and capillaries. The cell bodies of the Müller cell, the principal glial cell of the retina lies in the IPL, but their processes span the entire depth of the retina. Their apical processes form the external limiting membrane (ELM) and end-feet form the internal limiting membrane (ILM) (Figure 1.6) (230).

Figure 1.6 Normal anatomy of the retina

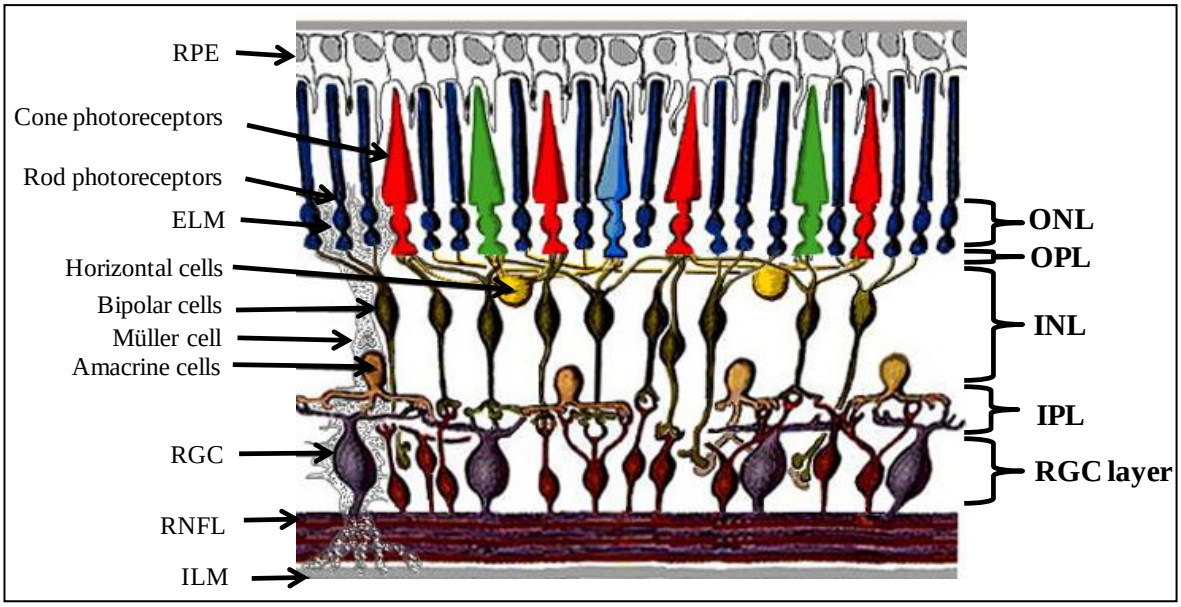

Figure 1.6 legend: The normal architecture of the human retina. RPE = retinal pigment epithelium; ELM = external limiting membrane; RGC = retinal ganglion cell; RNFL = retinal nerve fibre layer; ILM = internal limiting membrane; ONL = outer nuclear layer; OPL = outer plexiform; INL = inner nuclear layer; IPL = inner plexiform layer. (Image adapted from (231))

1.11.2 Normal GABA activity in the retina

GABA is the major inhibitory neurotransmitter in the retina. GABAergic pathways in the retina modulate neural transmission from photoreceptors to bipolar cells (in the OPL), and from bipolar cells to RGC (in the IPL) (225). In the OPL, inhibitory synaptic interactions are mediated by horizontal cells. In the IPL, inhibitory circuits are driven by amacrine cells of which around 50% are GABAergic (Figure 1.7).

Three types of GABA receptors are found in the IPL (Figure 1.7), the ionotropic $GABA_A$ and $GABA_C$ receptors, and the metabotropic $GABA_B$ receptors. Both $GABA_C$ and $GABA_A$ receptors are found on bipolar cell axon terminals, whereas only $GABA_A$ receptors are found on amacrine and ganglion cell dendrites (225). Activity at the pre-synaptic, $GABA_A$ and $GABA_C$ receptors modulate neurotransmitter release from the bipolar cells (225). $GABA_C$ receptors have a higher affinity for GABA than $GABA_A$ receptors (227) and give rise to a more sustained inhibitory response than that generated by $GABA_A$ receptors (225;228). The combination of both receptor sub-types on the bipolar-cell axon terminal allows a dynamic response to a range of GABA concentrations (225;228). The distribution of $GABA_A$ and $GABA_C$ receptors differs for each bipolar-cell type with rod bipolar cells having the highest ratio of $GABA_C$ to $GABA_A$ receptors compared to cone ON-bipolar and OFF-bipolar cells (228).

Termination of GABA signaling is achieved by active transport of GABA from the synaptic cleft via GAT-1 into the pre-synaptic GABAergic amacrine cell and by GAT-3, and to a lesser extent GAT-1, into surrounding Müller cells (232;233). Within the amacrine cell or Müller cell, GABA is metabolized by the mitochondrial enzyme GABA-transaminase (GABA-T) (1) (Figure 1.7).

Figure 1.7 Normal GABA in the retina at the level of the inner plexiform layer

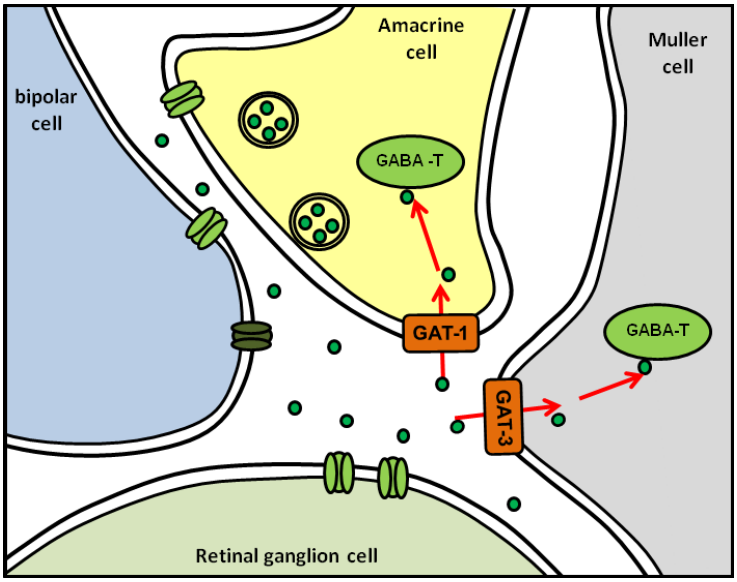

Figure 1.7 legend: In the IPL, pre-synaptic bipolar cell activity is modulated via GABAergic amacrine cells, through activity at $GABA_A$ (light green) and $GABA_C$ (dark green) receptors. GABA activity is terminated by uptake via high affinity GABA-transporters (GAT) into the pre-synaptic GABAergic amacrine cell and surrounding Müller cells, where it is metabolised by GABA-transaminase (GABA-T)

1.11.3 VGB in the retina

In mice and rats, exposure to VGB leads to a dose-dependent decrease in GABA-T activity and an increase in GABA concentration in several CNS regions, including cerebellum, pons, midbrain, striatum, hippocampus, hypothalamus, frontal cortex, dorsal cortex, spinal cord and retina (9;10;14-19). However, studies have consistently shown that the effects of VGB are particularly pronounced in the retina where after a single dose, VGB levels are substantially higher than they are in brain and spinal cord (15;17). Sills et al. reported concentrations of VGB in the retina were up to five times higher than any other CNS region (15). In another study VGB concentration was up to 18 times higher in retina than brain (17). In addition, inhibition of GABA-T activity (14;15;17;234;235) and associated increase in GABA concentration (14;15;17;234) are

significantly more pronounced in the retina than elsewhere in the CNS. In rats receiving a one-off dose of 1000 mg/kg VGB, retinal concentrations of GABA-T were reduced to less than 22% of control animals, with GABA concentration elevated to 260% of control animals (15) (Table 1.6). Comparatively, the dorsal cortex showed the greatest effect of VGB on the brain with GABA-T activity reduced to 54% of control activity, and GABA levels 195% of control levels (Table 1.6) (15).

Table 1.6 Percentage difference in GABA-T activity and GABA concentration in different CNS regions in VGB-exposed* rats compared to control rats

	Cerebellum	Pons	Hippocampus	Frontal cortex	Dorsal cortex	retina
GABA concentration	150.6%	178.8%	140.0%	171.7%	195.0%	261.3%
GABA-T activity	59.2%	68.3%	60.3%	68.3%	53.5%	21.4%

Results are expressed as the mean percentage concentration, or activity, compared to the control group (rats injected with saline). Table adapted from (15).

* Rats were exposed to a one-off dose of 1000 mg/kg of VGB

GABA = γ-aminobutyric acid; GABA-T = GABA transaminase; CNS = central nervous system; VGB = vigabatrin

The distribution of retinal GABA was also changed after VGB exposure. In non-exposed control animals GABA-immunoreactivity was localised in the IPL, in GABAergic amacrine cell bodies in the INL, and in occasional cell bodies in the GCL (presumed to be displaced amacrine cells) (234;236). In VGB-exposed animals significant GABA-immunoreactivity was detected in Müller cells as vertical streaks of staining extending through the depth of the retina to the ELM (234). In addition, there was increased staining in the amacrine cell bodies and in the IPL (234). In healthy control animals Müller cells fail to show staining for GABA, as any GABA transported

into Müller cells via GAT is rapidly metabolised by GABA-T (237). The prominent Müller cell staining seen in VGB-exposed animals suggests that the inhibition of GABA-T leads to abnormal accumulation of GABA in these cells (234). The retinal distribution of GABA-T was unchanged in VGB-exposed animals, although there appeared to be a decrease in the density of GABA-T immunoreactivity particularly in the IPL (234).

1.12 Retinal pathology in VGB-exposed animals

The toxic effects of VGB on the retina were first described in animals more than a decade before it was found to be associated with visual field loss in humans. In 1987 Butler et al. examined retinal sections from albino and pigmented rats exposed to VGB for 90 days. In the albino rats, diffuse changes were seen in the ONL including structural disorganisation, migration of photoreceptor nuclei toward the RPE and loss of photoreceptor nuclei (64). In addition, the frequency of retinal lesions and the severity of the lesions showed dose dependence. Only 1/30 rats exposed to 30mg/kg/day of VGB developed retinal lesions, compared to 24/30 rats exposed to 300mg/kg/day. Conversely, in the pigmented rats no retinal lesions were detected even after exposure to 300mg/kg/day of VGB.

1.12.1 Outer retinal pathology in VGB-exposed animals

Subsequent studies of the effects of VGB exposure on retinal morphology in albino animals have found similar changes to the outer retina as those described by Butler et al. Disorganisation of the ONL has been consistently reported (238-242) (Figure 1.8), which is associated with migration of photoreceptor nuclei toward the RPE (238;240-

242) and the OPL (238) (Figure 1.8), and irregularities in the structure of the ELM (239).

Figure 1.8 Disorganisation of the ONL in VGB-exposed rats

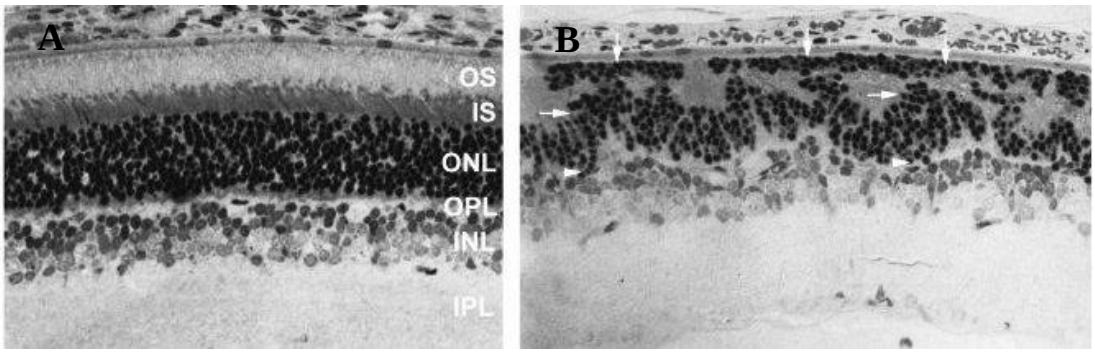

Figure 1.8 legend: Figure **(A)** shows a normal retinal section from a non-exposed control rat. Note the highly organised retinal structure with distinct demarcation of individual retinal layers. Figure **(B)** is taken from a VGB-exposed rat. Note the disorganisation of the retinal layers, particularly the ONL (white horizontal arrows), and the migration of photoreceptor nuclei toward the RPE (white vertical arrows). Figure taken from (238)

OS = outer segment; IS inner segment; ONL = outer nuclear layer; OPL = outer plexiform layer; INL = inner nuclear layer; IPL = inner plexiform layer

Immunohistochemical studies have revealed further pathological changes involving photoreceptors, including abnormal morphological changes in cone inner/outer segments (238;240;242) which were not restricted to areas of ONL disorganisation, but were also seen in areas with apparently normal retinal structure (238). In addition, a decrease in the density of cone inner/outer segments was found (238;241;242), with signs of photoreceptor degeneration in some areas (detected using TUNNEL staining for evidence of DNA fragmentation) (238). Under electron microscopy, abnormal photoreceptors showed vacuolization of the inner segment, disruption and dilatation of discs, and formation of membranous bodies in the outer segments (238). Changes in the

OPL have also been noted, with withdrawal of rod photoreceptor synapses towards the retinal pigment epithelium (240). Cone photoreceptor synapses were found to stay localised within the OPL, although they were found not to be as uniformly organised as cone photoreceptor synapses in the retinas of non-exposed control animals (240). In conjunction with the withdrawal of rod photoreceptor synapses (240), neuronal plasticity was seen to occur, with rod bipolar cells extending their dendrites past the OPL, deep into the ONL (240-242), to form ectopic synapses with the withdrawing rod photoreceptor cells (240).

All of the pathological changes described in the outer retina after VGB exposure have been noted in albino strains of rats and mice (64;238-242). In the study by Butler et al. exposure to 300mg/kg/day of VGB led to pathological changes in the retina in 80% of albino rats. Conversely, pigmented rats exposed to the same amount of VGB, and maintained in the same environment (12 hour dark/light cycles with light intensity of 260 lux), developed no retinal lesions (64). In addition, pigmented rabbits exposed to VGB showed no difference in the intensity and distribution of staining of cone inner/outer segments, or in the number of cone/inner outer segments, compared to non-exposed rabbits (243).

Albino rats are known to develop retinal pathology after excessive light exposure which is similar to that seen in the VGB-exposed albino rats (64). In the study by Butler et al. albino rats not exposed to VGB and maintained in the same light conditions as the VGB-exposed albino rats, did not develop retinal pathology (64). Thus the morphological changes in the albino VGB-exposed rats could not solely be explained

by phototoxicity (64). The influence of light on VGB retinotoxicity was explored by Izumi et al. Albino rats injected with a single dose of VGB were maintained under two different light conditions; either a 12 hour light/dark cycle (light intensity 300-500 lux), or 24 hours of light (light intensity 6000-8000 lux) (239). In rats exposed to 24 hours of light, the retina showed changes similar to those described previously in VGB-exposed albino animals. Conversely, VGB-exposed rats maintained in a 12 hour light/dark cycle showed no retinal abnormalities (239). In the same study, the effect of VGB and light exposure were assessed ex vivo in retinal sections from normal, healthy rats. Retinal sections were suspended in artificial CSF with added VGB and exposed to either 20 hours of darkness or light (light intensity 20000 lux). In addition, control retinal sections were suspended in artificial CSF alone or with added GABA, and subject to the same light conditions. The retinal sections exposed to VGB and 20 hours of light showed changes comparable with those seen in albino rats. In addition, the effect of VGB and light exposure was dose- and time-dependent, with pathology observed more frequently after suspension in higher concentrations of VGB and after exposure to longer durations of light. In contrast, retina exposed to VGB and maintained in 20 hours of darkness showed no pathological changes. Retina exposed to GABA showed no pathological changes under light or dark conditions (239).

These findings suggest that VGB sensitises the already sensitive albino retina to light, enhancing its phototoxic effect and promoting retinal degeneration (63-65). Furthermore, whilst VGB and light exposure resulted in pathological changes in retinal slices, application of GABA under the same light conditions was not retinotoxic (239), suggesting that high levels of GABA alone may be insufficient to lead to retinotoxicity and VAVFL in humans.

1.12.2 Other retinal pathology in VGB-exposed animals

In VGB-exposed albino rats and mice, abnormalities involving Müller cells have been reported. Increased GFAP immunoreactivity in Müller cells was found in areas of disorganisation and in some areas of normal retinal structure (238;241;242). In highly disorganised retinal areas, GFAP-immunoreactive Müller cell processes extended beyond the ELM into the layers of the photoreceptor inner/outer segments (238). This also occurred in some normal-appearing areas suggesting that VGB-induced gliotic changes were occurring throughout the retina (238).

In VGB-exposed rabbits (of unknown strain), GFAP immunoreactive Müller cells were detected in the peripheral and central retina with some cells showing abnormal morphology (236). No immunoreactive Müller cells were seen in non-exposed rabbits (236). Studies of VGB-exposed pigmented rabbits have found no indication of altered Müller cell morphology or function (243;244). However, in one of these studies, VGB-exposed pigmented rabbits were maintained for a 4-5 month treatment-free period before sacrifice and enucleation of the eye (244). The authors suggested that the pathological changes in Müller cells that had been previously found in VGB-exposed rabbits may only present during VGB exposure and might be reversible on cessation of therapy (244). Alternatively, differences in the findings between studies may be related to different rabbit strains used in each study (i.e. pigmented or albino strains), or differences in the duration or amount of VGB exposure between studies (243).

1.12.3 Reversibility of VGB-associated retinal pathology in animals

Two studies have examined whether VGB-associated retinal pathology may be reversible on VGB withdrawal. In a study by Kjellstrom et al. rabbits exposed to VGB

for 12 months were maintained for a 4-5 month treatment-free period before sacrifice and enucleation of the eye (244). No difference in retinal morphology was detected using immunohistochemical techniques between the VGB-exposed and non-exposed animals. Similarly, Duboc et al. assessed the effect of a "recovery period" on VGB-exposed albino rats. After VGB exposure, animals were given either a two-day or a 43-day recovery period before sacrifice and enucleation of the eye (238). Animals in both the two-day and 43-day recovery period groups showed the same outer retinal pathology as described in other VGB-exposed albino animals. Fewer animals in the 43-day recovery group showed the retinal changes, and the areas of pathology were reduced in size compared to the two-day recovery group (238).

1.13 Retinal pathology in VGB-exposed humans

Only one pathological study of the retina and optic nerve from a single individual with VAVFL has been reported (162). The individual had been exposed to VGB for 28 months prior to death at a maximum daily dose of 6g/day. Prior to death the individual reported "visual difficulties" and one month prior to death perimetry using HVFA 30-2 showed VAVFL. At post mortem examination the retina showed almost complete loss of RGC in the periphery, with less severe involvement of RGC in the macula, and severe atrophy of the RNFL. There was some loss of nuclei from the INL and ONL and atrophy of the IPL, OPL and RNFL. The optic nerve was severely atrophic (around a third of its normal size) with relative preservation of fibres projecting form the macula compared to those projecting form the peripheral retina. The optic tracts also showed some atrophic changes (162).

1.14 The retinal nerve fibre layer in VGB-exposed individuals

Although the precise mechanisms of VGB retinotoxicity are unknown, there is evidence to suggest that in humans RGC loss is implicated (80;101;146;147;162;165). RNFL atrophy (97;106;147;183;198) and optic atrophy (101;147;183) are the most common abnormalities detected using fundoscopy or fundus photography. These clinical observations are supported by finding that RGC loss was the most prominent retinal pathological change seen in a post mortem study of an individual with VAVFL (162). However, assessment of the fundus through direct examination, slit-lamp biomicroscopy and using fundus photography, reveals that in most individuals with VAVFL, the fundus appears normal with no evidence of RNFL loss or optic atrophy (78;94;95;97;101;104;106;112;116;120;121;128;130;147;148;164;196). Even in individuals with severe VAVFL (i.e. visual field less than 20^{o} eccentricity), the fundus can be normal (139;146).

1.14.1 The normal retinal nerve fibre layer

The RNFL is an inner-retinal layer composed of the axons of RGC. Projecting RGC axons are organised into bundles which extend in radial wedge-shaped sectors from the retinal periphery to the ONH where the RGC axons exit the globe of the eye forming the optic nerve (245;246). The nerve fibre bundles maintain horizontal topographic organisation of RGC axons, allowing little, if any, lateral dispersion of axons between bundles (247). Consequently, the projecting RGC axons follow a specific trajectory, such that axons from RGC in neighbouring retinal locations project to discrete areas of the ONH (Figure 1.9) (246-249).

Figure 1.9 Topographic projections of RGC axons in the RNFL

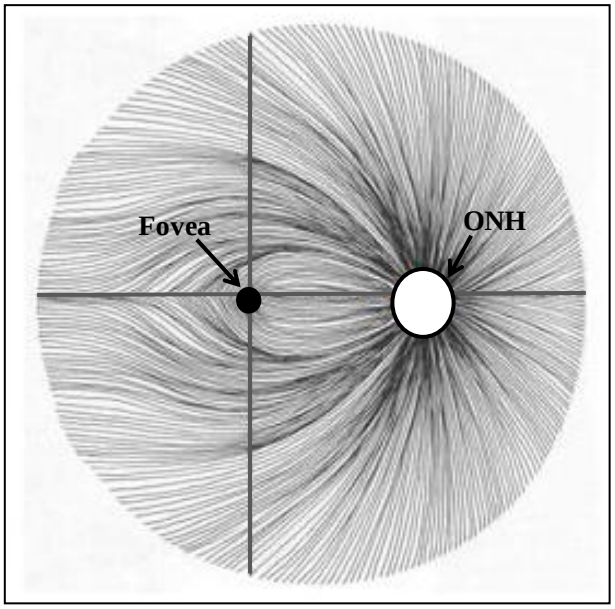

Figure 1.9 legend: RGC axons project from the retinal periphery to the ONH where they exit the globe of the eye forming the optic nerve. The RGC axons follow a specific topographic trajectory, such that axons from RGC in neighbouring retinal locations project to discrete areas of the ONH.

Grey vertical line = vertical meridian; grey horizontal line = horizontal meridian; ONH = optic nerve head

RGC axons in the nasal hemifovea, and caecocentral area, project directly towards the ONH in a rectilinear course, to enter at its most temporal aspect (246-249) (Pollock). Axons from RGC in the temporal hemifovea and extrafoveal area project in an arcuate course to avoid the rectilinear central projections, entering the ONH supero- and infero-temporally (246-249). At increasing distances from the horizontal raphe, axons in the temporal peripheral retina take an increasingly arcuate course to enter the ONH at the superior and inferior poles (246-249). Fibres from RGC in the nasal periphery, take a radial trajectory and enter the ONH on the nasal side (247-249) (Figure 1.9). RGC axons respect the horizontal meridian (grey horizontal line on Figure 1.9), such that

axons from the superior retina do not cross the horizontal meridian, and enter the ONH at its superior pole, and RGC axons in the inferior retina enter at the inferior pole (246).

In the RNFL in the area immediately surrounding the ONH (the peripapillary RNFL (ppRNFL)), the organisation of the converging RGC axons creates a "double hump" configuration. The ppRNFL is thickest at the superior and inferior poles of the ONH and thinnest in the nasal and temporal aspects of the ONH (250;251).

1.14.2 Imaging the ppRNFL

Assessment of the ppRNFL around the ONH not only allows the acquisition of information about the structural integrity of the RGC axons (i.e. by measuring ppRNFL thickness), but can also provide information about the retinal location of any focal pathology, owing to the topographic organisation of the RGC axons at the ONH (250). Several instruments are available that allow quantitative imaging of the ppRNFL including optical coherence tomography (OCT), scanning laser polarimetry and scanning laser opthalmoscopy (252). The diagnostic abilities of each of these instruments in diseases affecting the ppRNFL (e.g. glaucoma) have been extensively evaluated, and there is little difference in the capabilities between the three technologies (253-255).

In the output from each of these instruments, quantitative summary measures of ppRNFL thickness are provided including average thickness around the circumference of the ONH, and thickness in defined areas (e.g. temporal, superior, nasal and inferior ONH areas).

1.15 Imaging the ppRNFL in VGB-exposed individuals

In 2004 Choi et al. suggested the potential for using RNFL imaging in VGB-exposed individuals (198). They showed that in an individual with VAVFL and atrophy of the peripheral RNFL, evident using red-free fundus photography, thinning of the ppRNFL could be detected using OCT. The pattern of ppRNFL thinning detected using OCT was consistent with the clinical and photographic features, showing ppRNFL thinning restricted to the ONH areas receiving RGC axons from the peripheral retina (198).

After the initial report of ppRNFL thinning in VGB-exposed individuals (198), subsequent studies using OCT (119;198;229;256), scanning laser ophthalmoscopy (229) and scanning laser polarimetry (257), confirmed that the ppRNFL was significantly thinner in VGB-exposed individuals compared to healthy controls and non-exposed individuals with epilepsy (Table 1.7).

Table 1.7 Summary of studies using ppRNFL imaging in VGB-exposed individuals

Reference	Number of VGB-exposed	Method	Main finding
Choi 2004 (198)	1	TD-OCT (Stratus model) 3.4mm fixed diameter scan	ppRNFL thinning was consistent with photographic and clinical abnormalities
Wild 2006 (229)	21	TD-OCT (Stratus model) Proportional circle scan	100% of individuals with VAVFL were below the 95% confidence limit for normality ppRNFL was significantly thinner in VGB-exposed with VAVFL compared to VGB-exposed with normal visaul fields, non-exposed individuals and healthy controls
Durnian 2008 (257)	8	SLP (GDx VCC)	100% of individuals with VAVFL showed abnormal ppRNFL thinning
Lawthom 2009 (256)	27	TD-OCT (Stratus model) 3.4mm fixed diameter scan	100% of individuals with VAVFL showed ppRNFL thinning in the nasal quadrant*
Ardagil 2010 (119)	14	TD-OCT (Stratus model) 3.4mm fixed diameter scan	ppRNFL was significantly thinner in VGB-exposed compared to non-exposed and healthy controls
Moseng 2011 (258)	9	TD-OCT (Stratus model) 3.4mm fixed diameter scan	ppRNFL was significantly thinner in VGB-exposed individuals with VAVFL compared to non-exposed, there was an increased frequency of ppRNFL thinning compared to non-exposed*

TD-OCT = time-domain optical coherence tomography; SLP = scanning laser ophthalmoscopy; VCC = variable corneal compensation

*compared to the manufacturers' normative database

1.15.1 ppRNFL thickness in individuals with VAVFL

In individuals with VAVFL, the ppRNFL was significantly thinner compared to non-exposed individuals with epilepsy (119;229;258) and compared to healthy controls

(119;229). Furthermore, using OCT, Wild et al. showed that individuals with VAVFL had significantly thinner ppRNFL compared to VGB-exposed individuals with normal visual fields (229), suggesting that the development of VAVFL may be related to loss of RGC axons. Average ppRNFL thickness was plotted as a function of mean sensitivity to illustrate a possible relationship between ppRNFL thinning and the degree of visual field loss. However, no statistical analysis or discussion of the trend was made by the authors (229). Reinspection of the data does not appear to show an association between the two measures.

1.15.2 The pattern of ppRNFL thinning in individuals with VAVFL

A pattern of ppRNFL thinning associated with VGB exposure, that is in agreement with the pattern of RNFL and ONH atrophy observed using fundus photography (147;183), has been suggested. In individuals with VAVFL, ppRNFL thickness was compared to ppRNFL thickness data from healthy controls provided in the manufacturers' normative database[2]. Individuals with ppRNFL thickness falling below the 5th percentile of the manufacturers' normative database were considered to have abnormal thinning. All individuals (n=11) with VAVFL showed abnormal ppRNFL thinning in the nasal quadrant leading to the suggestion that ppRNFL attenuation in the nasal quadrant should be used as a biomarker for VGB toxicity (256). Conversely, the ppRNFL in the temporal quadrant is relatively preserved with few individuals showing abnormal thinning in this area (119;256;259).

1.15.3 ppRNFL thickness in VGB-exposed individuals with normal visual fields

Thinning of the ppRNFL was also found in some VGB-exposed individuals with normal visual fields (229;256). The pattern of ppRNFL thinning was similar to that

[2] See 1.19.3

seen in individuals with VAVFL, with thinning detected in the superior, nasal and inferior quadrants, but preservation of the ppRNFL thickness in the temporal quadrant (256). These findings may represent individuals with subtle pathological changes in the retina that do not result in functional changes that are detectable using standard white-on-white perimetry, and thus provide promising evidence that ppRNFL imaging may be a more sensitive measure of VGB retinotoxicity than does perimetry (256).

1.15.4 The relationship between ppRNFL thickness and VGB exposure

Using OCT, ppRNFL thickness in the nasal quadrant was found to correlate with cumulative VGB exposure, with increasing VGB exposure related to decrease ppRNFL thickness (256). However, in a study using scanning laser polarimety no correlation was found between any ppRNFL thickness measure and cumulative VGB exposure or duration of VGB exposure (257). In an OCT study by Wild et al., average ppRNFL thickness was plotted as a function of cumulative VGB exposure and of duration of VGB exposure (229). However, no statistical analysis or discussion of the trend was made by the authors. On reinspection of the data there does not appear to be an association between either measure of VGB exposure and average ppRNFL thickness. The disagreement between studies is probably due to the small number of subjects included, and larger studies are needed to fully appreciate the relationship between the amount and duration of VGB exposure and the degree of ppRNFL thinning.

1.16 ppRNFL thickness in non-exposed individuals with epilepsy

In some non-exposed individuals with epilepsy, ppRNFL thinning was detected as compared to the normative database of ppRNFL thickness provided by the

manufacturer[3] (229;256). In a study by Lawthom et al. 3/13 non-exposed individuals showed abnormal thinning in at least one of the ppRNFL quadrants, although all showed normal average ppRNFL thickness (256). The individuals all had normal visual fields and no clinical reason was found for the attenuation. The authors suggested that the abnormal finding in these individuals was most likely due to misalignment of the subject during scanning or misplacement of the scan circle (256). In an OCT study of 45 individuals with epilepsy exposed to carbamazepine or valproate monotherapy, no difference in ppRNFL thickness was found compared to healthy controls (260).

1.17 ppRNFL imaging for clinical use in VGB-exposed individuals

Based on these OCT studies (Table 1.7), ppRNFL imaging has been proposed as a useful tool in the assessment of VGB-exposed individuals, providing a sensitive and specific indicator of VAVFL (119;229;256). In particular Lawthom et al. suggested that ppRNFL attenuation in the nasal quadrant should be used as a biomarker for VGB toxicity (256).

In the US, where VGB was recently licensed, the manufacturers of VGB (Lundbeck) require an assessment form to be completed at each opthalmological examination of individuals undergoing VGB therapy which is to be returned to the manufacturers after completion. The form includes a section for OCT assessment, requiring the interpretation of the OCT as "normal, abnormal or uninterpretable" (261). In addition, a recent report on the recommendations for visual testing in VGB-exposed individuals compiled by an "expert panel" of neurologists, ophthalmologists and visual

[3] For details See 1.19.3

electrophysiologists, included OCT in the suggested visual evaluation protocol, particularly when perimetry is unreliable or inconclusive (262). In a briefing document compiled for the FDA during the application for approval of the licensing of VGB in the US, it was stated that "It is highly likely that OCT will be the primary modality of assessing VGB retinal effects within 5 years" (263).

At the present time however, the exact role of OCT in the management of VAVFL is uncertain (262). The available OCT studies have been on a small number of individuals, and the precise relationship between the degree of ppRNFL thinning and the severity of VAVFL is unknown. In the expert panel's report on the recommendations for visual testing in VGB-exposed individuals, it was stressed that currently OCT should be considered as an "exploratory test" (262). Furthermore, although it has been suggested that ppRNFL imaging may provide an alternative tool to assess individuals who are unable to perform perimetry (229;256;262), this has not been formally assessed, and the repeatability of measurements has not been validated in a population of individuals with epilepsy.

1.18 Optical coherence tomography

1.18.1 Introduction to OCT

OCT (264) is an optical imaging tool that allows non-invasive, high resolution, cross sectional imaging of biological tissue microstructure in vivo (264;265). OCT imaging is analogous to ultrasound; however, instead of sound waves, low-coherence light is used to obtain images based on the optical properties of the tissue (264;265). Images are generated by measuring the time delay and the magnitude of backscattered and back-

reflected light from the various tissue microstructures (266;267). Detailed imaging of discrete tissue architecture relies on the ability to detect difference in the optical properties of adjacent structures (268).

The axial image resolution of OCT is determined by the bandwidth of the light-source (267). Axial resolutions achievable with commercially available OCT instruments ranges from 4 - 10µm (265), compared to standard clinical ultrasound which has a resolution of 0.1 – 1mm (269). Transverse resolutions are dependent on the spot size of the light beam on the tissue, and in retina transverse resolutions of around 20µm are typically achieved (270;271). The cross-sectional image (tomograph) generated from OCT imaging has been referred to as an "optical biopsy" (265), as it provides images of tissue microstructure similar to those seen under a microscope, that are not obtainable with any other non-invasive techniques (266;267).

The main disadvantage of OCT is that light (unlike sound waves in clinical ultrasound) is substantially scattered by most biological tissues. Attenuation of the light from this scattering limits the imaging depth to around 2mm (265;269), compared to standard clinical ultrasound which can reach depths of up to 10cm (269). The limited penetration depths make OCT imaging impractical for many clinical applications. The retina, however, is particularly accessible to OCT imaging as the transparent tissues of the lens, cornea and ocular media, allow transmission of light from the OCT instrument to the retina with minimal scattering and attenuation (267). Because of this, the clinical use of OCT has developed most rapidly in ophthalmology for imaging the microstructure of the retina and optic nerve head (267), and will be further discussed here with reference to retinal imaging.

1.18.2 The basic principles of OCT

The basic principles of OCT are illustrated in Figure 1.10. Low-coherence light (800-1400 nm wavelength) from a superluminescent diode is directed into a fibre-optic Michaelson interferometer. At the interferometer the incident light beam is split into a reference arm and a sample arm via a partially reflective mirror. Light in the reference arm is reflected back to the interferometer from a reference mirror. At the same time, the light beam in the sample arm is incident upon a scanning mechanism, which under computerised control, focuses the beam onto the retina in a discrete location. The light beam is then backscattered or reflected from the retina, via the scanning mechanism, back to the interferometer. At the interferometer light from the reference mirror, and that from the retina, are combined producing an optical interference pattern on the surface of a photodetector (264;266;270).

The raw signals received at the photodetector are processed into an individual A-scan, which represents the depth-resolved reflectivity profiles of the retina at the discrete location on which the beam was focused by the scanning mechanism. Movement of the scanning mechanism allows the light beam in the sample arm to "sweep" across the retina in a predetermined scan pattern (e.g. a single-line (Figure 1.11)) enabling the acquisition of multiple sequential A-scans in a desired pattern and location (272). After processing, multiple individual A-scans acquired during a scan session are assembled into a two-dimensional cross-sectional image (B-scan) (Figure 1.10 and 1.11). Using some OCT technologies, a series of B-scans in a raster pattern can be taken to generate three-dimensional OCT images (Figure 1.11).

Figure 1.10 Basic principles of OCT

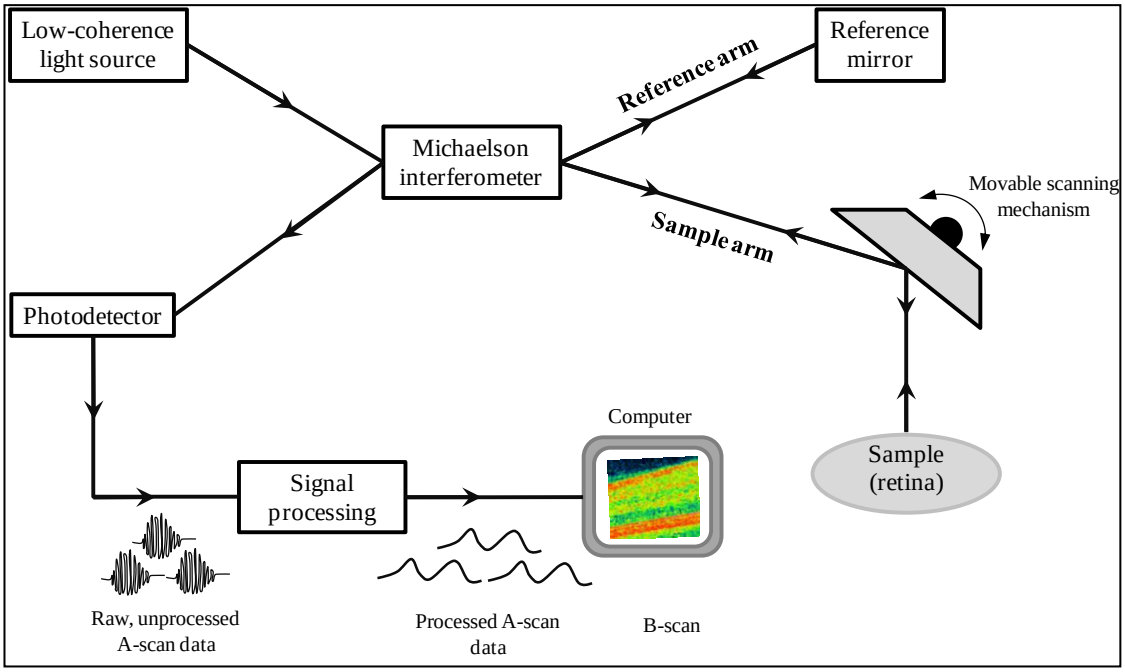

Figure 1.10 legend: The basic mechanisms of optical coherence tomography (OCT) of the retina. Figure adapted from (273)

Figure 1.11 Assembly of processed A-scan data into a tomograph

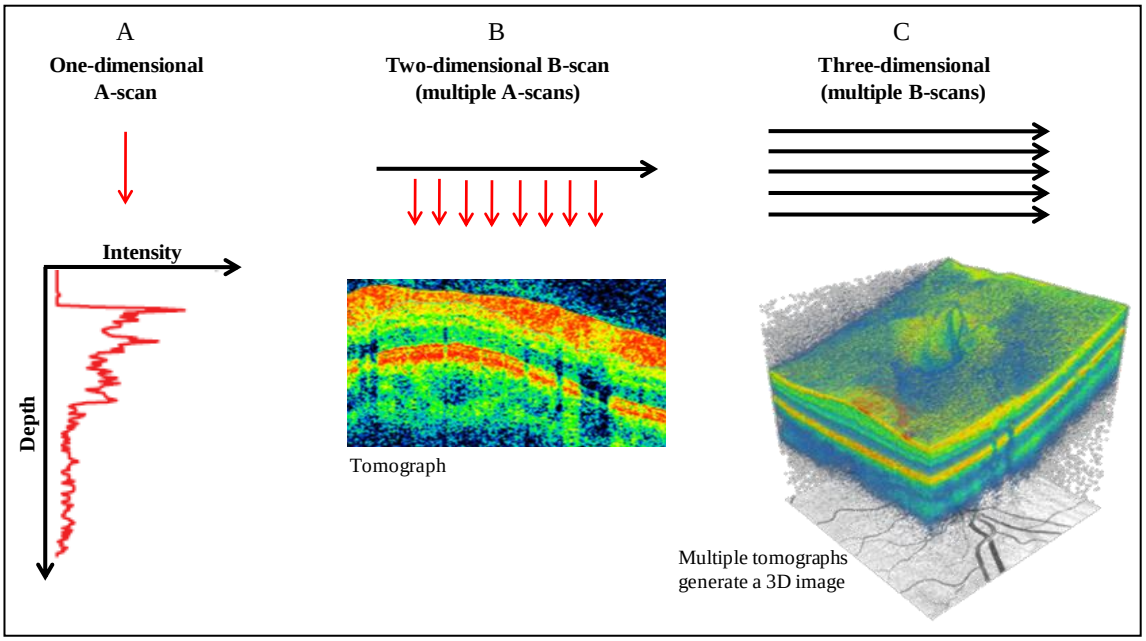

Figure 1.11 legend: **(A)** The individual A-scan (red arrow) represents the depth-resolved reflectivity profiles of the tissue being scanned. **(B)** Multiple A-scans (red arrows) are

assembled into a B-scan (black arrow) to produce the two-dimensional tomograph. **(C)** Using some OCT technologies, a series of B-scans (black arrows) in a raster pattern can be taken to generate three-dimensional OCT images.

1.18.3 OCT technology

Several OCT instruments are commercially available, the first of which was released in 1995 and utilised time-domain technology. The most recent instrument to be released based on this technology was the Status OCT (Carl Zeiss Meditec, Inc., Dublin, CA, USA) (271). More recently, OCT instruments utilising spectral-domain (also called Fourier-domain) technology (e.g. Cirrus HD-OCT (Carl Zeiss Meditec, Inc., Dublin, CA, USA)) have been developed, and comprise the latest generation of commercially available OCT instruments.

Although the basic principles of time-domain OCT (TD-OCT) and spectral-domain OCT (SD-OCT) are the same (Figure 1.10), they utilise different mechanisms to resolve the axial depth of structures within the tissue being scanned, resulting in significant differences in scanning speed, and axial resolution (271;274;275).

1.18.3.1 TD-OCT (Stratus OCT)

In TD-OCT the depth and relative positions of the retinal structures are determined sequentially by moving the reference mirror and analysing the interference patterns between the reflected reference light at known distances, and the reflected light from different scattering sites in the sample (276;277).

The dependence on movement of the reference mirror to enable depth resolution, and the requirement of sequential resolution of light reflected from various depths, limits image acquisition speed to around 400 A-scans per second. Using this technology, the latest commercially available OCT model (Stratus OCT, Carl Zeiss Meditec, Dublin,

CA, USA) allows acquisition of a single-line B-scan, comprised of 512 adjacent A-scans, within 1.28 seconds, with axial resolution of around 10µm (277).

1.18.3.2 SD-OCT (Cirrus OCT)

In SD-OCT, depth resolution is not obtained by mechanical manipulation of the reference mirror, but by including a spectrometer in the detector arm. The spectrometer allows the interference pattern obtained from the light reflected from the stationary reference arm, and that reflected from all scattering sights (i.e. at all depths) in the sample, to be collected simultaneously on the photodetector (278). The interference pattern then undergoes Fourier transformation to produce the A-scan image (275;277).

Because the light reflected from different scattering sights in the sample are measured simultaneously, as opposed to sequentially with TD-OCT, the process is up to 100 times faster (279) with data acquisition speeds of around 27,000 A-scans per second. Cirrus OCT (Carl Zeiss Meditec, Dublin, CA, USA), acquires a 6x6mm cube of data consisting of 40,000 A-scans, in less than 1.49 seconds.

1.18.4 The OCT image (retinal tomograph)

After processing, multiple individual A-scans acquired during a scan session are assembled into a two-dimensional cross-sectional image (B-scan) (Figure 1.11). Using SD-OCT, a series of B-scans in a raster pattern can be taken to generate three-dimensional OCT images (Figure 1.11). The final processed images are displayed in the OCT output using a colour-scale (or grey-scale) to represent the logarithm of the intensity of the reflected signal (265;266;268;270;272). Typically, the red end of the colour spectrum represents areas of high reflectivity with the blue end corresponding to areas of low reflectivity (264;268) (Figure 1.12).

The laminated appearance of the retinal tomograph suggested that individual retinal layers might be distinguished by differences in their optical properties (280). To determine the retinal structural components represented in OCT images, studies compared cross-sectional retinal tissue, seen under light microscopy, with corresponding retinal OCT scans, in humans (264;281) and in animals (268;280;282) (Figure 1.12). In the OCT image, a distinct layer of high reflectivity at the vitreoretinal interface corresponded to the RNFL (264;268;280). Other highly reflective layers were compatible with the IPL, OPL and RPE (268;280-282). Retinal areas of low reflectivity corresponded with the location of the photoreceptor inner and outer-segments and the INL and ONL (Figure 1.12 (268;270;280-282).

Figure 1.12 The relationship between the OCT tomograph and retinal histology

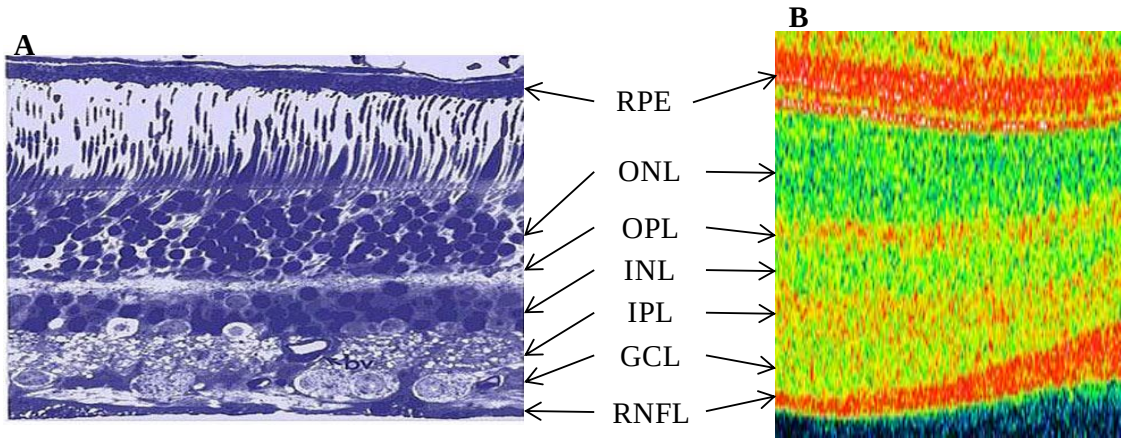

Figure 1.12 legend: The retinal substructures observable on light microscopy **(A)** have unique optical properties which produce distinct layers in the OCT tomograph **(B)**. Light microscopy image **(A)** taken from (231)

For the commercially available OCT instruments, various scanning protocols have been developed which allow targeted imaging of particular retinal locations depending on the

structure of interest. The tomograph obtained from each scanning protocol is provided in the manufacturers' summary report and can be used to detect retinal pathology through direct observation. In addition to the tomograph, the summary report provides quantitative data (e.g. retinal thickness), summary quantitative data (e.g. average retinal thickness in defined retinal areas), and normative data on various retinal structural measurements.

1.19 Using OCT to image the ppRNFL

In the OCT tomograph the RNFL appears as a distinct layer of high reflectivity at the vitreoretinal interface (264;268;280) (Figure 1.12). Interest in developing methods to image and measure RNFL thickness was stimulated by the need for more objective, repeatable tools for use in glaucoma management, where retinal ganglion cell loss and associated RNFL attenuation are pathological features (283). Algorithms developed for OCT to measure RNFL thickness employ a circular scan centred on the ONH (in the peripapillary area) (Figure 1.13) (283). As all RGC axons project through the retina in the RNFL to leave the orbit in the optic nerve (Figure 1.9), measuring peripapillary RNFL (ppRNFL) thickness dictates that the measurement sample contains projections from all RGC axons throughout the retina.

1.19.1 Measuring ppRNFL thickness

The thickness of the ppRNFL is calculated firstly by determining the borders of the ppRNFL. This is achieved using segmentation software which uses "edge-detection" algorithms to recognise changes in reflectivity patterns in the OCT signal (276;283;284). The anterior border of the ppRNFL is detected by an early sharp rise in the signal intensity as the light passes through the minimally reflective vitreous into the

highly reflective RNFL. Similarly the posterior border of the ppRNFL is defined by a sharp decrease in signal intensity as the light leaves the RNFL and passes into the less reflective structures of the adjacent inner retina. Once the inner and outer borders of the ppRNFL have been established, the thickness in micrometers can be determined between these borders (276;283;284). This process is carried out for each individual A-scan. Measures of ppRNFL thickness that are provided in the manufacturers' summary report are based on the ppRNFL thickness measurements from each of the individual A-scans.

1.19.2 ppRNFL thickness scanning methods

The impact of the dramatic difference in scanning speed between TD and SD-OCT is highlighted in the scanning protocols used by each instrument from which ppRNFL thickness is determined. In TD-OCT the instrument acquires three sets of 256 A-scans in a 3.46mm diameter circle around the ONH within 1.3 seconds of scanning time. The ppRNFL measurements provided in the manufacturers' summary report are calculated from an average of the three sets of scans. In SD-OCT instrument acquires a 6x6mm cube of data centred on the ONH, consisting of 40,000 A-scans, in 1.48 seconds. A 3.46mm diameter circle of data comprised of 256 A-scans, centred around the ONH is extracted from the cube of data. The ppRNFL measurements provided in the manufacturers' summary report are calculated from the 3.46mm diameter circle of data.

1.19.3 The manufacturers' summary reports

After scan acquisition, each OCT instrument provides ppRNFL thickness data in the manufacturers' summary reports. The reports included summary measures of ppRNFL thickness include the average ppRNFL thickness (around the whole ONH), and the ppRNFL thickness in 90^o quadrants and 30^o sectors (Figure 1.13). Regions of the ppRNFL are referred to according to their location around the ONH. The four 90^o

quadrants are referred to as temporal, superior, nasal, and inferior quadrants. The twelve 30^{o} sectors are referred to as temporal (Temp), temporal-superior (TS), superior-temporal (ST), superior (Sup), superior-nasal (SN), nasal-superior (NS), nasal (Nas), nasal inferior (NI), inferior-nasal (IN), inferior (Inf), inferior-temporal (IT) and temporal-inferior (TI) sectors (Figure 1.13). A temporal-superior-nasal-inferior-temporal (TSNIT) plot is also provide in the manufacturers' summary report, which graphically represents the ppRNFL thickness around the whole ONH across each of the 256 individual A-scans (Figure 1.13).

In addition to providing quantitative ppRNFL thickness data, the ppRNFL thickness is classified according to which percentile it falls into, based on the manufacturers' database of age-corrected normal values. ppRNFL thickness values for all summary measures (average, 90^{o} quadrants, 30^{o} sectors and TSNIT plots), are colour-coded according to which percentile they fall into. Values falling into the $\leq 95^{th}$–>5^{th} percentile are colour coded as green, $\leq 5^{th}$–>1^{st} percentile are coloured yellow and those falling into $\leq 1^{st}$ percentile are coloured red (Figure 1.13).

Details of the normative database in the TD-OCT (Stratus OCT, software version 4.0, Carl Zeiss Meditec, Dublin, CA) have been made available. The normative data base is comprised of 328 subjects aged 18 – 85 of whom 155 (48%) were men. The ethnic groups included in the database were "Caucasian" (63%), "Hispanic" (24%), "African American" (8%), "Asian" (3%), "Asian Indian" (1%) (285).

Details of normative data for the SD-OCT model are not currently available.

Figure 1.13 The manufacturers' summary report of ppRNFL thickness data

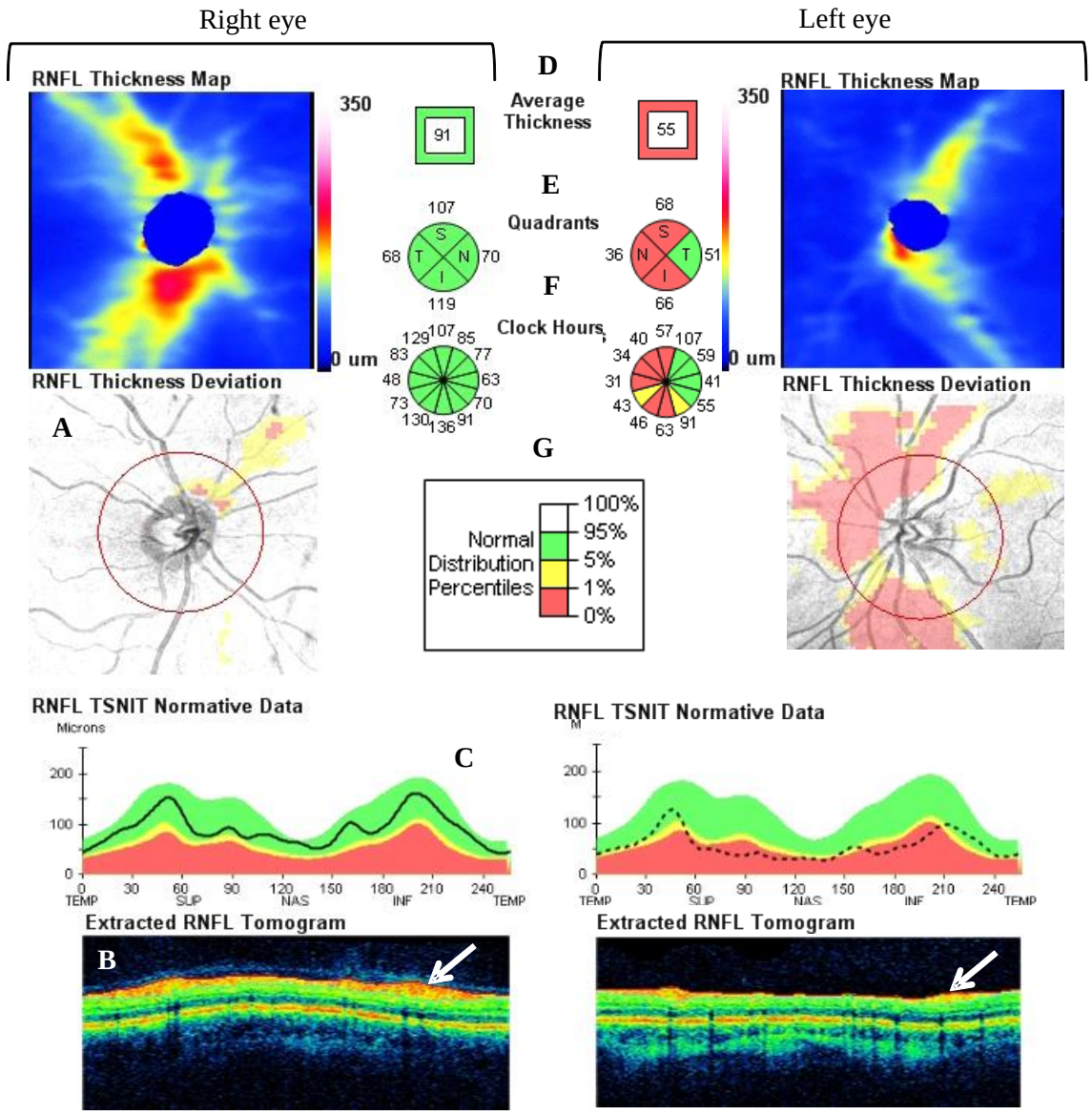

Figure 1.13 legends: Data provided in the manufacturers' summary report of ppRNFL thickness. Data illustrated on the left-hand side of the report is taken from the right eye. Data illustrated on the right-hand side of the report is taken from the left eye

(A) The 3.46mm diameter scan circle composed of 256 A-scans (red circle), centred on the ONH.

(B) The ppRNFL tomograph. The most superficial red/yellow layer (white arrow) is the ppRNFL from which the summary measures of ppRNFL thickness and the TSNIT profile are taken.

(C) The TSNIT profile is plotted from measures of ppRNFL thickness taken from the ppRNFL tomoraph (B). Both the TSNIT profies and the ppRNFL tomograph (B) show the "unfolded" 3.46mm circle of ppRNFL thickness data composed of 256 ppRNFL scans. The scan number is shown on the horizontal axis. The ppRNFL thickness is shown in the vertical axis. The black line represents the individual's ppRNFL thickness profile. The individuals ppRNFL thickness is compared to the manufacturers' normal distribution percentiles (G).

(D) The average ppRNFL thickness around the whole ONH. The colour represents which normal distribution percentile the individual's average ppRNFL thickness falls into (G). The average ppRNFL thickness in the right eye (left-hand side of the report) is 91µm and is classified as normal (green). The average ppRNFL thickness in the left eye (right-hand side of the report) is 55µm and is classified as abnormal (red).

(E) The average ppRNFL thickness in 90^{o} quadrants around the ONH. The colour of each quadrant represents which normal distribution percentile the individual's mean ppRNFL thickness by quadrant falls into (G).

(F) The average ppRNFL thickness in 30^{o} sectors around the ONH. The colour of each sector represents which normal distribution percentile the individual's mean sectorial ppRNFL thickness by sector falls into (G).

(G) The normal distribution percentiles for ppRNFL thickness. ppRNFL thickness is classed as normal (i.e. green area, $\leq 95^{th}$–>5^{th} percentile); showing borderline attenuation (i.e. yellow area, $\leq 5^{th}$–>1^{st} percentile); or showing abnormal thinning (i.e. red area, $\leq 1^{st}$ percentile).1.10

1.20 Current problems regarding the clinical management of VAVFL

Guidelines as to the management of VAVFL are available, recommending suitable assessment techniques based on developmental age. However, these may not account for individuals unable to perform perimetry (286), and often recommend investigative techniques which have not shown consistent sensitivity or specificity for detecting VAVFL (229;261;262;286).

1.20.1 The ophthalmological examination

The ophthalmological history and examination will largely be normal in the majority of individuals with VAVFL. Up to 90% of individuals with VAVFL are asymptomatic and symptoms of "bumping into things" or "tunnel vision" may only occur when VAVFL is severe. The asymptomatic nature of VAVFL adds difficulty to monitoring VGB-exposed individuals, as pathological changes to visual function may go unnoticed until follow-up appointments. In addition, individuals may be reluctant to attend for ophthalmological follow-up when they perceive that their vision is normal. Colour vision, visual acuity and contrast sensitivity are also typically normal, even in individuals with severe VAVFL. In most individuals with VAVFL examination of the fundus will reveal a normal retina (78;94;95;97;101;104;106;112;116;120;121;128;130;147;148;164;196). The presence of RNFL loss and optic atrophy detected using fundoscopy or photography probably indicates already advanced pathology (147).

1.20.2 Perimetry

The gold standard for assessing VAVFL is using perimetry. However, between 5 and 40% of adults with epilepsy are unable to perform perimetry (106), and in many others perimetric results may be unreliable and inconclusive (229). Repeated visual field testing is often needed, after which results can still prove difficult to interpret (182). These issues are further exaggerated in children where perimetry is often unachievable. It is estimated that up to 80% of VGB-exposed children are unable to perform formalized perimetric testing (122;131;287). In infants perimetry is not possible, creating a great source of contention when considering prescribing VGB for infantile spasms (263).

1.20.3 Electrodiagnostics

ERG abnormalities including increased latency and reduced amplitude of the photopic b-wave, reduced OP amplitudes and reduced 30Hz flicker response have been suggested as markers for VAVFL. However, non-exposed individuals with epilepsy and VGB-exposed individuals with normal visual fields may also show these abnormalities. In addition, some individuals with VAVFL have normal ERG. The VEP and PERG are normal in most individuals with VAVFL. In addition these techniques reflect central retinal function and therefore may be insensitive to peripheral retinal disease.

No electrodiagnostic measure has consistently shown sufficient sensitivity or specificity in identifying individuals with VAVFL (229).

1.20.4 ppRNFL imaging

Based on the OCT studies discussed previously (Table 1.7) ppRNFL imaging has been suggested as a useful tool in the assessment of VGB-exposed individuals, providing a sensitive and specific indicator of VAVFL (119;229;256). In particular Lawthom et al. suggested that ppRNFL attenuation in the nasal quadrant should be used as a biomarker for VGB toxicity (256).

At the present time however, the exact role of OCT in the management of VAVFL is uncertain (262). The available OCT studies have been on a small number of individuals, and the precise relationship between the degree of ppRNFL thinning and the severity of VAVFL is unknown. In an "expert panel's" report on the recommendations for visual testing in VGB-exposed individuals it was stressed that currently OCT should be considered as an "exploratory test" (262). Furthermore, although it has been suggested that ppRNFL imaging may provide an alternative tool to assess individuals who are unable to perform perimetry (229;256;262), this has not been

formally assessed, and the repeatability of measurements has not been validated in a population of individuals with epilepsy.

1.21 Summary of problems regarding the use of VGB

The use of VGB has been limited by the risk of irreversible VAVFL. However, trepidation regarding its use is augmented because of problems in the clinical management of VAVFL (as described above), particularly in those unable to perform perimetry, as well as several uncertainties regarding the natural history of VAVFL. Of note, many studies have reported conflicting findings regarding the prevalence, progression and risk of VAVFL. In addition, the pathological mechanisms of VAVFL are still unknown. From a detailed review of the literature, the main issues regarding the use of VGB and the management of VAVFL include:

- Problems in the clinical management of VAVFL, particularly in those unable to perform perimetry.
- Uncertain and conflicting evidence as to the risk factors for VAVFL, particularly with regard to cumulative VGB exposure and duration of VGB exposure.
- The pathological mechanisms of VAVFL are unknown.
- The natural evolution of VAVFL with continued VGB exposure is unclear, particularly over long exposure periods.

1.22 Hypotheses and aims of the study

The aims of this study were to address some of the current problems regarding the use of VGB and the management of VAVFL by exploring the potential of OCT ppRNFL imaging in a large population of VGB-exposed individuals.

Hypothesis:

Measurement of ppRNFL thickness using OCT is a suitable tool to use in VGB-exposed individuals, providing an indirect assessment of the presence of VAVFL, particularly in those unable to perform perimetry.

Aims to test this hypothesis:

- Establish whether more VGB-exposed individuals are able to complete OCT ppRNFL imaging compared to formal perimetric testing.
- Determine if ppRNFL thickness measurements show adequate repeatability in VGB-exposed individuals.
- Identify the relationship between ppRNFL thickness and visual field size in VGB-exposed individuals.

Hypothesis:

Particular clinical, demographic and therapeutic risk factors increase the risk of VAVFL and thus may also be associated with the risk of ppRNFL thinning in VGB-exposed individuals.

Aims to test this hypothesis:

- Explore the effect of clinical, demographic and therapeutic characteristic on ppRNFL thinning in VGB-exposed individuals.

- Identify whether ppRNFL thinning occurs in non-exposed individuals with epilepsy, and determine what factors may be associated with ppRNFL thinning in this population.

Hypothesis:

VAVFL progresses with continued VGB-exposure over long follow-up periods. Furthermore, the ppRNFL may also show a progressive pattern of thinning with increasing VGB-exposure.

Aims to test this hypothesis:

- Explore the evolution of visual field size over a substantial follow-up period in individuals continuing VGB therapy.
- Determine whether a pattern of ppRNFL thinning can be identified in VGB-exposed individuals, and to explore the relationship between the amount of VGB exposure and patterns of ppRNFL thinning.

Chapter 2 Methods

2.1 Subjects and recruitment

2.1.1 Ethics

This project was approved by the Joint Research Ethics Committee of the National Hospital for Neurology and Neurosurgery and UCL Institute of Neurology and by other relevant institutional ethics committees. All participants provided written, informed consent.

2.1.2 Subjects and recruitment

301 individuals with epilepsy and 90 healthy individuals participated in the study between September 2008 and June 2010. Individuals with epilepsy were recruited from two epilepsy centres: the National Hospital for Neurology and Neurosurgery, Queen Square, London, (which includes the National Society for Epilepsy at Chalfont), and Stichting Epilepsie Instellingen Nederland. All individuals, with a diagnosis of epilepsy, who were able to provide informed consent, were eligible for invitation to participate in the study. Healthy individuals were recruited from research groups and employees at the National Society for Epilepsy.

2.1.3 Exclusion criteria

Individuals were excluded if they had diabetes, glaucoma or other known ocular disease, a family history of glaucoma or past history of trauma or surgery to the eye or orbit. Individuals with a refractive error of more than 4.50 diopters mean sphere and more than 2.5 diopters cylinder were also excluded (288). Seven of the 391 participants were excluded from the study according to these criteria and did not undergo any further testing.

Healthy individuals were excluded if they had a history of epilepsy or current or previous exposure to an antiepileptic drug.

2.1.4 Subject Groups

After exclusion of seven individuals based on the exclusion criteria, 384 individuals remained in the study, including 294 individuals with epilepsy and 90 healthy controls. Individuals were grouped according to a diagnosis of epilepsy, exposure to VGB and the OCT model on which they were assessed[4] (Figure 2.1).

Figure 2.1: Organisation of participants into Groups

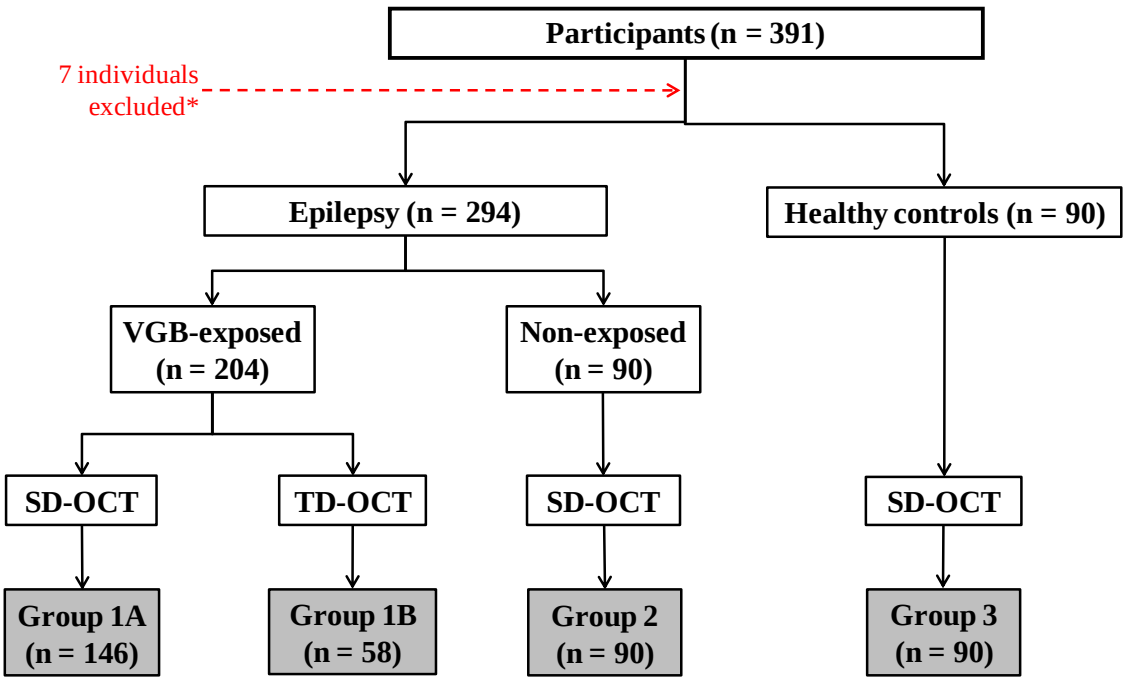

Figure 2.1 legend: Individuals were grouped according to a diagnosis of epilepsy, exposure to VGB and the OCT model on which they were assessed. VGB-exposed individuals were assessed using with SD-OCT or TD-OCT. All non-exposed individuals and healthy controls were assessed using SD-OCT.

[4] Details of the two OCT technologies are discussed in 1.18.3

VGB = vigabatrin; SD-OCT = spectral-domain optical coherence tomography; TD-OCT = time-domain optical coherence tomography.

2.1.4.1 Group 1A and Group 1B: VGB-exposed

VGB-exposed individuals included individuals currently being treated with VGB (on-VGB), and individuals previously exposed to VGB (off-VGB). VGB-exposed individuals were assessed using one of two OCT models; spectral-domain OCT (SD-OCT) or time-domain OCT (TD-OCT). Group 1A included 146 VGB-exposed individuals with epilepsy assessed using SD-OCT. Group 1B included 58 VGB-exposed individuals with epilepsy assessed using TD-OCT.

2.1.4.2 Group 2: Non-exposed

Group 2 included 90 individuals with epilepsy with no history of VGB exposure (non-exposed). All individuals in Group 2 were assessed using SD-OCT.

2.1.4.3 Group 3: Healthy controls

Group 3 included 90 healthy individuals with no history of epilepsy or antiepileptic drug exposure. All individuals in Group 3 were assessed using SD-OCT.

2.2 Demographic, clinical and therapeutic data

Demographic data for each Group are displayed in Table 2.1.

Table 2.1 Demographic and clinical data according to Group

	Group 1A	**Group 1B**	**Group 2**	**Group 3**
	VGB-exposed individuals with epilepsy	VGB-exposed individuals with epilepsy	Non-exposed* individuals with epilepsy	Healthy controls
Number of participants	146	58	90	90
Mean age (years) [SD]	45.9 [±11.4]	46.1± 10.6	39.5 ± 11.4	41.9 ± 13.1
Sex (% males)	51.4	59.3	40.0	40.0
Mean duration of epilepsy (years) [SD]	32.2 [±10.4]	35.3 ± 8.6	22.5 ± 12.8	NA
Mean age of onset (years) [SD]	8.9 [±7.1]	13.9 ± 8.7	14.0 ± 8.7	NA
Mean cumulative VGB exposure (grams) [SD]	2281.0 ± 3255.7	7041.4 ± 5921.9	0	NA
Median cumulative VGB exposure (grams) [range]	1061.0 [10-20085]	7581.0 [259-21105]	0	NA
Mean duration of VGB exposure (months) [SD]	41.3 ± 46.6	104.8 ± 82.3	0	NA
Median duration of VGB exposure (months) [range]	21.0 [1-230]	126.0 [3-231]	0	NA
Mean maximum daily VGB dose	2798.6 [1070.4]	2746.6 [965.6]	0	NA

(milligrams) [SD]				
Median maximum daily VGB dose (milligrams) [range]	2000 [500-5000]	3000 [500-5000]	0	NA

VGB = vigabatrin; *non-exposed = not exposed to VGB

For individuals with epilepsy, all clinical and demographic data were obtained from the medical records. Sources of information included out-patient clinic letters and in-patient admission and discharge summaries and drug charts. For the healthy controls, demographic data were obtained from direct questioning. The relevant clinical variables and the criteria used to classify them are shown in Table 2.2. Clinical, demographic and therapeutic data for each individual were only included in any analyses if evidence of that variable could be obtained from the medical records. For example, the presence or absence of a history of febrile seizures was only recorded for an individual if it was explicitly discussed in the clinical records. If an explicit record of any clinical variable was not found these data were regarded as missing.

Table 2.2 Criteria used to define clinical features

Clinical feature	Definition/method of determination
VGB-exposed	Individuals with any current or previous exposure to VGB, as determined from the information available in the medical notes. There were no minimum criteria in terms of the duration of exposure or dose received.
Duration of VGB exposure	The time in months that the individual was exposed to VGB, as determined from the information available in the medical notes. (See 2.1.x for further details of determination).
Cumulative VGB exposure	The total amount of VGB in grams that an individual was exposed to, as determined from the information available in the medical notes. (See 2.1.x for further details of determination).
Maximum daily VGB dose	The maximum daily dose of VGB, in milligrams, that an individual received, as determined from the information available in the medical notes.
Non-exposed	Individuals with no history of VGB exposure, as determined from the information available in the medical notes.
Epilepsy phenotype	Phenotypes were classified according to the criteria described by Kasperaviciute et al. (289) adapted from the International League Against Epilepsy revised organisation of phenotypes in epilepsies (290).
Duration of epilepsy	The length of time in years between the year of diagnosis* of epilepsy as recorded in the medical notes, and the year of inclusion in the study. (e.g. epilepsy diagnosed in 1973, inclusion in the study in 2009, duration of epilepsy = 36 years).
Drug-resistant epilepsy	Adapted from the International League Against Epilepsy Commission on Therapeutic Strategies (291). Individuals who: a) have had one or more seizures (of any type) in the year preceding the most recent follow-up b) have had three drug trials which are adequate and

	appropriate. i) Appropriate means the drug is recommended by NICE or licensed for the type of seizures in question ii) The drug was tried for a sufficient length of time at an adequate dosage - maximum tolerated daily dose usually, or if clinician has documented that the drug has shown lack of efficacy. Length of time should be for at least the maximum duration between seizures. Seizures should have occurred during treatment with each drug. c) No documented non-epileptic attacks during any of the drug trials above d) No documented regular (>2 times) non-compliance causing seizures
Learning disability	Individuals described by their epilepsy consultant, in the medical notes, as having learning disability or cognitive impairment.
History of febrile seizures	Individuals who have a record of febrile seizures in their medical notes.
History of status	Individuals who have a record of status in their medical notes
History of head injury	Individuals who have a record of a head injury in their medical notes.
History of neurosurgery	Individuals who have a history of neurosurgery involving the brain parenchyma.
History of smoking	Individuals who were current, or ex-smokers.
Exposure to other AEDs (e.g. carbamazepine)	Any current or previous exposure to any AED, as determined from the information available in the medical notes, was documented. There were no minimum criteria in terms of the duration of exposure or dose received. For each AED individuals were classed as "exposed" or "non-exposed".

VGB = vigabatrin; NICE = National Institute for Health and Clinical Excellence; AED = antiepileptic drug

*Often the age of the individual at the time of the diagnosis was given instead of the year of diagnosis.

2.2.1 Choosing relevant clinical and demographic variables

The demographic and clinical data to be obtained from the medical records were chosen based on previous studies of risk factors for VAVFL, and on studies of ppRNFL thickness in other neurological disease. Other clinical variables that are thought to be associated with neuronal injury in epilepsy were also chosen.

2.2.1.1 VAVFL risk factors

Male gender (92;94;95;97;98;103;137;167) and co-medication with other AEDs (particularly valproate) (108;114;164), have been shown to be associated with risk of VAVFL and were chosen as variables. Smoking was also suggested as a possible risk factor for VAVFL in a preliminary analysis in one study (92) and was also included. In addition, excessive tobacco and alcohol use is associated with the development of a toxic-nutritional optic neuropathy (tobacco-alcohol amblyopia) which can manifest with changes in ppRNFL thickness (292).

2.2.1.2 ppRNFL in neurological disease

The presence of learning disability was chosen as a clinical variable as an association between cognitive function and ppRNFL thickness has been found in studies of individuals with multiple sclerosis where ppRNFL thinning is associated with cognitive disability (293). In healthy, young individuals ppRNFL thickness was found to be associated with level of cognitive functioning (294).

A history of neurosurgery involving the brain parenchyma was also chosen. Individuals who have had surgical resections involving the visual pathways (e.g. anterior temporal lobe resections for hippocampal sclerosis) may show ppRNFL thinning as a result of

retrograde trans-synaptic degeneration. In a recent study, ppRNFL thinning was detected in individuals with acquired occipital lobe lesions, providing evidence for trans-synaptic degeneration of the visual pathway that is detectable using OCT (295).

2.2.1.3 Neuronal injury

Clinical factors that have been associated with neuronal injury and cell death were also chosen. Local and global neuronal losses related to certain clinical factors may involve the visual pathways, leading to ppRNFL thinning through trans-synaptic degeneration. Duration of epilepsy was selected as widespread neuronal abnormalities and atrophy have been associated with longer duration of epilepsy (296-300), indicating that in some individuals progressive brain atrophy can occur with continuing seizure activity (299). Status epilepticus (301), febrile seizures (302) and head injury (303) are also associated with neuronal injury and cell death, and thus were included as clinical variables.

2.2.2 Calculating cumulative VGB exposure and duration of VGB exposure

The duration of VGB exposure and the cumulative VGB exposure were calculated from information available in the medical notes.

The duration of VGB exposure was calculated using Excel by inputting the first date of VGB exposure; the "start date" and the last date of VGB exposure; the "end date", and determining the time in months between these two dates.

For individuals who were prescribed VGB on an out-patient basis, the exact "start date" was not known. In these cases the date of the out-patient clinic (as determined from the clinic letter) where VGB was first prescribed, was used as the "start date". Where the date of the out-patient clinic was not know (i.e. it was not included in the clinic letter and could not be found elsewhere in the out-patient notes) the date of the clinic letter

was used. For individuals prescribed VGB on an in-patient basis the date of the first VGB dose, as given in the drug chart, was used as the "start date".

For individuals prescribed VGB on an out-patient basis the "end date" was determined from information provided in the last available clinic letter in which the individual was still receiving VGB. The "end date" was calculated using available withdrawal schedules or advice regarding withdrawal provided in the clinic letter. Withdrawal information was calculated from the date of the out-patient clinic, or clinic letter (as described above). Clinic letters succeeding the letter which outlined withdrawal information were carefully checked to ensure that VGB therapy had been discontinued. For individuals withdrawn from VGB on an in-patient basis the date of the last VGB dose, as outlined in the drug chart, was used as the "end date". For individuals who were still receiving VGB at the time of the study, the date of participation in the study was used as the "end date".

The cumulative VGB exposure was calculated using Excel, and was determined by multiplying the total daily dose of VGB (in grams) by the duration of therapy (in days). For example, a total daily dose of 2.5 grams for 1095 days would equate to a cumulative VGB exposure of 2.5 x 1095 = 2,737.5 grams. The "start date" and "end date" of a specified daily dose were determined from information available in the medical notes as described above for the calculation of duration of VGB exposure.

Most individuals included in the study underwent several changes in VGB daily dose over the duration of VGB exposure. For these individuals a "start date" and an "end date" were determined for each daily dose, as described above for the calculation of duration of VGB exposure and the cumulative VGB exposure was determined for each of these periods. See Table 2.3 for an example.

Table 2.3 Example of how cumulative VGB exposure was calculated

Daily dose (KG)	Start date	End date	Days	Cumulative dose (KG)
0.5	8.8.1995	21.8.1995	14	7
1.0	22.8.1995	18.9.1995	28	28
2.0	19.9.1995	12.2.1996	147	294
1.5	13.2.1996	26.2.1996	14	21
1.0	27.2.1996	12.3.1996	14	14
0.5	13.3.1996	26.3.1996	14	7
		Cumulative VGB exposure (KG)		**371**

VGB exposure data were only included for individuals who had a complete historical reference of VGB exposure. This included reference to starting VGB, reference to any dose changes and reference to VGB withdrawal. If cumulative VGB exposure, duration of VGB exposure, or maximum daily VGB dose could not reliably be deduced from the available clinical records, VGB dose data were regarded as missing. The most common reasons for missing VGB exposure data included exposure to VGB before referral to the National Hospital for Neurology and Neurosurgery (in these cases it was known that the individual had been exposed to VGB but the details of exposure were often not available or were incomplete); and missing clinic letters or outpatient notes which provided data on VGB start dates, VGB dose changes and VGB withdrawal schedules.

2.3 Examination and test procedures

All examinations and test procedures were undertaken at the same visit and by the same operator (LMC)[5].

2.3.1 Examinations undertake

Information sheets were provided to all individuals participating in the study and informed consent was obtained[6]. All individuals underwent a screening questionnaire and visual assessment to determine suitability for the study (see exclusion criteria). Subsequently, depending on the group that the individual belonged to, individuals were assessed using GKP and OCT (Table 2.4). For individuals recruited from Stichting Epilepsie Instellingen Nederland, instructions for GKP and OCT were provided in Dutch[7].

[5] For fourteen individuals a retrospective analysis of the evolution of VAVFL was carried out (see Chapter 3). Some of the visual field examinations included in this analysis were not performed by LMC, and were taken at multiple test sessions over a ten-year period by several experienced operators.

[6] Information sheets and consent forms are provided in the Appendix 1

[7] For the Dutch translation of OCT and GKP instruction, please see Appendix 3

Table 2.4 The order of examination and assessment for all individuals included in the study

Order of assessment	Examination/assessment	Participants included
1st	Information sheets are provided, the study is explained to the participant and informed consent is obtained	All participants
2nd	A screening questionnaire[8] is used to exclude subjects according to the criteria. Visual acuity, colour vision and refractive status are assessed.	All participants
3rd	The visual field is assessed using GKP	Individuals in Group 1A and Group 1B*
4th	ppRNFL imaging is undertaken using OCT	All participants*

GKP = Goldmann kinetic perimetry; OCT = optical coherence tomography

*not including those participants who were excluded after the initial screening questionnaire and assessment

2.3.2 Screening

All individuals underwent a screening questionnaire[10] and examination based upon the exclusion criteria. Refractive status was determined using a focimeter. Best corrected visual acuity was assessed using a six-meter Snellen chart and a near chart. Colour vision was examined using the Ishihara pseudoisochromatic test. Individuals who met the exclusion criteria did not undergo any further examination or test procedures. Individuals who were found to have an unexplained impairment of colour vision or visual acuity, that could not be corrected with a pinhole or appropriate lens were also excluded at this stage and were referred for further ophthalmological examination.

[8] See Appendix 2 for the exclusion criteria questionnaire.

2.4 Perimetry

The visual field was examined using GKP for all VGB-exposed individuals (Group 1A and Group 1B). Individuals in Group 2 and Group 3 did not undergo perimetric testing.

2.4.1 Choosing a perimetric technique

There is controversy over whether VAVFL should be assessed using automated static or manual kinetic perimetry (122). Screening strategies recommended by the Royal College of Ophthalmologists include using either an automated static suprathreshold two- or three-zone age-corrected strategy, to at least 45^{o} eccentricity (e.g. HVFA 120-point or Octopus 07), or kinetic perimetry using GKP (III4e and I4e or I2e stimuli) (286).

Automated perimetry has been recommended by some groups who have suggested that VAVFL is more frequently detected using automated perimetry (92;140). However, these studies have not compared the use of each technique in the same group of individuals to determine if either method is superior. The range of prevalence of VAVFL reported in the literature using each method is similarly wide, (19 – 92% for manual kinetic perimetry (96;110); 17 – 89% for automated static perimetry (94;116)).

An advantage of using automated perimetry is that it is largely operator-independent (108), allowing standardisation of the assessment technique and avoiding the variability introduced by an examiner (304). Manual kinetic perimeters are not always accessible (108), and depend on a skilled, trained operator (122;304-307), who may not be available (108).

The use of some of the standard automated visual field assessment programmes (e.g. HVFA 30-2 and 24-2 programmes) may miss mild to moderate peripheral visual field

defects that do not extend into the central visual field (97;101;108;116;122). Even those recommended automated programmes may not survey the far periphery of the visual field. For example the Humphrey 120-point programme surveys within an eccentricity of 50^{o} nasally, 60^{o} temporally, 40^{o} superiorly, and 55^{o} inferiorly. The normal extent of the visual field is 60^{o} nasally, 100^{o} temporally, 60^{o} superiorly, and 75^{o} inferiorly. Therefore mild peripheral visual field defects may be missed. GKP allows the visual field to be assessed out to 90^{o} in all planes, thus most of the peripheral visual field can be assessed using this technique.

Many individuals with epilepsy are unable to meet the demanding requirements of automated perimetry (81;93;95;110). Manual kinetic perimetric techniques, including GKP, allow a constant interaction between the operator and patient, enabling the testing to be guided by the individual being examined (304;305). In individuals with poor fixation, poor attention or cognitive impairment a more reliable visual field can often be obtained by a skilled operator using GKP (308). The operator dependence of GKP also introduces disadvantages, in particular, operator bias my influence the recorded visual field (309) (see 8.1.1 for further discussion of this).

GKP has been suggested as a preferential technique for detecting VAVFL because of the ability to survey the majority of peripheral visual field in a short period of time, and its possible superior sensitivity for detecting peripheral visual field defects (310). Importantly, more individuals are able meet the requirements of this technique (94;96;97;104;110;122;137). For these reasons GKP was chosen to examine the visual field of VGB-exposed individuals in the present study.

2.4.2 Perimetric method

Visual fields were assessed using a Goldmann kinetic perimeter (Haag Streit, UK). Where perimetry was performed it was always carried out first to ensure that the results of the OCT scan could not produce any operator bias in the visual field acquisition.

Both eyes were examined, where possible, using V4e, I4e and I2e stimuli. Appropriate full-aperture spectacle correction was used for examination of the central 30^o of the visual field. Monocular vision was examined, with the non-tested eye fully occluded using an eye patch. The right eye was always examined first. Individuals were positioned in the headrest and allowed to adapt to the luminance of the background sphere for 1-2 minutes. During this time the procedure was explained to the subject and the subject's eye was moved into the correct position by adjustment of the headrest. Fixation was carefully monitored by direct visualisation of the fixating eye. The V4e target was presented first and the full isopter plotted, followed by the I4e and I2e targets. Before examination of the peripheral visual field, the target was always presented into a central area of the visual field to ensure that the individual understood the instructions and was responding appropriately to the stimulus (i.e. by pressing the response buzzer). By doing this the reaction time of the subject could also be assessed, helping to guide the examination.

The target was presented in the far peripheral visual field and moved along each of twelve meridians, spaced 30^o apart, toward the point of fixation. The target was moved at a velocity of approximately 4^o per second (311), which was adjusted according to the needs of the subject being examined. A velocity of 4^o per second was chosen as it has been shown to be the optimal rate of movement to improve the time efficiency of the procedure without significantly influencing the effect of reaction time on the response

(311). Other stimulus velocities have also been suggested, including 2^o (312) and 5^o (313) per second. The blind spot was assessed using the I4e isopter.

2.4.3 Calibration of perimeter

The Goldmann kinetic perimeter was regularly calibrated according to the manufacturers' instructions (312) to ensure that the target luminance and background sphere luminance were correct and did not change between examination periods. The target luminance was maintained at 1000 apostilbs. The background sphere luminance was maintained at 31.5 apostilbs.

2.4.4 Exclusion of visual field data

Visual fields were excluded if they were determined to be unreliable by the operator. A disadvantage of using GKP is that there are no objective methods to determine visual field reliability, and thus unreliable visual fields must be determined subjectively by the examiner. Factors known to contribute to the reliability of a recorded visual field were considered, including fixation accuracy, false positive and false negative responses (199). Fixation was carefully monitored by the operator, and assessments in which repeated loss of fixation occurred were deemed unreliable. Assessments from individuals showing a high number of false positive responses (i.e. frequently pressing the buzzer when no light stimulus was presented to them) were also determined as unreliable. Where individuals showed highly variable responses to the same stimulus examinations were also recorded as unreliable. In addition the shape of the recorded visual field was assessed, particularly in individuals in whom visual field tests were subjectively determined to be unreliable. Visual fields showing a spiral or star-shaped pattern are typically associated with functional visual field loss rather than true visual pathway pathology (314;315) and are regarded as indications of poor reliability of a

visual field result (315). All of these factors were taken into account when excluding visual field test results from the analysis.

Visual fields with homonymous defects were excluded from the visual field analysis. Previous studies have included these visual field data, excluding the quadrant or hemifield displaying the defect (99;106;113). In this study, these visual fields were excluded as the radial extent of the visual field is not uniform throughout, (i.e. the normal monocular visual field extends to around 100^{o} temporally, 60^{o} nasally, 60^{o} superiorly and 75^{o} inferiorly). Exclusion of a hemifield or quadrant from the analysis may result in an over- or under-estimation of the visual field size (Figure 2.2).

Figure 2.2: Quantifying the visual field using MRD

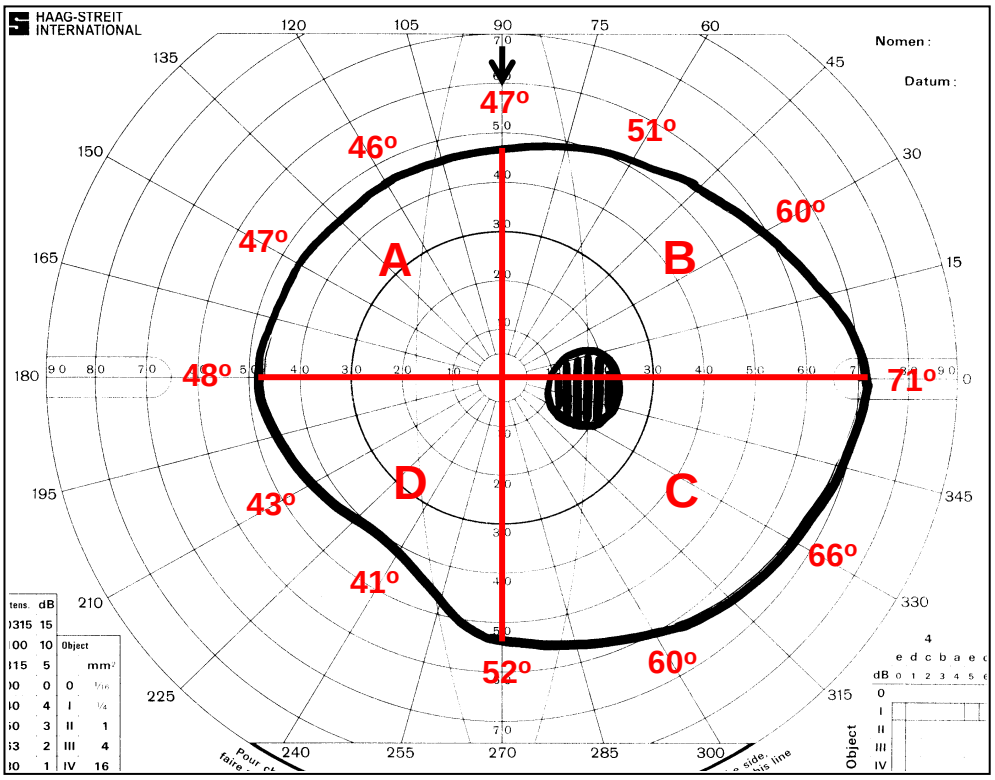

Figure 2.2 legend: An example of a normal visual field assessed using the I4e isopter. The visual field is quantified using MRD, by measuring the radial distance in degrees, from fixation, at 12 points, 30^{o} apart (starting at 90^{o}) (black arrow), and calculating the average radial distance.

The size of the visual field (using mean radial degrees (MRD)) was calculated using the whole visual field, and then after excluding quadrants or hemifields. Whole visual field= 53 MRD; exclude A = 54 MRD; exclude B = 52 MRD; exclude C = 51 MRD; exclude D = 55 MRD; exclude A+D = 58 MRD; exclude B+C = 46 MRD.

2.5 Quantifying and classifying visual field data

Studies of VAVFL have used various methods and criteria to quantify and classify visual field results from GKP. These methods are outlined in Table 2.5. Those criteria that have been utilised to classify the presence and severity of VAVFL are shown in Table 2.6.

Table 2.5 Methods and criteria used to quantify VAVFL as assessed by manual kinetic perimetry in different studies

Reference	**Method used to quantify visual field loss**
Newman 2002 (95) Best 2005 (148) Kinirons 2006 (99) Kinirons 2006 (168) **This study**	The MRD was determined from the I4e isopter by measuring the radial distance in degrees, from fixation, at 12 points, 30^{o} apart, and calculate the average radial distance.
Miller 1999 (106) Paul 2001 (111) Krauss 2003 (105) Toggweiler 2001 (118)	The MRD was determined from the V4e isopter by measuring the radial distance in degrees, from fixation, at 12 points, 30^{o} apart, and calculate the average radial distance.
Toggweiler 2001	The radius of the V4e isopter is measured in degrees in the temporal, superior, nasal and inferior meridians
Wild 1999 (97) Wild 2009 (92)	The radius of the I4e isopter is measured in degrees in the temporal, superior, nasal and inferior meridians
Kalviainen 1999 (104)	The radius of the IV4e isopter was measured in degrees in the

Nousiainen 2001 (100)	temporal, superior, nasal and inferior meridians
Hardus 2000 (94) Hardus 2000 (152) Hardus 2001 (137)	The Esterman Grid – The Esterman grid comprises 100 dots, each dot represents1% of an intact visual field. The Grid was placed over the recorded visual field. The percentage visual field loss was calculated from the number of dots that fall outside the area of the V4e isopter (i.e. within the area of the visual field defect).
Hardus 2001 (137) Hardus 2001 (136) Hardus 2003 (151)	The surface method – A line was drawn through 24 bisection points of the 15-degree spaced meridians for the V4e isopter. The surface inside this line was calculated using Excel (Microsoft, Redmond, WA, USA).
van der Torren 2002 (109)	The extent in degrees of the nasal visual field (to the nearest 5 degrees)
Schmitz 2002 (108)	The radius of the III4e isopter was measured in the temporal and nasal meridian. The findings of both eyes were summed and divided by two.
Comaish 2002 (135)	Visual field plots were scanned into a computer and the areas contained within the I4e isopter were measured using ImageJ software. The results were summed for the two eyes
Vanhatalo 2002 (122)	Temporal visual field in degrees using the largest isopter tested
Arndt 2002 (164)	The area of perception (in square degrees) was determined for each test without blind-spot subtraction.
Schmidt 2002 (149) Schmidt 2004 (174)	The radius of the III4e isopter was measured in the nasal, the nasal inferior (225° or 315°) and the temporal axis. The findings of both eyes were summed and divided by two.
Sergott 2010 (93)	The radius of the V4e and IV4e isopter measured in degrees in the temporal and nasal meridians

MRD = mean radial degrees

Table 2.6 Methods and criteria used to classify VAVFL as assessed by manual kinetic perimetry in different studies

Reference	Criteria used to classify visual fields
Wild 1999 (97) Wild 2009 (92) **This study**	See Table 2.7 for details
Kalviainen 1999 (104) Nousiainen 2001 (100) Sorri 2000 (316) Vanhatalo 2002 (122)	Normal = >70^{o} in the temporal meridian Mildly abnormal = 50–70^{o} in the temporal meridian Severely abnormal = <50^{o} in the temporal meridian (with the largest isopter tested)
Miller 1999 (106)	Minor constriction = 10-15 degrees less than the MRD in non-exposed individuals Significant constriction = 20-25 degrees less than the MRD in non-exposed individuals
Hardus 2001 (137) Hardus 2001 (136) Hardus 2003 (151)	Loss of more than 14% (equivalent to two standard deviations) of the visual field surface area in one eye compared to the visual field surface area of 24 healthy controls. Using the V4e isopter. The surface area of a visual field was determined using Excel.
van der Toren 2002 (109)	VAVFL = <50^{o} in the nasal meridian (stimulus size unknown)
Malmgren 2001 (96)	Visual field "contraction" = <80^{o} in the temporal meridian or <40^{o} in the nasal meridian. Using the V4e isopter
Schmitz 2002 (108) Schmidt 2002 (149)	(compared to baseline visual field size) Normal – constriction of <10° (III/4e) and <5° (I/2e) – any change, if the amount of fluctuation was similar Mild changes – constriction of between 10° - 25° (III/4e) and/or 5–10° (I/2e) Severe changes

	– constriction of >25° (III/4e) and/or >10° (I/2e)
Jensen 2002 (121)	Normal = >40◦ in the nasal meridian and > 60◦ in the temporal meridian Mildly abnormal = 40-20◦ in the nasal meridian and 60-30◦ in the temporal meridian Severely abnormal = <20^{o} in the nasal meridian and <30^{o} in the temporal meridian (Using the IV4e isopter)
Arndt 2002 (164)	moderate VAVFL = visual field area of <2SD of the mean value obtained in healthy controls severe defect = visual field area of <3SD of the mean value obtained in healthy controls
Sergott 2010 (93)	Normal = >80◦ in the temporal meridian Mildly impaired = 60—80◦ in the temporal meridian Moderately impaired = 30—<60◦ in the temporal meridian Severely impaired = <30◦ in the temporal meridian Using the V4e or IV4e isopter (averaged for the 2 eyes)
Newman 2002 (95)	Severe VAVFL = ≤30 MRD
Kinirons 2006 (99)	Constricted visual field = MRD more than two standard deviations below the average MRD from non-exposed individuals Severely constricted visual field = MRD <30 degrees
Toggweiler 2001 (118)	VAVFL = <60 MRD. Using the V4e isopter

2.5.1 Quantifying visual field size

In this study the mean radial degrees (MRD) method was used to quantify the size of the visual field. The MRD was determined using the I4e isopter, and was calculated by measuring the radial distance in degrees, from fixation, at 12 points, 30^{o} apart (from 0^{o} – 120^{o}), and calculating the average radial distance (Figure 2.2).

This method has been used previously in several studies of VAVFL (95;99;105;106;111;118;153;168), including four studies which have been carried out fully, or in part, in the department that this study was conducted (National Hospital for Neurology and Neurosurgery) (95;99;148;168).

This method of quantification of visual field size was chosen because the quantitative value obtained reflected the visual field size in all meridians, i.e. the size of the whole visual field contributed to the obtained MRD value for the visual field. Other classification methods have assessed the extent of only part of the visual field (e.g. the temporal meridian) (108;108;109;122). Assessment of the whole visual field was felt to be important as VAVFL is known to affect the entire periphery of the visual field, and is not confined to particular hemifields, quadrants or regions (e.g. the arcuate regions).

Other methods used to quantify the size of the visual field that have utilised the whole visual field include the Esterman grid (94;137;152) and the surface method (136;137;151). The Esterman method comprises a grid of 100 points, each one representing 1% of the visual field. Any points that lie outside of the outer boundaries of the visual field are counted to determine the percentage visual field loss. The disadvantage of this method is that there is an unequal distribution of points over the visual field (e.g. the inferior-temporal quadrant contains 40 points, whilst the superior-nasal contains only 19) (137), with few points in the far periphery, meaning that small changes in the peripheral visual field may be missed.

2.5.2 Classifying visual field size

Several criteria have been used classify the visual field (Table 2.6). This allows the visual field to be classified as normal or abnormal, as well as describing the severity of the abnormality (e.g. mild VAVFL or severe VAVFL).

Some studies have used visual field results from control populations (either non-exposed individuals with epilepsy or healthy controls) to define the criteria used to classify VAVFL. Typically, an abnormal visual field is one where the quantitative measure of visual field size (e.g. radial degrees in the temporal meridian) is more than two standard deviations below the control group mean for that measure (99;136;137;151;164).

There are several issues with using a control group to classify the presence and severity of VAVFL. Firstly, whilst it may be easy to classify an "abnormal" visual field (e.g. by using a cut off of more than two standard deviations below the control group mean visual field size), it becomes more difficult in using criteria to describe the severity of VAVFL (e.g. mild, moderate and severe VAVFL). Most studies that have used a control group to define VAVFL have only defined visual fields as "normal" or "abnormal" (99;136;137;151). The severity of VAVFL varies widely (12;96;97;106) (Figure 1.3), and this classification method may not be sufficient to describe and classify VAVFL. Secondly, the recorded visual field size may be influenced by factors not related to visual impairment (for further discussion see Chapter 3), including psychomotor slowing, cognitive impairment, delayed reaction time, poor attention and concentration. In individuals with epilepsy this may lead to an underestimation of the visual field size. Using a healthy control group to set the criteria for normality may lead to an overestimation of the prevalence of VAVFL in VGB-exposed individuals because of differences in the ability to perform the test, rather than because of true visual

pathology. Lastly, differences in the control populations used between studies might influence the reported prevalence of VAVFL making results difficult to compare between studies.

For these reasons, a control group was not used to define the presence or severity of VAVFL, and an absolute classification criterion was selected for use in this study. The visual field was classified as being normal or showing either mild, moderate or severe VAVFL, using the criteria described by Wild et al. (97) (Table 2.7).

Table 2.7 Guidelines for the classification of severity of visual field loss for kinetic perimetry according to the I4e isopter (97)

	Meridian			
VAVFL classification	**Temporal** (extent in degrees)	**Superior** (extent in degrees)	**Nasal** (extent in degrees)	**Inferior** (extent in degrees)
Normal	>70^{o}	>40^{o}	>45^{o}	>50°
Mild	50-70^{o}	35-40^{o}	35-45^{o}	45-50^{o}
Moderate	30-50^{o}	20-35^{o}	20-35^{o}	25-45^{o}
Severe	<30^{o}	<20^{o}	<20^{o}	<25^{o}

These criteria were used as they were the only criteria to take into account all four of the major meridians (temporal, superior, nasal, inferior), whereas most other classification systems used only took into account the extent of the nasal and/or temporal meridian (Table 2.6).

2.5.3 Reliability of visual field quantification and classification method

The methods chosen to quantify and classify the visual field require the examiner to make a subjective assessment of the extent of the visual field in each meridian. To

determine whether the chosen methods had adequate intra- and inter-rater reliability, a subset of 25 visual fields were analysed.

To determine intra-rater reliability, visual fields were quantified and classified immediately after acquisition by L.M.C. Several months later the visual fields were re-examined, quantified and classified by the same examiner who was blinded to the initial classification. To determine the inter-rater reliability, visual fields were quantified and classified immediately after acquisition by L.M.C. At a later date they were assessed by a second examiner, who was blinded to the initial quantification and classification, and to the individuals medical and drug history. MRD data were analysed using intraclass correlation coefficient (ICC) (317). Visual field classification data were analysed by determining Cohen's kappa (κ) (318).

Visual field quantification using MRD showed high intra- and inter-rater agreement (Table 2.8). Visual field classification showed "substantial" intra-rater agreement, and "moderate" inter-rater agreement (Table 2.8). The good reliability of the visual field quantification and classification methods confirmed that these methods were suitable for use in the present study.

Table 2.8 Intra- and inter-rater reliability of visual field quantification and classification method

	MRD ICC (95% CI)	Classification κ (p value)
Intra-rater	0.995 (0.989 – 0.998)	0.709 (p<0.001)
Inter-rater	0.995 (0.990 – 0.998)	0.523 (p<0.001)

ICC = intraclass correlation coefficient; CI = confidence interval; κ = Cohen's kappa.

Interpreting ICC: an ICC of zero indicates no agreement between the measures, an ICC of one indicates perfect agreement between measures (319).

Interpreting Cohen's kappa: a κ of zero indicates that the agreement between the measures is no better than that which would be obtained by chance. A κ of one indicates perfect agreement between measures. The value of κ can be judged as providing agreement that is poor ($\kappa \leq 0.20$); fair ($0.21 \leq \kappa \leq 0.40$); Moderate ($0.41 \leq \kappa \leq 0.60$); substantial ($0.61 \leq \kappa \leq 0.80$) or good ($\kappa \geq 0.81$) (318;319).

2.6 Optical Coherence Tomography

All individuals participating in the study underwent ppRNFL imaging using OCT. In individuals undergoing perimetry (Group 1A and Group 1B), OCT was performed after perimetric testing was completed.

2.6.1 OCT scan method

For all ppRNFL scans, the contralateral eye was occluded and individuals were positioned in the head rest and asked to look into the OCT lenses and fixate on an internal target. The optic disc was clearly visualised, and the scan-circle was centred on the optic disc. Polarisation was machine-optimised, either with the automatic tool or

manually. Individuals were asked to maintain fixation and to avoid blinking whilst the scan was taken. Where possible each participant underwent two ppRNFL thickness scans on each eye. ppRNFL imaging was carried out using two commercially available OCT models. One instrument utilised time-domain technology; the Stratus OCT (Carl Zeiss Meditec) and one utilised spectral-domain technology; the Cirrus OCT (Carl Zeiss Meditec, Dublin, CA)[9].

2.6.2 Pupil dilation

In individuals in whom clear visualisation of the optic disc was not possible, and in whom adequate OCT signal strength (see 2.6.5) was not achieved, pupils were dilated using 1% tropicamide drops. OCT scans were performed 15-20 minutes after application of drops. Pupil dilation was avoided where possible because of the increased assessment time, risk of angle closure in predisposed individuals (320) and side effects of pain and blurred vision after application of the drops (321). Recent studies have shown that providing that a clear image of the fundus can be visualised, and an adequate signal strength obtained (see 2.6.5), pupil dilation does not have a significant effect on measurements of ppRNFL thickness (321-323).

2.6.3 Time-domain OCT

A commercially available TD-OCT (Stratus OCT, software version 4.0, Carl Zeiss Meditec, Dublin, CA) was used to assess VGB-exposed individuals recruited from specialist epilepsy clinics at the Queen Square Site of the National Hospital for Neurology and Neurosurgery. These individuals comprised Group 1A.

2.6.3.1 Why TD-OCT was chosen

The use of a TD-OCT instrument for the assessment of a subset of VGB-exposed individuals was chosen to enable comparison of results with those currently presented in

[9] See 1.18.3 for a description of difference between two OCT technologies

the literature. Four studies (119;229;256;258) and one case report (198) have described the use of ppRNFL imaging using OCT in VGB-exposed individuals, all of which have used TD-OCT.

2.6.3.2 The TD-OCT ppRNFL scanning protocol

For the TD-OCT instrument, two ppRNFL scanning protocols are available; the "Proportional Circle Scan" and the "Fast Retinal Nerve Fibre Layer Thickness Scan". The "Proportional Circle Scan" was used by Wild et al. in the first study to describe ppRNFL thinning in individuals with VAVFL (229). In this scan protocol the radius of the scan circle is based on an increment of the vertical diameter of the ONH (229). This technique can be used to allow for differences in ONH size between individuals, as ppRNFL thickness decreases with increasing distance from the ONH (324-326). The disadvantage of this technique is that the choice of the increment is arbitrary, and may be difficult to standardise between studies (229). In addition, the reproducibility of ppRNFL thickness measures was found to differ with various scan circle diameters (283;325). The current clinical standard for obtaining ppRNFL thickness measures using OCT is by using a fixed diameter scan circle of 3.46mm (327). Using this scan diameter was found to provide the most reproducible ppRNFL thickness measures compared to other scan circle diameters (283;325).

The "Fast Retinal Nerve Fibre Layer Thickness Scan" protocol, which has been used in the most recent studies of OCT ppRNFL imaging in VGB-exposed individuals (119;256;258), adheres to this clinical standard by utilising a fixed-diameter circular scan of 3.46mm. The normative database within the Stratus OCT was created using this scan protocol, and comparison of ppRNFL thickness measures with the normative data can only be made with scans acquired using this scan method. Although this scan

protocol uses a fixed diameter scan circle, the 3.46mm diameter is considered large enough to encompass the whole ONH, without any overlap, in most eyes (229).

In this study individuals were scanned using the "Fast Retinal Nerve Fibre Layer Thickness" protocol. This protocol was selected to allow for comparison of data with the manufacturers' normative database. In addition, the ppRNFL thickness measure available from the SD-OCT instrument, which was used for imaging Group 1A, Group 2 and Group 3 in this study, utilises a 3.46mm fixed-diameter circle of data.

The "Fast Retinal Nerve Fibre Layer Thickness Scan" utilises a circular scan comprised of 256 A-scans, centred on the optic nerve head. Three circular-scans are acquired in succession, over 1.3 seconds. The ppRNFL thickness is determined by the instrument's internal software from an average of the three scans and displayed in the manufacturers' summary report, the "RNFL Thickness Average Analysis Report" (Figure 1.13).

2.6.4 Spectral domain-OCT

SD-OCT was used in the assessment of all healthy individuals (Group 3), non-exposed individuals with epilepsy (Group 2) and in VGB-exposed individuals recruited from the Chalfont Epilepsy Centre and from SEIN (Group 1A).

2.6.4.1 Why SD-OCT was chosen

Although all previous studies of OCT ppRNFL imaging in VGB-exposed individuals have been conducted using TD-OCT, the latest generation of OCT instruments that became available at the start of this study utilised spectral domain technology. The differences between SD-OCT and TD-OCT are discussed in Chapter 1 (1.18.3).

VGB has recently received a license for use in the US and studies using OCT in VGB-exposed individuals are currently underway (263). These studies are likely to utilise the

latest SD-OCT technology, thus the use of SD-OCT in the assessment of the majority of the individuals included in this study will make the results more comparable to any future research in this area.

2.6.4.2 The SD-OCT ppRNFL scanning-protocol

To measure ppRNFL thickness the "Optic Disc Cube 200x200" protocol was used. This protocol generates a 6x6mm grid of data by acquiring 200 horizontal scans each composed of 200 A-scans, centred on the optic nerve head. Using the "Glaucoma Analysis" algorithm, a 3.46mm diameter circle of data, made up from 256 A-scans, is extracted from the grid. From this circle of data ppRNFL thickness is calculated and displayed in the "Glaucoma Analysis Report" and the "ONH and RNFL Thickness OU Analysis Report".

2.6.5 Exclusion of OCT data

Only data from the right eye were used in the analysis[10]. All scans were assessed for their quality and were excluded if they were off-centred, had significant movement artefacts, missing data (Figure 2.3), or a signal strength of less than six (arbitrary units). The signal strength is determined by the OCT software from the signal to noise ratio and the signal-uniformity within the scan (328). A signal strength, on a scale of one to ten (arbitrary units), is given for each scan, where ten denotes excellent scan quality and one denotes poor scan quality (329). For clinical purposes a cut-off signal strength of five out of ten (arbitrary units) is recommended by the manufacturer. However, for research purposes, studies have used a higher cut-off (329) as low signal strength can lead to an underestimation of the ppRNFL thickness (330).

[10] See Chapter 2

Figure 2.3 An example of ppRNFL scans that did not fulfil the quality control criteria

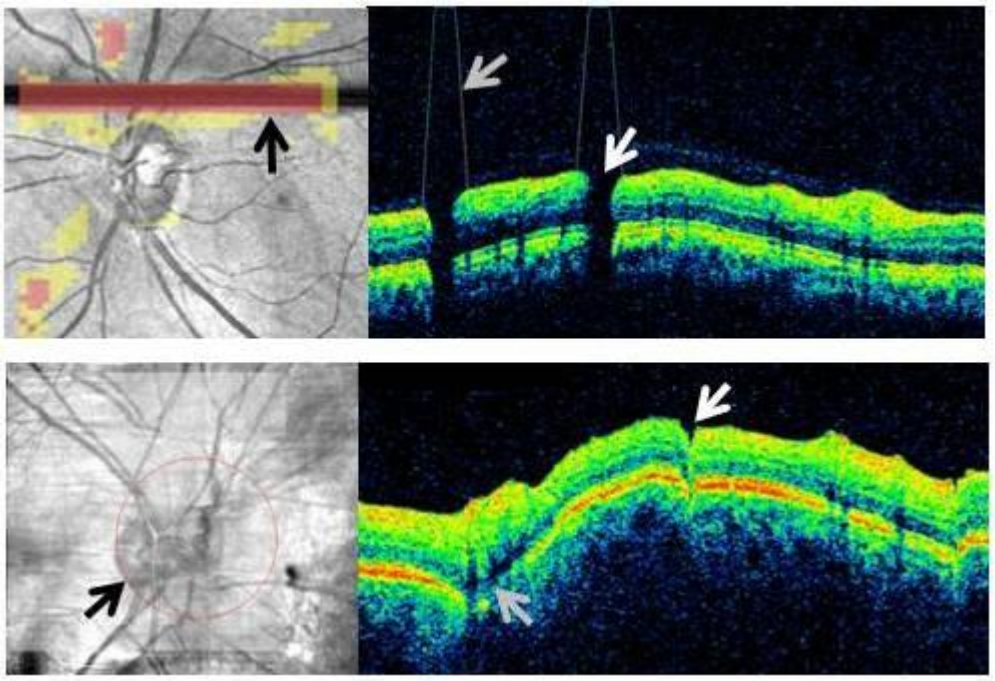

Figure 2.3 legend: **(A)** Blinking during ppRNFL scan. The black arrow indicates on the fundus image the areas affected by the blink. The blink results in missing sections of data from the tomograph (white arrow). The inbuilt software cannot detect the borders of the ppRNFL in these areas (grey arrow). (**B)** Significant eye movement during the ppRNFL scan. The retinal image is blurred and the scan-circle (shown in red) is off-centred (black arrow). The tomograph is jagged (white arrow) and irregular resulting in poorly defined ppRNFL boundaries. The individual retinal layers cannot clearly be identified in some areas (grey arrow).

2.7 Quantifying and classifying ppRNFL thickness data

2.7.1 Quantifying ppRNFL thickness – manufacturers' summary report

Quantitative ppRNFL thickness data were obtained from the manufacturers' summary reports (Figure 1.13). Summary measures that were analysed include the average ppRNFL thickness (around the whole ONH), and the ppRNFL thickness in 90^{o} quadrants and 30^{o} sectors (Figure 2.4 A-C).

2.7.2 Quantifying ppRNFL thickness – A new summary measure

For individuals assessed using SD-OCT, the ppRNFL thickness data from each of the 256 A-scans was exported to a personal computer using Research Browser Software (Version 5) (Carl Zeiss Meditec, Dublin, CA). From this the 256 A-scans were combined to form an additional summary measure of 64 segments around the ONH each comprised of four A-scans. (Figure 2.4D).

Figure 2.4: The distribution of summary measures of ppRNFL thickness around the optic nerve head

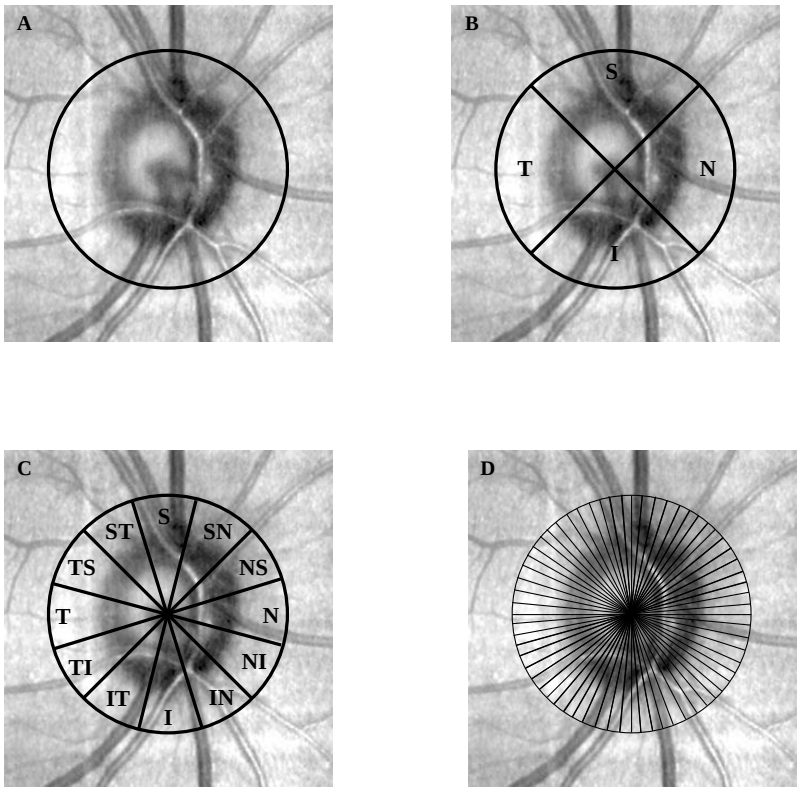

Figure 2.4 legend: Summary measure of ppRNFL thickness provided by in the manufacturers' summary report include the average ppRNFL thickness around the whole of the ONH **(A)**, in 90^{o} quadrants **(B)**, in 30^{o} sectors **(C)**. In addition a new summary measure was created comprised of 64 segments **(D)**.

2.7.3 Classifying ppRNFL thickness

In addition to quantifying thickness, the ppRNFL thickness was classified according to which percentile it fell into, based on the manufacturers' normative database. In the manufacturers' summary report the ppRNFL thickness values are colour-coded according to which percentile they fall into. Values falling into the $\leq 95^{th}$–>5^{th} percentile are colour coded as green, $\leq 5^{th}$–>1^{st} percentile are coloured yellow and $\leq 1^{st}$ percentile are coloured red (Figure 1.13). In this study, ppRNFL thickness was classed as being normal if it fell into the $\leq 95^{th}$–>5^{th} percentile (green area); showing borderline

attenuation if it fell within the ≤ 5th–>1st percentile (yellow area); or showing thinning if it was within the ≤1st percentile (red area) (Figure 1.13).

In a "guide to interpreting OCT output" available from the manufacturers' website the normal distribution percentiles have not been defined as "normal", "borderline" or "abnormal", as used in this study, although the ≤1st percentile is described to be "considered outside normal limits" (331). However, the classification system that was adopted for this study has frequently been used to classify ppRNFL thickness in other areas of research, particularly in glaucoma (332) where OCT ppRNFL imaging is widely used. Although theses definitions are somewhat arbitrary, these percentiles (and associated colour coding) are commonly used in the clinical setting to aid the clinician in the assessment of the integrity of the ppRNFL and to monitor any changes over time.

It is important to stress that 5% of normal healthy individuals with no eye-disease will fall within the "borderline" area, and 1% of normal healthy individuals with no eye-disease individuals with fall within the "abnormal" area (285).

2.8 Data analysis

Many individuals had ppRNFL thickness scans from both the right and left eyes that fulfilled the quality control criteria[11]. Only data from one right eye scan from each individual was included in the analysis.

A "one-eye design" (333) was chosen for this study so that standard statistical techniques could be applied to the data without increasing the risk of Type 1 errors.

[11] As described in 2.4.5

Analyses in which both eyes of an individual are used ("two-eye designs") (333) require particular statistical approaches. This is because within an individual data from one eye are more likely to be similar to data from the other eye of the same individual, than it is from another eye from a different individual, i.e. within a subject the data from each eye will be highly correlated (unless there is unilateral eye disease) (333;334). This is due to multiple factors including genetic and environmental effects that will act within an individual to influence any structural or functional parameters (334). In standard statistical analysis, data should be independent, and failure to take account of between-eye correlation in a "two-eye design" can lead to an overestimation of the precision of the statistical values (333;334). A "two-eye design" can be used in the analysis, however, data from both eyes should be averaged and the average value can be treated with the same standard statistical techniques as a "single-eye design" (333). Alternatively, more complex statistical approaches are needed to determine the contribution to the outcome measure of variance arising from between-subject factors and those arising from within-subject factors (333). A further complicating factor is added to both of these "two-eye design" approaches when some individuals only have data from one eye. In this study, whilst many individuals had data from both eyes, some individuals only had data from only one eye.

For a "one-eye" design, the eye to be entered into the analysis can either be chosen at random, or can be chosen to be always the right eye, or always the left eye (334). Initially a random-eye approach was going to be used in this study; however analysis of a subset of the data from individuals in Group 1A and Group 3 suggested that the right-eye measures were significantly thicker than the left eye measures[12]. Recently, this observation has also been made in a group of 248 healthy volunteers, where the average

[12] Data provided in Appendix 4

ppRNFL thickness in the right eye was 0.52µm thicker than the average ppRNFL thickness in the left eye, which reached statistical significance (335). Thus only the right eye was chosen from each individual to use in the analysis

In individuals who had two right-eye ppRNFL scans that met the quality control criteria, the scan with the highest signal strength was used in the analysis. If both scans had equal signal strength, the most recently[13] obtained scan was selected.

2.8.1 Quantitative and categorical outcome measures

For ppRNFL thickness and visual field size, data were available as both quantitative and categorical measures (Table 2.9). Analysis of data included exploration of both quantitative and categorical measures of ppRNFL thickness and visual field size.

Table 2.9 Categorical and quantitative data obtained from OCT and perimetry for analysis

Method	Quantitative measure	Categorical measure
OCT	Absolute ppRNFL thickness in a given area (µm)	Normal (≤95th–>5th percentile*)
		Borderline thinning (≤ 5th–>1st percentile*)
		Abnormal thinning (≤1st percentile*)
Perimetry	Mean radial extent of the I4e isopter (degrees)	Normal#
		Mild VAVFL#
		Moderate VAVFL#
		Severe VAVFL#

*According to the manufacturers' normative database

[13] In terms of the time-of-day as all scans from an individual were acquired on the same day.

#According to criteria defined by Wild et al. (97)

For the analysis of absolute measures of ppRNFL thickness, data obtained from Group 1B could not be analysed alongside data from Group 1A, Group 2 or Group 3 as differences in the acquisition methods between the two OCT instruments used do not currently allow these data to be pooled for these analyses (336).

All data analysis was performed using SPSS (version 17.0, SPSS, Chicago). Data from the right eye were used in all analysis. Continuous variables were checked for normality and appropriate parametric or non-parametric analyses were applied. Statistical significance was determined at the 5% level, unless otherwise stated.

Chapter 3 The natural evolution of VAVFL in individuals who continue VGB therapy

3.1 Introduction

It is widely accepted that once established, VAVFL is stable and does not progress with continued VGB exposure. Several follow-up studies of individuals who continue VGB therapy have shown no progression of VAVFL over time (81;100;111;148-150) (Table 3.1), although others have suggested that progression can occur (81;139;151;152) (Table 3.1).

Studies of the evolution of VAVFL in individuals continuing VGB therapy have followed participants for short periods of time (typically less than four years) (Table 3.1). In one case report which has shown the evolution of visual field size with continued VGB exposure over a longer period, the visual field size showed a significant decrease after ten years of VGB use, suggesting that VAVFL may progress in some individuals after many years of VGB exposure (139).

Table 3.1: Summary of follow-up studies reporting changes in the visual field with continued VGB exposure

Reference	Number of participants	Follow-up (months)	Conclusion	How the data were analysed
Clayton 2010 (139)	1	120	Progression	Observation
Kinirons 2006 (99)	41	6 - 67	No progression	Criteria [a]
Hardus 2000 (152) *Hardus 2003 [b] (151)*	11 *5*	13 - 61 37 - 47	Progression *Progression*	Statistical test [b] *Statistical test [b]*
Best 2005 (148)	16	18 - 43	No progression	Observation Statistical test [b]
Lawden 1999 (81)	1	39	No progression	Observation
Nousiaien 2001 (100)	26	4 - 38	No progression	Observation Statistical test [b]
Schmidt 2002 (149)	4	12 - 24	No progression	Observation Statistical test [b]
Graniewski-Wijnands 2002 (150)	9	18	No progression	Observation
Paul 2001 (111)	15	12	No progression	Observation Statistical test [b]
Lawden 1999 (81)	1	11	Progression	Observation

The table is organised in order of the length of the follow-up period. Observation = progression of VAVFL was determined from either direct observation and qualitative evaluation of serial visual field data, or from observation of serial quantitative measure of VAVFL, typically plotted in a graphical format (e.g. serial MRD measurements shown graphically in (139))

[a] when analyzing progression or recovery of visual fields, the authors considered a change in MRD of ≤5% as stable, of 6–10% as indeterminate, and of >10% as pathologic change.

[b] Either a paired-samples T-test or a Wilcoxon Signed Rank Test was used to determine a statistically significant difference in visual field size between tow predefined test points.

Italics = Hardus 2003 (151) reports five individuals who were included in the earlier report (152) of 11 individuals.

The severity of VAVFL varies widely (12;96;97;106), with some individuals showing very mild loss of the far periphery of the visual field (94;96;116) whilst others develop a very severe constriction extending to involve the central 30^{o} of the visual field (96;101;109;139). In addition, a continuum of severity of associated retinal pathology, including retinal nerve fibre layer thinning (183), and optic atrophy (147) have also been described. Frisen et al. suggested that RNFL attenuation associated with VAVFL may be progressive with continued VGB exposure. A "staging system" based on the photographic appearance of the RNFL was developed, with atrophy initially only detectable in the nasal peripapillary area and later progressing to involve the superior and inferior poles of the ONH (147).

The range of severity of VAVFL and associated retinal pathology may be suggestive of a progressive evolution of VGB retinotoxicity with continued VGB exposure (96;147;183). The lack of evidence to suggest VAVFL is progressive with continued VGB exposure may be due to short follow up periods or inappropriate statistical or observational approaches to the data.

Understanding the evolution of VAVFL with continued VGB exposure over a long period of time is essential for optimal patient management, and for enabling decisions to be made about the risks and benefits of continued VGB therapy. For example, from clinical experience, some individuals maintain seizure freedom on VGB, greatly improving their quality of life and enabling them to drive (180). If VAVFL is

progressive, or can develop after many years of VGB therapy, eligibility to drive may be jeopardised due to the development of visual field loss (179). In addition, although in most individuals VAVFL is asymptomatic, in severe cases it can be disabling, greatly affecting quality of life (106).

3.1.1 Aims

The aim of this study was to assess the natural evolution of VAVFL over a ten year period in individuals continuing VGB therapy.

3.2 Methods

3.2.1 Subjects

Fourteen individuals who were currently taking VGB were included in the study. Individuals were participants from Group 1A and Group 1B. All individuals had originally participated in a study of VAVFL at the National Hospital for Neurology and Neurosurgery commencing in 1999 (95) and had been taking VGB since before the original study. All individuals were being followed up routinely in the National Hospital for Neurology and Neurosurgery Neuro-Ophthalmology Department because of continued VGB exposure.

3.2.2 Perimetry

All individuals were examined on at least one occasion by the author (LMC), according to the methods described[14]. Other examinations of the visual field were performed as part of the individual's on-going neuro-opthalmological assessment related to their VGB exposure, and as part of other studies of VAVFL (95). These examinations were

[14] See Chapter 2

undertaken by several skilled operators according to clinical protocol, which is in keeping with those methods described.

3.2.3 Data analysis

All visual fields were quantified using the MRD method[15] for the right eye, using the I4e isopter. This method was also used in the original study of these individuals commencing in 1999 (95). All visual field assessments were quantified and analysed by the author (LMC). Reliability of the visual field was determined based on the operator's comments on the visual field chart and in the medical notes.

The first recorded visual-field assessment whilst on VGB (Test 1), and the latest recorded visual-field assessment whilst still taking VGB (Test 2) were selected from each individual to use in part of the analysis. Follow-up time was defined as the time in months between Test 1 and Test 2 and was determined from the medical notes according to the method described[16]. The visual fields taken during Test 1 and Test 2 were classified according to criteria set out by Wild et al. (97).

3.3 Results

3.3.1 Subject data

Data from fourteen individuals and 176 visual field tests were available. Two visual field tests were excluded, (one each from participant 5 and 7), as the operator had indicated that the results were unreliable, leaving 174 visual field tests available for

[15] See Chapter 2

[16] See 2.2.2

analysis. One individual included in this study (Subject 12), has recently been reported by our group (139).

Details of VGB exposure, follow-up time and visual field size for each participant are shown in Table 3.2. The average follow-up time was 128 months (range 104-148). At the time of Test 1, the mean cumulative VGB exposure was 4737 grams; the mean duration of VGB exposure was 65 months. At Test 2, the mean cumulative VGB exposure was 11,677 grams; the mean duration of VGB exposure was 192 months (Table 3.2).

3.3.2 Visual-field classification

Visual fields were classified according to criteria set out by Wild et al. (97). At Test 1 9/14 (64.3%) individuals had VAVFL. At Test 2 13/14 (92.9%) individuals were classified as showing VAVFL. Six individuals had progressed by at least one class (e.g. from normal to mild VAVFL). Seven individuals remained within the same class. One individual (Subject 2) showed an improvement from "moderate VAVFL" to "mild VAVFL", but only when considering data at Test 1 and Test 2 (Table 3.2).

3.3.3 Visual-field size

A Wilcoxon Signed Rank Test showed that the latest visual field (Test 2) was significantly smaller than the first visual field (Test 1) ($z=-2.48$; $p<0.05$; Table 3.2). The average difference between the visual field size at Test 1 and Test 2 was 7.5 MRD.

Table 3.2 VGB exposure and visual field data for each Subject

Subject (number of visual field tests)	**Cumulative VGB exposure (grams)**		**Duration of therapy (months)**		**Follow-up (months)**	**Test 1**		**Test 2**		**Rate of change of MRD/ KG of VGB exposure***
	Test 1	**Test 2**	**Test 1**	**Test 2**		**MRD**	**Classification**	**MRD**	**Classification**	
1 (8)	7606	13806	122	230	108	52	Normal	38	Mild	-1.3
2 (10)	6570	14427	84	213	129	32	Moderate	39	Mild	-0.4
3 (17)	3134	11654	45	185	140	34	Moderate	28	Moderate	-1.1
4 (13)	2086	8640	35	144	109	50	Normal	33	Moderate	-2.2
5 (16)	1220	3141	58	190	132	50	Normal	51	Normal	-1.8
6 (16)	4286	8961	43	170	127	38	Mild	37	Mild	-1.4

7 (9)	7398	20085	91	230	139	35	Moderate	29	Moderate	-0.9
8 (6)	221	4432	5	139	134	25	Moderate	28	Moderate	-0.9
9 (4)	6299	12627	112	216	104	52	Normal	43	Mild	-0.6
10 (13)	11629	16247	121	235	114	46	Normal	30	Moderate	-3.7
11 (17)	1367	7154	20	164	144	34	Moderate	26	Moderate	-1.6
12 (21)	6297	18950	49	197	148	32	Moderate	1	Severe	-2.7
13 (10)	2516	10250	36	162	126	41	Mild	38	Mild	-2.4
14 (14)	5632	13106	83	216	133	36	Mild	31	Moderate	-1.1
Average (SD)	**4737**	**11677**	**64.6**	**192 (32.4)**	**127.6 (14.0)**	**39.8 (8.8)**		**32.3 (11.3)**		

VGB = vigabatrin; MRD = mean radial degrees; Test 1 = first visual field examination taken whilst on VGB; Test 2 = latest visual field examination taken whilst on VGB

3.3.4 Individuals with normal visual fields at Test 1

Five individuals (Subjects 1, 4, 5, 9 and 10) had normal visual fields at Test 1 (Table 3.2). At Test 2 one individual still showed a normal visual field, two individuals showed mild VAVFL and two showed moderate VAVFL. The average visual field size at Test 1 for these five individuals was 50 MRD, at Test 2 it was 39 MRD. The average difference between the visual field size at Test 1 and Test 2 was 11.0 MRD.

3.3.5 Evolution of VAVFL

The cumulative VGB exposure at the time of each visual field examination was determined, and a graph of cumulative VGB exposure and MRD, at successive examinations over the follow-up period, was plotted for each individual (Figure 3.1). A linear trendline was added to each graph, taking into account all available visual field data for that individual (Figure 3.1). The trendlines for all individuals showed a negative trend, suggesting an overall decrease in the visual field size with increasing cumulative VGB exposure. Fluctuations in visual field size above and below the trendline were seen for all individuals (Figure 3.1).

3.3.6 Rate of change of visual field size

The rate of change of the visual field size was determined for each individual from the slope of the trendline and ranged from 0.4 to 3.7 MRD per kilogram of cumulative VGB dose (Table 3.2).

Figure 3.1: Visual field size in relation to cumulative VGB exposure for each Subject

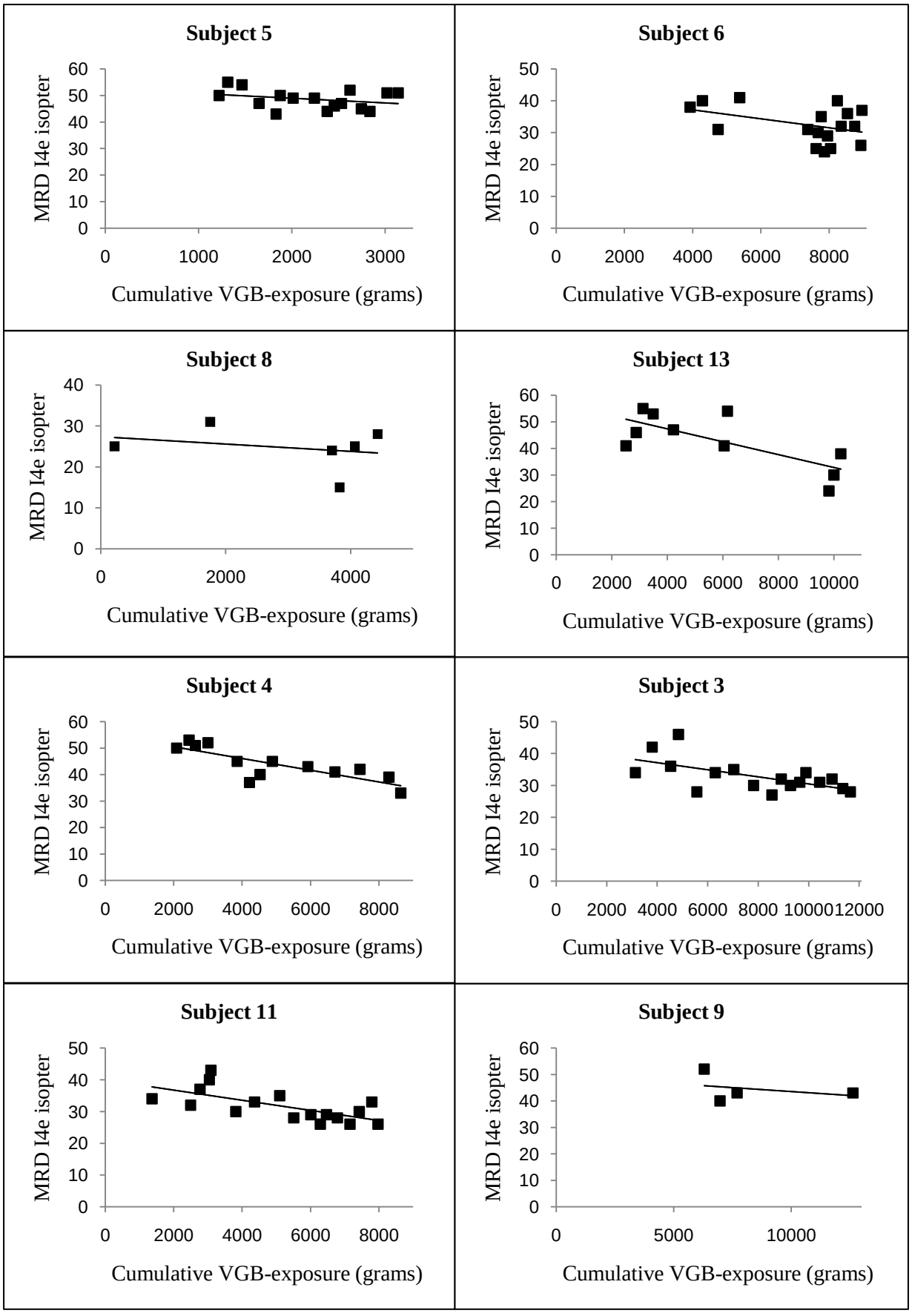
Subject 5
MRD I4e isopter
0
10
20
30
40
50
60
0
1000
2000
3000
Cumulative VGB-exposure (grams)
Subject 6
MRD I4e isopter
0
10
20
30
40
50
0
2000
4000
6000
8000
Cumulative VGB-exposure (grams)
Subject 8
MRD I4e isopter
0
10
20
30
40
0
2000
4000
Cumulative VGB-exposure (grams)
Subject 13
MRD I4e isopter
0
10
20
30
40
50
60
0
2000
4000
6000
8000
10000
Cumulative VGB-exposure (grams)
Subject 4
MRD I4e isopter
0
10
20
30
40
50
60
0
2000
4000
6000
8000
Cumulative VGB-exposure (grams)
Subject 3
MRD I4e isopter
0
10
20
30
40
50
0
2000
4000
6000
8000
10000
12000
Cumulative VGB-exposure (grams)
Subject 11
MRD I4e isopter
0
10
20
30
40
50
0
2000
4000
6000
8000
Cumulative VGB-exposure (grams)
Subject 9
MRD I4e isopter
0
10
20
30
40
50
60
0
5000
10000
Cumulative VGB-exposure (grams)

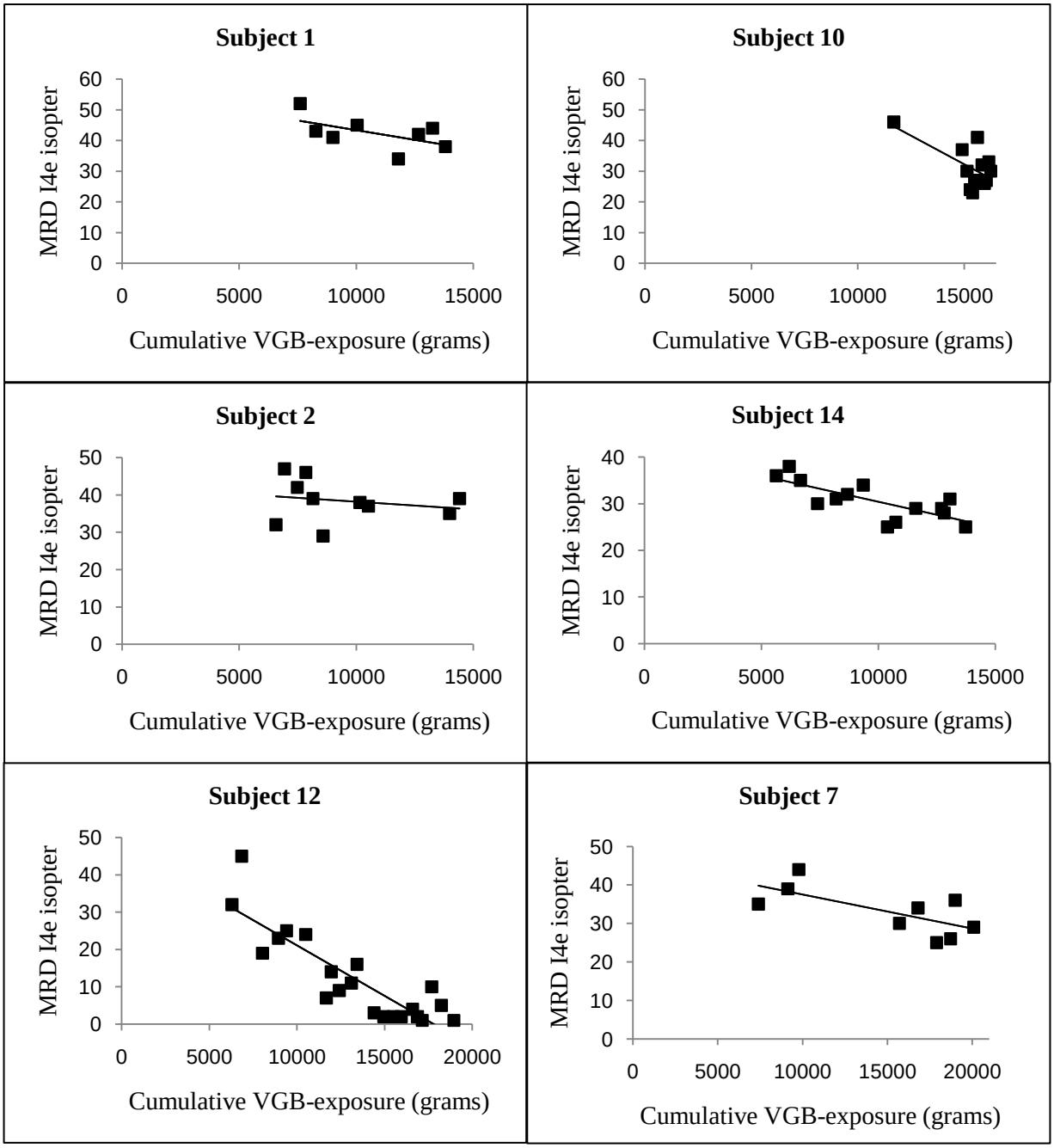

Figure 3.1 legend: Graphs for each individual showing the visual field size in MRD at each successive examination (represented by ♦), in relation to the cumulative VGB exposure at that time. Graphs are numbered according to the subject number, and are shown in order of increasing cumulative VGB exposure. A linear trendline was added to each scatter-plot.

VGB = vigabatrin; MRD = mean radial degrees

3.3.7 Fluctuations in visual field size

Fluctuations in visual field size above and below the trendline were seen for all individuals (Figure 3.1). The scatterplot for Subject 5 is highlighted (Figure 3.2). Over

relatively small increases in cumulative VGB exposure, the MRD shows variable fluctuation above and below the trendline (red arrows; Figure 3.2). However, overall a trend for decreasing visual field size with increasing cumulative VGB exposure is still apparent.

Figure 3.2: Fluctuations in visual field size between test sessions

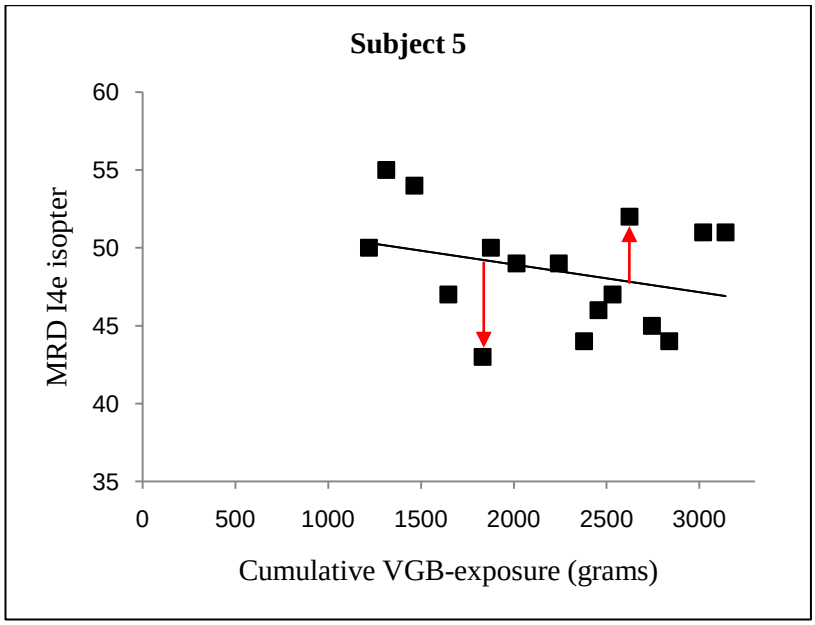

Figure 3.2 legend: A scatterplot of MRD and cumulative VGB exposure is shown for Subject 5. Over a small increase in cumulative VGB exposure there is a high degree of fluctuation in the visual field size above and below the trendline over successive test sessions (red arrows). Overall the trendline shows a negative trend

3.4 Discussion

This is the longest follow-up study of VAVFL in individuals continuing VGB therapy, and shows the evolution of VAVFL over successive test sessions with increasing VGB exposure. The results suggest VAVFL progresses with continued VGB use over a ten-

year follow-up period. The prevalence of VAVFL increased from 64% at Test 1 to 93% at Test 2. All individuals included in the study showed a trend for decreasing visual field size with increasing cumulative VGB exposure when all fields for an individual were taken into account (Figure 3.1). Our results concur with Hardus *et al.* who reported an increase in the percentage visual field loss with continued VGB use over a 13 – 61 month follow-up period in 11 individuals (152). In addition, individual cases have been described of VAVFL progression with continued VGB exposure (81;99;111;139;148). The majority of studies, however, have reported that once established, VAVFL is stable and does not progress further with continued VGB use (81;100;111;148-150). The ambiguity regarding the evolution of VAVFL with continued VGB exposure may be due to a number of factors. Good, prospective data on the course of VAVFL with continued VGB use are lacking (99), and most studies, including the present study, rely on retrospective analysis of visual field data acquired by different examiners over many years. Furthermore, perimetry has inherent limitations which may make it impractical to detect changes in the visual field over time in VGB-exposed individuals, particularly if these changes are small and follow-up periods are short.

3.4.1 Problems with measuring the visual field

In many individuals with epilepsy, perimetric results may be unreliable and inconclusive and repeated visual field testing is often needed, after which results can still prove difficult to interpret (229). In the present study, evaluation of serial visual field tests showed a variable degree of fluctuation in visual field size above and below the trendline (Figure 3.1 and 3.2). These fluctuations are likely to represent variability in visual field size that is not related to VGB-associated pathological change in visual function, but are the result of both subject-related and examiner-related factors (337).

Subject-related factors that may influence the recorded visual field include fatigue (338), reaction time (339), an inadequate understanding of the task (337;340) and a "learning effect" (159) whereby individuals show an improvement of the visual field over subsequent test sessions related to improved performance and familiarity with the task, rather than true improvement in visual function (159;160). In healthy individuals assessed using Goldmann kinetic perimetry, the visual field size was found to fluctuate by up to 16% between test sessions (341). In individuals with visual impairment due to retinitis pigmentosa, the fluctuation in visual field size not related to disease progression was as high as 50% between sessions in some individuals (341). In individuals with epilepsy, fluctuations in visual field size may be exaggerated. Certain antiepileptic drugs (342;343), seizures, the underlying cause of the epilepsy and psychosocial factors (344) can impair cognition, attention and psychomotor speed, all of which are integral to performing perimetry reliably. As these factors may fluctuate over time, their influence on the recorded visual field may also fluctuate, exaggerating the normal variability in visual field size between test sessions, and making it difficult to detect true pathological change (337).

Examiner-related factors may also contribute to the variability in the recorded visual field particularly when using a manual perimetric technique (e.g. Goldmann kinetic perimetry) as was utilised in the present study (306). The speed and direction of movement of the light-stimulus which is used to assess the visual field is operator-dependant. Although optimal rates of stimulus movement have been suggested (311;313), the speed and technique used by an operator during an assessment may be influenced by the subject's performance and ability, the time constraints of the clinical setting and the examiner's skill and experience (304;311). In addition, the instructions given by the examiner to the individual on how to perform the assessment can affect the

obtained visual field (340). As a result, the visual field assessment is difficult to accurately standardise between examiners, and inter-examiner factors will add to the variability in the recorded visual field between test sessions (304;345).

3.4.2 Problems with detecting and defining progression of VAVFL

Several studies of VAVFL have attempted to overcome the effects of "normal" fluctuation on detecting progression of VAVFL by using criteria to define pathological change in visual field, including a change in the visual field of ≥10% (99) or of more than 10 MRD (95;148). The disadvantage of using these arbitrary criteria to define progression of VAVFL is that they may result in missing small pathological changes in the visual field size (99). For example, whilst all individuals in the present study show a trend for progression of VAVFL when all visual field tests were considered, only four individuals (Subjects 1, 4, 10 and 12) show a decrease in visual field size of ≥ 10 MRD when comparing the visual field size at Test 1 and Test 2. Similarly, whilst Hardus et al. reported VAVFL progression with continued VGB use, the average percentage loss in the visual field size had only increased by 4.2% and 3.5% for the right and left eyes respectively (152).

In the present study, the rate of decrease in the visual field size over the ten-year observation period was between 0.4 and 3.7 MRD per kilogram of cumulative VGB exposure suggesting that although progression of VAVFL occurs, for most individuals the degree of change with increasing VGB exposure is small. This degree of change may be difficult to detect clinically if serial results are assessed subjectively for evidence of progression (337), a method that has been utilised in some studies of VAVFL (Table 1). In addition, when follow-up periods are short, as in previous studies of progression of VAVFL (Table 1), any change in the visual field may be too small to detect.

Failure to detect progression of VAVFL in some studies may also relate to the analysis used. In the present study Subject 2 showed an apparent improvement in the visual field from moderate VAVFL at Test 1to mild VAVFL at Test 2 (Table 3), when considering only these two time points. However, when all time points were considered, the trendline indicated a progressive decrease in visual field size over the follow-up period (Figure 3.1). Similarly, Subject 5 was classified as having normal visual fields at Test 1(50 MRD) and at Test 2 (51 MRD), however, the trendline applied to all available visual field results shows a progressive decrease in the visual field size of 1.8 MRD per KG of cumulative VGB exposure (Figure 3.1; Table 3.2). Many studies of VAVFL progression have utilised analysis techniques where only two visual field test points are used to determine whether a change in the visual field size has occurred (Table 2). If any of the test points used were significantly influence by non-pathological subject-related or examiner-related variability then the analysis may fail to detect a change in the visual field size. Although the present study is also subject to all the subject- and examiner-related factors discussed, the advantage of the present study is that for each individual all available reliable visual field test results were used in the evaluation of progression of VAVFL (Figure 3.1). By plotting the visual field results from multiple examinations over a protracted period, no presumptions need to be made about the influence of subject-related and examiner-related variability on the visual field, enabling trends to be detected despite the inter-test fluctuations in visual field size.

3.4.3 The progression of VAVFL

Although the progression of VAVFL with continued VGB use may be small and difficult to detect clinically it is important to note that the rate of progression of VAVFL appears to differ between individuals. For example, in the present study, Subject 2 and Subject 12 were followed up over similar VGB exposure durations (cumulative VGB-

exposure from around 6000 to 15,000 grams). Both individuals had similar visual field results at the beginning of the assessment period. However, in the ensuing follow-up period, the average rate of loss for Subject 12 deteriorated was higher (2.7 MRD/kg cumulative VGB-exposure), developing severe VAVFL to less than 10^{o} eccentricity, whilst Subject 2 showed a more slowly progressive course (0.4 MRD/kg cumulative VGB-exposure), with the visual field size showing little change with increasing VGB use (Table 3.2; Figure 3.1). The inter-individual differences in the rate of progression of VAVFL with continued VGB use described in this study may account for some of the variation in inter-individual susceptibility to VAVFL seen in individuals exposed to similar amounts of VGB, and may help to explain the conflicting findings regarding the relationship between the amount and duration of VGB exposure and the risk and severity of VAVFL.

At the time of Test 1 the average duration of VGB exposure was more than five years, and 9/14 individuals had already developed VAVFL. It cannot be assumed that the true pattern of visual field loss is actually linear, or that the progression of visual field loss observed in the present study represents the pattern and rate of progression of VAVFL prior to, or subsequent to, the observation period. Patterns and rates of VAVFL progression my change throughout an exposure period, occurring in a slowly progressive and/or rapid pattern of onset and change. Prospective longitudinal studies including baseline visual field examinations prior to VGB exposure are needed to fully elucidate the pattern of VAVFL onset and progression.

The finding of intra-individual variation in the rate of progression of VAVFL with continued VGB use may have implications for phenotyping in drug response studies of VAVFL. Current understanding of the relationship between VGB-exposure and visual field loss come from cross sectional studies typically looking at visual field size after a

given VGB exposure. However, the rate of change in the visual field size with increasing cumulative VGB-exposure may provide a stronger indicator of an individual's risk of developing significant VAVFL, and may provide a more useful measure to consider in the management of individuals continuing VGB therapy.

3.4.4 New tools are needed

The multifactorial contributions to the variability in the recorded visual field, particularly in a population of individuals with epilepsy, suggest that perimetry may not be the most appropriate tool for monitoring visual dysfunction in VGB-exposed individuals. Subtle pathological changes in the visual field may go undetected until significant VAVFL has developed, at which point visual field loss may be symptomatic and have a negative impact on the individuals quality of life (97;106). New methods to assess VGB-exposed individuals for the effects of VGB retinotoxicity are needed, particularly in individuals in whom perimetry is unreliable or unfeasible. ppRNFL thinning measured using OCT has been suggested to be a sensitive and specific indicator of VAVFL (256). OCT provides an objective quantitative tool that provides highly repeatable measures of retinal structure in healthy individuals (346) and in individuals with visual impairment (346;347). If structural changes in the retina, such as ppRNFL thinning, are associated with the development of VAVFL as has been suggested (229;256), they may be detectable before VAVFL becomes apparent using perimetry (348).

For OCT ppRNFL imaging to be clinically valuable in individuals with VAVFL, any detectable structural changes must show an association with functional visual impairment. Additionally the technique must be suitable for use within a population of individuals with epilepsy, and show good repeatability of its measurements within that population.

3.5 Conclusion

In summary, VAVFL shows progression with continued VGB exposure over a ten-year period. However, this progression may be subtle and difficult to detect using perimetry. Assessing VAVFL using perimetry has inherent limitations and new methods are undoubtedly needed to monitor VGB-exposed individuals.

Chapter 4 The ppRNFL in VGB-exposed individuals; exploring the relationship between ppRNFL thickness and visual field size

4.1 Introduction

It has been suggested that imaging of the ppRNFL using OCT provides a sensitive and specific indicator of VAVFL, and should be considered in all people commencing VGB (256). ppRNFL thinning detected using OCT has been described in a small number of patients with VAVFL (229;256), but no studies have explored the relationship between ppRNFL thickness and visual field size in VGB-exposed individuals. Wild et al. reported average ppRNFL thickness as a function of Mean Sensitivity (derived using standard automated perimetry) for 20 individuals with VAVFL, although no statistical analysis of any association was discussed (229). To optimize the clinical application of ppRNFL imaging in VGB-exposed individual, it is important to understand the relationship between this structural measure, and functional VAVFL (349).

The value of any tool in the assessment of VGB-exposed individuals depends partly upon the repeatability of its measurements within that population. Structural measures of the retina using OCT show high repeatability and reproducibility in healthy subjects (346), and in people with glaucoma (346;347). A significant source of variability in ppRNFL thickness measures, can arise from differences in scan alignment (350), which can occur as a result of changes in the subjects fixation during scanning. During perimetric testing I have observed that inability to adequately fixate on a visual target provides a common source of measurement error in individuals with epilepsy, and

therefore may contribute to measurement error during OCT, and reduce its clinical utility in this setting.

4.1.2 Aims

The aims of this study were to determine the repeatability of OCT ppRNFL thickness measurements in a VGB-exposed population and to explore the relationship between ppRNFL thickness and visual field size, to establish whether OCT is a suitable tool to use in VGB-exposed individuals.

4.2 Methods

4.2.1 Subjects

VGB-exposed individuals from Group 1A and Group 1B, and healthy controls (Group 3) were included in the study.

4.2.2 Perimetry

Individuals from Group 1A and Group 1B underwent perimetric testing according to the methods described. Individuals in Group 3 were not assessed using perimetry.

4.2.3 OCT

All individuals were assessed using OCT. Individuals from Group 1A and Group 3 were assessed using SD-OCT. Individuals from Group 1B were assessed using TD-OCT.

4.2.4 Data analysis

For the analysis of absolute values of ppRNFL thickness, data obtained from Group 1B could not be analysed alongside data from Group 1A and Group 3 as differences in the

acquisition methods between the two OCT instruments used do not currently allow these data to be pooled for these analyses (336).

4.3 Results

4.3.1 Subjects and performance

204 VGB-exposed individuals (Group 1A and 1B) and ninety healthy controls (Group 3) participated in the study. Demographic details of each Group are shown in Table 2.1 (Chapter 2). 39 (19.1%) were unable to perform perimetry reliably due to inability to cooperate. 13 (6.4%) individuals were also unable to perform OCT (all of whom could not perform perimetry). 26/39 (66.7%) of the individuals who were unable to perform perimetry could complete OCT. Visual field data were excluded or missing for a further 34 individuals and OCT for 11 individuals, (Table 4.1). Overall, OCT images were acquired for 180 VGB-exposed individuals (129 for Group 1A, 51 for Group 1B); visual field data for 131; 126 individuals had both sets of data (84 from Group 1A, 42 from Group 1B). OCT data were available for all individuals in Group 3.

Table 4.1 Reasons for missing or excluded OCT and visual field data for all VGB-exposed individuals

	Visual field	OCT
Total recruited	**204**	**204**
Unable to perform task	39[17]	13[a]
Unable to perform task due to small pupils (OCT only) or physical disability	5	5[b]
Visual field data excluded from analysis due to non-VAVFL visual field defect[c]	18	NA
Data not available	11[d]	6[e]
Total available for analysis	**131**	**180**
Total with both visual field and OCT data	**126**	

OCT = optical coherence tomography; VAVFL = vigabatrin associated visual field loss

[a] All individuals were also unable to perform visual field i.e. all included in the 39 individuals with missing visual field data.

[b] Two individuals refused dilating drops and image acquisition was not possible with Stratus OCT.

[c] Including visual field defects due to intracranial surgery, traumatic injury, infarction or other known structural lesion.

[d] Individuals were unable to be present for the visual field examination.

[e] OCT data were not available for the right eye. Data fitting the quality control criteria were available for the left eye, however these was not used in the analysis.

[17] OCT data from individuals who were unable to perform perimetry were compared against OCT data from individuals from whom visual field data was available, to determine whether there was a difference between the two populations. Results can be seen in Appendix 5.

4.3.2 Repeatability

The intra-session repeatability of ppRNFL imaging was assessed from consecutive scans from the same eye that were suitable. 99 individuals from Group 1A, and 30 individuals from Group 1B, had sequential scans from the same eye taken at the same visit which fulfilled the quality control criteria. The intraclass correlation coefficient (ICC) and 95% confidence intervals (CI) for average RNFL thickness and for each of the 90^{o} quadrants are shown in Table 4.2.

Table 4.2 ICC and 95% CI for average ppRNFL thickness and for ppRNFL thickness in each of the 90^{o} quadrants in Group 1A and 1B

ppRNFL area	**Group 1A** ICC (95% CI)	**Group 1B** ICC (95% CI)
Average	0.987 (0.981 – 0.992)	0.985 (0.970 – 0.993)
Superior	0.968 (0.952 – 0.978)	0.966 (0.931 – 0.984)
Nasal	0.923 (0.888 – 0.948)	0.909 (0.820 – 0.956)
Inferior	0.977 (0.966 – 0.985)	0.981 (0.960 – 0.948)
Temporal	0.956 (0.935 – 0.970)	0.893 (0.790 – 0.948)

ICC = intraclass correlation coefficient; CI = confidence interval

Group 1A = VGB-exposed individuals assessed using spectral-domain OCT

Group 1B = VGB-exposed individuals assessed using time-domain OCT

Interpreting ICC: an ICC of zero indicates no agreement between the measures, an ICC of one indicates perfect agreement between measures (319)

4.3.3 The prevalence of VAVFL

67/131 (51.1%) individuals showed VAVFL, according to criteria set out by Wild et al. (97). Of these 30 (44.8%) showed mild, 29 (43.3%) moderate and 8 (11.9%) severe VAVFL (Table 4.3).

Table 4.3 The frequency and severity of VAVFL in Group 1A and Group 1B

	Group 1A N=87	Group 1B N=44	Total N=131
VAVFL	39 (44.8)	28 (63.6)	67 (51.1)
Mild	20 (51.3)	10 (35.7)	30 (44.8)
Moderate	17 (43.6)	12 (42.9)	29 (43.3)
Severe	2 (5.1)	6 (21.4)	8 (11.9)

VAVFL = vigabatrin associated visual field loss; Group 1A = VGB-exposed individuals assessed using SD-OCT; Group 1B = VGB-exposed individuals assessed using TD-OCT

4.3.4 Distribution of ppRNFL thinning across Groups

The number of individuals showing ppRNFL thinning according to the manufacturers' normative database was determined. Individuals from Group 1A and Group 1B were assessed collectively as each OCT instrument compares quantitative ppRNFL thickness data against its own normative database. Average ppRNFL thickness and ppRNFL thickness in each of the 90^{o} quadrants were analysed. For average ppRNFL thickness, 58/180 (32.2%) VGB-exposed individuals showed abnormal ppRNFL thinning (i.e. $\leq 1^{st}$ percentile) and 20.0% of VGB-exposed individuals showed borderline changes (i.e. $\leq$

5^{th}–>1^{st} percentile). Abnormal ppRNFL thinning was most frequently seen in the superior and inferior quadrants, (38.9% and 31.1% of individuals respectively), followed by the nasal quadrant (9.4% of individuals). The temporal quadrant showed ppRNFL thinning in only 6.1% of individuals (Figure 4.1). 112/180 (62.2%) individuals showed ppRNFL thickness changes (either ≤1^{st} percentile or ≤5^{th}–>1^{st} percentile) in at least one of the 90^{o} quadrants.

In agreement with the manufacturer's normative database, >95% of individuals in Group 3 showed normal ppRNFL thickness (i.e. ≤95^{th}–>5^{th} percentile) for average ppRNFL thickness and for each of the 90^{o} quadrants (Figure 4.1). Similarly, ≤1% of individuals in Group 3 showed ppRNFL thickness in the abnormal range (i.e. ≤1^{st} percentile) for average ppRNFL thickness and for the temporal, nasal and inferior 90^{o} quadrants. Only one individual (1.1%) showed abnormal superior quadrant thinning (Figure 4.1).

Figure 4.1: The percentage of VGB-exposed and healthy individuals showing thinning for average ppRNFL thickness and for ppRNFL thickness in each of the 90^{o} quadrants

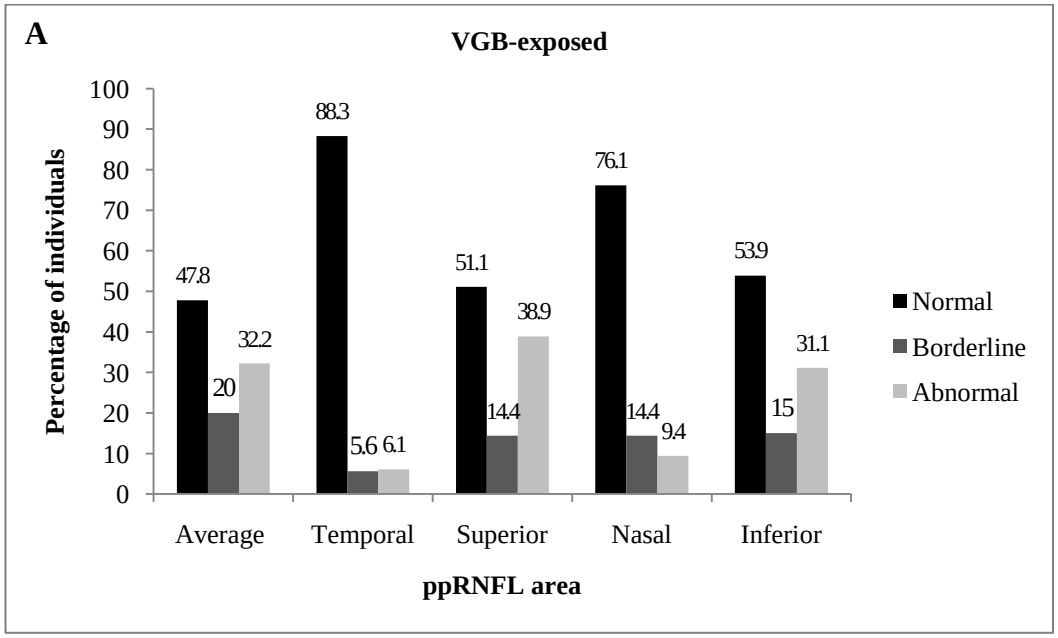

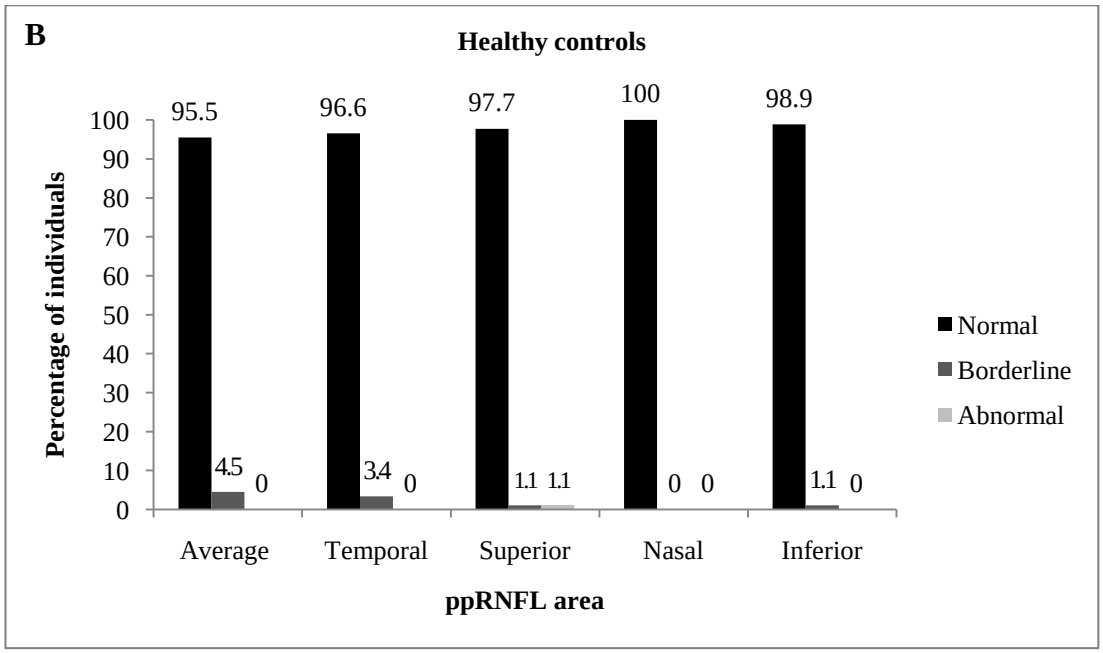

Figure 4.1 legend: The percentage of VGB-exposed individuals **(A)** and healthy controls **(B)** showing normal, borderline and abnormal ppRNFL thickness in each of the 90^{o} quadrants.

ppRNFL = peripapillary retinal nerve fibre layer; VGB = vigabatrin; Normal = ppRNFL thickness ≤95th–>5th percentile, according to the manufacturers' normative database; Borderline = ppRNFL thickness ≤5th–>1st percentile, according to the manufacturers normative database;

Abnormal = ppRNFL thickness $\leq 1^{st}$ percentile according to the manufacturer's normative database

4.3.5 ppRNFL thickness by Group

The average ppRNFL thickness, and the thickness in each of the 90^{o} quadrants for each Group is shown in Table 4.3. The ppRNFL was significantly thinner in Group 1A than in Group 3 for all measures ($p<0.01$; Table 4.4).

Table 4.4 ppRNFL thickness in Group 1A, 1B and 3

ppRNFL area	Group 1A (N =129)	Group 1B (N=51)	Group 3 (N=90)
Average thickness (±SD) (µm)	78.9 (±12.4)*	77.5 (±16.3)	94.4 (±8.8)
Superior thickness (±SD) (µm)	94.6 (±20.2)*	92.8 (±26.2)	115.9 (±13.9)
Nasal thickness (±SD) (µm)	62.9 (±10.3)*	58.4 (±19.4)	73.8 (±10.6)
Inferior thickness (±SD) (µm)	98.8 (±20.8)*	96.6 (±22.0)	122.8 (±14.4)
Temporal thickness (±SD) (µm)	58.9 (±10.1)*	62.3 (±11.5)	65.2 (±10.2)

ppRNFL = peripapillary retinal nerve fibre layer; SD = standard deviation

Group 1A – VGB-exposed patients assessed using spectral-domain OCT

*Statistically significant difference in ppRNFL thickness between Group 1A and Group 3 ($p<0.01$; Bonferroni adjusted)

Group 1B and 3 were not compared as groups were assessed using different OCT models[18]

[18] See 1.18.3

4.3.6 Distribution of ppRNFL thinning according to visual field classification

The number of individuals showing ppRNFL thinning according to the manufacturers' normative database was determined. All individuals from Group 1A and Group 1B were assessed collectively as each OCT instrument compares quantitative ppRNFL thickness data against its own normative database.

In individuals with VAVFL, abnormal ppRNFL thinning was seen most frequently in the superior and inferior quadrants (68% and 51.6% of individuals, respectively). The temporal quadrant was the least frequently affected with 85.9% of individuals showing normal ppRNFL thickness in this quadrant.

In VGB-exposed individuals with normal visual fields the superior quadrant most frequently showed abnormalities. 21% of VGB-exposed individuals with normal visual fields showed either abnormal or borderline ppRNFL thickness in this quadrant.

Figure 4.2 The percentage of VGB-exposed individuals showing thinning for average ppRNFL thickness and for ppRNFL thickness in each of the 90^{o} quadrants according to visual field classification

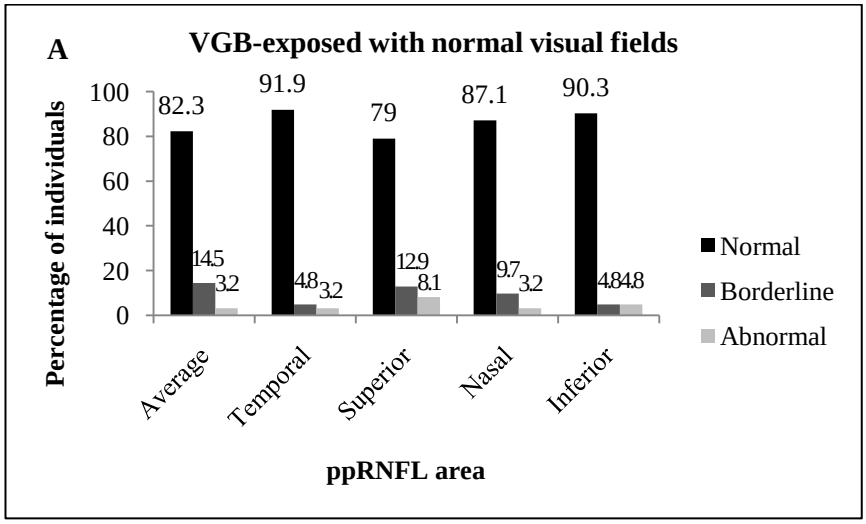

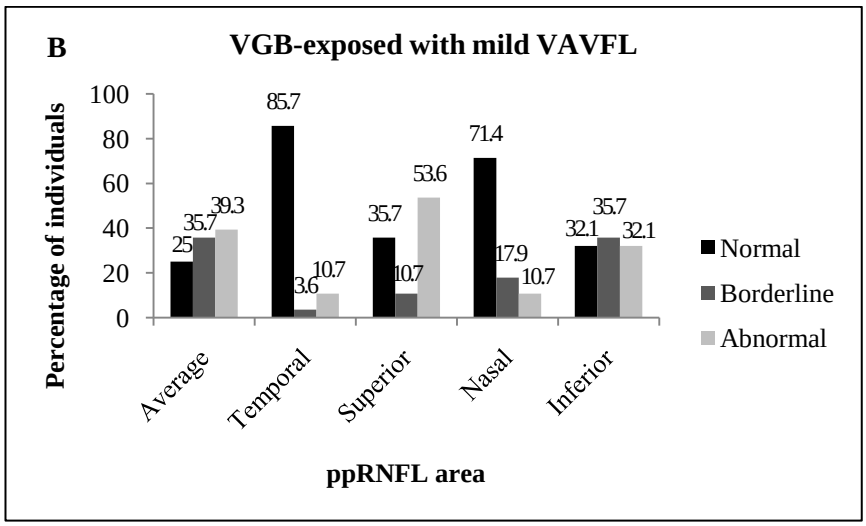

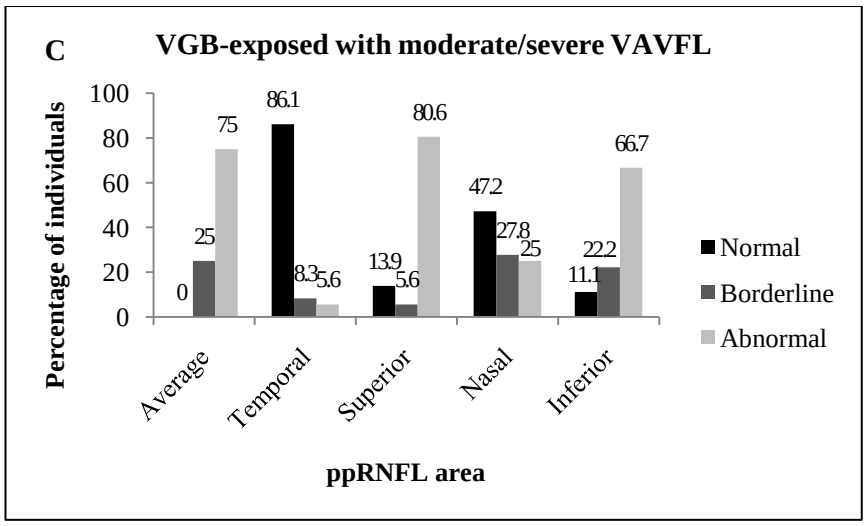

Figure 4.2 legend: The percentage of VGB-exposed individuals with normal visual fields **(A)** mild VAVFL **(B)**, and moderate/severe VAVFL **(C),** showing normal, borderline and abnormal ppRNFL thickness in each of the 90^{o} quadrants.

ppRNFL = peripapillary retinal nerve fibre layer; VGB = vigabatrin; Normal = ppRNFL thickness $\leq 95^{th}$–>5^{th} percentile, according to the manufacturers' normative database; Borderline = ppRNFL thickness $\leq 5^{th}$–>1^{st} percentile, according to the manufacturers normative database; Abnormal = ppRNFL thickness $\leq 1^{st}$ percentile according to the manufacturer's normative database.

4.3.7 ppRNFL thickness according to visual field classification

The ppRNFL thickness in individuals grouped according to their visual field classification (i.e. normal, mild VAVFL, moderate VAVFL or severe VAVFL) is shown in Table 4.5. The ppRNFL was significantly thinner ($p \leq 0.01$) in individuals with VAVFL compared to those with normal VFs in all ppRNFL areas, excluding the temporal quadrant.

Table 4.5 ppRNFL thickness in Group 1A and Group 1B according to visual field classification

ppRNFL area	Group 1A		Group 1B	
	Normal visual fields (N=47)	VAVFL (N=37)	Normal visual fields (N=15)	VAVFL (N=27)
Average thickness (±SD) (μm)	86.8 (8.6)	69.7 (9.6)*	94.4 11.7	71.1 10.2*
Temporal thickness (±SD) (μm)	60.4 (11.0)	58.0 (8.7)	62.9 8.5	62.5 12.8
Superior thickness (±SD) (μm)	108.2 (13.5)	80.4 (17.1)*	120.7 14.7	81.5 17.1*
Nasal thickness (±SD) (μm)	66.5 (10.1)	56.5 (10.1)*	75.1 19.4	50.9 13.3*
Inferior thickness (±SD) (μm)	111.7 (12.3)	83.8 (15.2)*	119.0 16.7	89.3 14.1*

*Statistically significant difference between individuals with normal visual fields and individuals with VAVFL ($p \leq 0.01$; Bonfferoni adjusted)

4.3.8 The frequency of ppRNFL thinning according to visual field classification

126 VGB-exposed individuals had both visual field and OCT data. The number of individuals showing ppRNFL thinning (either $\leq 1^{st}$ percentile or $\leq 5^{th}$–>1^{st} percentile) in at least one of the 90^{o} quadrants, according to visual field classification, was determined (Table 4.6). 64/126 (50.8%) individuals had VAVFL. 82/126 (65.1%) showed ppRNFL changes in at least one of the 90^{o} quadrants. 100% of individuals with moderate or severe VAVFL showed ppRNFL thickness changes in at least one of the

90^o quadrants. 37.1% of individuals with normal visual fields showed ppRNFL thickness changes in at least one of the 90^o quadrants.

Table 4.6 The frequency of ppRNFL thinning in VGB-exposed individuals according to visual field classification

	Visual field classification			
	Normal	Mild	Moderate	Severe
Normal ppRNFL	39 (62.9%)	5 (17.9%)	0	0
ppRNFL thinning	23 (37.1%)	23 (82.1%)	28 (100%)	8 (100%)

Normal ppRNFL = all 90^o quadrants fell within $\leq 95^{th}$ – $>5^{th}$ percentile

ppRNFL thinning = ppRNFL thickness fell into either $\leq 1^{st}$ percentile or $\leq 5^{th}$–$>1^{st}$ percentile in at least one 90^o quadrant

4.3.9 ppRNFL and MRD

126 VGB-exposed individuals had both visual field and OCT data, eighty-four from Group 1A and forty-two from Group 1B. A scatter plot of MRD and average ppRNFL thickness is shown for Group 1A and Group 1B in Figures 4.3 and 4.4 respectively. Individuals within each group were further classified according the severity of their visual field loss (97) (Figure 4.3A and 4.4A), and according to which percentile their ppRNFL thickness fell into (Figure 4.3B and 4.4B). There was a strong correlation between MRD and average ppRNFL thickness for Group 1A ($r = 0.73$, $p < 0.001$; Figure 4.3), and Group 1B ($r = 0.77$, $p < 0.001$; Figure 4.4).

The coefficient of determination was calculated to explore how much of the variance in MRD was explained by average ppRNFL. For Group 1A, $R^2 = 0.53$, for Group 1B, $R^2 = 0.59$: i.e. just over one half of the variance in MRD can be explained by average ppRNFL thickness.

Figure 4.3: Correlation between the average ppRNFL thickness and MRD in individuals from Group 1A

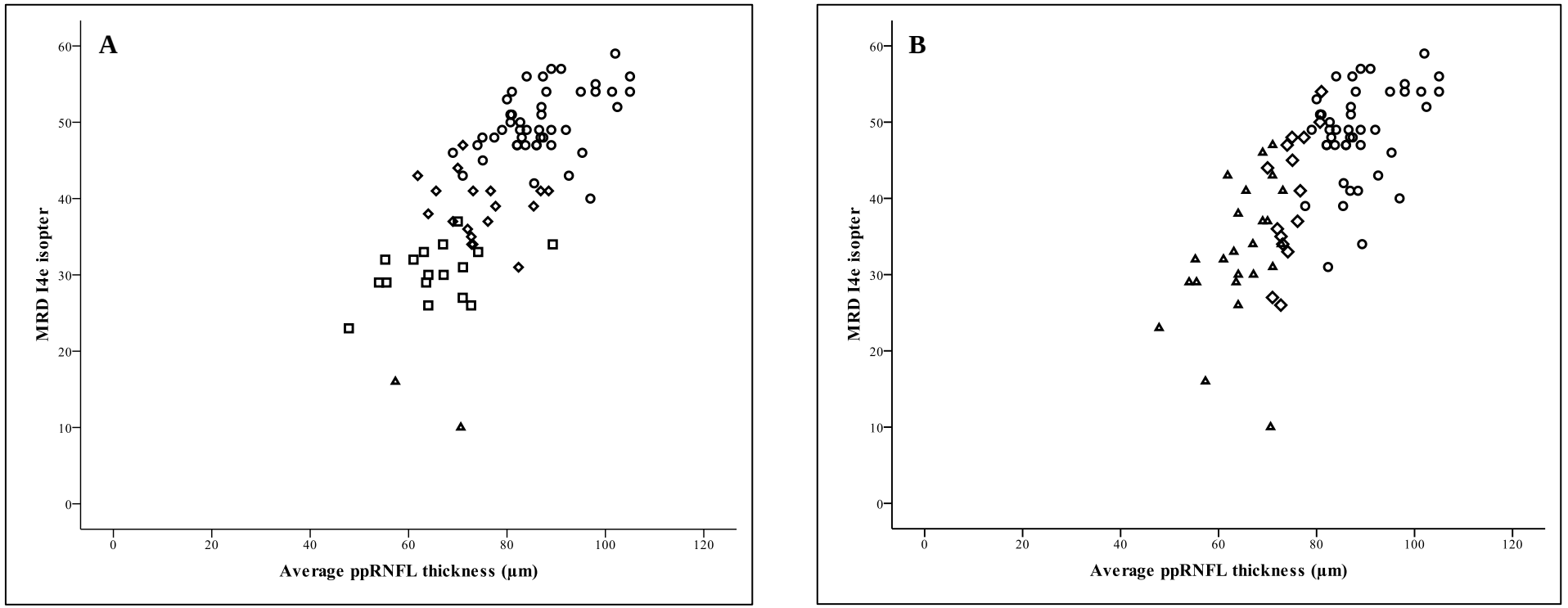

Figure 4.3 legend: There was a correlation between visual field size (MRD) and average ppRNFL thickness in Group 1A. (**A)** Individuals were classified according to the degree of VAVFL (97). Normal (○); mild (◊); moderate (□); severe (Δ). (**B)** Individuals were classified according to which percentile ($\leq 95^{th}$–>5^{th}, $\leq 5^{th}$–>1^{st}, $\leq 1^{st}$) the average ppRNFL thickness falls into, based on the manufacturers' normative database. Normal (○); borderline (◊); abnormal (Δ).

Figure 4.4: Correlation between average ppRNFL thickness and MRD in individuals from Group 1B

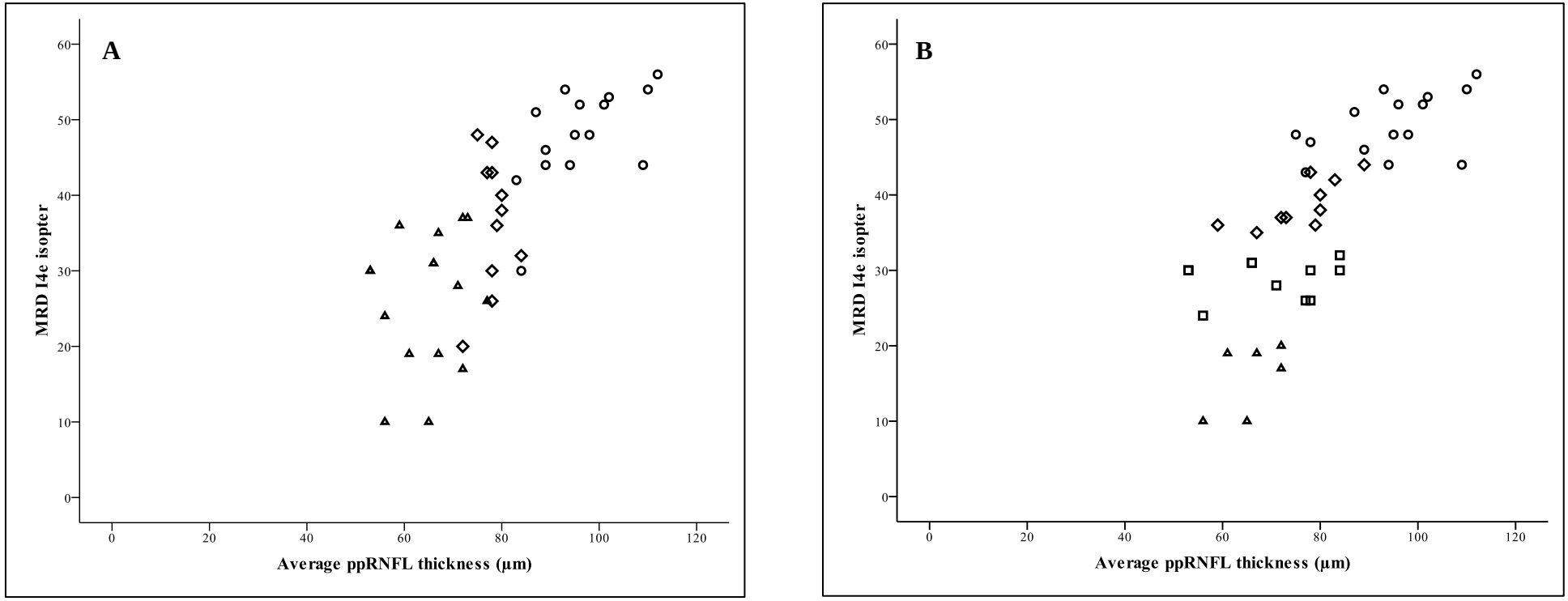

Figure 4.4 legend: There was a correlation between visual field size (MRD) and average ppRNFL thickness in Group 1B. **(A)** Individuals were classified according to the degree of VAVFL (97). Normal (○); mild (◊); moderate (□); severe (Δ). **(B)** Individuals were classified according to which percentile (≤95th–>5th, ≤ 5th–>1st, ≤1st) the average ppRNFL thickness falls into, based on the manufacturers' normative database (285). Normal (○); borderline (◊); abnormal (Δ).

4.4 Discussion

The present study has investigated the prevalence of ppRNFL thinning in a large group of VGB-exposed individuals. In addition, the relationship between structural retinal changes and functional visual field defects was explored. The findings confirm the presence of ppRNFL thinning in VGB-exposed individuals and suggest a linear relationship between average ppRNFL thickness and visual field size measured by MRD. Additionally, ppRNFL thickness measured using OCT was shown to be highly repeatable in a VGB-exposed population of individuals with epilepsy. The importance of the findings from this study are twofold: firstly, they demonstrate the potential for using ppRNFL imaging in the assessment of VGB-exposed individuals, particularly its potential for use in individuals unable to perform perimetry. Secondly, the underlying retinal pathology leading to visual dysfunction is still debated and the structure-function relationship described in this study may provide evidence of the mechanisms leading to irreversible VAVFL.

4.4.1 OCT in individuals unable to perform perimetry

This study found that 19.1% of VGB-exposed individuals were unable to perform reliable perimetry. This is in agreement with previous observations which have found that between 5 and 40% of VGB-exposed individuals could not perform accurate visual field testing (229;256).

Perimetry demands a high degree of attention and co-operation from the subject being examined. Individuals with cognitive impairment may not be able to appreciate the demands of the task. Perimetry requires that the subject maintain fixation for several minutes whilst performing a motor response (i.e. pressing a buzzer) to a moving stimulus presented in their peripheral vision. To realise the task accurately and reliably

requires adequate attention (351), concentration and psychomotor function as well as an understanding of what is required (340). Impairment in any of these domains can impair the subject's ability to perform the task adequately. The time taken to obtain a reliable visual field result can be up to ten minutes or more to enable a thorough assessment of each eye accurately using a range of large and small isopters. This adds further burden to a subject who may fatigue easily, or be unable to maintain sufficient concentration and attention for long periods. These issues are further exaggerated in children where perimetry is often unachievable. It is estimated that up to 80% of VGB-exposed infants and children are unable to perform formalized perimetric testing (122;131;287). In infants perimetry is not possible, creating a great source of contention when considering prescribing VGB for infantile spasms (263), particularly as any signs of VAVFL may not be apparent to parents or carers until the visual field loss is severe (122).

ppRNFL scanning using OCT may provide an alternative tool for the assessment of VGB-exposed individuals, particularly those who are unable to perform reliable perimetry (229). In the present study, only 6.4% of individuals were unable to undergo OCT, and 67% of individuals who were unable to perform perimetry were able to complete OCT. Whilst ppRNFL scanning using OCT does require a degree of co-operation from the subject under examination, it does not require the subject to respond to a stimulus, thus the result is less dependent on the abilities of the individual. To obtain a satisfactory ppRNFL scan, the subject is required to maintain fixation on a target for less than two seconds, without blinking whilst the scan is being performed. With an SD-OCT instrument the scan circle does not have to be accurately aligned around the ONH before the scan is taken as the cube of data obtained during a scan allows movement of the scan circle after acquisition into the required position. In

addition, inbuilt centering software automatically centres the scan around the optic nerve head after it has been acquired. The ability to adjust the scan circle after acquisition, allows shorter chair time for the subject (as this can all be done after the subject has left), which is important particularly in individuals with attention difficulties, and allows for less precise fixation during scanning.

OCT imaging has proved an effective tool in paediatric eye care (352) and been used successfully in the evaluation of children with demyelinating disease (353) and glaucoma (354) and in infants with retinopathy of prematurity (355;356) and shaken baby syndrome (357). Studies using standard table-top TD-OCT in healthy children and children with eye disease have included children from as young as three years old (354;358). In addition, a newly-developed hand-held SD-OCT instrument has allowed the acquisition of retinal images in infants and children whilst in the supine position, both under anaesthesia or sedation (355-357) and without any sedation (355;356). Studies using handheld devices have included infants from 32 weeks old (355).

Current guidelines for assessing VAVFL recommend formal perimetry for individuals with a developmental age of eight years or more, and ERG and confrontation testing for younger subjects, or for those unable to perform perimetry (262;359). ppRNFL imaging using OCT is a useful tool to assess VGB-exposed individuals. In the present study more subjects were able to perform OCT than perimetry, and the technique requires a short chair-time. OCT may be of particular benefit in assessing VGB-exposed individuals who are unable to complete reliable perimetric testing.

4.4.2 ppRNFL imaging is repeatable

In the present study it was shown that measures of ppRNFL thickness using OCT are highly repeatable in VGB-exposed individuals with epilepsy. The ICCs reported in this

study are in keeping with those reported in healthy subjects (346), and in individuals with glaucoma (346;347). 129/180 (71.7%) patients had two OCT scans which were both of adequate quality to include in the analysis[19]. In the remaining individuals only one OCT scan fulfilling the quality control criteria was available for analysis and in some individuals multiple attempts to obtain a high quality OCT scan may be needed. In the clinical setting, stringent quality control criteria should be applied when both performing and evaluating OCT measures of ppRNFL thickness. Some of the most important criteria to consider when obtaining and evaluating ppRNFL thickness scans are outlined here.

4.4.2.1 Signal strength

A signal strength of at least five out of ten (arbitrary units) (as recommended by the manufacturer) should be obtained, as low signal strength can lead to an underestimation of the ppRNFL thickness (330) (Figure 4.5). Consideration of signal strength may be or particular importance when evaluating sequential scans for changes in ppRNFL thickness over time. An apparent decrease in ppRNFL thickness may be related to poor signal strength rather that actual ppRNFL thinning. For example, in the present study, a healthy individual from Group 3 underwent OCT. The first scan revealed an average ppRNFL thickness of 76µm falling within the $\leq 5^{th}$–>1^{st} percentile (borderline thinning). The signal strength was noted to be 5/10 (arbitrary units), and the scan was repeated. Subsequent scans revealed a normal ppRNFL (average ppRNFL thickness 84µm; $\leq 95^{th}$–>5^{th} percentile).

[19] According to the quality control criteria described in 2.6.5

Figure 4.5: The effect of signal strength on measures of ppRNFL thickness

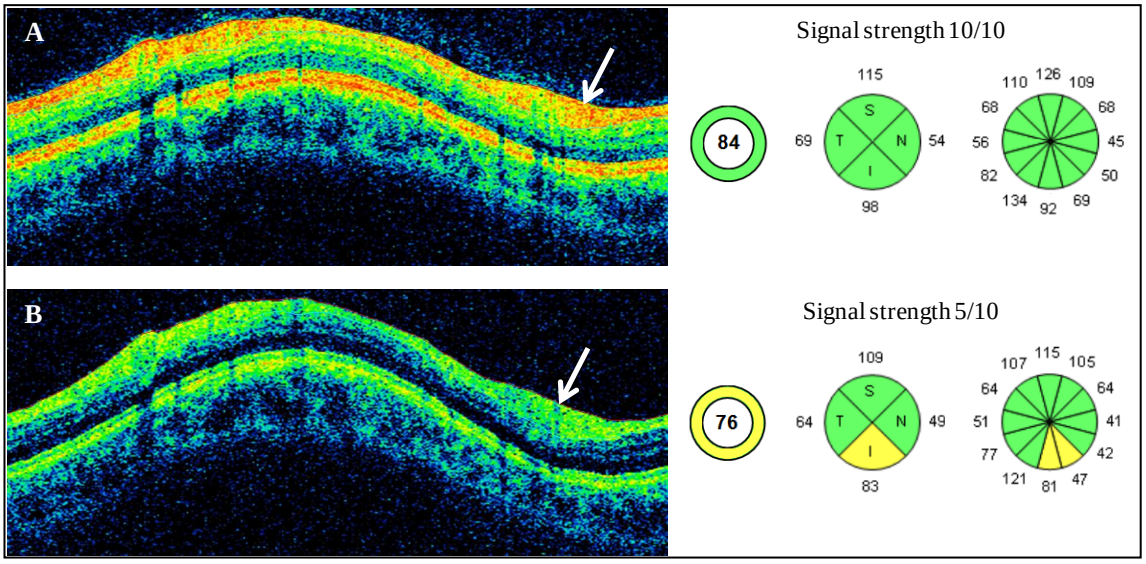

Figure 4.5 legend: Two ppRNFL thickness scans taken during the same scanning session from the right eye of a healthy individual in Group 3. The retinal tomograph with optimal signal strength (10/10 arbitrary units) **(A),** shows a bright red/yellow ppRNFL (white arrow). The corresponding summary measures indicate a normal ppRNFL thickness (average thickness 84µm). In the retinal tomograph with a low signal strength (5/10 arbitrary units) **(B)**, the individual retinal layers (including the ppRNFL (white arrow)) are not as clearly discernable. The summary measures suggest borderline thinning of the ppRNFL (average thickness 76µm); however, this is related to the low signal strength and consequent difficulties with the software algorithm in detecting the ppRNFL boundaries, rather than actual retinal pathology.

4.4.2.2 Movement artefacts and missing data

Where there are significant movement artefacts or missing data, the inbuilt algorithm is unable to detect the inner and outer boundaries of the ppRNFL and ppRNFL thickness cannot be accurately established (Figure 4.6). The effect of incomplete data on measures of ppRNFL thickness can be seen in Figure 4.6. ppRNFL scans taken from an individual during blinking (Figure 4.6B) and eye movement (Figure 4.6C), show markedly different measures of ppRNFL thickness compared to those obtained from a high quality scan (Figure 4.6A). The presence of movement artefacts and missing data

(e.g. due to blinking during scan acquisition) can be evaluated easily by reviewing the fundus image and tomograph immediately after it is obtained. Fundus images and tomographs that demonstrate these irregularities (Figure 4.6) should be discarded and repeated where necessary.

Figure 4.6: The effect of movement artefacts and missing data on measures of ppRNFL thickness

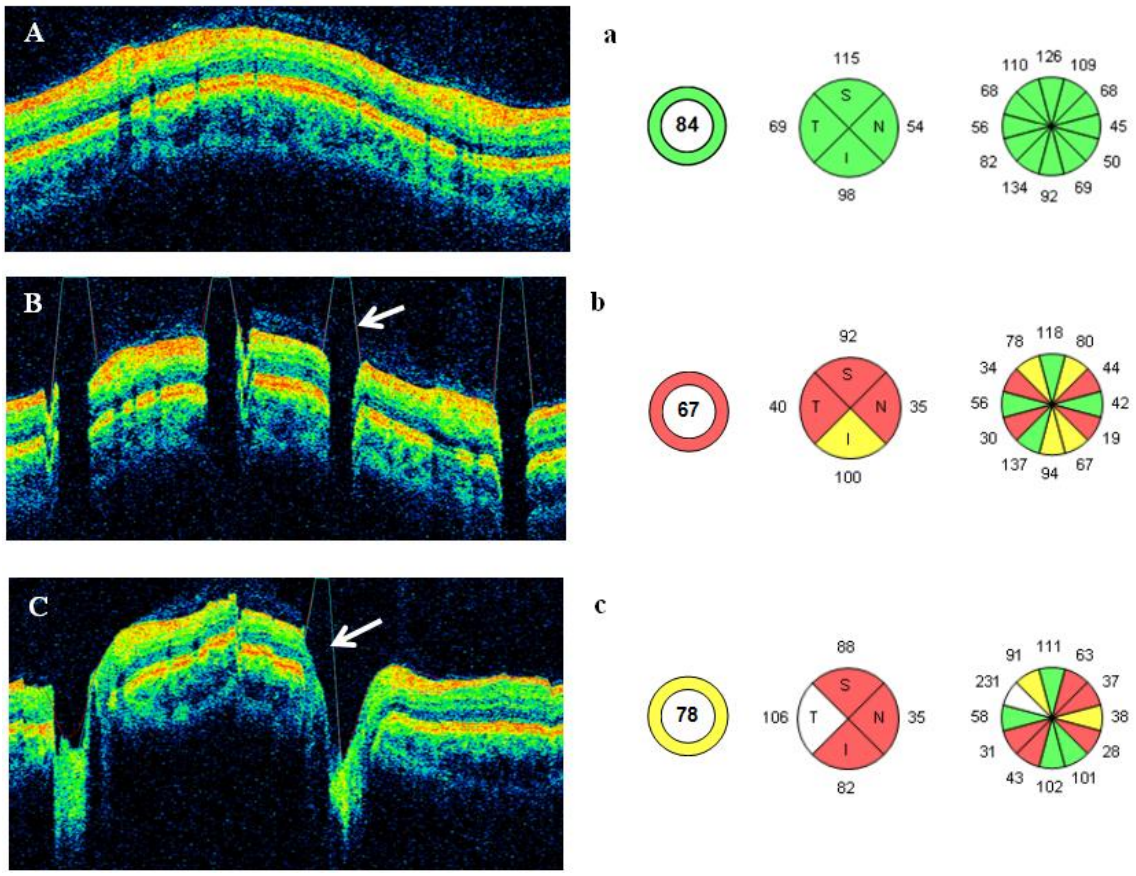

Figure 4.6 legend: Retinal tomographs and ppRNFL thickness data from the right eye of an individual taken during the same test session. **(A)** shows a high quality scan; **(B)** shows a scan with missing data due to blinking during scan acquisition, and failure of the software algorithm to detect ppRNFL boundaries (white arrow); **(C)** shows a scan with significant movement artefact and failure of the software algorithm to detect ppRNFL boundaries (white arrow). The effect of incomplete data on measures of ppRNFL thickness can be seen in the corresponding

summary measures of ppRNFL thickness (**(b)** and **(c)**) which are markedly different from the measures obtained from a high quality scan of the same individual **(a)**.

4.4.2.3 Failure to detect ppRNFL boundaries

Even in apparently good quality scans (i.e. those without movement artefacts or missing data), the acquired tomograph should be carefully evaluated to ensure that the inner and outer boundaries of the ppRNFL have been accurately established by the software algorithm. Small abnormalities in the ppRNFL thickness may go undetected due to image post-processing (360). In addition, incidental retinal abnormalities such as posterior vitreous detachment may lead to a distortion of the ppRNFL boundary detection resulting in inaccurate measures of ppRNFL thickness (e.g.; Figure 4.7).

Figure 4.7: The effect of distortion of the ppRNFL boundaries

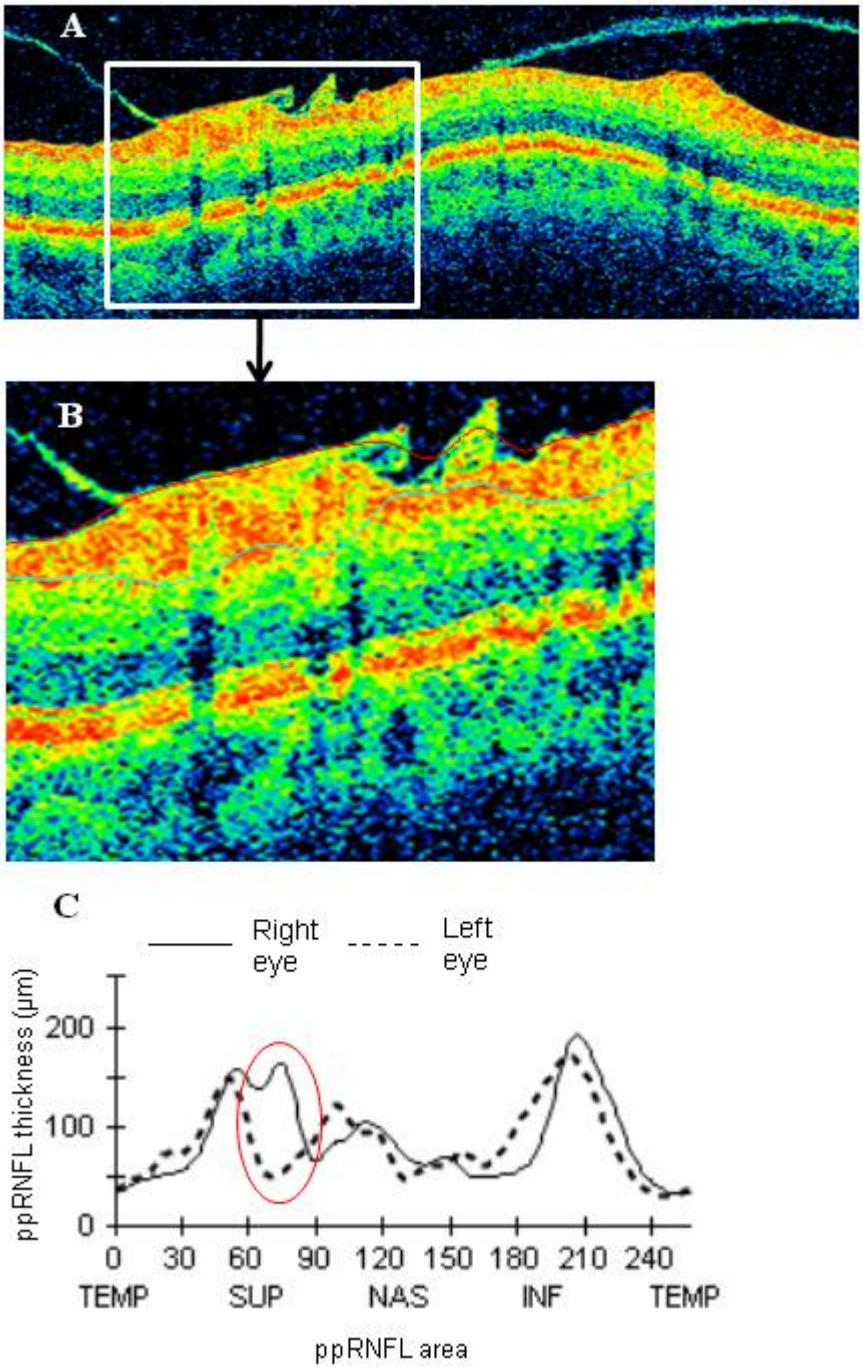

Figure 4.7 legend: Careful inspection of an apparently high quality tomograph **(A)** reveals distortion of the ppRNFL boundary due to posterior vitreous detachment **(B)**. The effect of this on measures of ppRNFL thickness can be seen by comparing the TSNIT plot for each eye **(C)**. ppRNFL thickness is largely symmetrical between the eyes; however, where the ppRNFL boundary is distorted, the ppRNFL thickness is significantly thicker than in the fellow normal eye (red circle).

4.4.2.4 Scan circle placement

The location of the scan circle around the ONH can affect the ppRNFL thickness measurement (327;361) (Figure 4.8). The ppRNFL becomes increasingly thicker at closer proximity to the ONH (362), thus if the scan circle is not accurately centred on the ONH ppRNFL measurements may appear thickener (or thinner) than would be expected if the scan was aligned accurately, and may be interpreted as falsely normal or abnormal (361). This was demonstrated in a VGB-exposed individual from Group 1A. Displacement of the scan circle temporally, superiorly, nasally and inferiorly (Figure 4.8B, C, D and E, respectively) resulted in ppRNFL thickness values that deviated from those recorded when the scan circle was centred on the ONH (Figure 4.8A). Although the average ppRNFL thickness did not change substantially with scan displacement, the ppRNFL thickness in the 90^{o} quadrants and 30^{o} sectors was significantly affected. For example, the ppRNFL thickness in the superior quadrant measured 63µm when the scan circle was centred on the ONH, 73µm when the scan was displaced temporally and 44µm when the scan was displace superiorly (Figure 4.8).

The SD-OCT model used in the present study possesses inbuilt software allowing both automatic and manual centring of the circular scan around the optic disc after scan acquisition. Other OCT models (including the TD-OCT model used in the present study) do not allow this function, and scan alignment is made by the operator before the scan is acquired. In the present study, ppRNFL measurements taken from Group 1A (using SD-OCT) had a lower variability than those taken from Group 1B (TD-OCT). This is in agreement with previous findings in healthy volunteers and in individuals with glaucoma, and probably reflects the shorter scanning time and automatic centring of the circular scan around the optic disc with the newer equipment that utilises spectral-domain technology (363).

Figure 4.8: The effect of scan circle placement on measures of ppRNFL thickness

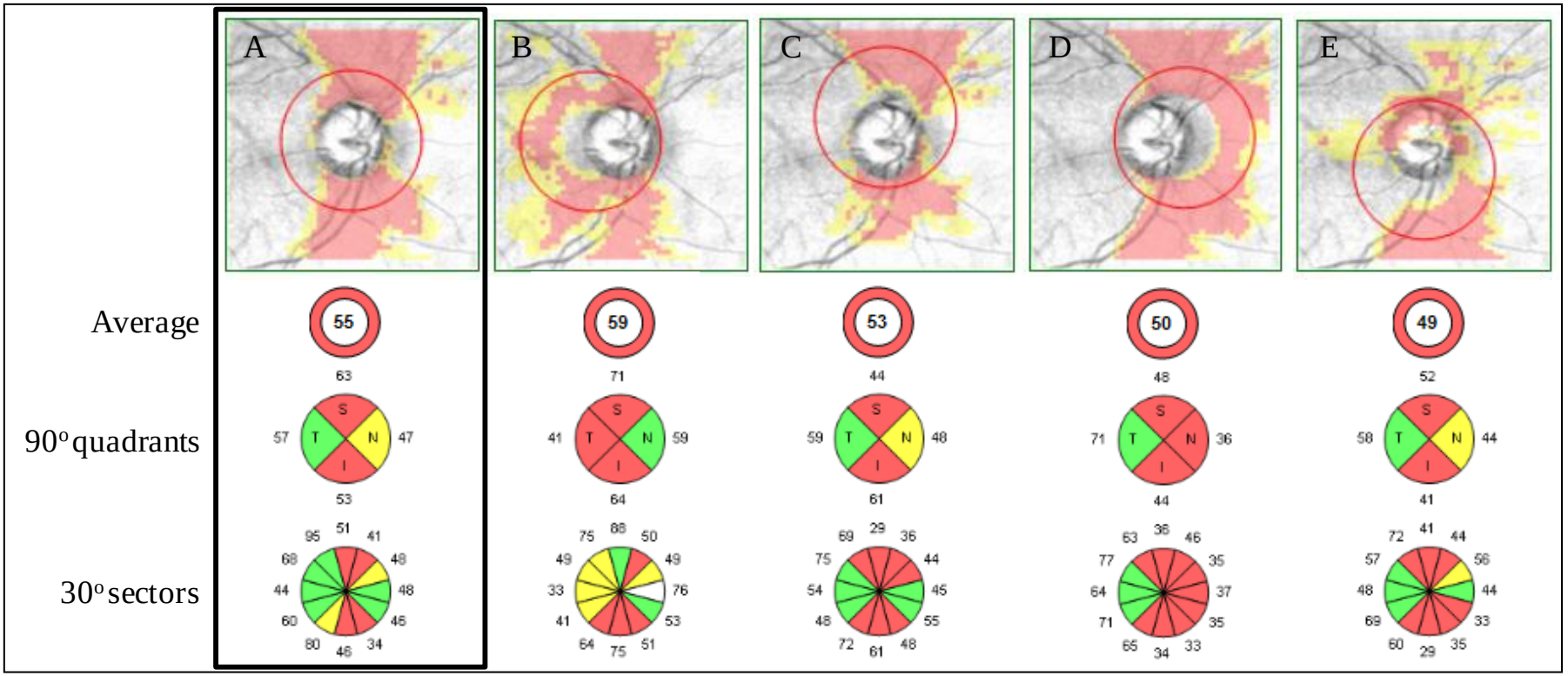

Figure 4.8 legend: A ppRNFL thickness scan was acquired from the right eye of a VGB-exposed individual in Group 1A. The scan circle, which was automatically centred on the ONH **(A)**, was manually displaced after scan acquisition. Displacement of the circular scan, relative to the ONH, temporally **(B)**, superiorly **(C)**, nasally **(D)** or inferiorly **(E)** resulted in ppRNFL thickness values that deviated from those recorded when the scan circle was centred on the ONH.

4.4.3 Prevalence of VAVFL

51.1% of VGB-exposed individuals included in the present study had VAVFL. Previous studies have reported the prevalence of VAVFL to be between 17 and 92% in adults (140), and between 6 and 65% in children (Table 1.1). Recently, a systematic review of observational studies investigating the prevalence of VAVFL was published (91). The review identified 32 studies which met the inclusion criteria, and found that the random-effects estimate for the proportion of vigabatrin-exposed individuals with visual field loss was 52% and 34% for adults and children, respectively (91).

The large range in the reported prevalence of VAVFL could be due to a number of factors (also see Chapter 1). In the present study, visual fields were classified according to the criteria set out by Wild et al. (97). However, studies have used various perimetric techniques to assess the visual field and different methods and criteria to quantify and classify VAVFL (Table 2.5 and 2.6) which could result in differences in the reported prevalence. For example, Vanhatalo et al. defined a normal visual field as one in which the temporal meridian extended beyond 80^{o} eccentricity. However, they showed that if the criteria for normality were reduced by 10^{o} (i.e. a normal visual field was one in which the temporal meridian extended beyond 70^{o} eccentricity) the reported prevalence of VAVFL within the population decreased from 55% to 23% (122). A further contribution to the variation in reported prevalence of VAVFL may come from the VGB exposure characteristics of populations included in each study. Studies including individuals with a long duration of VGB exposure and high cumulative VGB exposure may show higher prevalence of VAVFL compared to studies in which individuals received a lesser degree of VGB exposure. In the present study, the prevalence of VAVFL was 44.8% in Group 1A and 63.6% in Group 1B. All individuals in each Group were assessed by the same operator using GKP and the visual field results were

quantified and classified by the same examiner using the same methods and criteria. However, the mean duration of VGB exposure and the mean cumulative VGB exposure were higher for Group 1B than for Group 1A (Table 2.1) which could account for the difference in prevalence of VAVFL between the Groups.

4.4.4 Prevalence of ppRNFL thinning

In agreement with previous studies (119;229) the present study showed that the ppRNFL was significantly thinner in VGB-exposed individuals compared to healthy controls. In addition it was confirmed that the ppRNFL was significantly thinner in VGB-exposed individuals with VAVFL compared to VGB-exposed individuals with normal visual fields (229).

The prevalence and distribution of ppRNFL thinning was determined according to the manufacturers' normative database. Overall, 62.2% of individuals showed ppRNFL thickness changes (either $\leq 1^{st}$ percentile or $\leq 5^{th}$–>1^{st} percentile) in at least one of the 90^{o} quadrants. Abnormal ppRNFL thinning was most frequently seen in the superior and inferior quadrants, (38.9% and 31.1% of individuals respectively), followed by the nasal quadrant (9.4% of individuals), with few individuals (6.1%) showing thinning in the temporal quadrant.

A pattern of ppRNFL thinning with relative preservation of the temporal quadrant has been described previously in VGB-exposed individuals with VAVFL (198;229;256;258) and is in keeping with the reported pattern of RNFL and optic atrophy detected using fundus photography in which RGC projecting to the temporal aspect of ONH are relatively preserved (147;183;198).

The distribution of ppRNFL thinning detected in the present study, differs from that which has been reported previously. Lawthom et al. reported that in individuals with

VAVFL the nasal quadrant was the most affected quadrant with 11/11 individuals showing ppRNFL thinning (either $\leq 1^{st}$ percentile or $\leq 5^{th}$–>1^{st} percentile) (256). In the study by Lawthom et al. TD-OCT was used and individuals with VAVFL were analysed independently of VGB-exposed individuals with normal visual fields. For comparison, the ppRNFL data from individuals in Group 1B (assessed using TD-OCT), who had VAVFL were compared with the data provided by Lawthom et al. (Table 4.7). The main difference between the OCT findings in the present study and in the study by Lawthom et al. was in relation to the nasal quadrant. In the present study 40.8% of individuals with VAVFL in Group 1B had normal nasal quadrant ppRNFL thickness, whereas 100% of individuals in the study by Lawthom et al. showed ppRNFL abnormities (either $\leq 1^{st}$ percentile or $\leq 5^{th}$–>1^{st} percentile) in the nasal quadrant. In addition, abnormal thinning ($\leq 1^{st}$ percentile) in the superior quadrant was seen considerably more frequently in the present study compared to the study by Lawthom (63.0% and 18.2% of individuals, respectively) (Table 4.7).

The differences in the distribution of ppRNFL thinning between studies are difficult to explain as both studies used the same TD-OCT model and compared data against the same normative database. In addition, all individuals included were classified as showing VAVFL. However, different perimetric techniques, and thus visual field classification criteria, were used in each study. Lawthom et al. used automated perimetry (Humphrey visual field analyser 30-2 program) which only assesses the visual field out to 30^{o} eccentricity. Conversely, in the present study GKP was used

Table 4.7 Comparison of ppRNFL thickness data between individual from Group 1B with VAVFL (N=27) and individuals with VAVFL from Lawthom et al. (N=11) (256)

	Normal ppRNFL thickness (% of individuals)		Borderline ppRNFL thickness (% of individuals)		Abnormal ppRNFL thickness (% of individuals)	
ppRNFL area	**Lawthom**	**This study**	**Lawthom**	**This study**	**Lawthom**	**This study**
Average	0	11.1	27.3	29.6	72.7	59.3
Temporal	100	81.5	0	11.1	0	7.4
Superior	36.4	25.9	45.5	11.1	18.2	63.0
Nasal	0	40.8	27.3	29.6	72.7	29.6
Inferior	27.3	25.9	45.5	37.0	27.3	37.0

11 individuals with VAVFL were included in the study by Lawthom et al. 27 individuals with VAVFL were included from the present study.

which assess the visual field out to 90^{o} eccentricity. It is possible that individuals included in the study by Lawthom et al. had more severe VAVFL than individuals included in the present study, as those with mild VAVFL, not encroaching on the central 30^{o} may not have been included in the VAVFL group in their study. The distribution of ppRNFL thinning may be associated with the severity of VAVFL and thus may differ between studies depending on the severity of VAVFL within a study population. In agreement with the findings in the present study, a recent study using TD-OCT in nine individuals with VAVFL found that 4/9 (44.4%) individuals had normal ppRNFL thickness ($\leq 95^{th}$–>5^{th}) in the nasal quadrant (258).

Based on their findings Lawthom et al. suggested that ppRNFL thinning in the nasal quadrant should be used as a biomarker for VGB toxicity. The discrepancy in findings

between their study and this one shows that further studies are needed to elucidate the pattern of VGB-associated ppRNFL thinning before screening recommendations can be made. The pattern of ppRNFL thinning in VGB-exposed individuals will be discussed further in Chapter 6.

4.4.5 ppRNFL thickness and VAVFL

To compare the ability of OCT ppRNFL imaging to identify retinal structural abnormalities, and Goldmann kinetic perimetry to identify abnormalities of visual function, the results of individuals who undertook both test procedures were analysed. 51% of individuals were classified as having VAVFL whereas 65% were identified as showing thinning[20] in at least one of the 90^{o} quadrants. Interestingly 37% of individuals classified as having normal visual fields showed ppRNFL thinning in at least one of the 90^{o} quadrants, suggesting that thinning of the ppRNFL may be detected before VAVFL becomes clinically apparent. This does not necessarily imply that significant structural change (i.e. RGC loss) must take place before VAVFL occurs. In fact, in this study a linear relationship was observed between ppRNFL thickness and visual field size which would imply that they occur together (i.e. ppRNFL thinning is linearly related to visual field loss) (348). However, because perimetric results are highly variable, even among healthy individuals with normal visual fields (337;341), and the test is subjective and difficult to quantify, the ability to detect clinically significant VAVFL in the early/mild stages may be difficult (348).

In five individuals with mild VAVFL, the ppRNFL thickness was normal in all four 90^{o} quadrants. There are a number of possible explanations for this. Firstly, these individuals could actually have normal visual fields; however, because of psychomotor

[20] Includes <5th percentile and <1st percentile

slowing, impaired reaction time or other cognitive dysfunction, the visual field may have been recorded as smaller than it actually was. Secondly, the ppRNFL also includes a non-axonal component, including glial cells and blood vessels. When ppRNFL thickness is taken to be representative of RGC axon number, it presumes that the non-axonal component of the ppRNFL is equal between individuals and does not change in response to RGC axon loss (348). However, this may not be the case. Some individuals may have a larger contribution to ppRNFL thickness from non-neuronal cells which may maintain their ppRNFL thickness within normal limits despite significant RGC axon loss, thus making ppRNFL imaging less able to detect VAVFL that perimetry. Lastly, dysfunctional RGC (as opposed to dead RGC) may contribute to visual impairment despite maintaining structural integrity. In this case, VAVFL may be apparent in some individuals with normal ppRNFL thickness.

All of the individuals with moderate and severe VAVFL showed ppRNFL thinning in at least one 90^{o} quadrant, suggesting that when VAVFL is advanced both instruments are likely to have sufficient ability to identify individuals who have visual impairment. The value of ppRNFL imaging in this instance might be in detecting the progression of retinal toxicity in individuals who continue VGB therapy, as perimetry may not be sensitive enough to detect subtle changes in VAVFL, particularly over short observation periods[21].

4.4.6 Structure-function relationship

In this study, a strong linear relationship was observed between visual field size and average ppRNFL thickness in VGB-exposed individuals. A relationship between ppRNFL thinning detected using OCT and visual field loss (or reduced visual acuity)

[21] See chapter 3

has been described previously for several diseases including glaucoma (348;349;364), autosomal dominant optic atrophy (365), non-arteritic anterior ischemic optic neuropathy (366) and optic neuritis (367-369). In all of these diseases the principal mechanism of visual impairment is dysfunction or death of RGC in the retinal area corresponding to the visual deficit, due to injury of the RGC axon (370).

Atrophy of the RNFL has also been described in diseases of the outer retina where visual dysfunction is related to degeneration of rod and cone photoreceptors (371). In post mortem eyes from individuals with retinitis pigmentosa, a variable degree of RGC loss was apparent; yet there was little evidence to suggest that RGC loss contributed significantly to the degree visual dysfunction (372). In some individuals with little or no light perception and markedly decreased or absent photoreceptors, the RGC number and RNFL remain within normal limits (372;373). ppRNFL thinning detected using OCT has also been described in individuals with retinitis pigmentosa (374-376) (and other retinal dystrophies including autosomal recessive cone-rod dystrophies (377)). However, no association was found between the degree of ppRNFL thinning and the severity of visual field loss (or change in visual acuity) in any of the studies (374-376). In the retinal dystrophies it is likely that RGC death, and ppRNFL atrophy, occurs as a result of trans-synaptic degeneration after photoreceptor death or dysfunction (371;372); however, it is not the major contributor to visual impairment in such diseases (377).

4.4.7 Mechanisms of VAVFL

The strong association seen in the present study between ppRNFL thinning and decreasing visual field size provides some evidence that irreversible VAVFL may be related to RGC injury. The underlying retinal pathology associated with VAVFL is unknown, and previous animal and human pathological, electrophysiological, clinical and imaging studies have implicated all retinal cell types from the RPE to the RGC.

4.4.7.1 Animal studies – the outer retina

Pathological studies of animals exposed to VGB have consistently reported structural abnormalities in the outer retina, including disorganisation of the ONL with migration of photoreceptor nuclei towards the RPE (64;238-242) and morphological abnormalities and atrophy of cone photoreceptors (238;240-242). It is important to note, that almost all animal studies of VGB retinotoxicity have been carried out on albino strains of mice and rats and probably represent a sensitizing effect of VGB on the retina making the photoreceptors more susceptible to light damage (64;65). The pathological changes described in VGB-exposed albino animals did not occur when they were reared in darkness or low light conditions (63;239). Furthermore, these changes were not seen in pigmented animals exposed to VGB (63-65;243).

4.4.7.2 Human electrophysiological studies – the inner retina

In VGB-exposed individuals electrophysiological data have shown abnormalities in measures reflecting both rod and cone photoreceptor pathways involving the RPE, amacrine cell, bipolar cell and Müller cell function (see 1.10). On the basis of human ERG data most studies have concluded that the mechanisms of VAVFL lie in the inner retina, involving disordered transmission between bipolar, Müller, amacrine and RGCs (81;112;121;146;153). The relationship between ERG abnormities and VAVFL has been explored. In several studies a correlation has been described between reduced amplitude of the b-wave (reflecting bipolar and Müller cell finction) and decreased visual field size (105;109;135;150;151). However, others have reported that OP amplitude (amacrine cell function) (103;112;135) and the 30Hz flicker amplitude (cone pathway function) (106;134) correlate with the severity of VAVFL.

Although the electrophysiological findings almost certainly implicate an effect of VGB on inner retinal electrophysiology, careful inspection of the literature reveals that in

most studies electrophysiological abnormalities are not synonymous with VAVFL, i.e. for all ERG measures that have been found to be abnormal in individuals with VAVFL, they have also been found to be normal in other studies. Further, the same ERG measures are found to be abnormal in some individuals with normal visual fields. The reasons for this are not known. Differences in findings between studies may relate to differences in the VGB-exposed populations included, differences in the electrophysiological methods and analysis of recordings, and differences in the definitions and classification of "normal" and "abnormal" results between studies. However, even within the same studies, where techniques and classifications are standardised across subjects, some individuals on VGB with VAVFL can show ERG abnormalities where others have normal ERG findings (101;104;120;150).

Clearly not all ERG abnormalities are associated with the mechanisms that lead to VAVFL (145). Some aspects of the ERG changes may be physiological, and result directly from the effect of increased GABA concentrations on normal synaptic transmission (145;214). Furthermore, chronic increases in extracellular GABA concentration may lead to down-regulation of GABA receptors (378) and GABA transporters, resulting in changes in retinal electrophysiology that may persist after VGB withdrawal. Other changes in the ERG may reflect pathological abnormalities in retinal electrophysiology, which result from injury to inner retinal cells leading to irreversible changes in cell function and neurotransmission.

4.4.7.3 Human clinical, imaging and pathological studies – the retinal ganglion cells

Inspection of the fundus, either directly or with fundus photography, reveals a normal retina and optic nerve in most individuals with VAVFL (95;147). However, in some individuals, optic disc pallor (78;81;97;101;120;147;183), and atrophy of the peripheral RNFL (78;81;105;106;147;183;198) can be seen. These clinical observations are

supported by findings from a post mortem study of a single individual with VAVFL which found almost complete loss of RGCs, and severe atrophy of the RNFL, in the peripheral retina (162). Recently, the effect of VGB toxicity on RGC has received new attention, as findings from retinal imaging studies further implicate RGC pathology in VAVFL. The ppRNFL is significantly thinner in VGB-exposed individuals compared to healthy controls (119;229) or non-exposed individuals with epilepsy (119;229;258). In addition, VGB-exposed individuals with VAVFL show significantly thinner ppRNFL than VGB-exposed individuals with normal visual fields (229) suggesting that RGC loss may be related to the development of VAVFL.

The strong association seen in the present study between ppRNFL thinning and decreasing visual field size provides further evidence that irreversible VAVFL may be related to loss of RGC (162). If irreversible VAVFL were predominantly due to dysfunction or death of other retinal cells, then it would be unlikely that such a relationship would be seen. For example, if irreversible visual field loss were related to photoreceptor death or dysfunction, and RGC death and ppRNFL atrophy were the result of trans-synaptic degenerative processes, one would expect to see visual field loss in some cases without RGC loss (and ppRNFL thinning) as is seen in retinitis pigmentosa and other retinal degenerations (372;373). Similarly if death or dysfunction of other inner retinal cells including amacrine, bipolar and Müller cell, were directly responsible for irreversible VAVFL, then a more consistent relationship would be expected to be seen between ERG abnormalities and visual field loss. Studies using mfERG add further weight to this argument. Several mfERG studies have demonstrated that electrophysiological abnormalities in individuals with VAVFL are diffuse and are not limited to, or associated with, areas of visual field loss (81;120;134;153).

4.4.8 Mechanisms of VGB retinotoxicity - a theory

Several hypotheses of the mechanisms of VAVFL have been suggested based on the available clinical, electrophysiological and pathological human and animal data, yet there is a lack of unified understanding that brings together, and explains, all of the abnormal findings from various studies of VGB retinotoxicity. From the findings of the present study, alongside a detailed consideration of the existing literature on the effects of VGB on the human and animal visual pathway, a theory is proposed as to the mechanisms of VGB retinotoxicity and the development of abnormal retinal electrophysiology, ppRNFL thinning and VAVFL (Figure 4.9).

VGB irreversibly inhibits GABA-T leading to an accumulation of GABA in retinal cells expressing GABA-T, particularly in Müller cells (234) (Figure 4.9). In addition, VGB increases extracellular GABA by stimulating GABA release (14;23) and reducing GABA uptake (16;23;25) (Figure 4.9). These two mechanisms of VGB-associated increases in retinal GABA (intracellular GABA accumulation and increased extracellular GABA) might have differential effects on retinal physiology and structure.

The high levels of extracellular GABA may alter the physiology of retinal cells expressing GABA receptors, particularly in the highly GABA-immunoreactive IPL of the inner retina, where GABAergic amacrine and interplexiform cells make synaptic connections with GABA receptor-expressing bipolar cells and RGCs. The effect of increased extracellular GABA (alongside alterations in intracellular GABA metabolism) could have both short-term and long-term effects on inner-retinal physiology. Short-term effects may be directly related to increased GABA concentrations in the retina, and are likely to be physiological and reversible on cessation of VGB exposure and return of normal GABA-T activity. The long-term effects of elevated extracellular GABA could be both physiological and/or pathological. Persistently elevated retinal GABA could

result in up- or down-regulation of GABA receptors, GABA-transporters, enzymes involved in normal GABA metabolism and proteins involved in synaptic GABA release. Changes in the expression of these proteins in response to high GABA levels may contribute to abnormal retinal physiology during VGB exposure. Some of the abnormalities may reverse after VGB withdrawal, whilst others may persist. The long- and short-term changes in inner-retinal physiology as a result of elevated GABA may account for the abnormalities reported in the ERG which suggest a predominant effect of VGB on inner retinal function, particularly involving amacrine and bipolar cells.

As extracellular GABA increases, concurrently the inhibition of GABA-T leads to accumulation of GABA within retinal Müller cells (234). Chronic accumulation of GABA within the Müller cell may lead to Müller cell dysfunction and gliosis resulting in loss of normal trophic support and regulation of extracellular environment and release of neurotoxic factors. As a consequence RGC loss occurs (see Chapter 6) manifesting as ppRNFL thinning, optic atrophy and VAVFL.

This theory suggests that VGB-induced increases in retinal GABA may have multiple influences on retinal physiology and structure through several distinct but interrelated mechanisms. Those mechanisms associated with abnormalities in the ERG and EOG may not be directly related to those associated with ppRNFL thinning and the development of VAVFL. Whilst the various mechanisms are inextricably linked, they may exist independently of each other to varying degrees. This model may explain why electrophysiological abnormalities have not consistently been shown to be associated with the presence of, or severity of, VAVFL, and why no electrodiagnostic measure has shown sufficient sensitivity or specificity in identifying individuals with VAVFL (229). Furthermore, it demonstrates how the findings from the present study integrate with and compliment the wealth of earlier research on VGB retinotoxicity.

Figure4.9 A theory as to the mechanisms of VGB retinotoxicity and VAVFL

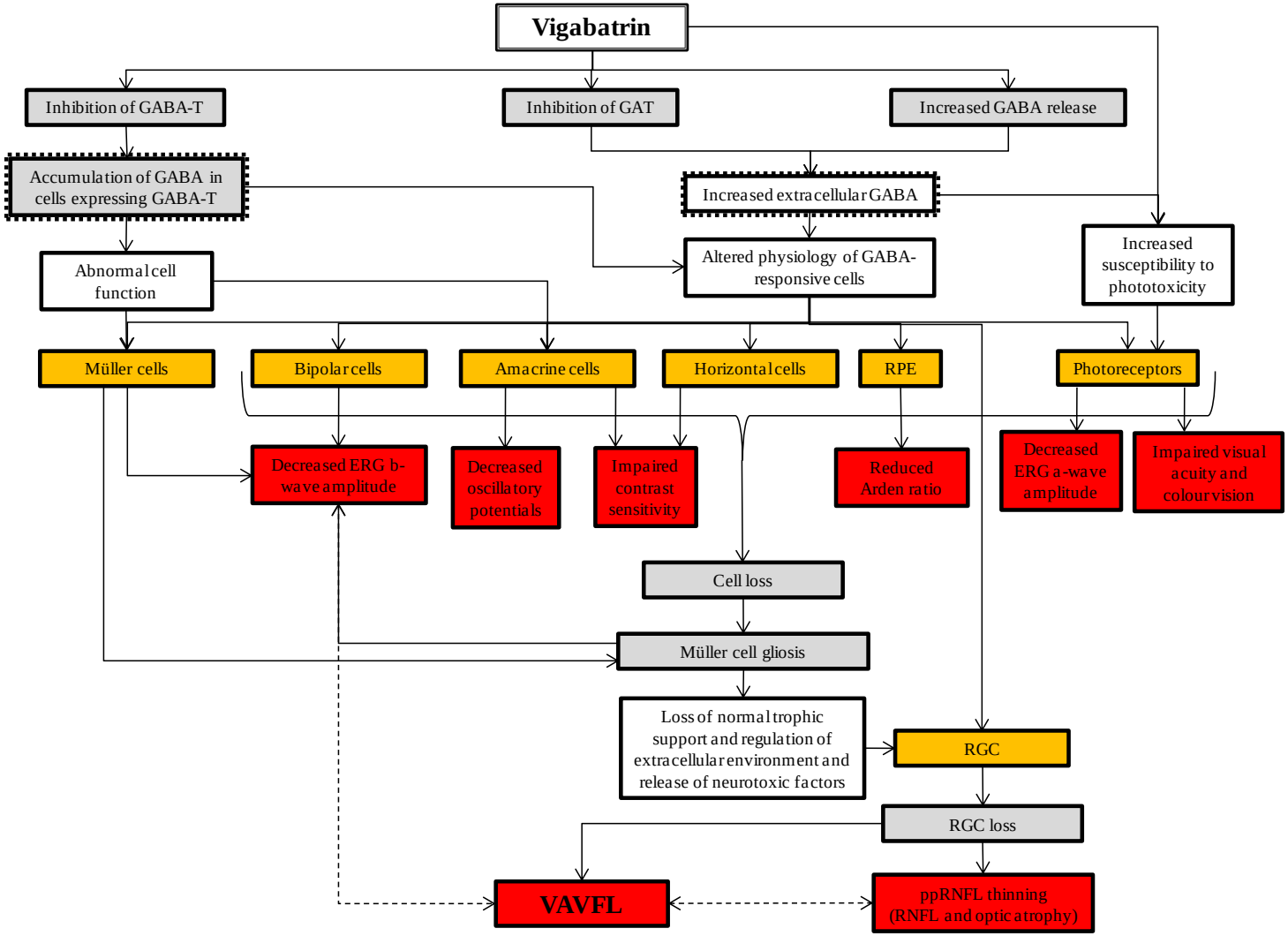

Figure 4.9 legend: GABA = γ-aminobutyric acid; GABA-T = GABA-transaminase; GAT = GABA-transporter; RPE = retinal pigment epithelium; ERG = electroretinogram; RGC = retinal ganglion cell; ppRNFL = peripapillary retinal nerve fibre layer; RNFL = retinal nerve fibre layer; VAVFL = vigabatrin associated visual field loss

Orange boxes = retinal cells; red boxes = human clinical/diagnostic findings; Grey boxes = human and animal pathological/experimental findings; white boxes = theoretical processes; Dashed arrows = clinical/diagnostic findings that have frequently been shown to be associated with each other; Grey dashed line and boxes with grey text = observations only made in VGB-exposed albino rats and mice

4.4.8.1 Summary

VGB appears to have an effect on several retinal cell types, including irreversible, pathological structural and functional changes, as well as reversible physiological changes probably related to elevated GABA concentrations. The mechanisms of VGB toxicity are unknown, and whilst it is apparent that RGC axon loss does occur, there is no clear evidence as to whether the RGC is a primary target of VGB toxicity, or whether RGC axon loss occurs secondary to other retinal cell dysfunction or death. It is possible that the mechanisms responsible for the electrophysiolgocal changes seen in some VGB-exposed individuals are distinct from those related to the development of VAVFL.

Distinguishing those mechanisms that are responsible for irreversible VAVFL is integral to identifying the best screening techniques to use in VGB-exposed individuals. Longitudinal studies using perimetry, retinal electrophysiology and OCT imaging are needed to further elucidate the relationship between the measurements obtained with these techniques to provide a better understanding of the mechanisms and time course of VGB retinotoxicity. Further human pathological data are also needed to better characterise the pathological changes that occur in the retina in VGB-exposed individuals.

Chapter 5 Factors associated with ppRNFL thinning in VGB-exposed individuals

5.1 Introduction

Around 50% of VGB-exposed individuals will develop VAVFL (91) yet currently it is unknown which individuals are most at risk. Whilst some individuals maintain normal visual fields after many years of VGB exposure, others develop severe VAVFL after relatively low VGB doses. Identification of factors that predispose to VAVFL may allow for safer prescribing of VGB in selected individuals (168).

Recently, a large, multicentre study of VAVFL in 386 VGB-exposed adults and children identified higher duration of VGB exposure, and higher mean daily dose of VGB, to be risk factors for VAVFL (92). Several other studies have reported increased risk of VAVFL with increasing cumulative VGB exposure (81;96;113;122;137;163), duration of VGB exposure (81;94;96;108;118;126;137;164), maximum daily VGB dose (107) and mean daily VGB dose (92;109;137) (Table 5.7). Conversely, several other studies have reported no effect of cumulative VGB exposure (95;97-100;104;109;124;164), duration of VGB exposure (95;97;99;100;109;122;124;128;135), maximum daily VGB dose (99;102;108) or mean daily dose (124;126;128;165) on risk of VAVFL (Table 5.7).

The large, multicentre study also reported male gender as a risk factor for VAVFL (92), which is in agreement with previous findings (92;94;95;97;98;103;137;167). Males were more than two times as likely to develop VAVFL compared to females (92;140).

Conversely, other studies have found no increased risk of VAVFL associated with male sex (100;104;122;135).

Increased risk of VAVFL has also been associated with increasing age (108) and co-medication with valproate (108;114;164). However, most demographic, clinical and therapeutic factors have shown no association with increased risk of VAVFL, including; exposure to other AEDs (94;97;137), number of other AEDs exposed to (108;112), age (97;112;122;135), epilepsy syndrome (104;113), duration of epilepsy (94;112), temporal lobe lesions (94), history of status (94) or poor cognitive performance (122).

ppRNFL thickness, measured using OCT, provides an easily quantifiable and repeatable measure of VGB-associated retinal pathology that is highly correlated with the degree of VAVFL[22]. No studies have yet explored factors associated with ppRNFL thinning in VGB-exposed individuals. Identifying factors that are associated with ppRNFL thinning may aid in evaluating the benefits and risks of initiating, or discontinuing, VGB therapy.

5.1.1 Aims

The aims of this study were to identify demographic, clinical and therapeutic factors associated with ppRNFL thinning in VGB-exposed individuals. For comparison of the data acquired in this study with other studies of VAVFL, a relationship between the amount of VGB exposure and the severity of VAVFL was also explored.

[22] See Chapter 4

5.2 Methods

5.2.1 Subjects

VGB-exposed individuals from Group 1A and Group 1B were included in this study.

Demographic details of each Group are provided in Table 2.1[23].

5.2.3 Data analysis

For the analysis of MRD and VGB exposure, data from Group 1A and Group 1B were combined.

For the analysis of clinical, demographic and therapeutic factors and their association with ppRNFL thickness only data from individuals in Group 1A were included. ppRNFL thickness data from Group 1A and Group 1B cannot be combined due to differences in data acquisition between the two instruments (336) and thus data must be analysed separately. In Group 1B OCT data were only available for 51 individuals of whom only 32 had VGB exposure data available, thus the Group was considered to be too small for multivariate analysis.

Data from Group 1B was explored using univariate analysis independently of Group 1A data in analysis regarding cumulative VGB exposure and duration of VGB exposure and ppRNFL thickness.

To determine clinical and therapeutic factors associated with average ppRNFL thickness, statistical analysis of the data (from Group 1A) were completed in three stages in a similar approach to that used by Wild et al. in the analysis of risk factors for VAVFL (92). Firstly, all demographic, clinical and therapeutic variables were explored using univariate analysis to determine whether an association existed with average

[23] See Chapter 2

ppRNFL thickness. Correlation analysis was used for continuous variables (e.g. cumulative VGB exposure and age). Categorical variables (e.g. history of febrile seizures) were explored using independent samples T-test. A p-value of ≤ 0.05 was considered significant. Parametric and non-parametric tests were applied depending on the distribution of the data.

In the second stage, all categorical and continuous variables that were found to be significant in the first analysis were then entered into a standard linear regression model with average ppRNFL thickness as the dependent variable. Finally, variables that were retained in the standard linear regression model ($p \leq 0.05$) were then entered into a final standard linear regression model to determine the combined and unique contribution of each of the variables to the average ppRNFL thickness.

5.3 Results

5.3.1 Subjects and clinical data

Clinical and therapeutic data were obtained from the medical notes as outlined in Chapter 2. OCT data were available for 129 individuals in Group 1A, but, complete clinical and therapeutic data could not be obtained for all individuals[24]. The number of individuals in Group 1A who had OCT data and data regarding each of the clinical and therapeutic factors used in the analysis are shown in Table 5.1.

5.3.2 Relationship between visual field size and VGB exposure

Individuals from Group 1A and Group 1B were included in the analysis. A correlation was found between MRD and cumulative VGB exposure ($r=-0.622$; $p<0.001$;

[24] See Chapter 2

Figure5.1A), duration of VGB exposure (r=-0.525; p<0.001; Figure 5.1B) and maximum daily VGB dose (r=-0.44; p<0.001; Figure 5.1C).

Table 5.1 The number of individuals in Group 1A (with OCT data) with data on each clinical variable

Clinical variable	Total number of individuals with data
Age	129
Gender	129
Cumulative VGB exposure	92
Duration of VGB exposure	92
Max daily VGB dose	92
Duration of epilepsy	120
Age at onset	120
Total number of AEDs exposed to	116
Learning disability	120
Epilepsy phenotype	121
Homonymous visual field defect	84*
History of febrile seizures	97
History of head injury	111
History of status	100
Smoker	59**

*determined from visual field examinations undertaken as part of this study

**data on smoking history was not available from individuals recruited from SEIN

Figure 5.1 Correlation between cumulative vigabatrin-exposure (A), duration of VGB exposure (B) and maximum daily VGB dose (C) and visual field size

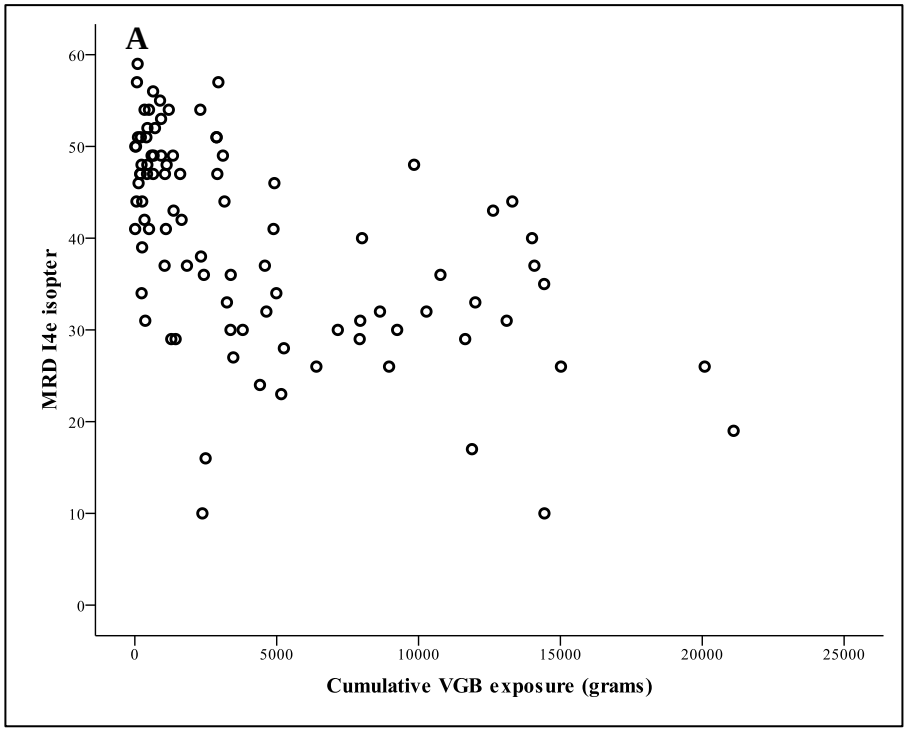

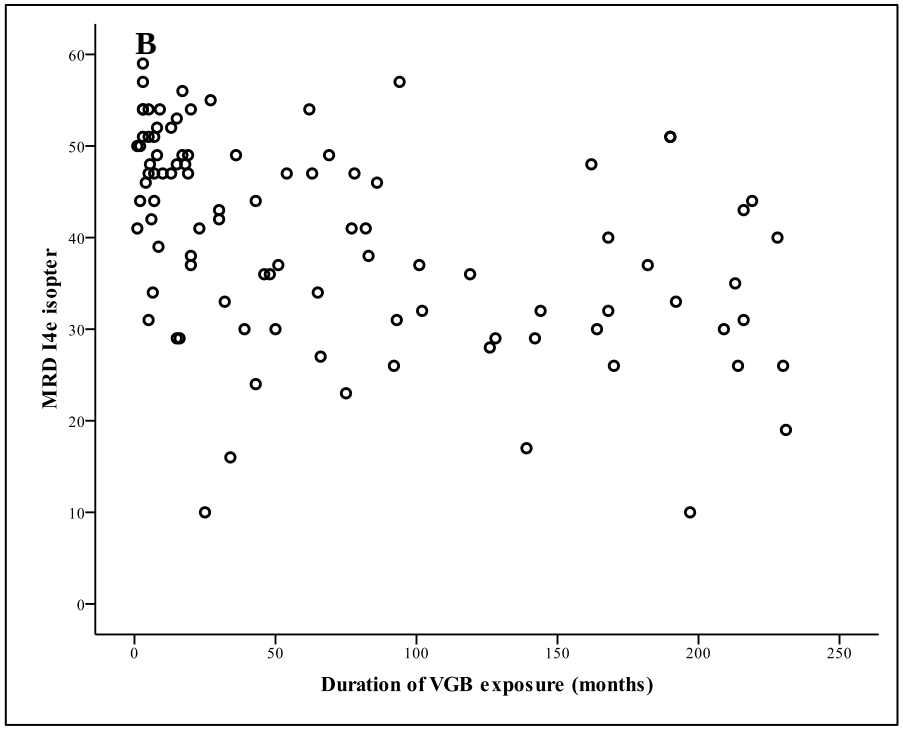

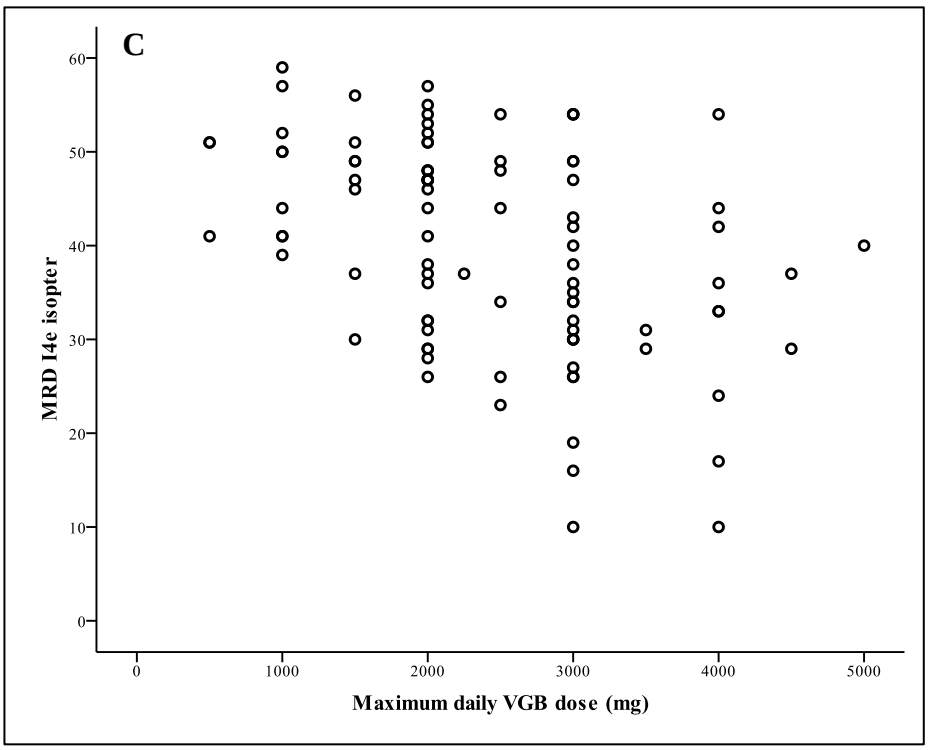

Figure 5.1 legend: Increasing cumulative vigabatrin exposure **(A)**, duration of VGB exposure **(B)** and maximum daily VGB dose **(C)** correlated with decreasing visual field size as measured using MRD.

ppRNFL= peripapillary retinal nerve fibre layer; VGB = vigabatrin

Individuals were grouped according to the severity of VAVFL as defined by Wild et al. (97). The median values of the VGB exposure variables for each Group are shown in Table 5.2.

Table 5.2 The amount of VGB exposure in individuals grouped according to visual field classification

	Normal (N=42)	**Mild VAVFL (N=19)**	**Moderate VAVFL (N=26)**	**Severe VAVFL (N=5)**
Median cumulative VGB exposure (grams) [range]	653.5 [15-14000]	2331.0 [10-14427]	5825.5* [239-20085]	11883.0* [2381-21105]
Median duration VGB exposure (months) [range]	15.0 [1-219]	44.5 [1-228]	97.5* [7-230]	139.0* [25-231]
Median maximum daily VGB dose (milligrams) [range]	2000 [500-4000]	2750 [500-5000]	3000* [1500-4500]	3500* [3000-4000]

VAVFL – vigabatrin associated visual field loss

*significantly different compared to VGB-exposed individuals with normal visual fields ($p<0.008$)

Kruskal-Wallis tests showed a significant difference in cumulative VGB exposure, duration of VGB exposure and maximum daily VGB dose between Groups ($p<0.05$). Post-hoc comparisons were made using Mann-Whitney U tests between each Group. A Bonferroni adjusted p value of 0.008 was used to allow for multiple testing.

In the post-hoc analysis, cumulative VGB exposure, duration of VGB exposure and maximum daily VGB dose were significantly higher ($p<0.008$) in individuals with moderate VAVFL compared to individuals with normal visual fields, and in individuals with severe VAVFL compared to individuals with normal visual fields. No statistically significant differences were found between other Groups.

5.3.3 Step 1 – exploring clinical and therapeutic factors associated with average ppRNFL thickness

5.3.3.1 Continuous variables

In Group 1A, a correlation was found between average ppRNFL thickness and cumulative VGB exposure, duration of VGB exposure and maximum daily VGB dose (Table 5.3; Figure 5.2). No correlation with average ppRNFL thickness was found for age, duration of epilepsy, age of epilepsy onset or number of AEDs exposed to (Table 5.3).

Table 5.3 Correlations between average ppRNFL thickness and continuous variables

	Correlation coefficient (r)	p-value
Cumulative VGB exposure	-0.53	< 0.001
Duration of VGB exposure	- 0.41	<0.001
Maximum daily VGB dose	-0.36	< 0.001
Age	-0.05	0.59
Duration of epilepsy	-0.17	0.17
Age of epilepsy onset	0.12	0.33
Number of AEDs exposed to	-0.19	0.14

5.3.3.2 Relationship between VGB therapy and average ppRNFL thickness in Group 1B

The relationship between VGB exposure and average ppRNFL thickness was also explored for Group 1B. In Group 1B there was no correlation between cumulative VGB exposure, duration of VGB exposure or maximum daily VGB dose and average ppRNFL thickness (r = -0.21 p=0.26; Figure 5.3A; r= - 0.17; p=0.33; Figure 5.3B; r =-0.17; p=0.33; Figure 5.3C respectively).

Figure 5.2 Correlation between cumulative vigabatrin-exposure (A), duration of VGB exposure (B) and maximum daily VGB dose (C) and average ppRNFL thickness for Group 1A

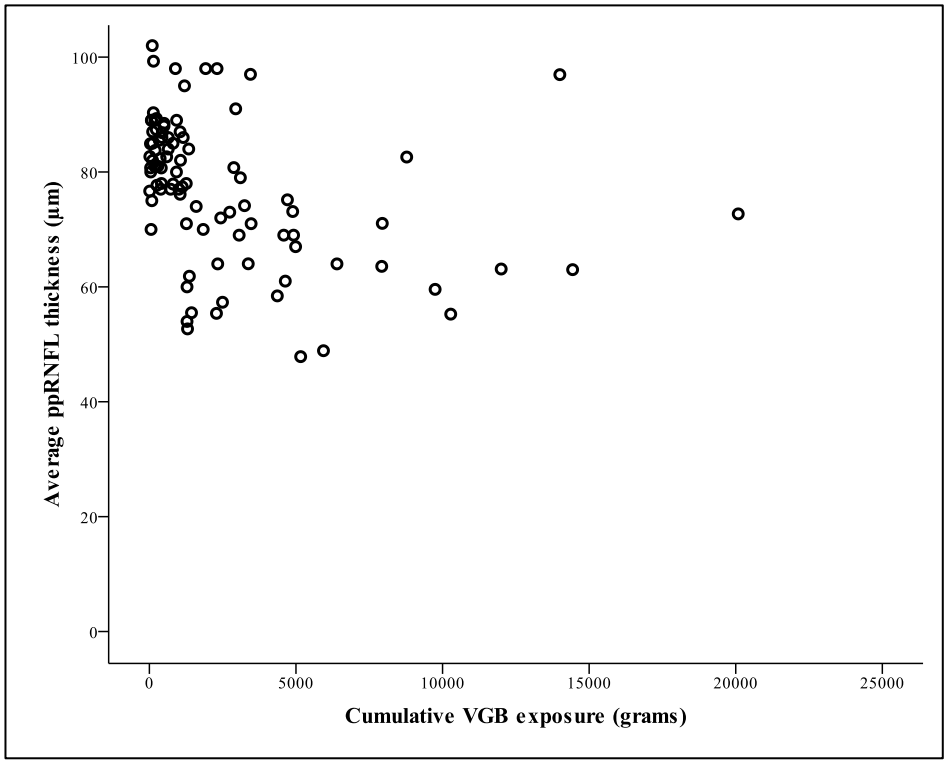

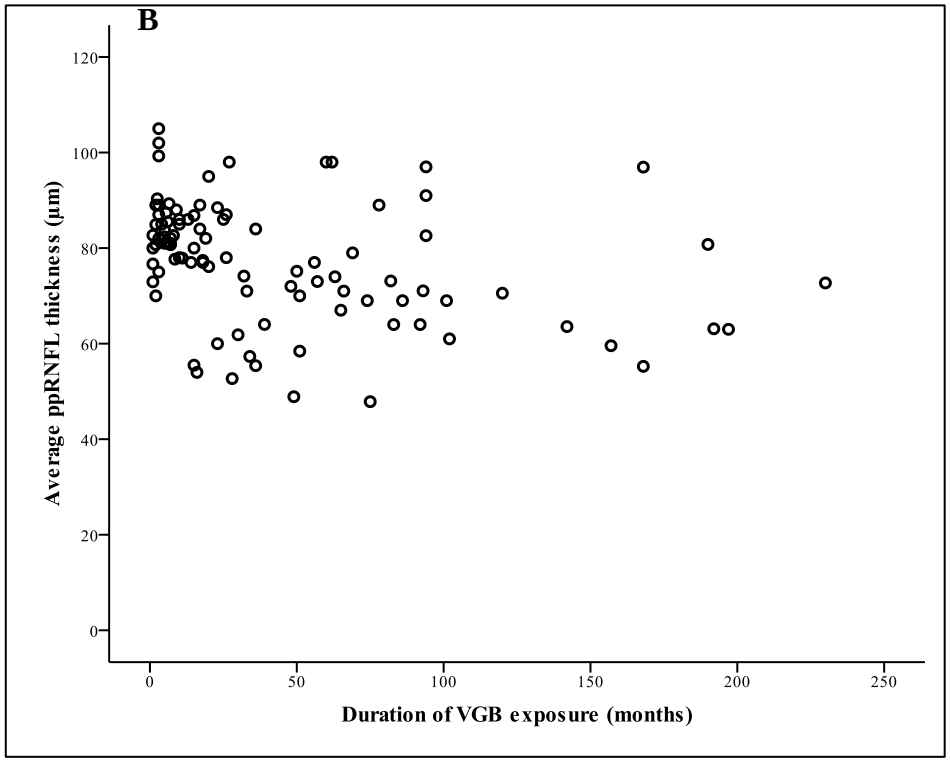

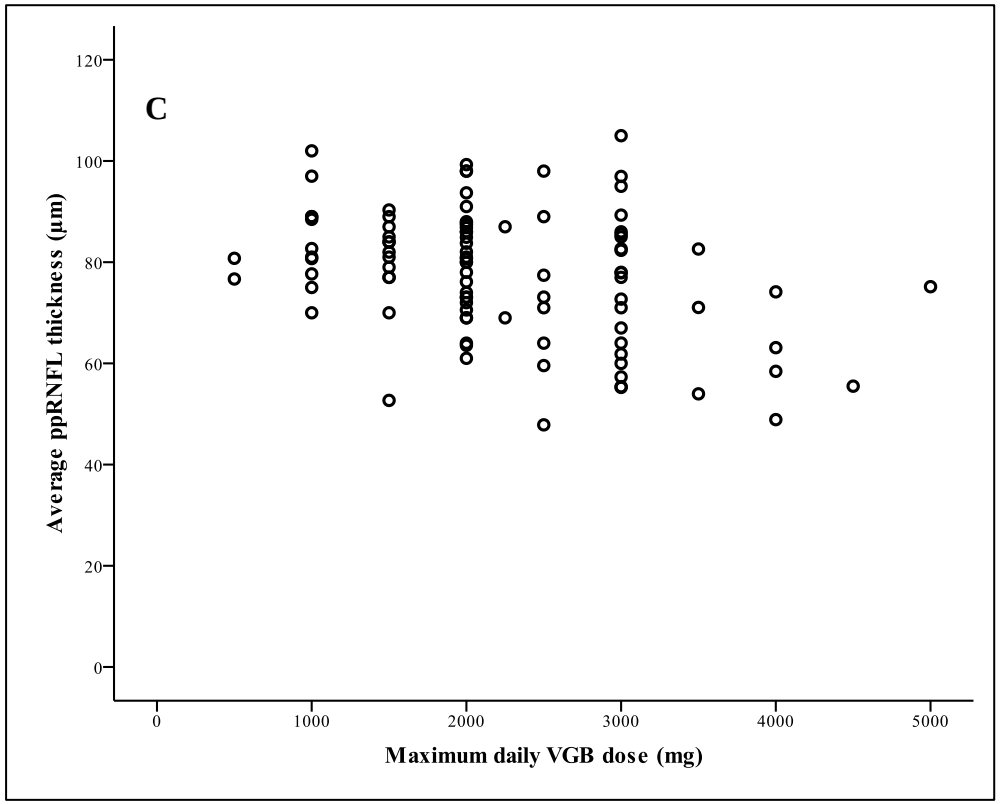

Figure 5.2 legend: Increasing cumulative vigabatrin-exposure **(A)**, duration of VGB exposure **(B)** and maximum daily VGB dose **(C)** correlated with decreasing average ppRNFL thickness.

Figure 5.3 Correlation between cumulative vigabatrin-exposure, and duration of VGB exposure, and average ppRNFL thickness for Group 1B

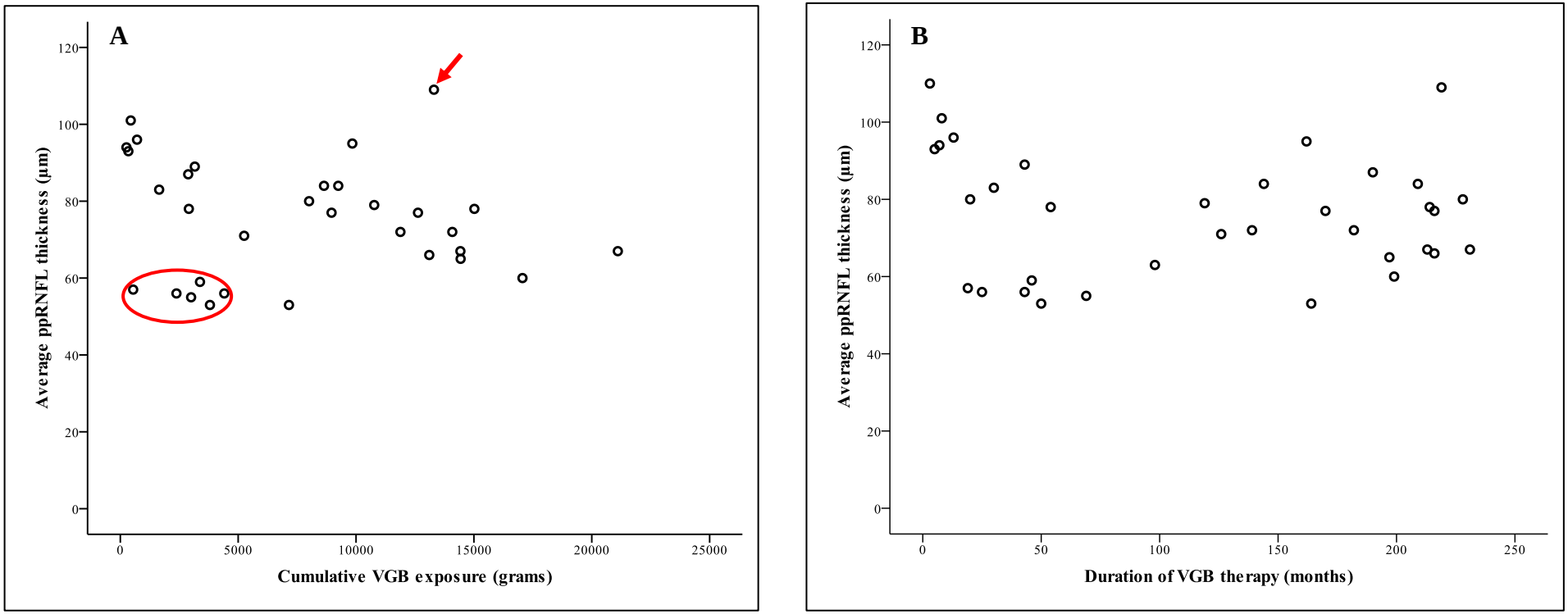

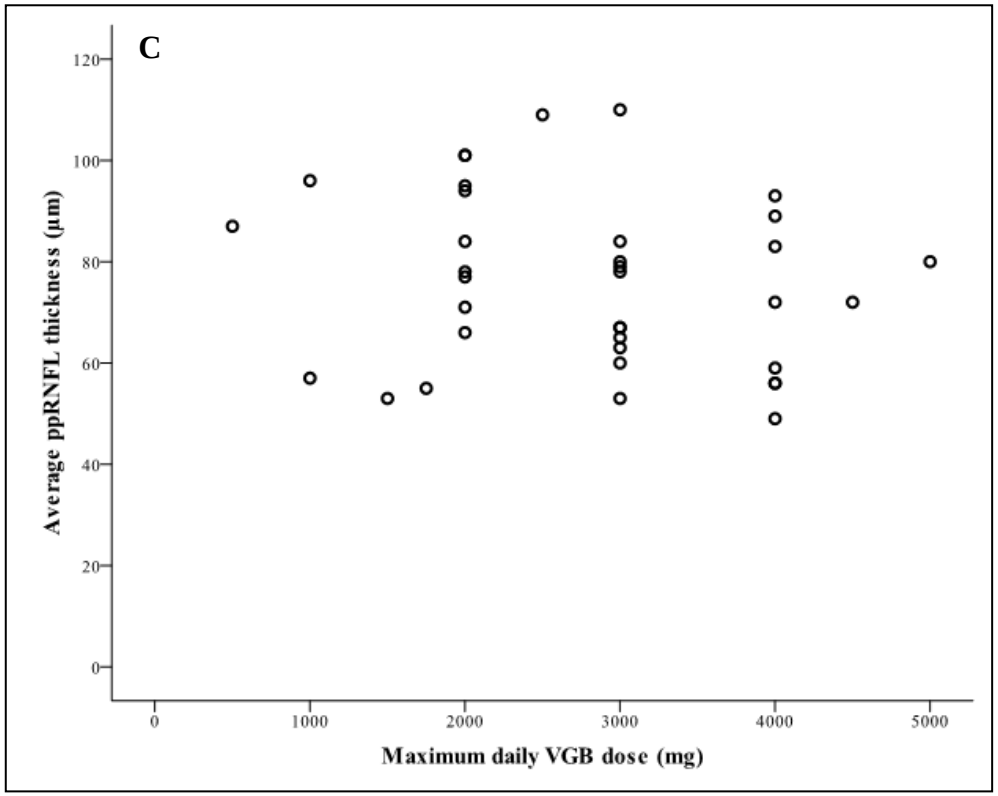

Figure 5.3 legend: In individuals in group 1B there was no correlation between cumulative vigabatrin-exposure **(A)**, duration of VGB exposure **(B)** and maximum daily VGB dose **(C)** and average ppRNFL thickness. Individuals may develop significant ppRNFL thinning after receiving a relatively small cumulative VGB exposure (red circle), whilst others maintain normal ppRNFL thickness despite receiving a large cumulative VGB exposure (red arrow).

5.3.3.3 Categorical variables

The effect of particular clinical features on average ppRNFL thickness was explored using independent samples T-tests. The ppRNFL was significantly thinner in males compared to females (75.3µm and 82.2µm, respectively; p<0.001) and in individuals with homonymous visual field defects compared to those without (72.1µm and 79.7µm, respectively; p=0.01). There was no effect of any other clinical factor, or exposure to any other AED on ppRNFL thickness (p>0.05; Table 5.4).

Table 5.4 Mean average ppRNFL thickness according to clinical and therapeutic factors

	Mean average ppRNFL thickness (µm) (number of individuals)		P value
Variable	**Yes**	**No**	
Smoker	82.2 (15)	77.7 (44)	0.28
History of status	79.5 (14)	77.4 (86)	0.63
History of head injury	78.6 (15)	79.1 (96)	0.93
History of febrile seizure	79.5 (19)	79.1 (78)	0.92
Sex	Male 75.3 (63)	Female 82.2 (66)	<0.001*
LD	78.3	76.8	0.67
Homonymous visual field defect	72.1 (21)	79.7 (63)	0.01*
Acetazolamide	78.7 (28)	76.9 (88)	0.61
Clobazam	77.4	78.6	0.79

	(93)	(23)	
Clonazepam	78.5 (38)	76.9 (78)	0.64
Ethosuximide	78.7 (11)	79.6 (105)	0.87
Felbamate	71.3 (7)	79.4 (109)	0.06
Gabapentin	76.2 (50)	81.1 (66)	0.09
Lacosamide	78.4 (10)	78.9 (106)	0.89
Lamotrigine	79.1 (92)	75.8 (24)	0.45
Levetiracetam	76.7 (83)	81.2 (33)	0.29
Oxcarbazepine	76.9 (43)	79.0 (73)	0.76
Phenobarbital	75.9 (49)	80.5 (67)	0.10
Pregabalin	75.4 (82)	79.7 (34)	0.34
Primidone	75.5 (22)	79.0 (94)	0.14
Phenytoin	76.9 (85)	80.3 (31)	0.40
Valproate	77.4 (90)	78.1 (26)	0.88
Topiramate	78.6 (69)	78.5 (47)	0.99
Tiagabine	76.2 (25)	78.0 (91)	0.64
Zonisamide	80.2 (19)	76.5 (97)	0.32

*significant difference

Only one individual had never been exposed to carbamazepine therefore it was not included in the analysis

At the time of testing less than 5 individuals had been exposed to each of ACTH and chlordiazepoxide therefore these antiepileptic drugs were not included in the analysis.

Epilepsy type

Individuals with hippocampal sclerosis (N=34); malformations of cortical development (N=18) and individuals with partial epilepsy of unknown cause (N=40) were compared using one-way ANOVA. There was no significant difference in average ppRNFL thickness between these groups ($p>0.05$).

Individuals with other epilepsy types included those with angioma or vascular malformation, stroke, infection, neurocutaneous syndromes, tumour and trauma. These individuals were not included in the analysis due to the small numbers of individuals within each group.

5.3.4 Step 2 – Multiple regression

In step one of the analysis, cumulative VGB exposure, duration of VGB exposure, maximum daily VGB dose, sex and homonymous visual field defect were found to be significantly associated with average ppRNFL thickness. These variables were entered into a standard linear regression model to determine the combined and unique contribution of each VGB exposure variable to average ppRNFL thickness.

The total model explained 30.8% of the variance in average ppRNFL thickness (R Square = 0.308; $p<0.001$). The contribution of each individual variable in the model was compared (Table 5.5). Cumulative VGB exposure and duration of VGB exposure did not contribute uniquely to this model (cumulative VGB exposure (beta=0.019; $p=0.935$), duration of VGB exposure (beta=-0.283, $p=0.201$).

Table 5.5 Standardised Beta coefficients and p-values for all variables in the Step 2 model

Variable	Beta	p-value
Cumulative VGB exposure	0.019	0.94
Duration of VGB exposure	0.283	0.20
Maximum daily VGB dose	0.296	0.01*
Gender	0.228	0.02*
Homonymous visual field defect	0.246	0.01*

*Significant ($p<0.05$)

The regression analysis showed that cumulative VGB exposure and duration of VGB exposure were highly correlated ($r=0.88$; $p<0.001$), indicating multicollinearity. When multicollinearity is present within a regression model, results regarding the contribution of individual variables to the model may be misleading (e.g. a p-value may not indicate significance, even though the variable is contributing). In this case, one of the contributing variables should be omitted from the model (379)[25]. As cumulative VGB exposure was calculated from duration of VGB exposure and daily VGB dose (which includes maximum daily VGB dose), cumulative VGB exposure was excluded from the model.

5.3.5 Step 3 – The final model

A final model was created after excluding cumulative VGB exposure. The total model explained 30.8% of the variance in average ppRNFL thickness (R Square = 0.308;

[25] In some cases collinear variables can also be combined to form one new independent variable which can then be included in the model.

p<0.001). The contribution of each individual VGB exposure variable in the final model was compared (Table 5.6), and showed that all of the variables included in the model contributed significantly (p<0.05) to average ppRNFL thickness. Maximum daily VGB dose made the strongest unique contribution to average ppRNFL thickness (beta -0.291), uniquely contributing to 8.1% of the total variance in average ppRNFL thickness, (derived from squaring the Part correlation coefficient (-0.285^2 x 100)) (379).

Table 5.6 Standardised Beta coefficients and p-values for all variables in the final model

Variable	**Beta**	**p-value**	**Part correlation coefficient**
Duration of VGB exposure	-0.267	0.007*	-0.261
Maximum daily VGB dose	-0.291	0.003*	-0.285
Sex	-0.228	0.02*	-0.227
Homonymous visual field defect	-0.246	0.01*	-0.245

*Significant (p<0.05)

5.4 Discussion

5.4.1 Clinical and therapeutic factors associated with average ppRNFL thickness

This is the first study to explore clinical and therapeutic factors associated with ppRNFL thinning in VGB-exposed individuals. Cumulative VGB exposure, duration of VGB exposure, maximum daily VGB dose, male gender and the presence of a homonymous visual field defect were found to be independently associated with

average ppRNFL thickness in individuals in Group 1A. After entering these variables into a standard linear regression model, cumulative VGB exposure was excluded due to multicollinearity with duration of VGB therapy. A final model showed that duration of VGB exposure, maximum daily VGB dose, male gender and the presence of a homonymous visual field defect were both independently and collectively associated with average ppRNFL thickness and explained 30.8% of the variance in average ppRNFL thickness.

5.4.2 The relationship between VGB exposure and VGB retinotoxicity

Although a correlation was found between average ppRNFL thickness and cumulative VGB exposure, duration of VGB exposure and maximum daily VGB dose for Group 1A (Figure 5.2), no association was found for Group 1B (Figure 5.3). Only one other study has discussed the relationship between ppRNFL thickness measured using OCT, and degree of VGB exposure. Lawthom et al. demonstrated a weak correlation between increasing cumulative VGB exposure and decreasing ppRNFL thickness in the nasal quadrant in 27 individuals (256). Conversely, using scanning laser polarimetry, cumulative VGB exposure and duration of VGB exposure were not found to correlate with any measures of ppRNFL thickness, (including average, superior, inferior and nerve fibre indicator), in eight VGB-exposed individuals (257).

The inconsistency in findings between studies, and within this study, regarding the relationship between the degree of VGB exposure and the degree of ppRNFL thinning reflects the contradicting evidence in the literature concerning the relationship between increasing VGB exposure and increased risk of VAVFL. In the present study, increasing cumulative VGB exposure, duration of VGB exposure and maximum daily VGB dose were associated with decreasing visual field size (as measured using MRD) (Figure 5.1). In agreement, increasing cumulative VGB exposure

(81;96;113;122;137;163), duration of VGB exposure (81;94;96;108;118;126;137;164), maximum daily VGB dose (107) and mean daily VGB dose (92;109;137) have been associated with increased risk of VAVFL in some studies (Table 5.7). However, several other studies have reported no effect of cumulative VGB dose (95;97-100;104;109;124;164), duration of therapy (95;97;99;100;109;122;124;128;135), maximum daily VGB dose (99;102;108) or mean daily dose (124;126;128;165) on risk of VAVFL (Table 5.7).

Table 5.7 Summary of studies exploring an association between the amount of VGB exposure and the risk of VAVFL

Reference	Number of individuals	Method to determine association between VGB exposure and VAVFL	Association between VGB exposure and VAVFL		
			Cumulative VGB exposure	Mean daily VGB dose	Duration of VGB exposure
Wild 2009 (92)	386	Individuals were grouped by visual field classification. Groups included "VAVFL" and "no VAVFL" Univariate analysis was used to identify variables associated with VAVFL. Significant variables from this analysis were then put into a step-wise multivariate logistic regression model. Variables retaining significance in the model were transformed into categorical variables and odds ratios were determined	N[d]	Y	Y
Hardus 2000 (94)	109	Individuals were grouped by duration of VGB exposure. Groups included "0-2years", "2-4years" and ">4years VGB exposures" Differences in the amount of visual field loss (using the Esterman grid) between groups was assessed using one way ANOVA	NA	NA	Y[c]
Newman 2002 (95)	100	Individuals were grouped by visual field classification. Groups included visual	N	NA	N

		field size of ">30MRD" and "<30MRD" Differences in VGB exposure between groups were assessed using ANOVA○			
Malmgren 2001 (96)	99	Individuals were grouped by visual field classification. Groups included "normal" and "visual field loss" Differences in VGB exposure between groups was assessed using a Mann Whitney U test	Y	NA	Y
Nicolson 2002 (98)	98	Individuals were grouped by cumulative VGB exposure. Groups included "<2KG", "2-4KG", "4-6KG", "6-10KG", ">10KG cumulative VGB exposure" Differences in the frequency of visual field loss between the groups were assessed using a chi squared test●	N	NA	NA
Kinirons 2006 (99)	93	Correlation between visual field size (MRD) and VGB exposure variables	N	N[a]	N
This paper	**92**	**Spearman correlation between visual field size (MRD) and VGB exposure variables** **Individuals were grouped by visual field status. Groups included "normal", "mild VAVFL", "moderate VAVFL" and "severe VAVFL"** **Differences in VGB exposure were assessed using A Kruskall Wallis test**	**Y[β]**	**Y[aβ]**	**Y[β]**

		with post-hoc analysis using Mann-Whitney U Test			
Hardus 2001 (137)	92	Correlation between percentage visual field loss and VGB exposure Linear regression to identify factors associated with visual field size	Y	Y	Y
Vanhatalo 2002 (122)	91	Individuals were grouped by visual field classification. Groups included "normal" and "abnormal" visual fields Differences in VGB exposure between the groups were assessed using T-tests Linear regression of temporal visual field extent and VGB exposure variables*	Y*	NA	Y* #
Nousiainen 2001 (100)	60	Linear regression using the extent of the visual field in the Temporal, Superior, Nasal or Inferior meridians and VGB exposure	N	NA	N
Arndt 2002 (164)	52	Correlation between visual field size and VGB exposure	N	NA	Y
Wild 1999 (97)	42	Individuals were grouped by visual field classification. Groups included "VAVFL" and "non-VAVFL"** Individuals were grouped by duration of VGB exposure. Groups included "<4 years" and ">4 years of VGB exposure" No statistical tests applied	N	NA	N

Tseng 2006 (102)	34	Individuals were grouped by visual field classification. Groups included "no visual field defect", "visual field defect" Differences in VGB exposure between the groups were assessed using Mann Whitney U test and Fisher's Exact Test. Logistic regression was also performed.	N	N[a]	N
Kalviainen (1999) (104)	32	Correlation between the extent of the visual field in the Temporal, Superior, Nasal or Inferior meridians and VGB exposure	N	NA	N
Conway 2008 (107)	31	Multiple regression between severity of visual field loss and VGB exposure	N	Y[a]	N
Werth 2006 (124)	30	Pearson correlation between visual field size and VGB exposure ◊	NA	N	N
van der Torren (109)	29	Correlation between extent of nasal visual field and VGB exposure	N	Y	NA
Harding 2000 (165)	26	Individuals were grouped by visual field classification. Groups included "no VAVFL", "mild/moderate VAVFL" and "severe VAVFL" No statistical tests applied.	Y	N	N
Schmitz 2002 (108)	23	Individuals were grouped by visual field classification. Groups included "visual field loss" and "no visual field loss". Differences in VGB exposure between groups were assessed using Mann Whitney U test	NA	N[a]	Y

Manuchehri 2000 (113)	20	Spearman correlation between percentage total visual field loss and VGB exposure	Y	NA	NA
Gross-Tsur 2000 (126)	17	Biserial correlation between "ocular dysfunction"♦ and VGB exposure	NA	N	Y
Lawden 1999 (81)	16	Individuals were grouped by visual field classification. Groups included "VAVFL" and "no VAVFL" No statistical tests applied.	Y	NA [a, b]	NA[b]
Ascaso 2003 (128)	15	Individuals were grouped by visual field classification. Groups included "normal" or "visual field defect" Differences in VGB exposure between the groups were assessed using T-tests□	NA	N	N
Toggweiler 2001 (118)	15	Repeated measures ANOVA with VGB exposure variables as covariates	NA	NA	Y[∞]
Comaish 2002 (135)	14	Correlation between visual field size and VGB exposure	NA	NA	N
Frisen 2004 (163)	10	Linear regression between "hit rate" in the temporal and nasal visual field and VGB exposure	Y	NA	NA

Where "no statistical tests were applied" conclusions regarding differences in VGB exposure between groups were made on observations of the data.

[a]Maximum daily VGB dose analysed

[b]Summary measures of these available in paper but not statistically assessed or discussed by authors

[c]However, there was a plateau effect (i.e. there was no difference in % visual field loss in the 2-4 year exposure and 4-6 year exposure groups)

[d]Lost from multiple regression after duration of therapy and mean daily dose added (due to multicollinearity)

#There was a significant difference in cumulative VGB exposure between the "normal" and "abnormal" visual field groups, but no significant difference was found for the duration of VGB exposure between groups (independent samples T-test).

*Using linear regression a correlation was found between the temporal extent of the visual field and the cumulative VGB exposure and duration of VGB exposure. However, there was no relationship when the extent of the nasal visual field was used.

**The "no VAVFL" group was comprised of 12 individuals, 2 of whom had "unreliable" visual field test results and 6 had "uninterruptable" test results. Some of these individuals may have had VAVFL

♦Measures of "ocular dysfunction" included abnormalities in perimetric studies, VEP and ERG

□Only 3 individuals in the "visual field defect" group

●No post-hoc analysis (there appeared to be a difference between the <2 (30%) and > 10 kg (53%) group)

○The ">30MRD" group would include individuals with normal visual fields and individuals with mild/moderate visual field loss

◊Non-commercial arc-perimeter used which may not be accurate enough to detect small changes in the peripheral visual field

[β]Post-hoc analysis revealed statistical differences ONLY between individuals with normal visual fields and those with either moderate or severe VAVFL

∞There was no association for the inner-most isopter tested (I1e)

The conflicting findings between studies regarding the relationship between the degree of VGB exposure and the development of retinotoxic sequela (i.e. ppRNFL thinning and VAVFL) may be due to several factors.

5.4.2.1 Small sample sizes

A number of the studies exploring associations between VGB exposure variables and risk of VAVFL have been based on small populations. Eleven of the 25 studies identified in this review of the literature included 30 or fewer participants (Table 5.7). Small studies may have insufficient power to detect a significant association between VGB exposure and risk of VAVFL. For example Ascaso et al. (128) reported no difference in the duration of VGB exposure, and mean daily VGB dose between individuals with and without VAVFL. However, the study included only 15 individuals with just three individuals comprising the VAVFL group. In some studies statistical analysis was not performed (possibly due to small sample sizes), and conclusions regarding VGB exposure variables and risk of VAVFL were based upon observations of the data (81;165).

Within a VGB-exposed population there appear to be "extreme responders", i.e. those individuals who develop significant VAVFL or ppRNFL thinning after receiving a relatively small exposure to VGB (Figure 5.3), and others who maintain normal vision and ppRNFL thickness despite receiving a large exposure (Figure 5.3). These "outliers" within a dataset may affect the ability to identify correlations and association between variables, particularly if the number of observations is small (380). In Group 1B, extreme responders were particularly apparent (Figure 5.3). In this Group only 32 individuals had both OCT and VGB dose data, the small sample size and the presence of extreme responders could account for the lack of association seen in the present study in Group 1B between the degree of VGB exposure and ppRNFL thickness.

5.4.2.2 The visual field variable

In this study the visual field was analysed as both a continuous (quantitative) variable (i.e. visual field size as measured by MRD) and a categorical variable (i.e. "normal", "mild VAVFL", "moderate VAVFL" and "severe VAVFL"). Other studies have also used both approaches (Table 5.7). For analysis of the visual field and its association with the degree of VGB exposure, the visual field recorded from the chosen perimetric technique has to be quantified and/or classified according to certain criteria. The lack of a standardised method to quantify and classify visual field size (or the size of a visual field defect) has resulted in the use of different techniques in different studies (see Table 2.5 and 2.6). For example, in a study of 91 VGB-exposed children, a correlation was found between the degree of VGB exposure (cumulative exposure and duration of exposure) and the extent of the temporal visual field (in degrees). However, no correlation was found between the degree of VGB exposure (cumulative exposure and duration of exposure) when the extent of the nasal visual field (in degrees) was analysed (122). In a different study, a relationship was found between decreasing size of the outer isopters (V4e, I4e, I3e and I2e) of the visual field and increasing duration of VGB exposure; however, the size of the inner-most isopter was not associated with duration of VGB exposure (118).

Similarly, when classifying VAVFL, differences in the criteria used to determine whether a visual field shows normal, mild or severe VAVFL may contribute to the variation in results seen between studies. In some studies, determination of the relationship between VAVFL and the degree of VGB exposure was carried out by comparing individuals grouped according to visual field status (i.e. VAVFL or normal visual fields) (81;92;95-97;102;108;122;128;134). The majority of these studies however, have used different criteria to classify the visual field (Table 2.6). For

example, Vanhatalo et al. classified a normal visual field as one in which the largest isopter tested using Goldmann kinetic perimetry (usually the V4e) extended by more than 70^{o} in the temporal meridian, whilst Malmgren et al. used a cut off of 80^{o} in the temporal meridian.

5.4.2.3 Accurate VGB exposure data

Most studies of VAVFL are retrospective and determination of VGB exposure is made from the clinical notes. VGB-exposed individuals can often have complex medical histories with multiple hospital referrals making accurate determination of the amount of, or duration of, VGB exposure difficult (94). In the present study, data on cumulative VGB exposure, duration of VGB therapy and maximum daily VGB dose was only included for an individual if a complete history of the VGB exposure were available in the clinical notes (see Chapter 2). If records describing VGB exposure were missing, prohibiting calculation of VGB exposure (e.g. clinic letters describing initiation or withdrawal of VGB, or letter describing VGB dose changes), the VGB exposure data were considered missing for that individual. Although every effort was made to calculate the VGB exposure variables as accurately as possible it may not represent the individual's actual VGB exposure. Around a quarter of individuals are estimated to be non-compliant with their recommended AED regime (381). Even if the individual is fully compliant, and follows the exact recommendations made in a clinic letter (e.g. increase VGB dose by 1000mg), the actual dates that the individual put into place these recommendations cannot usually be determined. The date of the clinic was used in the calculation of duration of VGB exposure and cumulative VGB exposure; but the individual may not have implemented the changes until sometime after the clinic date. These difficulties with accurately determining VGB exposure may also contribute to the variations in findings between studies.

5.4.3 Male sex and ppRNFL thinning

In the present study, male sex was found to be associated with ppRNFL thinning in VGB-exposed individuals after controlling for VGB exposure. This is in agreement with several other studies that have found male sex to be a risk factor for VAVFL (92;94;95;97;98;103;137;167) (Table 1.4). Sex differences in whole retinal thickness at the level of the macula, measured using OCT, have been reported, with males having significantly thicker retinas compared to females (382-384). However, OCT measures of ppRNFL thickness generally show no gender difference in healthy volunteers (Table 5.8). Only two studies have reported thinner ppRNFL in males compared to females, in the temporal (385) and inferior quadrant (386). This suggests that the susceptibility of males to VAVFL and ppRNFL thinning may not be due to sex differences in RGC number and ppRNFL thickness, but due to other factors that have no influence of RGC integrity in the healthy retina.

Table 5.8 Summary of studies comparing ppRNFL thickness measured using OCT between healthy males and females

Reference	Number of individuals	OCT model	Findings
(387)	146	TD-OCT	No difference
(285)	328	TD-OCT	No difference
(385)	199	TD-OCT	Temporal quadrant thinner in males
(386)	312	TD-OCT	Inferior quadrant thinner in males
(388)	99	TD-OCT	No difference
(389)	460	TD-OCT	No difference
(390)	201	TD-OCT	No difference
(391)	109	TD-OCT	No difference
(392)	170	SD-OCT	No difference
(393)	100	TD-OCT	No difference

TD-OCT = time-domain optical coherence tomography; SD-OCT = spectral-domain optical coherence tomography

In mice and rats there is evidence for sexual dimorphism in CNS GABAergic systems in certain brain regions, including sex differences in GABA concentrations (394;395); GABA receptor subunit expression (394); GABA synthesis (396) and electrophysiological properties of some GABAergic neurones (397).

Susceptibility of males to VGB retinotoxicity may be related to sex differences in retinal GABAergic systems (135), such as differences in GABAergic cell numbers, expression of GABA receptors, GABA synthesis and release and GABA metabolism. In male rats, GABA accumulation in the substantia nigra was significantly higher than in female rats up to 10 minutes after sacrifice (396). Since GABA degradation via GABA-T is oxygen-dependent, and presumed to stop immediately after death (396), the accumulation of GABA post mortem probably reflects continued GABA-synthesis (396), suggesting that in the substantia nigra GABA synthesis is greater in males than in females (396). Similar sexual dimorphism may also exist in the retinal GABAergic system. Greater GABA synthesis in the retina in males compared to females could explain the increased susceptibility to VGB retinotoxicity in males. Higher levels of synthesised GABA may lead to increased synaptic GABA release resulting in augmented accumulation of GABA in the retina in males after exposure to VGB.

5.4.4 Age and ppRNFL thickness

Histological studies of human retina have shown that the number of RGC axons decreases with age (398-400). This age-related thinning can be detected using OCT ppRNFL imaging, which shows a decreases in ppRNFL thickness with age at a rate of between 0.16 and 0.44 μm per year (285;390;401;402). No effect of age on ppRNFL thickness was found in this study. It is likely that any small effect of age on the ppRNFL thickness is masked by the greater effects of VGB on the ppRNFL thickness.

5.4.5 Other antiepileptic drugs and ppRNFL thickness

It has been suggested that combination therapy with VGB and valproate may be associated with increased risk of VAVFL (108;114;164). However, in two studies that

have reported this (108;114), the association between combination therapy with VGB and valproate and the development of VAVFL was based on a small sample of individuals (403). In the study by Ardnt et al. (114) only one individual was treated with VGB and valproate combination therapy. Although this individual developed severe VAVFL; in the same study, severe VAVFL was also reported in individuals receiving VGB monotherapy and VGB and carbamazepine combination therapy. Furthermore in a large study of 386 VGB-exposed individuals, concomitant exposure to any other AED was not associated with risk of VAVFL (92). In addition, valproate monotherapy is not associated with visual field abnormalities (404;405) or retinal electrophysiological abnormalities (405). However, in a study of individuals receiving VGB combination therapy with either carbamazepine (N=31) or valproate (N=21), those receiving valproate had significantly smaller visual fields compared to those receiving carbamazepine, despite similar cumulative VGB exposure and duration of VGB exposure between the two groups (164).

No effect of exposure to valproate was found in the present study. However, only "exposure" to each AED was assessed, AEDs taken in combination with VGB were not evaluated, and thus a combination effect of VGB and valproate cannot be ruled out. Valproate increases whole brain levels of GABA (406) probably through inhibition of succinate semialdehyde dehydrogenase, resulting in elevated levels of succinate which inhibits GABA-T activity (407). Inhibition of GABA-T by both VGB and valproate when used concomitantly could lead to increased risk of VGB retinotoxicity. Further studies are needed to assess the risk of VAVFL with concomitant AED use during VGB-exposure.

5.4.6 Homonymous visual field defects and ppRNFL thickness

The ppRNFL was significantly thinner in individuals with homonymous quadrantinopic or hemianopic defects than in individuals without homonymous defects. Twenty one individuals had a homonymous visual field defect that was detected on visual field testing. One individual had "left sided cavitatory brain damage" and homonymous hemianopia, one individual had ischaemic brain damage following a ruptured aterio-venous malformation and a homonymous hemianopia, and one individual had Sturge-Weber syndrome and a homonymous hemianopia. 18/21 individuals had had a homonymous quadrantinopia from resection of epileptogenic foci (16/18 from the temporal lobe, 2/18 from the parietal lobe).

Homonymous visual field defects are a common complication of epilepsy surgery, particularly after anterior temporal lobe resection, and occur due to damage to the anterior aspect of the optic radiation, (Meyer's loop) (Figure 5.4). The incidence of visual field defects after temporal lobe resection is estimated to be between 15 and 100% (408;409).

In individuals with lesions to the optic radiation, ppRNFL thinning may result from retrograde trans-synaptic degeneration. In humans, retrograde trans-synaptic degeneration of RGC as a result of post-geniculate visual pathway lesions is controversial (410), and was not thought to occur (411). Miller and Newman reported normal, healthy optic discs, with no indication of atrophy, in an individual with a homonymous hemianopia following a cerebro-vascular accident 57 years previously (412). Conversely, several other case reports suggest that optic atrophy (413-415), RNFL thinning (416) and degeneration of the anterior visual pathway (414) can be seen between 6 and 35 years following an occipital lobe lesion (413-415). In non-human

Figure 5.4 Projections of the optic radiation and Meyer's loop in the anterior temporal lobe

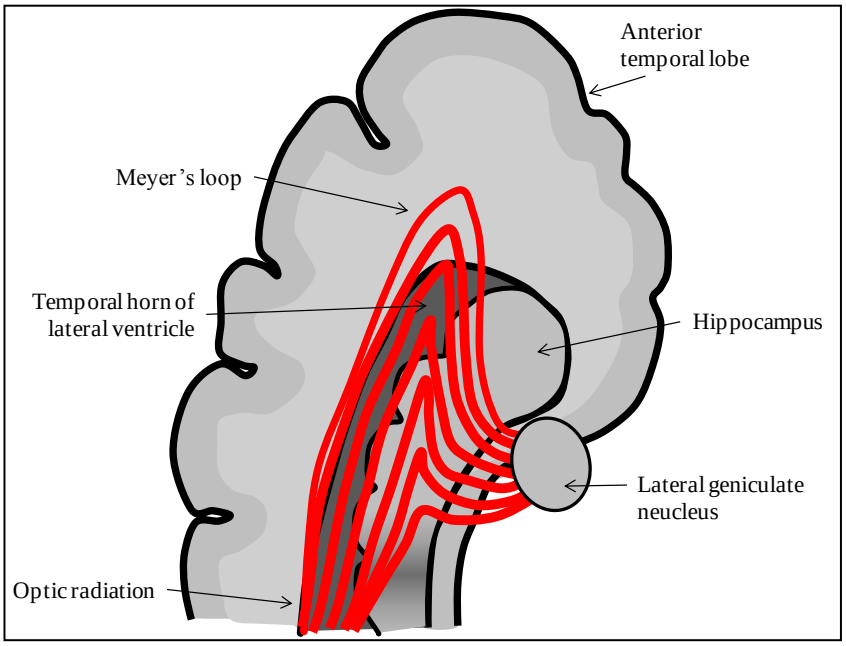

Figure 5.4 legend: The optic radiations are shown in red. The anterior aspect of the optic radiation (Meyer's loop) takes a ventral course into the anterior temporal lobe. Surgical resection of the anterior temporal lobe can result in damage to nerve fibres in Meyer's loop leading to a homonymous superior quadrantinopia.

primates RGC atrophy is observed after occipital lobectomy (417), excision of the striate cortex (418), and after small lesions to the striate cortex (419).

Recently, thinning of the ppRNFL has been detected using OCT in individuals with homonymous hemianopia secondary to congenital (295;420) and acquired lesions (295) of the occipital cortex. Additionally, in two individuals with homonymous hemianopia resulting from acquired lesions to the striate cortex, degeneration of the ipsilateral optic tract was detected using MRI (410). These studies suggest that retrograde trans-synaptic degeneration occurs in the human visual pathway and that in some individuals this can be detected using OCT imaging of ppRNFL thickness (295). The presence of

retrograde trans-synaptic degeneration of RGC resulting from lesions to the optic radiation has not been systematically explored. However, the data from this study suggest that this may occur after lesions from surgical procedures (e.g. anterior temporal lobectomy).

A limitation of studying the effects of lesions to the optic radiations on the ppRNFL thickness in this population is that VGB has a significant effect on the ppRNFL thickness (229;256). The true effect of optic radiation lesions on the ppRNFL may be hidden or exaggerated by the effect of VGB. Additionally as this was a cross-sectional study, the thinner ppRNFL in the individuals with homonymous visual field defects cannot definitely be attributed to the lesion, but may be related to another factor.

Prospective, longitudinal studies are needed to determine whether retrograde trans-synaptic degeneration occurs after acquired lesions to the optic radiation (e.g. as a result of anterior temporal lobectomy). There is particular scope for this in individuals with epilepsy undergoing anterior temporal lobe resections, who will usually undergo pre and post surgical perimetry and in whom OCT ppRNFL imaging could be included in the assessment. However, the duration of time between optic radiation lesion and RGC atrophy is uncertain, and may not be clinically detectable opthalmoscopically for up to 35 years after the insult (414), if ever (256;412). OCT ppRNFL imaging provides a technique that may detect subtle loss of RGC axons before it is clinically detectable using opthamoscopy (295). Recently Jindahra et al. presented an abstract describing longitudinal changes in ppRNFL thickness, using OCT, in seven individuals with post-geniculate visual pathway lesions. In three individuals with hemianopia, ppRNFL thinning was evident at three months post injury and showed a trend from further decline over a one year follow-up period (421).

In disagreement with the present study, the work presented by Jindahara found no ppRNFL thing in individuals with homonymous quadrantinopia (421). Homonymous superior quadrantinopia is a common complication of temporal lobectomy, and 16/18 of the individuals with homonymous visual field defects included in the present study had this visual field defect. The risk of VAVFL in individuals with post-geniculate visual pathway lesions has not been systematically explored. Often visual field test results showing a homonymous visual field defect are excluded from analyses because of the confounding effect on quantification of visual field size[26]. However, interestingly, one of the few studies that has reported that VAVFL progresses with continued VGB exposure was in individuals who had undergone temporal lobe surgery (152). In the study reported by Hardus et al. (152) only surgical candidates were included, so a comparison could not be made about the progressiveness of VAVFL in individuals who had not undergone surgery. It is possible that loss of neurons post-synaptic to RGC after post-geniculate visual pathway injury (i.e. as a result of temporal lobe surgery) may make the RGC more susceptible to VGB toxicity. Thus in individuals not exposed to VGB, post-geniculate lesions resulting in quadrantinopias do not result in a significant degree of RGC loss that can be detected using OCT. However, in VGB-exposed individuals with already "injured" RGC as a result of VGB toxicity, further injury to the visual pathway may be exaggerated.

5.4.7 Genetic variation and ppRNFL thickness

Genetic variation may play a role in the development of VAVFL (168) and ppRNFL thinning. Heredity studies have demonstrated that genetic factors are strong determinants of ppRNFL thickness (393;422). Individual variation in RGC number prior to VGB exposure could contribute to susceptibility to VGB-induced ppRNFL

[26] See 2.4.4

thinning, and explain the degree of variability seen in ppRNFL thickness between individuals. Curcio and Allen found that in healthy human retina the total number of RGC ranged from 710,000 to 1.54 million (423). These findings are in keeping with RGC axon number in human optic nerve, which has been shown to range from 730,000 to 1.7 million (399;424;425). Individuals with lower numbers of RGC (and thinner ppRNFL) may be more susceptible to the effects of diseases, or processes, which target the RGC apparatus (398;423;426) and may be at greater risk of developing VAVFL at lower VGB doses.

Males sex was found to be associated with ppRNFL thinning after VGB exposure. OCT studies show that ppRNFL thickness does not differ between healthy males and females (Table 5.8) suggesting that baseline RGC number may not be the only contribution to susceptibility to VGB retinotoxicity. Genetically-determined differences in retinal GABAergic pathways including differences in GABAergic cell number and GABA-transporter and GABA receptor expression; and GABA metabolism, including differences in GABA-T activity, may also increase or decrease risk of VGB retinotoxicity in an individual. In a previous study, three candidate genes were found to be associated with increased risk of VAVFL including a gene encoding $GABA_B$ receptor (GABRR1/2) and two genes encoding GABA-transporters (GAT1/3 and GAT2). However, no significant association was found on replication of the study by the same authors in a second independent cohort (168). The initial genetic association found in the study by Kinirons et al. (168) probably represents a false positive result. A real association between the gene variants detected in their study, or indeed other variants, cannot be ruled out. The study may have been underpowered to detect variants of small effect; in addition findings may have been confounded by variability in the visual field measurement (168). A chosen phenotype must be reliably and consistently

determined (427) as phenotype variation may influence the ability to identify causal variants (428). Perimetry is subject to multiple confounding influences on the recorded visual field, which may be further exaggerated in individuals with epilepsy (see Chapter 3) and thus may not provide the most suitable phenotype for the assessment of genetic determinants of VGB toxicity. OCT ppRNFL imaging may provide a more robust phenotype to use in pharmacogenetic studies of VAVFL. As part of the work carried out for this study it was shown that in a VGB-exposed population OCT ppRNFL thickness measures are highly repeatable (Chapter 4). In addition, measures of ppRNFL thickness are objective and easily quantifiable and are not subject to the same degree of subject-related and examiner-related variability as perimetry. Additionally, as more patients are able to complete OCT than can complete perimetry (Chapter 4), this will allow collection of larger numbers of VGB-exposed individuals and increased study power. Future studies should explore whether particular genetic variants are associated with ppRNFL thickness in VGB-exposed individuals.

Chapter 6 Patterns of ppRNFL thinning in VGB-exposed individuals

6.1 Introduction

Although the precise mechanisms of VAVFL are not known, it is becoming increasingly evident that RGC loss is implicated. In a single post mortem study from an individual with VAVFL pathological analysis of the retina and optic nerve revealed severe loss of RGC and their axons in the peripheral retina, with relative preservation of RGC in the central retina (162). A similar pattern of RGC atrophy has also been reported in studies using fundus photography to assess the integrity of the RNFL and ONH. Frisen et al. describe a series of 21 VGB-exposed children all of whom showed a distinct pattern of RNFL atrophy (147). In some individuals, atrophy of the RNFL was confined to the nasal peripapillary area. In others the areas of atrophic RNFL extended to involve the superior and inferior poles of the ONH. Conversely, the temporal ppRNFL was spared in all cases (147). In addition, a unique pattern of "inverse" (183) or "C-shaped" (147) optic atrophy has been described in VGB-exposed individuals, resulting from loss of RGC axons from the nasal aspect of the ONH with preservation of those in the temporal portion.

This pattern of RGC atrophy has been described as "inverse" optic atrophy, to distinguish it from the more common pattern of temporal optic atrophy, and macula RNFL attenuation, seen with toxic-nutritional optic neuropathies (183). In the toxic-nutritional optic neuropathies visual impairment typically involves central visual pathways, a caecocentral visual field defect, decreased visual acuity and abnormal

colour vision with atrophy of RGC subserving the fovea, parafoveal area and caecocentral area and atrophy of the temporal aspect of the ONH (248).

Conversely, VGB toxicity is associated with a bilateral, symmetrical, concentric visual field defect, affecting the peripheral visual field and sparing central vision (97). Even in individuals with severe VAVFL the central visual field is spared and colour vision and visual acuity are typically normal (101;139;146). The pattern of RNFL attenuation and optic atrophy seen in VGB-exposed individuals is consistent with a pathological process involving RGC in the peripheral retina, resulting in peripheral visual field loss. RGC axons in the temporal peripheral retina, take an increasingly arcuate course to enter the ONH at the superior and inferior poles (247-249). Axons from RGC in the nasal retina (including the nasal periphery), take a radial trajectory and enter the ONH on the nasal side (247-249).

More recently a pattern of ppRNFL thinning, detected using OCT, has been explored in individuals with VAVFL. In agreement with the appearance of the RNFL and ONH in studies using fundus photography, studies using OCT have reported a relative preservation of the ppRNFL thickness in the temporal quadrant (119;229;256;258). In addition, varying degrees of ppRNFL thinning in the nasal, superior and inferior quadrants have been reported (119;229;256;258). Lawthom et al. found that 100% of individuals with VAVFL showed ppRNFL thinning in the nasal quadrant (256). Conversely, in a study by Moseng et al. the distribution of ppRNFL thinning was equal across the superior, inferior and nasal quadrants, with 55.6% of individuals showing thinning in each of these areas (258). However, both of these studies were small with 11 individuals include in the study by Lawthom et al. and 9 individuals in the study by Moseng et al. In a larger study of 64 individuals with VAVFL carried out as part of this work, the number of individuals showing ppRNFL thinning in each of the 90^{o} quadrants

was assessed (see 4.3.6). The superior and inferior quadrants most frequently showed ppRNFL thinning (68.8% and 51.6% of individuals, respectively), with only 18.8% of individuals with VAVFL showing thinning in the nasal quadrant.

The differences in findings between the studies may be related to the criteria used to define ppRNFL thinning. In the studies by Lawthom et al. (256) and Moseng et al. (258) ppRNFL thinning was defined as a measure falling below the 5^{th} percentile of the manufacturers' normative database. Conversely in the study carried out as part of this work, ppRNFL thinning was defined as measures falling within the $\leq 1^{st}$ percentile of the manufactures' normative database. In addition, in the studies by Lawthom et al. (256) and Moseng et al. (258) TD-OCT was used to determine ppRNFL thickness, whereas in this study both TD-OCT and SD-OCT were used.

To make a reliable comparison of the results between the three studies, data from individuals with VAVFL included in this study who were examined using TD-OCT were extracted. The definition for ppRNFL thinning as applied to the Lawthom et al. and Moseng et al. studies was applied to these data (Table 6.1).

The main difference between the studies was that whilst Lawthom et al. reported nasal quadrant thinning in 100% of individuals, only 55-60% of individuals were found to show abnormal nasal quadrant thickness in this study, and in the study carried out by Moseng et al. (Table 6.1).

Table 6.1 Comparison of the reported pattern of ppRNFL thinning in individuals with VAVFL across three studies using the same TD-OCT model

	Abnormal ppRNFL thinning ($\leq 5^{th}$ percentile of the manufacturers' normative database)		
	Lawthom (256) (N=11)	**Moseng (258) (N=9)**	**This (N=27)**
Temporal	0	22.2	18.5
Superior	63.6	55.6	74.1
Nasal	100	55.6	59.2
Inferior	72.7	55.6	74.1

TD-OCT = time-domain optical coherence tomography

The differences in the distribution of ppRNFL thinning are difficult to explain as all studies used the same TD-OCT model, and ppRNFL thickness scan protocol, and compared data against the same normative database. In addition, all individuals were classified as showing VAVFL. Different perimetric techniques, and thus visual field classification criteria, were used in each study. Lawthom et al. used automated perimetry (Humphrey visual field analyser 30-2 program) which only assesses the visual field out to 30^{o} eccentricity. Conversely in this study Goldmann kinetic perimetry was used which assess the visual field out to 90^{o}, and in the study by Moseng et al., the full-field 120-point screening test was used which examines out to 60^{o} eccentricity. It is possible that individuals with mild VAVFL, not encroaching on the central 30^{o} could have been missed in the study by Lawthom et al. and those wild mild VAVFL may be contributing to the differences in findings between the studies.

Different patterns of ppRNFL thinning may be associated with various stages of VAVFL, or degree of VGB exposure. Frisen et al. suggested that RNFL attenuation associated with VAVFL may be progressive with continued VGB exposure. A "staging system" based on the photographic appearance of the RNFL was developed, with atrophy initially only detectable in the nasal peripapillary area and later progressing to involve the superior and inferior poles of the ONH (147) (Table 6.2). Later stages involving the temporal aspect of the ONH may also occur (147).

Table 6.2 Staging of ppRNFL atrophy in VGB-exposed individuals using fundus photography

Stage	Appearance of the RNFL
1	Partial atrophy of the nasal quadrant
2	Severe atrophy of the nasal quadrant with partial atrophy of the nasal sectors of the superior and inferior quadrants
3	Severe atrophy of the nasal quadrant and severe atrophy of the nasal sectors of the superior and inferior quadrants with partial atrophy of the temporal sectors of the superior and inferior quadrants
4	Severe atrophy of the nasal quadrant and severe atrophy of the superior and inferior quadrants

Table adapted from Frisen et al. (147)

Based on their findings Lawthom et al. suggested that ppRNFL thinning in the nasal quadrant should be used as a biomarker for VGB toxicity, however, the discrepancy in findings between OCT studies shows that further investigation is needed to elucidate the pattern of VGB-associated ppRNFL thinning before screening recommendations can be

made. If ppRNFL imaging is to be used in the assessment of VGB-exposed individuals as has been suggested (256;259), then the precise characteristics of VGB-associated ppRNFL attenuation need to be determined. Understanding patterns of ppRNFL thinning after VGB exposure could aid clinicians in monitoring patients for retinal changes and may improve the ability to detect subtle change in the ppRNFL. Furthermore, if loss of RGC apparatus is progressive (147), discrete ppRNFL areas may show thinning early on (i.e. after a low dose of VGB). Knowledge of a particular pattern of ppRNFL thinning may facilitate early detection of subtle defects and improve screening strategies to prevent clinical visual field loss. In addition, if low cumulative doses of VGB do lead to subtle defects, this may have implications for trials of VGB as an anti-addiction therapy and in short-duration treatment strategies (142;429). A more complete understanding of patterns of RNFL atrophy may help reveal mechanisms of VGB toxicity.

6.1.1 Aims

To determine whether a pattern of ppRNFL loss can be identified in VGB-exposed individuals using OCT. Further this study will explore the relationship between cumulative dose of VGB and patterns of ppRNFL loss to determine whether subtle, discrete defects occur early after exposure.

6.2 Methods

6.2.1 Subjects

VGB-exposed individuals from Group 1A and non-exposed individuals with epilepsy (Group 2) were included in this study. The demographic details of individuals in Group 1A and Group 2 can be seen in Table 2.1[27]

6.2.2 VGB exposure groups

For 91 VGB-exposed participants from Group 1A, sufficient data were available to determine cumulative dose of VGB. These participants were further grouped according to cumulative VGB exposure. Group I included 41 participants with exposure to ≤1000 grams of VGB; Group II comprised 23 individuals with exposure to >1000≤2500 grams; Group III comprised 16 people with exposure to >2500≤5000 grams; Group IV included 11 individuals with exposure to > 5000 grams. Demographic details of each VGB exposure Group are presented in Table 6.3.

6.2.3 OCT

All individuals were assessed using SD-OCT

6.2.4 Data analysis

Where t-tests were used to explore differences in ppRNFL thickness across the twelve 30^{o} sectors, a Bonferroni adjusted p-value of 0.004 was used. Similarly in the analysis of 64 four-scan segments, a Bonferroni adjusted p-value of 0.0008 was used to allow for multiple testing (379).

[27] Chapter 2

Table 6.3 Characteristics of VGB-exposed individuals according to Group.

	Group I (n=41)	Group II (n=23)	Group III (n=16)	Group IV (n=11)
Cumulative VGB exposure	≤1000	>1000≤2500	>2500≤5000	>5000
Mean cumulative VGB exposure (grams) (SD)	341.3 (± 276.7)	1494.5 (± 469.5)	3834.4 (± 846.0)	9718.6 (± 3982.1)
Mean duration of VGB exposure (months) (SD)	9.8 (± 12.7)	36.1 (± 18.9)	78.3 (± 36.7)	131.4 (± 53.4)
Mean age (years) (SD)	49.6 (± 11.4)	46.9 (± 11.6)	47.6 (± 12.8)	43.8 (± 7.1)
Sex (male %)	63.0	56.0	43.8	72.0

VGB = vigabatrin; SD = standard deviation; Group I ≤1000 grams of VGB exposure; Group II >1000 ≤2500 grams of VGB exposure; Group III >2500 ≤5000 grams of VGB exposure; Group IV >5000 grams of VGB exposure

6.3 Results

Data from all individuals in Group 1A who were able to complete OCT were included in the analysis (n=129)[28]. 3/90 (3.3%) non-exposed individuals (Group 2) were unable to complete OCT and data from 87 individuals were used in the analysis.

[28] See Chapter 4

6.3.1 The ppRNFL in VGB-exposed versus non-exposed individuals

The ppRNFL thickness, and normal distribution percentiles, in each 30^{o} sector were compared between VGB-exposed individuals and non-exposed individuals.

6.3.1.1 ppRNFL thickness

The average ppRNFL thickness was significantly thinner in VGB-exposed individuals compared to non-exposed participants (78.9 and 88.8μm, respectively; $p \leq 0.004$). The ST, Sup, SN, NS, NI, IN, Inf and IT ppRNFL sectors were significantly thinner in VGB-exposed compared to non-exposed individuals ($p<0.004$; Table 6.4). The percentage difference in ppRNFL thickness in VGB-exposed compared to non-exposed participants was determined for each sector. The largest differences were found for the NS, IN and SN sectors (18.1%, 17.9% and 17.8% respectively; Table 6.4).

6.3.1.2 Frequency and distribution of ppRNFL thinning

The number of individuals showing ppRNFL thinning, according to the manufacturers' normal database, was determined for each of the 30^{o} sectors (Table 6.4). 28.8% of VGB-exposed individuals showed abnormal, (i.e. $\leq 1^{st}$ percentile), average ppRNFL thickness compared to 8.0% of non-exposed individuals. 19.2% showed borderline, (i.e. $\leq 5^{th}$–>1^{st} percentile), average ppRNFL thickness compared to 13.8% of non-exposed individuals. In VGB-exposed individuals, thinning was most frequently seen in the SN, IN, Inf and Sup sectors (32.0%, 25.6%, 24.8% and 21.6% respectively). Significantly more VGB-exposed participants were classified as showing abnormal ppRNFL thickness in the ST, Sup, SN, NS, IN and Inf sectors ($p<0.004$).

Table 6.4 ppRNFL thickness in each 30° sector. in VGB-exposed and non-exposed individuals

ppRNFL area	VGB-exposed (n=129) Thickness (µm)	Non-exposed (n=87) Thickness (µm)	Difference in ppRNFL thickness (non-exposed - exposed) (µm (%))	VGB-exposed Percentage showing ppRNFL thinning[a]		Non-exposed Percentage showing ppRNFL thinning[a]	
				≤1st	≤ 5th– >1st	≤1st	≤ 5th– >1st
Average	78.9*	88.8	10.2 (11.6)	28.8#	19.2	8.0	13.8
Temp	46.8	48.6	1.8 (3.7)	1.6	8.8	1.1	9.2
TS	70.2*	74.6	4.4 (5.9)	9.6	8.0	3.4	6.9
ST	113.3*	127.8	14.5 (11.3)	5.6#	16.8	1.1	6.9
Sup	92.8*	105.8	13.0 (12.3)	21.6#	9.6	9.2	8.0
SN	76.4*	92.9	16.5 (17.8)	32.0#	19.2	9.2	13.8
NS	71.7*	87.5	15.8 (18.1)	4.0#	15.2	1.1	4.6
Nas	57.6	58.3	0.7 (1.2)	3.2	2.4	1.1	5.7
NI	58.8*	65.6	6.8 (10.4)	3.2	8.0	2.3	4.6
IN	75.9*	92.4	16.5 (17.9)	25.6#	16.8	9.2	8.0
Inf	107.4*	124.1	16.7 (13.5)	24.8#	7.2	9.2	8.0
IT	111.4*	125.1	13.7 (11.0)	8.0	12.8	2.3	6.9
TI	59.6	63.0	3.4 (5.4)	1.6	8.0	1.1	4.6

ppRNFL = peripapillary retinal nerve fibre layer; VGB = vigabatrin; T = temporal; TS = temporal-superior; ST = superior-temporal; S = superior; SN = superior-nasal; NS = nasal-superior; N = nasal; NI = nasal-inferior; IN = inferior-nasal; I = inferior; IT = inferior-temporal; TI = temporal-inferior

[a]As defined by the manufacturers' normative database. The percentage of individuals falling within the abnormal (i.e. ≤1st percentile) and borderline (i.e. ≤ 5th–>1st percentile) are shown.

*Significant difference in ppRNFL thickness between exposed and non-exposed participants in these sectors ($p \leq 0.004$; independent samples T-test)

[#] Significant difference between number of VGB-exposed and non-exposed individuals classed as having abnormal ppRNFL thickness ($p < 0.004$; Chi squared test for independence)

6.3.2 ppRNFL thickness according to VGB exposure Group

The ppRNFL thickness in each 30^{o} sector was calculated for each VGB exposure Group (Table 6.5), and plotted as a graph (Figure 6.1). Significant differences in ppRNFL thickness were assessed using a one-way ANOVA with post hoc testing was carried out using Tukey HSD.

Table 6.5 ppRNFL thickness in each 30° sector in VGB-exposed individuals according to VGB exposure Group

ppRNFL area	Group I (n=40)	Group II (n=22)	Group III (n=16)	Group VI (n=11)	R squared
Average	84.3	74.0[x] *	73.2[x] *	66.0[x] *	0.33
Temp sector thickness (µm)	47.8	44.6	48.4	46.9	0.03
TS sector thickness (µm)	71.9	66.5	71.7	67.1	0.04
ST sector thickness (µm)	119.3	109.5[x]	107.6[x]	92.6[x] *	0.18
Sup sector thickness (µm)	104.8	85.7[x]	77.1[x] *	64.9[x] *	0.20
SN sector thickness (µm)	89.1	68.5[x] *	68.0[x] *	54.1[x] *	0.31
NS sector thickness (µm)	75.3[x]	67.6[x]	67.0[x]	58.9[x] *	0.27
Nas sector thickness (µm)	58.2	54.3	56.9	57.7	0.02
NI sector thickness (µm)	62.2	54.1[x]	54.3[x]	54.2[x]	0.13
IN sector thickness (µm)	86.1	71.6[x]	65.4[x] *	59.8[x] *	0.21
Inf sector thickness (µm)	120.0	100.5[x]	95.9[x] *	81.8[x] *	0.18
IT sector thickness (µm)	116.2	108.8[x]	106.9[x]	95.3[x]	0.12
TI sector thickness (µm)	60.4	56.6	58.9	57.9	0.03

ppRNFL = peripapillary retinal nerve fibre layer; VGB = vigabatrin; Temp = temporal; TS = temporal-superior; ST = superior-temporal; Sup = superior; SN = superior-nasal; NS = nasal-superior; Nas = nasal; NI = nasal-inferior; IN = inferior-nasal; Inf = inferior; IT = inferior-temporal; TI = temporal-inferior

Group I ≤1000 grams of VGB exposure; Group II >1000 ≤2500 grams of VGB exposure; Group III >2500 ≤5000 grams of VGB exposure; Group IV >5000 grams of VGB exposure

[x]ppRNFL thickness significantly thinner compared to non-exposed individuals ($p<0.05$)

*ppRNFL thickness significantly thinner compared to Group I ($p<0.05$)

Figure 6.1 Graph showing ppRNFL thickness across the 30° sectors according to VGB exposure Group

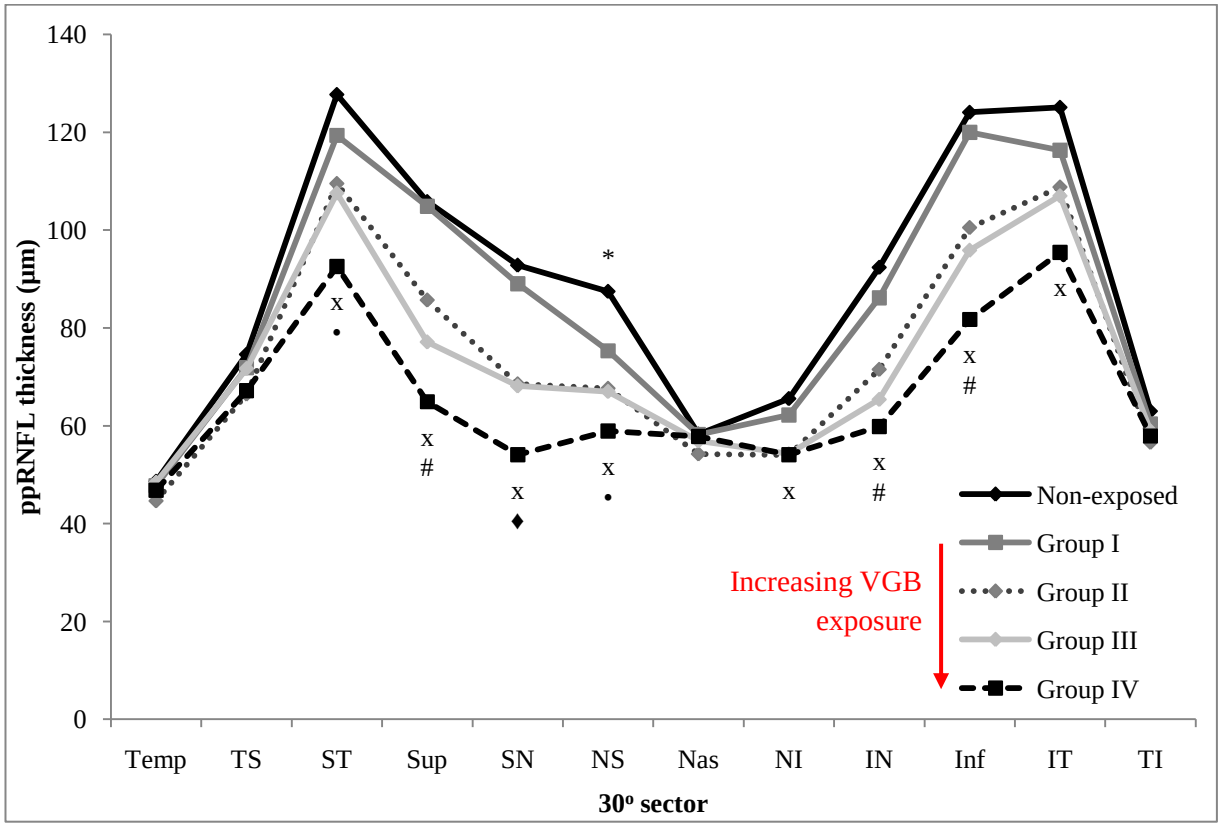

Figure 6.1 legend: The pattern of ppRNFL thinning according to cumulative VGB exposure. The ppRNFL is thinner in most areas with increasing cumulative VGB exposure. The temporal areas show no change in ppRNFL thickness with increasing VGB exposure.

***** Significant difference in ppRNFL thickness between non-exposed individuals and Group I ($p<0.05$)

× Significant difference in ppRNFL thickness between non-exposed individuals and Groups II, III and IV ($P<0.05$)

♦ Significant difference in ppRNFL thickness between Group I and Group II, III and IV ($p<0.05$)

Significant difference in ppRNFL thickness between Group I and Group III and IV ($p<0.05$)

● Significant difference in ppRNFL thickness between Group I and Group IV ($p<0.05$)

ppRNFL = peripapillary retinal nerve fibre layer; VGB = vigabatrin; Temp = temporal; TS = temporal-superior; ST = superior-temporal; Sup = superior; SN = superior-nasal; NS = nasal-superior; Nas = nasal; NI = nasal-inferior; IN = inferior-nasal; Inf = inferior; IT = inferior-temporal; TI = temporal-inferior; Group I ≤1000 grams cumulative VGB exposure; Group II >1000 ≤2500 grams cumulative VGB exposure; Group III >2500 ≤5000 grams cumulative VGB exposure; Group IV >5000 grams cumulative VGB exposure

6.3.2.1 VGB exposure Groups compared to non-exposed

The ppRNFL was significantly thinner in Groups II, III and IV compared to non-exposed individuals in the ST, Sup, SN, NS, NI, IN, Inf and IT sectors (Table 6.5; Figure 6.1).

In Group I the ppRNFL was found to be significantly thinner in the NS sector compared to non-exposed individuals. No differences were found for any other ppRNFL sectors in Group I compared to non-exposed individuals. A scatter plot of ppRNFL thickness in the NS sector and cumulative dose of VGB is shown for individuals in Group I (Figure 6.2). Four individuals were classified as shwing borderline ppRNFL thinning ($\leq 5^{th} > 1^{st}$ percentile)[29]. Data on the visual field status of 25/40 of the Group I patients were available [30]. According to criteria set out by Wild et al. (97) 19 individuals from Group I had normal visual fields, 5 had mild visual field loss and 1 showed moderate visual field loss.

There were no significant differences between any of the VGB exposure Groups and the non-exposed individuals in the Temp, TS, TI and Nas sectors.

[29] To determine whether the significant effect was driven by the four individuals showing borderline ppRNFL thickness they were excluded from the analysis. The repeated analysis still showed a significant difference in ppRNFL thickness in the NS sector in Group I compared to non-exposed individuals.

[30] From visual field testing carried out as part of study described in Chapter 4

Figure 6.2 ppRNFL thickness in the NS sector and cumulative dose of VGB for individuals in Group 1

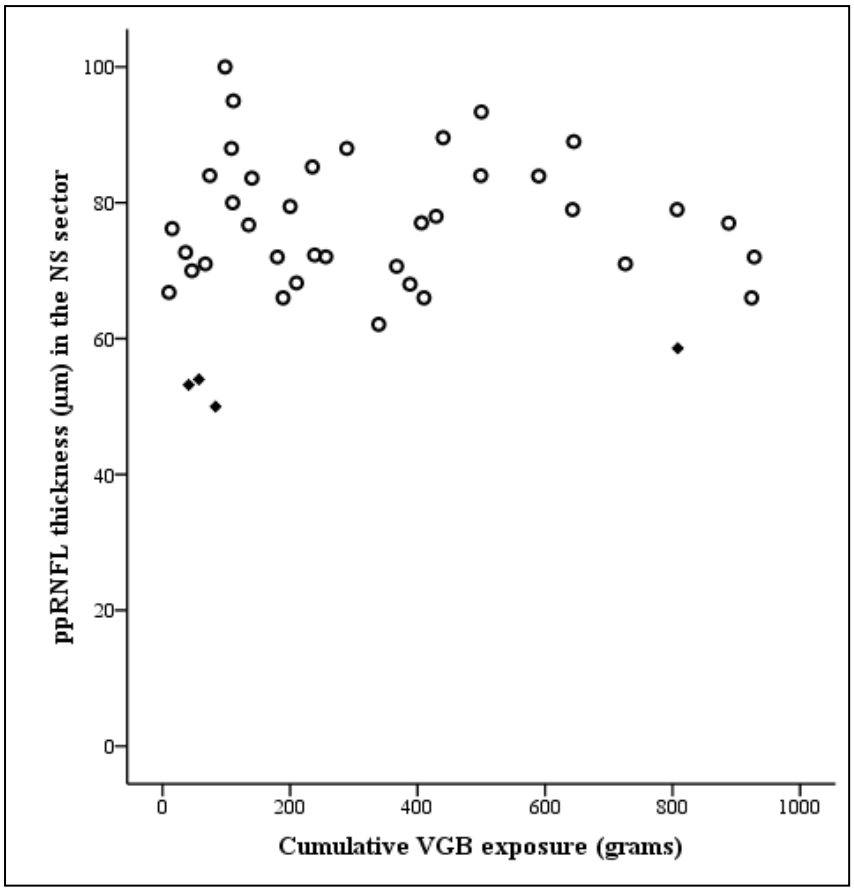

Figure 6.2 legend: ppRNFL = peripapillary retinal nerve fibre layer; VGB = vigabatrin; NS = nasal-superior; Group I ≤1000 grams of VGB exposure

○ Normal ppRNFL thickness (≤95th–>5th percentile according to the manufacturers' normative database)

♦ Borderline ppRNFL attenuation (≤ 5th–>1st percentile according to the manufacturers' normative database)

6.3.2.2 Inter-group comparison between VGB exposure Groups

Group II, III and IV all showed significantly thinner ppRNFL compared to Group I for the SN sector. Group III and IV also showed significantly thinner ppRNFL for the Sup,

IN and Inf sectors. In addition, the ppRNFL thickness was significantly thinner in Group IV than Group I in the NS and ST sectors. There were no significant differences in ppRNFL thickness between Groups II, III and IV for any sector.

The coefficient of determination was calculated to explore how much of the variance in ppRNFL thickness in each sector was explained by cumulative VGB exposure. R squared values ranged from 0.02 for the Nas sector to 0.31 for the SN sector (Table 6.5). The largest R squared values were found for the SN and NS sectors (0.31 and 0.27). Around a third of the variance in ppRNFL thickness in these sectors can be explained by cumulative dose of VGB (Table 6.5).

6.3.3 ppRNFL thickness according to VAVFL Group

The ppRNFL thickness in each 30^{o} sector was calculated according to each VAVFL classification (Table 6.6), and plotted as a graph (Figure 6.6). Individuals with moderate and severe VAVFL were combined owing to the small numbers in each group. Significant differences in ppRNFL thickness were assessed using a one-way ANOVA with post hoc testing was carried out using Tukey HSD.

Table 6.6 ppRNFL thickness in each 30° sector in VGB-exposed individuals according to VAVFL classification

ppRNFL area	Normal visual fields (n=47)	Mild VAVFL (n=18)	Moderate/severe VAVFL (n=19)
Temp sector thickness (µm)	47.3	47.3	46.3
TS sector thickness (µm)	72.5	69.5	67.1
ST sector thickness (µm)	125.5	110.3[x]	95.0[x]*
Sup sector thickness (µm)	109.7	83.3[x]*	72.4[x]*
SN sector thickness (µm)	89.4	69.2[x]*	53.2[x]*#
NS sector thickness (µm)	79.6x	67.1x*	56.3[x]*
Nas sector thickness (µm)	59.0	53.7	54.3
NI sector thickness (µm)	60.8	57.6	50.4[x]*
IN sector thickness (µm)	88.2	67.8[x]*	54.4[x]*
Inf sector thickness (µm)	127.3	95.6[x]*	77.3[x]*
IT sector thickness (µm)	119.6	111.7	97.2[x]*
TI sector thickness (µm)	61.6	59.4	58.3

ppRNFL = peripapillary retinal nerve fibre layer; VGB = vigabatrin; Temp = temporal; TS = temporal-superior; ST = superior-temporal; Sup = superior; SN = superior-nasal; NS = nasal-superior; Nas = nasal; NI = nasal-inferior; IN = inferior-nasal; Inf = inferior; IT = inferior-temporal; TI = temporal-inferior

[x]ppRNFL thickness significantly thinner compared to non-exposed individuals ($p<0.05$)

*ppRNFL thickness significantly thinner compared to VGB-exposed with normal visual fields ($p<0.05$)

#ppRNFL thickness significantly thinner compared to mild VAVFL ($p<0.05$)

Figure 6.3 Graph showing ppRNFL thickness across the 30° sectors according to VAVFL Group

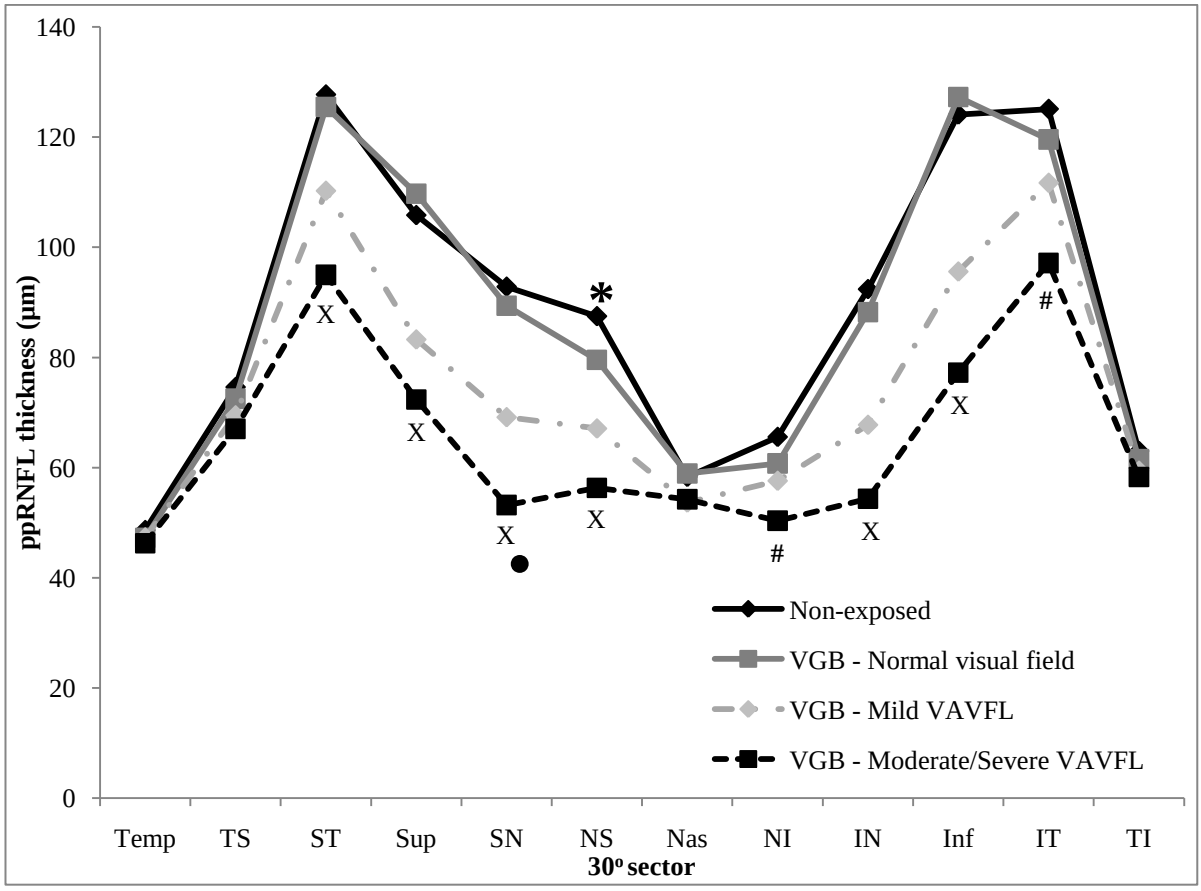

Figure 6.3 legend: The pattern of ppRNFL thinning according to severity of VAVFL. The ppRNFL is thinner in most areas with increasing severity of VAVFL. The temporal areas show no change in ppRNFL thickness with severity of VAVFL.

***** Significant difference in ppRNFL thickness between non-exposed individuals and VGB-exposed individuals with normal visual fields ($p<0.05$)

x Significant difference in ppRNFL thickness between non-exposed individuals and VGB-exposed individuals with mild VAVFL and moderate/severe VAVFL ($P<0.05$)

Significant difference in ppRNFL thickness between non-exposed individuals and VGB-exposed individuals with moderate/severe VAVFL ($P<0.05$)

● Significant difference in ppRNFL thickness between VGB-exposed individuals with mild VAVFL and VGB-exposed individuals with moderate/severe VAVFL ($p<0.05$)

ppRNFL = peripapillary retinal nerve fibre layer; VGB = vigabatrin; VAVFL = vigabatrin associated visual field loss; Temp = temporal; TS = temporal-superior; ST = superior-temporal; Sup = superior; SN = superior-nasal; NS = nasal-superior; Nas = nasal; NI = nasal-inferior; IN = inferior-nasal; Inf = inferior; IT = inferior-temporal; TI = temporal-inferior

6.3.3.1 VAVFL Groups compared to non-exposed

The ppRNFL was significantly thinner in individuals with mild VAVFL and in individuals with moderate/severe VAVFL compared to non-exposed individuals in the ST, Sup, SN, NS, IN and Inf sectors (Table 6.6; Figure 6.3) and in individuals with moderate/severe VAVFL only in the NI and IT sectors.

In VGB-exposed individuals with normal visual fields the ppRNFL was found to be significantly thinner in the NS sector compared to non-exposed individuals. No differences were found for any other ppRNFL sectors in VGB-exposed individuals with normal visual fields compared to non-exposed individuals.

There were no significant differences between any of the VAVFL Groups and the non-exposed individuals in the Temp, TS, TI and Nas sectors.

6.3.3.2 Inter-group comparison between VAVFL Groups

Individuals with mild VAVFL and individuals with moderate/severe VAVFL, showed significantly thinner ppRNFL compared to VGB-exposed individuals with normal visual fields for the Sup, SN, NS, IN and Inf sectors. Individuals with moderate/severe VAVFL also showed significantly thinner ppRNFL compared to VGB-exposed individuals with normal visual fields for the ST, IT and NI sectors. The only difference seen between individuals with mild VAVFL and individuals with moderate/severe VAVFL was in the SN sector where the ppRNFL was significantly thinner in individuals with moderate/severe VAVFL (Table 6.6; Figure 6.3).

6.3.4 ppRNFL thickness across 256 scans in VGB-exposed and non-exposed

For 71 VGB-exposed and 87 non-exposed participants, data were available to export the TSNIT profiles to a personal computer using Research Browser Software Version 5.0. A TSNIT profile for each group (VGB-exposed and non-exposed), was plotted from the 256 individual ppRNFL thickness scans (Figure 6.4).

A one-way between-groups multivariate analysis of variance was performed to investigate the effect of VGB exposure on ppRNFL thickness across 64 ppRNFL regions. There was a statistically significant difference between VGB-exposed and non-exposed individuals when all 64 ppRNFL were combined ($F(64, 88) = 1.75$, $p = 0.008$; Wilks' Lambda = 0.44; partial eta squared = 0.56). When each of the 64 ppRNFL areas were considered separately there was significant difference in 29 of the areas (Figure 6.4 and Figure 6.5) using a Bonferroni adjusted alpha level of 0.0008 (379). This included segments 10-14, 21-28 and 38-53 (Figure 6.4 and 6.5). For comparison, the location of the 64 four-scan segments and the twelve 30^o sectors were mapped onto the same figure (Figure 6.5).

Figure 6.4 ppRNFL thickness across 256 scans for VGB-exposed and non-exposed individuals

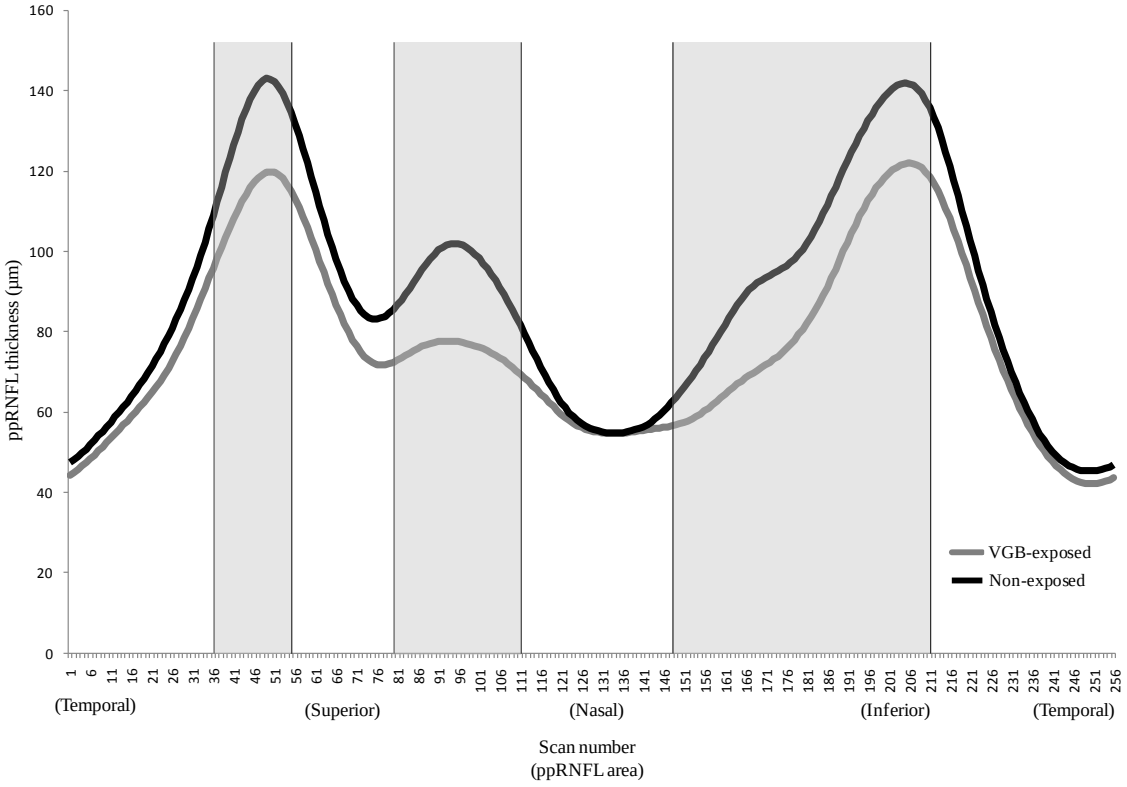

Figure 6.4 legend: ppRNFL = peripapillary retinal nerve fibre layer; VGB = vigabatrin; T = temporal; S = superior; N = nasal; I = inferior

Grey areas indicate significant ppRNFL thinning in VGB-exposed compared to non-exposed individuals ($p<0.0008$)

Figure 6.5 Distribution of ppRNFL thinning in the 64 four-scan segments

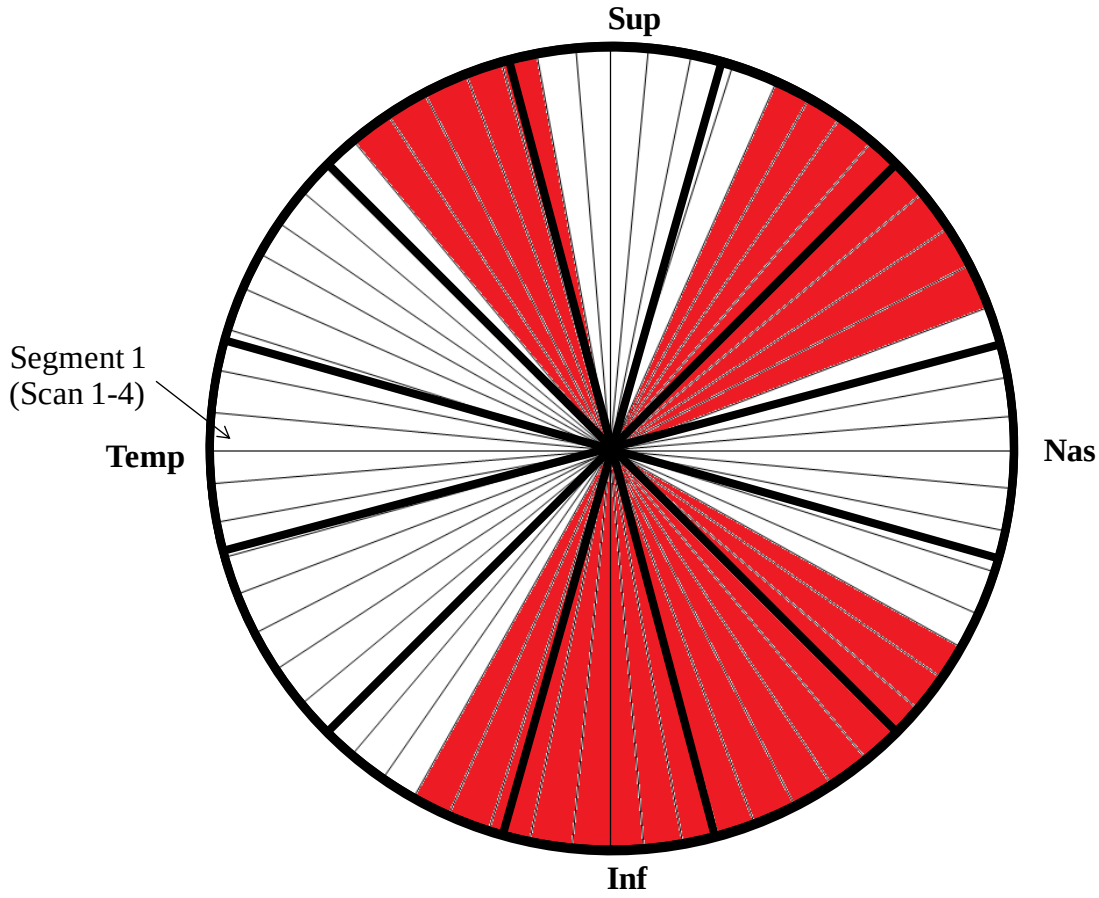

Figure 6.5 legend: Distribution of 64 four-scan segments on a ppRNFL scan compared with the distribution of the 30^{o} sectors (bold outline). Red areas indicate segments showing significantly thinner ppRNFL in VGB-exposed composed to non-exposed individuals within the 64 four-scan segments ($p<0.0008$).

ppRNFL = peripapillary retinal nerve fibre layer; Temp = temporal; TS = temporal-superior; ST = superior-temporal; Sup = superior; SN = superior-nasal; NS = nasal-superior; Nas = nasal; NI = nasal-inferior; IN = inferior-nasal; Inf = inferior; IT = inferior-temporal; TI = temporal-inferior

6.4 Discussion

This is the first study using OCT to explore in detail patterns of ppRNFL thinning in VGB-exposed individuals. Previous OCT studies have described patterns of ppRNFL thinning in a small number of individuals with VAVFL according to the 90^{o} quadrants provided in the manufacturers' summary report (256). In the present study patterns of ppRNFL thinning were explored across the twelve 30^{o} sectors provided in the manufacturers' summary report. In addition, a novel ppRNFL thickness summary measure was created comprising 64 four-scan segments, across which patterns of ppRNFL thinning could be determined in smaller ONH areas. Furthermore, patterns of ppRNFL thinning were determined according to cumulative VGB exposure and severity of VAVFL

6.4.1 Patterns of ppRNFL thinning in VGB-exposed compared to non-exposed individuals

The ppRNFL was significantly thinner in VGB-exposed individuals compared to non-exposed individuals in most of the 30^{o} sectors (Figure 6.6). Only the Temporal, TI and Nasal 30^{o} sectors showed no difference in absolute ppRNFL thickness between the Groups (Figure 6.6). In addition, in the TS sector there was no difference in the number of individuals showing ppRNFL thinning (i.e. $\leq 1^{st}$ percentile of the manufacturers' normative database) between the Groups (Figure 6.6). The relative preservation of the temporal ppRNFL in VGB-exposed individuals is in agreement with previous studies (198;229;256;257).

Figure 6.6 Difference in ppRNFL thickness between VGB-exposed and non-exposed individuals

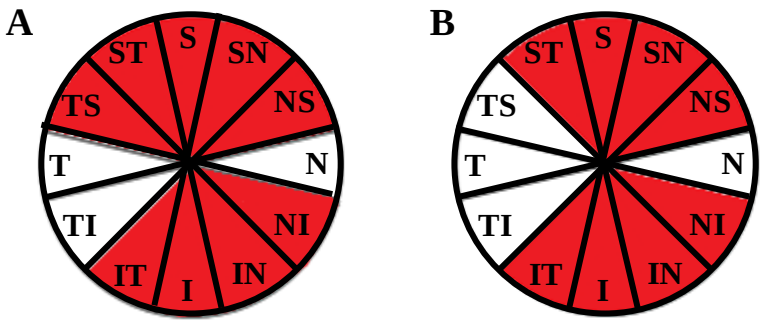

Figure 6.6 legend: **(A)** Red areas indicate 30° sectors showing significant difference in absolute ppRNFL thickness between VGB-exposed and non-exposed ($p<0.004$). **(B)** Red areas indicate 30° sectors showing a significant difference in the percentage of individuals showing abnormal ppRNFL thickness (i.e. $\leq 1^{st}$ percentile) according to the manufacturers' normative database between VGB-exposed and non-exposed individuals ($p<0.004$).

The ppRNFL was up to 18% thinner in VGB-exposed individuals compared to non-exposed individuals in some 30° sectors (SN, NS and IN), whilst in other 30° sectors there was little difference in ppRNFL thickness between Groups. In particular, the Nasal and Temporal 30° sectors were only 1.2% and 3.7% thinner, respectively in the VGB-exposed Group compared to the non-exposed Group. This suggests that there may be differential susceptibility of RGC to the retinotoxic effects of VGB, as some ppRNFL areas showed significant loss whilst others were relatively spared. Of importance is the variation in ppRNFL thinning between adjacent 30° sectors. For example, the NS, Nasal and NI 30° sectors all comprise the Nasal 90° quadrant, yet the percentage difference in ppRNFL thickness between VGB-exposed and non-exposed individuals was dissimilar across these 30° sectors. The NS 30° sector was the most affected sector with VGB-exposed individuals having a ppRNFL 18.1% thinner than

non-exposed individuals, whilst the adjacent Nasal sector was the least affected sector, with only a 1.2% difference between VGB-exposed and non-exposed individuals. The NI sector showed a modest 10.4% difference in ppRNFL thickness between the two Groups (Table 6.4). The variation in ppRNFL loss across adjacent sectors has a two-fold importance. Firstly, it suggests that ppRNFL thinning may occur in discrete areas, representing loss of distinct populations of RGC. Secondly it suggests that analysis of summary measures (e.g. the 90^{o} quadrants) provided in the manufacturers' summary reports, may be insufficient to detect subtle patterns of ppRNFL thinning, as adjacent areas of preserved ppRNFL thickness may mask any ppRNFL loss.

6.4.2 ppRNFL thinning in non-exposed individuals

An unexpected finding from this study was the high number of non-exposed individuals who showed ppRNFL thinning according to the manufacturers' normative database. 8% of individuals in Group 2 had an average ppRNFL thickness that fell within the $\leq 1^{st}$ percentile, and 13.8% of individuals fell into the $\leq 5^{th}$–>1^{st} percentile. The significance of these findings is explored further in Chapter 7. However, these results also have implications for the interpretation of the results in this study. As "epilepsy" may have an effect on ppRNFL thickness, all further discussion of the effect of VGB on ppRNFL thickness in VGB-exposed individuals is made in comparison to non-exposed individuals, rather than compared to healthy controls.

6.4.3 Effect of cumulative VGB exposure on the pattern of ppRNFL thinning

6.4.3.1 An early pattern of ppRNFL thinning

A major concern for VGB treatment strategies is whether irreversible retinal damage can occur after a short period of VGB exposure (429). This is a particular concern for

use of VGB as an anti-addiction medication (142), and for treatment of infantile spasms, where VGB may be used as first-line therapy. In this study significant ppRNFL thinning was found in the NS sector in individuals with a cumulative VGB exposure of less than 1000 grams (average cumulative VGB exposure 351 grams), compared to non-exposed individuals. This was the only 30^{o} sector to show a significant difference in ppRNFL thickness between these Groups, and suggests that thinning in the NS ppRNFL area may provide an early indication of VGB retinotoxicity.

It is uncertain why the ppRNFL in the NS 30^{o} sector may show thinning early in the course of VGB retinotoxicity. The peripheral, concentric characteristics of VAVFL, and the circumferentially-diffuse RNFL atrophy detected by fundus photography, suggest that VGB-associated RGC loss occurs relatively uniformly in the retinal periphery. There is no functional or structural evidence to suggest that RNFL loss associated with VGB toxicity is limited to, or defined by, RNFL bundles. In fact, it is probably this characteristic of uniform, peripheral RNFL loss (198) that makes detection of RNFL atrophy difficult by direct observation, or photography (147), and why ophthalmoscopic features of VGB retinotoxicity are generally absent, even in some individuals with severe VAVFL (i.e. visual field less than 20^{o} eccentricity) (139;146). In primate models of traumatic optic nerve damage, it was demonstrated that RNFL defects were not detectable using fundoscopy if lesions led to less than 50% reduction in RNFL thickness (430). If the lost RGC axons were grouped together, i.e. within a bundle, detection of RNFL atrophy was relatively easy. However, if loss of RGC axons occurred in a circumferential pattern, not limited to RNFL bundles, detection was more difficult as a greater number of RGC would need to be lost to reach the threshold for detection (430). In addition, diffuse RGC axon loss is more difficult to detect directly as areas of atrophic RNFL lack adjacent normal RNFL for comparison (431;432).

The mechanisms that may lead to preferential involvement of RGC projecting to the NS area of the ONH are unknown. Variations in local retinal anatomy, physiology or pharmacology may make these cells and/or axons particularly susceptible to VGB toxicity. Alternatively, RGC damage may be uniform throughout the retinal periphery, as is suggested from the characteristics of VAVFL, however, the NS ppRNFL area may receive a high proportion of peripheral RGC projections relative to central RGC projections, and thus proportionally more ppRNFL thinning occurs in this area early on.

Of interest, no individuals with less than 1000grams cumulative VGB exposure showed a ppRNFL thickness in the NS sector that fell into what is considered to be the abnormal range (i.e. $\leq 1^{st}$ percentile of the manufacturers' normative database), and only four individuals showed borderline changes (i.e. $\leq 5^{th}$–>1^{st} percentile) (Figure 6.2). The range in normal ppRNFL thickness (i.e. $\leq 95^{th}$–>5^{th} percentile of the manufacturers' normative database) in the NS 30^{o} sector was wide in both VGB-exposed and non-exposed individuals, with VGB-exposed individuals showing thickness ranging from 62 – 100µm (Figure 6.2). It is possible that small amounts of ppRNFL loss may occur early after VGB exposure but it may be difficult to detect this loss if relying on the manufacturers' summary report percentiles to assess the data. For example, in individuals with ppRNFL thickness in the NS on the upper-end of normal (e.g. > 100µm thick) significant ppRNFL loss in the NS sector (as much as 40% (or around 40µm) of the ppRNFL thickness), could occur before they would be considered to be showing borderline or abnormal changes in this sector. Significant ppRNFL loss could have occurred in some of the individuals included in the <1000grams cumulative VGB exposure Group, however, the degree of ppRNFL atrophy was not considerable enough to be detectable using the normal percentiles. In future studies using OCT in VGB-exposed individuals, baseline assessments of ppRNFL thickness should be undertaken

and absolute changes in ppRNFL thickness should be monitored. Using this technique it may be possible to detect early indications of VGB retinotoxicity, allowing well-informed decisions to be made about the risk and benefits of continued VGB exposure.

6.4.3.2 A progressive pattern of ppRNFL thinning

In the present study a clear trend was seen for decreasing ppRNFL thickness with increasing VGB exposure (Figure 6.1). However, after receiving a cumulative dose of more than 1000 grams (Groups II, III and IV) there was no significant difference in ppRNFL thickness at any of the 30^{o} sectors between Groups II, III and IV. This was most noticeable between Group II and Group III where although the mean cumulative VGB exposure was more than 2000grams higher in Group III, the pattern and degree of ppRNFL thinning was similar to that in Group II (Figure 6.1).

When each of the VGB exposure Groups comprised of individuals receiving >1000 grams cumulative VGB exposure (Groups II, III and IV) were compared against Group I (<1000g cumulative VGB exposure), the pattern of ppRNFL thinning in each Group appeared to suggested a progressive pattern of ppRNFL thinning across the 30^{o} sectors, i.e. with increasing VGB exposure each Group showed ppRNFL thinning in the same 30^{o} sectors as the previous Group, plus thinning in an additional combination of 30^{o} sectors (Figure 6.7). Interestingly, the NS sector which was the only sector found to show ppRNFL thinning in Group I compared to non-exposed individuals did not show further significant ppRNFL thinning until >5000g cumulative VGB exposure (Group IV). This could suggest that the RGC projecting to this ppRNFL area are susceptible to small amounts of VGB toxicity, yet the RGC that remain after the initial toxic insult are relatively insensitive to additional VGB exposure until later in the course of the toxicity. The reasons for this are unknown but may relate to differences in RGC size or subtype, or differences in the local retinal environment.

Figure 6.7 Difference in ppRNFL thickness in each 30^{o} sector between VGB exposure Groups

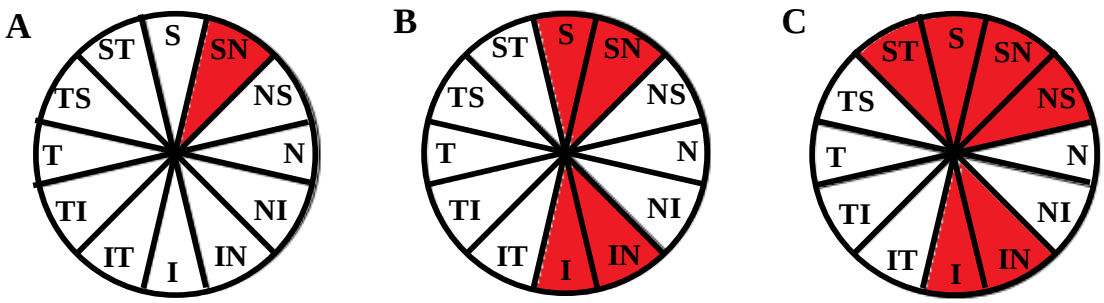

Figure 6.7 legend: Red areas indicate 30^{o} sectors showing significant difference in absolute ppRNFL thickness between Groups ($p<0.05$). **(A)** Group II compared to Group I. **(B)** Group III compared to Group I. **(C)** Group IV compared to Group I.

Whilst this is by necessity a cross-sectional study, the implication is that ppRNFL thinning progresses with increasing cumulative VGB exposure (147;152). This is in keeping with the earlier findings in this body of research that showed a progressive decrease in visual field size with continued VGB exposure over a ten-year follow-up period[31]. ppRNFL thinning occurs early on in the NS sector, progressing to involve adjacent superior areas (Figure 6.7A), later involving the inferior nasal ppRNFL (Figure 6.7B) and subsequently extending to involve more superior temporal areas (Figure 6.7C). It is important to note however, that the lack of significant difference in ppRNFL thickness seen between Groups II, II and IV (i.e. after >1000 grams cumulative VGB exposure) in any 30^{o} sector, suggests that progression may be slow

[31] See Chapter 3

with further increases in cumulative VGB exposure, and may be difficult to detect particularly if baseline ppRNFL thickness data are not available.

6.4.4 Effect of VAVFL severity on the pattern of ppRNFL thinning

In VGB-exposed individuals with normal visual fields the ppRNFL was significantly thinner in the NS sector compared to non-exposed individuals (Figure 6.8A). This is the same sector that was found to be significantly thinner in individuals who had less than 1000g cumulative VGB exposure, and adds further evidence that thinning in this ppRNFL sector may provide an early indication of VGB retinotoxicity, when VAVFL is clinically undetectable.

Figure 6.8 Difference in ppRNFL thickness in each 30^o sector according to VAVFL classification

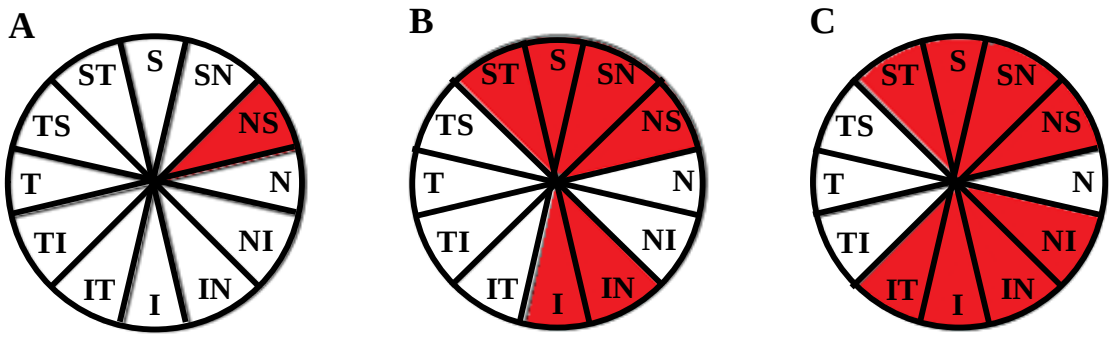

Figure 6.8 legend: Red areas indicate 30^o sectors showing significant difference in absolute ppRNFL thickness compared to non-exposed individuals (Group 2) ($p<0.05$)

(A) VGB-exposed individuals with normal visual fields compared to Group 2. **(B)** Individuals with mild VAVFL compared to Group 2. **(C)** Individuals with moderate/severe VAVFL compared to Group 2

In this body of research it has already been demonstrated that average ppRNFL thickness correlates with visual field size (measured using MRD)[32] in VGB-exposed individuals. In the present study a pattern of ppRNFL thinning associated with the severity of VAVFL is suggested. In individuals with mild VAVFL the pattern of ppRNFL thinning involves the superior and inferior poles of the ONH, extending into the nasal area and sparing the temporal aspect of the ONH, and involving the superior pole more extensively than the inferior pole (Figure 6.8B). In individuals with moderate/severe VAVFL there was further involvement of the ppRNFL in the inferior pole, however the temporal aspect of the ONH is still relatively spared (Figure 6.8C). These findings suggest that in VGB-exposed individuals who are unable to undergo perimetry a combination of the average ppRNFL thickness and the pattern of ppRNFL thinning may be useful surrogate markers of the presence of and severity of VAVFL. It is important to note that in a previous study of ppRNFL thickness in individuals with VAVFL thinning in the nasal 90^{o} quadrant was proposed as a bio-marker for VGB toxicity (256). However, in this body of work, nasal quadrant ppRNFL thinning was not present in more than 40% of individuals with VAVFL[33]. In the present study, the extreme nasal area (Nasal 30^{o} sector) does not appear to be preferentially susceptible to VGB toxicity, but thinning occurs predominantly in the nasal aspect of the superior and inferior poles, indicating that nasal quadrant attenuation may not be a suitable marker for VGB toxicity.

Exploration of the significance of subtle ppRNFL thinning after low VGB exposure and in VGB-exposed individuals with normal visual fields was limited by the cross-

[32] Chapter 4

[33] Individuals were assess n the same OCT model as those included in the study reporting that 100% of individuals with VAVAL had ppRNFL thinning in the nasal 90^{o} quadrant (See Chapter 4)

sectional nature of this study. Prospective longitudinal studies are needed to explore the evolution of ppRNFL loss and to establish whether subtle patterns of ppRNFL thinning, (particularly in the NS sector), after low doses of VGB, provide early predictors of which individuals will go on to develop VAVFL with continued VGB exposure. There is particular scope for such prospective studies currently within the United States where the Food and Drug Administration have recently approved VGB for use as a first-line therapy for infantile spasms, and as add-on therapy for adults with drug-resistant complex partial seizures (263;433).

6.4.5 Analysis of 64 four-scan segments

In this study it was noted that the ppRNFL in adjacent 30^{o} sectors showed variable susceptibility to VGB toxicity. For example, the NS sector showed significant thinning in VGB-exposed individuals with normal visual fields, and in individuals with small cumulative VGB exposure. In addition, the NS sector showed the largest difference in ppRNFL thickness in VGB-exposed compared to non-exposed individuals, with a mean ppRNFL thickness 18% thinner in VGB-exposed individuals. Conversely the adjacent Nasal 30^{o} sector did not show significant ppRNFL thinning in any analysis performed, even in individuals with more than 5000g cumulative VGB exposure and moderate/severe VAVFL. In addition, the mean Nasal ppRNFL thickness was only 1.2% thinner in VGB-exposed compared to non-exposed individuals.

It is possible that analysis of summary parameters, such as 90^{o} quadrants or 30^{o} sectors, may obscure or underestimate true areas of ppRNFL thinning (360) due to contributions from adjacent normal ppRNFL thickness. Therefore, the 256 ppRNFL scans that comprise the circle of ppRNFL thickness data were analysed independently of the manufacturers arbitrarily-divided output. Although the 64 sectors are also arbitrarily defined, they represent much smaller areas of the ONH than the twelve 30^{o} sectors so it

is more feasible that relevant areas of ppRNFL thinning may be found. Ideally the analysis would explore ppRNFL thickness in each of the 256 scan locations. However, this would require a much larger dataset to provide adequate power to detect significant differences. Significant ppRNFL thinning was found in VGB-exposed compared to non-exposed individuals in 29/64 of the four-scan segments (Figure 6.4). When aligned with the 30^{o} sectors, most of the abnormal 29 four-scan segments did not occupy the entire extent of the 30^{o} sectors (Figure 6.4). This suggests that if discrete areas of ppRNFL thinning occur within a 30^{o} sector, it may go undetected if neighbouring areas within the same 30^{o} sector are relatively preserved. This may contribute to the finding in the present study that although the absolute ppRNFL was significantly thinner in the NS 30^{o} sector in individuals with less than 1000grams cumulative VGB exposure, the ppRNFL thickness was still classified as being within the normal limits (i.e. within the $\leq 95^{th}$–>5^{th} percentile of the manufacturers' normative database) (Figure 6.2).

In the 64-segment analysis, preservation of the temporal area was found (Figure 6.4). In the inferior pole the pattern of thinning was comparable to that which was seen in VGB-exposed individuals after analysis of the 30^{o} sectors. Thinning in the superior pole was also found. However, the extreme superior aspect was spared with thinning demonstrated in the temporal-superior and nasal-superior areas. In agreement with the findings from the 30^{o}sector analysis, the most nasal aspect, and part of the nasal-inferior area, were unaffected (Figure 6.4). This dataset was too small to undertake the 64 four-scan segment analyses according to VGB exposure or severity of VAVFL. Further large studies are needed using this detailed analysis to determine if subtle changes in ppRNFL do occur after low VGB exposure.

Use of a smaller scan segments, such as the 64 four-scan segments described in this study, in the analysis of ppRNFL thinning, may prove useful in other diseases. For

example, in glaucoma, small wedge-shaped defects in the RNFL are common (434) and may not be detected by analysis of the manufacturers' arbitrarily-defined 30^o sectors or 90^o quadrants (360). Recently Leung et al. used the RNFL thickness deviation map provided in the Cirrus HD-OCT to characterise the pattern of RNFL defects in glaucoma, outside of the constraints of the manufacturers' summary reports (360). They found that the most common area of RNFL loss was in the inferio-temporal ONH area, between 270^o and 288^o (where 0^o is the temporal horizontal meridian). This area between 270^o and 280^o straddles two of the manufacturers' 30^o sectors, the inferior and IT sectors, which occupy 255-285^o and 285-315^o, respectively. Thus, analysis of the 30^o sectors to assess the integrity of the ppRNFL thickness may not reveal ppRNFL thinning until much later in the course of the disease, as areas of intact ppRNFL may mask areas of ppRNFL atrophy within a 30^o sector.

6.4.6 Pattern of ppRNFL thinning is in keeping with peripheral retinal pathology

It is suggested that the peripheral retina is particularly susceptible to VGB toxicity (84;101;216). The characteristics of VAVFL are of a peripheral and concentric visual field loss, with sparing of the central visual field, visual acuity and colour vision. Studies of animals exposed to VGB have described retinal changes that are commonly confined to the peripheral retina (64;238;243). In addition the only human pathological study of the retina and optic nerve from a VGB-exposed individual described severe loss of RGC in the peripheral retina, with relative sparing of cells in the central retina (162). Studies using wide field multifocal ERG, have suggested that retinal electrophysiological abnormalities are not diffuse, but are localised to areas of VAVFL in the peripheral retina (103).

The pattern of ppRNFL thinning described in the present study is in keeping with the proposed peripheral retinal pathology associated with VGB retinotoxicity and the characteristics of VAVFL. RGC axons entering the temporal aspect of the ONH, which were found to be spared in analysis of all VGB-exposed Groups are those from RGC in the fovea, extrafoveal area and caecocentral area which are responsible for central visual function. Conversely, RGC in the peripheral temporal retina, representing the peripheral nasal visual field, take an increasingly arcuate course to enter the ONH at the superior and inferior poles (247-249), those which were found to show ppRNFL thinning in VGB-exposed individuals. Axons from RGC in the nasal retina (including the nasal periphery) which represent the temporal visual field take a radial trajectory and enter the ONH on the nasal side (247-249).

6.4.7 Discussion of possible mechanisms of VGB-associated ppRNFL thinning with reference to the pattern of ppRNFL thinning

6.4.7.1 RGC size

Susceptibility of RGCs to VGB toxicity has been suggested to be dependent on the length of the non-myelinated segment of the RGC axon (147). Frisen et al. proposed that long RGC axons are preferentially susceptible to VGB toxicity, and in severe RNFL atrophy only RGC with short axons projecting to the central retina remain (147). Whilst this theory in part fits the pattern of atrophy seen in VAVFL, it is not entirely compatible with our understanding of RGC projections. Short axons are found around the entirety of the ONH projecting from RGC in the peripapillary area (247;435). If toxicity were dependent on length of unmyelinated axon, the ensuing visual field defect would be centred on the ONH (physiological blind spot), as short RGC axons were preserved. The pattern of visual field loss in severe VAVFL does not suggest that this is the case. As part of the work carried out for this study severe cases of VAVFL were

observed with only 10^{o} of central vision remaining, and in which the scotoma encompasses peripapillary visual function.

The pattern of ppRNFL thinning described in this study may indicate that susceptibility to VGB toxicity is related to the size of the RGC apparatus, and may be explained by regional variations in RGC characteristics and subtypes. In the non-human primate, RGC can be divided into two main classes based on size. The most numerous are the smaller P-cells (projecting to the parvocellular layers of the lateral geniculate nucleus (LGN)). Larger M-cells (projecting to the magnocellular layers of the LGN) comprise around 10% of the RGC population (230). RGC are not uniform throughout the retina. In the central retina proportionally more RGC are P-cells (230). RGC bodies are small (436-438), and densely-packed (423;436), with compact dendritic fields (439) and small axon diameters (440). With increasing eccentricity all of these attributes increase in size, so that in the peripheral retina RGC have larger cell bodies with expansive dendritic fields and larger axons (436-440). The majority of M-cells are found in the retinal periphery (230). Susceptibility of RGC with large cell bodies, dendritic fields or axon diameters to VGB toxicity would result in loss of peripheral RGC, with sparing of small cells in the central retina. This pattern of loss of RGC would lead to the characteristic peripheral visual field defect seen in VAVFL and would result in a pattern of ppRNFL thinning as described in this study.

Other regional differences in RGC characteristics have also been described. In the periphery, RGC soma sizes are smaller, and more densely-packed, in the nasal than in the temporal hemiretina at corresponding eccentricities (423;436;439). Greater susceptibility to VGB toxicity of larger RGC in the temporal periphery compared to the smaller RGC in nasal periphery, would be in agreement with the reported nasal predominance of VAVFL which has been reported by some groups (81;97;126). In the

nasal hemiretina, RGC along the nasal horizontal meridian compose the visual streak (423;436). Here RGC bodies are smaller (436) and more densely-packed (423;436) than RGC in the non-visual streak nasal retina. We found that axons projecting to the most nasal aspect of the ONH, (i.e. the Nas sector), were not affected by VGB exposure. The extreme nasal aspect of the ONH may be predominantly occupied by axons of RGC in the visual streak, which may be less susceptible to VGB toxicity due to their small size.

Susceptibility of RGC to injury based on size has been shown in several disease models (441). In animal models of glaucoma, RGC with large cell bodies showed an increased susceptibility to high intraocular pressure compared to RGC with small cell bodies (442-445). Furthermore, large RGC have been found to be selectively damaged in humans with glaucoma (398). In addition, large RGC have been shown to be more susceptible to neurotoxic injury (446;447). The mechanisms of selective RGC death is unknown, but may be related to differences in expression of receptors that may be stimulated by neurotoxic factors (445). For example, in an animal model of ocular hypertension, large RGCs expressing the NMDA receptor NR1 subunit were preferentially lost compared to RGCs expressing AMPA receptor GluR 2/3 subunits, suggesting that glutamate excitotoxicity may differentially affect cells expressing specific receptor subtypes (445). Susceptibility of large RGC in the peripheral retina may be related to differences in the expression of neurotransmitter receptors and transporters compared to small RGC in the central retina, resulting in differential susceptibility to VGB toxicity. Alternatively differences in axonal transport and repair mechanisms in some RGC may make them more susceptible injury (448). Particular RGC subtypes may account for this. Frisen et al. suggested that that RGC with large

axons may be more susceptible to VGB toxicity due to their larger surface area and thus greater potential exposure to VGB (147).

6.4.7.2 Müller cell density

An alternative pathological-mechanism that could account for the peripheral pattern of RGC loss after VGB exposure could be related to Müller cell dysfunction (101;216). Several groups have suggested that Müller cell dysfunction may play a significant role in the mechanisms leading to VAVFL (101;150;216;449). Müller cells are the principal glial cells of the human retina. After endogenous release, GABA is transported into Müller cells via the high affinity GABA transporters, GAT-3 and GAT-1 (233). Once inside the Müller cell, GABA is rapidly metabolised by the mitochondrial enzyme GABA-T (237). Due to the efficiency of this reaction, in healthy conditions Müller cells contain very low levels of intracellular GABA (26), and in retinal sections from healthy animals GABA is undetectable in Müller cells using immunhistochemical techniques (26;234;237;450). However, after exposure to VGB, which irreversibly inhibits GABA-T, retinal sections from rats showed significant GABA-immunoreactivity in Müller cells, demonstrated as vertical streaks of staining extending through the depth of the retina to the ELM (234). The prominent Müller cell GABA-immunoreactivity seen in VGB-exposed animals suggests that the inhibition of GABA-T leads to abnormal accumulation of GABA in these cells (234). In further support of this, VGB was found to accumulate in Müller cells in the peripheral retina in VGB-exposed non-human primates (451).

Differences in Müller cell density in the peripheral and central retina may account for the increased susceptibility of peripheral RGCs to VGB toxicity (101). In mammals, Müller cell density in the central retina is around 9000-17000 cells per mm^2 (452), with densities of up to 30,000 Müller cells per mm^2 in the parafoveal area in some species

(453). In the peripheral retina, Müller cell densities are much lower and are between 5000-8000 cells per mm^2 (452;453).

Presuming that VGB is equally distributed across the retina and is taken uniformly into Müller cells regardless of eccentricity, the inhibitory effects of VGB on GABA-T should lead to less accumulation of GABA in Müller cells in the central retina where cell numbers are higher, compared to in the periphery where cell numbers are comparatively low (101). In the peripheral retina where Müller cell density is low, VGB may inhibit a high proportion of the available GABA-T. Any remaining GABA-T that has not been inhibited by VGB may be unable to sufficiently metabolise GABA, resulting in accumulation within the Müller cell. In the central retina where Müller cell density is high, proportionally less GABA-T may be inhibited by VGB, leaving higher levels of active GABA-T able to metabolise the available GABA, and preventing accumulation within the Müller cell.

Chronic accumulation of GABA in the Müller cell may result in it becoming dysfunctional (216;449). In agreement with this, increased Müller cell GFAP expression has been reported in animals exposed to VGB (240-242). In some animals this was most notable in the peripheral retina (236;238) where other pathological retinal abnormalities were localised. Up-regulation of Müller cell GFAP is a sensitive marker of retinal injury (454), and further suggests that Müller cells may be implicated in mechanisms of VAVFL.

Müller cell dysfunction after VGB exposure is supported by human electrophysiological data. In VGB-exposed individuals, a reduction in the amplitude of the b-wave of the electroretinogram, which reflects combined Müller cell and bipolar cell function, has been demonstrated (101;104;120;138;150;154;196). Furthermore, the b-wave amplitude

reduction persists even after VGB withdrawal (150;151;153). In addition, of all retinal electrophysiological measures, the reduction in the b-wave amplitude has most consistently been shown to be correlated with the severity of VAVFL (105;109;135;150;151).

Although Müller cell dysfunction would not result in visual field loss itself (216), it may lead to loss of RGC by increasing their susceptibility to toxic stimuli (454). Müller cells are important regulators of the extracellular environment and supply metabolites and neurotrophic factors to retinal cells (26;450) including RGC (455). In addition, in experimental studies Müller cells have been found to protect RGC from glutamate excitotoxicity (456-459), hypoxia (459) and optic nerve injury (460), probably through uptake and metabolism of toxins and releases of neurotrophic factors (460). Müller cell dysfunction, as a consequence of GABA accumulation, may lead to RGC death (101). This could result from the lack of normal regulation of the RGC extracellular environment by the Müller cell. For example, Müller cells are also involved in glutamate uptake after synaptic release from bipolar cells and clearance of glutamate from the synaptic cleft by Müller cells is essential for the prevention of glutamate excitotoxicity (461). Impairment of normal glutamate uptake by Müller cells may result RGC death (462). RGC death as a consequence of glutamate excitotoxicity has implicated in glaucoma (463) and retinal hypoxia/ischemic (464) although this is controversial (465;466). In addition, under continued exposure to toxic or injurious conditions Müller cells may undergo gliotic changes, which may be associated with enhancing vulnerability of RGC to injury and induce RGC death, by release of cytokines (e.g. tumour necrosis factor-alpha (454;467;468)).

6.4.8 Summary

The ppRNFL is significantly thinner in VGB-exposed individuals compared to non-exposed individuals in a pattern consistent with the reported peripheral retinal pathology and the peripheral, concentric characteristics of VAVFL. After VGB exposure, ppRNFL thinning involves the superior and inferior poles of the ONH with relative sparing of the temporal and extreme nasal aspect of the ppRNFL. The pattern of ppRNFL thinning described in this study may reveal more about the mechanisms of VGB retinotoxicity. Differences in RGC size and/or Müller cell density may lead to differences in suggestibility between the peripheral and central retina to VGB toxicity.

ppRNFL thinning in the NS 30^{o} sector may occur early after VGB exposure in individuals with normal visual fields. With increasing VGB exposure ppRNFL thinning may progress to involve RGC projections in the superior and inferior poles of the ONH.

Caution should be exercised when exploring patterns of ppRNFL thinning according to the manufacturers' arbitrarily-defined 30^{o} sectors and 90^{o} quadrants which may obscure or underestimate true areas of thinning. Use of smaller scan segments, such as the 64 four-scan segments described in this study, in the analysis of ppRNFL thinning, may prove a useful tool for understanding patterns of ppRNFL thinning in VGB retinotoxicity and other disease involving RGC loss. Prospective longitudinal studies are needed to explore the evolution of ppRNFL thinning with continued VGB exposure and its relationship to the development of VAVFL. In addition, larger (possibly cross-centre) studies would enable analysis of ppRNFL thickness based on individual A-scan data, as opposed to using arbitrarily-defined ONH regions.

Chapter 7 ppRNFL thickness in individuals with epilepsy not exposed to vigabatrin

7.1 Introduction

In recent years there has been a resurgence of interest in studying the retina as a window to the brain and neurological disease processes (469-471). The retina has been described as an "outgrowth of the brain", and during development is formed by an optic outgrowth of the diencephalon. Thus pathological changes in the brain parenchyma may also be present in the retina. For example, one of the pathological hallmarks of Alzheimer's disease includes the accumulation of β-amyloid protein in the brain. Recently, in a mouse model of Alzheimer's disease, β-amyloid immunereactive plaques were detected in the retina, most prominently in the RGC layer (472). In addition RGC degeneration has been described in retinas from individuals with Alzheimer's disease (473). Thus the retina provides a unique window into the CNS, as unmyelinated axons (RGC axons in the RNFL) can be viewed easily and non-invasively using a variety of imaging techniques. In particular, imaging of the ppRNFL using OCT has been explored in several neurological diseases (474;475). Thinning of the ppRNFL has been reported in individuals with Alzheimer's disease (476;477), Parkinson's disease (478), Friedreich's ataxia (479), migraine (480), cerebral autosomal dominant arteriopathy with subcortical leukoencephalopathy (CADASIL) (481) and multiple sclerosis (with and without optic neuritis) (369;482). In individuals with multiple sclerosis, ppRNFL thickness correlated with disability scores, which included non-visual functions (e.g. motor function) (483), suggesting that in MS, damage to CNS white matter may be

detected by imaging of the ppRNFL (484). It is suggested that OCT imaging of the retina may provided insights into neurological disease pathogenesis, and ultimately may provide biomarkers for disease progression, and possibly for neuroprotection in clinical trials. In fact, OCT imaging has been incorporated into a number of large neurological clinical trials that will take place over the next decade (475).

Whilst several studies have explored ppRNFL thickness in individuals with epilepsy exposed to VGB (119;229;256;257), only one study has looked at individuals with epilepsy not exposed to VGB (260). In a study by Lobefalo et al. no difference was found in the ppRNFL between individuals with epilepsy (n=45) and age-matched healthy controls. The individuals included in the study were adolescents (age 11-18 years) with newly-diagnosed epilepsy and monotherapy with either carbamazepine or valproic acid for one year duration. In disagreement with the findings by Lobefalo et al. abnormal ppRNFL thinning has been described in non-exposed control populations in OCT studies of VAVFL (229;256). In the individuals with epilepsy not exposed to VGB (Group 2) included in the present study, 9% showed abnormal average ppRNFL thinning and 13.8% showed borderline changes[34].

In individuals with epilepsy, ppRNFL thinning may be associated with certain clinical features or prognostic factors. Understanding factors associated with ppRNFL thinning in non-exposed individuals may also help to identify risk factors for VAVFL.

7.1.1 Aims

The aim of this study was to determine if individuals with epilepsy not exposed to vigabatrin show ppRNFL thinning compared to healthy individuals. Furthermore, the study will explore factors that may contribute to ppRNFL thinning.

[34] See Chapter 6

7.2 Methods

7.2.1 Patients

Non-exposed individuals with epilepsy (Group 2) and healthy controls (Group 3) were included in the analysis.

7.2.2 OCT

All OCT ppRNFL imaging was carried out using SD-OCT.

7.3 Results

OCT ppRNFL data were available for 87 individuals with epilepsy not exposed to VGB (Group 2) and 90 healthy controls (Group 3).

7.3.1 ppRNFL thickness in non-exposed individuals with epilepsy compared to healthy individuals

Average ppRNFL thickness was significantly thinner in Group 2 compared to Group 3 (88.8µm and 94.4µm respectively; $p < 0.001$; Table 7.1). The superior, inferior and temporal quadrants were significantly thinner in Group 2 compared to Group 3 ($p<0.05$; Table 7.1)

Table 7.1 Average ppRNFL thickness and ppRNFL thickness in each of the 90° quadrants in Group 2 and Group 3

ppRNFL area	Group 2 N = 87	Group 3 N = 90	Group 2 Percentage showing ppRNFL thinning[a]		Group 3 Percentage showing ppRNFL thinning[a]	
			≤1st	≤ 5th– >1st	≤1st	≤ 5th– >1st
Average thickness (±SD) (µm)	88.8 (±10.9)*	94.4 (±8.8)	8.0	13.8	0	4.5
Superior thickness (±SD) (µm)	108.8 (±16.4)*	115.9 (±13.9)	10.3	8.0	1.1	1.1
Nasal thickness (±SD) (µm)	70.4 (±12.2)	73.8 (±10.6)	2.3	3.4	0	0
Inferior thickness (±SD) (µm)	113.9 (±18.5)*	122.8 (±14.4)	10.3	13.8	0	1.1
Temporal thickness (±SD) (µm)	62.1 (±9.2)*	65.2 (±10.2)	2.3	2.3	0	3.4

Group 2 = non-exposed individuals; Group 3 = healthy individuals

ppRNFL = peripapillary retinal nerve fibre layer;

*ppRNFL significantly thinner in Group 2 compared to Group 3 (P<0.05)

7.3.2 Clinical features associated with ppRNFL thinning in non-exposed individuals with epilepsy

For individuals in Group 2, independent samples T-tests were used to explore differences in ppRNFL thickness according to clinical and demographic features. There was no effect of gender, smoking, history of febrile seizures or drug resistance on ppRNFL thickness (p>0.05; Table 7.2). The ppRNFL was significantly thinner in

individuals with learning disability compared to individuals without learning disability (p=0.015; Table 7.2)

Table 7.2 Mean average ppRNFL thickness in Group 2 according to clinical features

	Average ppRNFL thickness (µm) (±SD)	
Sex	Male	Female
	87.1 (± 12.0)	90.0 (± 10.2)
	Yes	No
Smoker	89.2 (± 9.9)	87.4(± 12.4)
Drug-resistance	86.6 (± 11.5)	91.1 (± 10.5)
Learning disability	81.7 (± 9.9)*	89.1 (± 11.1)
History of febrile seizures	85.6 (± 8.1)	88.3 (± 11.3)

*ppRNFL significantly thinner in individuals with learning disability P = 0.015

7.3.3 History of neurosurgery and ppRNFL thickness

8/87 Individuals had undergone neurosurgery. Seven of theses were temporal lobe resections and one was an excision of a parietal haemagioma. ppRNFL thickness was compared between individuals who had undergone and those who had no history of neurosurgery. No significant difference in average ppRNFL thickness, or ppRNFL thickness in any the 90^{o} quadrants was found between the two groups, although there was a trend for decreased ppRNFL thickness in the inferior quadrant of individuals who had undergone neurosurgery (p>0.05) (Table 7.3).

Table 7.3 ppRNFL thickness in Group 2 individuals with a history of neurosurgery compared to individuals with no history of neurosurgery

ppRNFL area	History of neurosurgery	
	Yes (N=8)	No (N=79)
Average thickness (±SD) (μm)	87.1 (±9.3)	89.0 (±11.1)
Temporal thickness (±SD) (μm)	61.3 (±8.4)	62.2(±9.3)
Superior thickness (±SD) (μm)	110.3 (±19.1)	108.7 (±16.2)
Nasal thickness (±SD) (μm)	69.0 (±9.8)	70.6 (±12.4)
Inferior thickness (±SD) (μm)	107.6 (±19.2)	114.5 (±18.5)

7.3.4 Epilepsy type and ppRNFL thickness

Individuals with mesial temporal lobe epilepsy with hippocampal sclerosis (MTLE with HS) (N=20) were compared with individuals with partial epilepsy of unknown cause (N=31) (Table 7.4). There was no significant difference in average ppRNFL thickness. The ppRNFL was significantly thinner in the inferior quadrant in individuals with MTLE with HS compared to individuals with partial epilepsy of unknown cause (p=0.025; Table 7.4). Individuals with other epilepsy types included those with malformation of cortical development (N=11) and "other" types (including angioma or vascular malformation, stroke, infection, neurocutaneous syndromes, tumour and trauma) (N=25). These individuals were not included in the analysis due to the small numbers of individuals within each group.

Table 7.4 ppRNFL thickness in Group 2 individuals with MTLE with HS compared to individuals with partial epilepsy of unknown cause

ppRNFL area	MTLE with HS (N = 20)	Partial epilepsy of unknown cause (N = 31)
Average thickness (±SD) (µm)	84.4 (±9.2)	89.4 (±9.6)
Superior thickness (±SD) (µm)	104.5 (±17.1)	109.6 (±12.4)
Nasal thickness (±SD) (µm)	66.4 (±8.5)	70.2 (±11.7)
Inferior thickness (±SD) (µm)	104.9 (±17.6)*	117.2 (±17.9)
Temporal thickness (±SD) (µm)	63.3 (±10.3)	58.3 (±12.4)

ppRNFL = peripapillary retinal nerve fibre layer; MTLE + HS = Mesial temporal lobe epilepsy with hippocampal sclerosis

*ppRNFL significantly thinner in HS compared to cryptogenic P = 0.025

7.3.5 Age and duration of epilepsy and ppRNFL thickness

There was no correlation between age and average ppRNFL thickness (p=0.071) or age of epilepsy onset and average ppRNFL thickness (p=0.281). There was a weak correlation between duration of epilepsy and average ppRNFL thickness (r=-0.24; p=0.025; Figure 7.1). However, this was not found to be significant after controlling for age (p=0.15).

Figure 7.1 Scatter plot of average ppRNFL thickness and duration of epilepsy

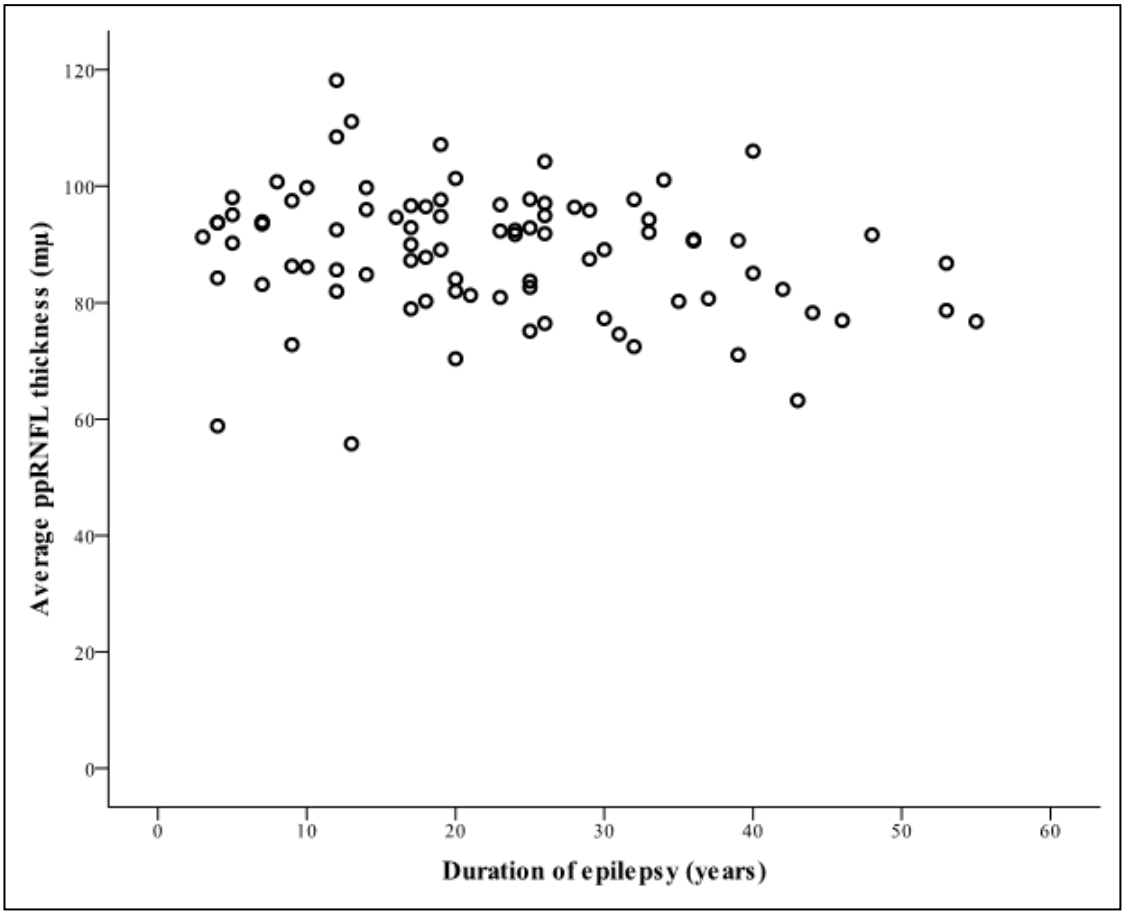

Figure 7.1 legend: There was a weak correlation between ppRNFL thickness and duration of epilepsy (r=-0.24; p=0.025; N=87) which was not found to be significant after controlling for age (p=0.15).

7.3.6 Antiepileptic drug exposure and ppRNFL thickness

There was no effect of exposure to any antiepileptic drug, (excluding vigabatrin), on ppRNFL thickness (p>0.05). No correlation was found between number of drugs used and mean ppRNFL thickness (r=-0.153, p=0.15).

7.4 Discussion

To my knowledge, this is the largest study to explore ppRNFL thickness in individuals with epilepsy not exposed to vigabatrin, and the first to explore clinical factors associated with ppRNFL thinning. We found that the ppRNFL is significantly thinner in individuals with epilepsy not exposed to VGB compared to age-matched healthy controls. 8.0% of individuals had average ppRNFL thickness that fell into the abnormal range, and 13.8% showed borderline changes, according to the manufacturers' normative database.

The findings from this study are in disagreement with the only other study of ppRNFL thickness in non-exposed individuals with epilepsy. In a study by Lobefalo et al. there was no difference in ppRNFL thickness in any of the four 90^{o} quadrants compared to age-matched healthy controls (260). The population included in the study by Lobefalo was dissimilar to the one included in this study (Table 7.5). In the study by Lobefalo, individuals had newly diagnosed epilepsy and exposure to only one AED (either carbamazepine or valproate monotherapy) for one year. In comparison, the population included in this study had exposure to between 1 and 15 AEDs and had a mean duration of epilepsy of 24 years Table 7.5). No further clinical details of the subjects epilepsy were provided in the study by Lobefalo et al. so we are unable to compare the populations on other clinical characteristics.

Table 7.5 Comparison of characteristics of individuals included in the study by Lobefalo et al. and the present study

	Lobefalo et al. (260) (N=45)	This study (N=89)
Age (years) [range]	15.7 [11-18]	37.3 [18-70]
Mean duration of epilepsy (years) [range]	1 [1]	24 [3-58]
Mean number of AEDs exposed to [range]	1 [1]	6 [1-15]
AEDs exposed to	CBZ, VPA	ACE, ACTH, CBZ, CDP, CLB, CLN, ETS, FBM, GBP, LAC, LEV, LTG, OXC, PB, PHT, PGB, PMD, TGB, TPM, VPA, ZNS

AED = antiepileptic drug; ACE = acetazolamide; ACTH = adrenocorticotrophic hormone; CBZ = carbamazepine; = CDP = chlordiazepoxide; CLB = clobazam; CLN = clonazepam; ETS = ethosuximide; FBM = felbamate; GBP = gabapentin; LAC = lacosamide; LEV = levetiracetam; LTG = lamotrigine; OXC = oxcarbazepine; PB = phenobarbital; PHT = phenytoin; PGB = pregabalin; PMD = primidone; TGB = tiagabine; TPM = topiramate; VPA = valproate; ZNS = zonisamide;

In agreement with this study, Lawthom et al. reported that 3/12 non-exposed individuals with epilepsy had a ppRNFL thickness that fell into the abnormal range (i.e. $\leq 5^{th}$ percentile of the manufacturers' normative database) in at least one 90^{o} quadrant, although all individuals showed normal average ppRNFL thickness. The authors postulated that the ppRNFL thinning in these individuals may be due to transynaptic retrograde degeneration because of long-standing cerebral lesions. However, they say that in an unpublished study of nine individuals with visual field defects from cortical

lesions, ppRNFL thickness was normal suggesting that trans-synaptic degeneration is not present, or is not identifiable using OCT. The authors concluded that the abnormalities probably arose due to misalignment of the subject or scan circle during the ppRNFL scanning procedure (256).

The reasons for ppRNFL thinning in individuals with epilepsy not exposed to VGB are uncertain. Atrophy of the optic nerve was found to be common in children presenting with their first unprovoked seizure, however in most cases this was thought to be related to neonatal birth injury (485). To my knowledge, the occurrence of optic atrophy in adults with epilepsy has not been explored.

7.4.1 Mechanisms of ppRNFL thinning in individuals with epilepsy

The cell body and proximal unmyelinated portion of the RGC axon lie within the retina, YET, MOST of the RGC axon is located outside the globe forming the intraorbital, intracanalicular and intracranial portions of the optic nerve, the optic chiasm and optic tract (230). More than 80% of RGC axons terminate in the lateral geniculate neucleus (LGN) of the thalamus, where they make synaptic connections with LGN relay neurones that project to the striate cortex. The projections to the striate cortex comprise the optic radiation (genicuolstriate fasciculus). Damage to any part of the visual pathway from the RGC body to the striate cortex could result in RNFL thinning detectable using OCT imaging. For example, in VGB-exposed individuals, primary or secondary toxic effects of elevated retinal VGB and/or GABA my lead to RNFL thinning due to RGC damage at the level of the retina (101)[35]. Conversely, RNFL thinning can also occur as a result of retrograde-transynaptic degeneration of RGC after lesions involving the occipital lobe (295;419;420). Some of the possible

[35] The hypothesis of this study

causes of ppRNFL thinning seen in non-exposed individuals with epilepsy in the present study are discussed here.

7.4.2 ppRNFL thinning as a result of retinotoxicity

In this study, no association was found between ppRNFL thinning and exposure to any particular AED. However, AEDs are commonly associated with retinal electrophysiological and visual functional abnormalities (176). After the initial reports of VAVFL, concerns were raised as to whether retinotoxicity was a class effect of GABAergic drugs. Early reports of visual field loss associated with exposure to tiagabine (486;487), a GAT-1 blocker, led to further concerns. However, subsequent studies showed that tiagabine was not associated with the development of visual field loss (105;192). In addition, rats exposed to a dose of tiagabine did not show increased retinal GABA concentrations, whereas rats exposed to VGB had retinal GABA concentrations of more than 260% of control animals (15). The proposed mechanisms of action of tiagabine are through blocking the high affinity GABA transporter GAT-1. This allows temporarily sustained synaptic GABA concentrations after endogenous release (488), but does not result in widespread increases in GABA concentrations (16).

In individuals receiving VGB, co-medication with valproate has received attention as a possible promoter of the retinotoxic effects of VGB (108;114;164). Valproate inhibits the enzyme succinate semialdehyde dehydrogenase, resulting in elevated levels of succuinate which is a potent inhibitor of GABA-T activity (407). Inhibition of GABA-T by both VGB and valproate when used concomitantly could lead to increased risk of VGB-retinotocicity. However, Wild et al., Lobefalo et al. and others (405) have found normal ppRNFL thickness in individuals receiving valproate monotherapy (229;260).

A retinotoxic class effect of the GABAergic AEDs is therefore unlikely (105;489). However, around 40% of retinal cells are GABA-immunoreactive (490) and thus pharmacological manipulation of GABAergic pathways by AEDs can be associated with retinal electrophysiological changes and visual impairment (176). In addition many AEDs with non-GABAergic mechanisms of action are also associated with visual side effects (176). Visual disturbances including diplopia, blurred vision, abnormal colour perception and nystagmus are relatively common side effects of many AEDs. These visual side effects are predominantly related to neurotoxic drug levels, over-dose or long-term use, and subside after the drug is reduced or withdrawn (for a review see (175;176)) and are not known to be related to long-term structural retinal changes

7.4.3 ppRNFL thinning as a result of brain pathology

It is becoming apparent that retrograde trans-synaptic degeneration can occur in the human visual pathway (295;420)[36]. High resolution in vivo imaging techniques such as OCT may be more sensitive at detecting subtle patterns of ppRNFL atrophy than has been previously achievable by direct clinical observation (295). Recently, thinning of the ppRNFL has been detected using OCT in individuals with homonymous hemianopia secondary to congenital (295;420) and acquired lesions (295) of the occipital cortex. Similarly, as part of this body of research it was found that the ppRNFL was significantly thinner in VGB-exposed individuals with homonymous quadrantinopic or hemianopic defects than in individuals without homonymous defects, after controlling for the amount of VGB exposure. This was suggested to be due to retrograde trans-

[36] See also 5.4.6

synaptic degeneration secondary to lesions in the optic radiation as a result of surgical resection of the temporal lobe[37].

7.4.4 Neurosurgery and ppRNFL thinning

In the present study, no difference in ppRNFL thickness was found in non-exposed individuals who had undergone neurosurgery. Although a trend for decreased ppRNFL thickness in the inferior quadrant was seen in individuals who had undergone surgery, where the average ppRNFL thickness was 107.6 µm, compared to individuals with no history of surgery where the thickness was 114.5µm. Only 8/87 individuals had a history of surgery and so the lack of significance may be due to the small numbers included in the study.

A weakness in this study was that visual fields were not routinely assessed in individuals with epilepsy not exposed to VGB, thus it was unknown whether any of the individuals who had undergone surgery showed homonymous visual field defects. Seven of the individuals who had a history of neurosurgery had undergone temporal lobe resections which are associated with post-operative visual field defects in between 15 and 100% of individuals (408). Visual field defects associated with temporal lobe resections (or other temporal lobe lesions) result from disruption of the optic radiations in the temporal lobe. The visual pathways are retinotopically organised, such that lesions in any part of the pathway will result in a defect in a known area of the visual field. After leaving the LGN, fibres in the optic radiation project in a retinotopicaly organised pattern, where fibres in the most anterior aspect of the optic radiation (Meyer's loop) are those which have received afferent input in the LGN from RGC in the inferior retina (including uncrossed RGC axons from the ipsilateral inferior temporal

[37] See 5.4.6

retina, and crossed RGC axons from the contralateral inferior nasal retina). Lesions involving the anterior optic radiation result in a defect of the superior quadrant of the visual field, immediately adjacent to the vertical meridian, ipsilateral to the lesion (409). Lesions involving the anterior portion of the optic radiation (Myers loop) resulting in homonymous superior quadrantinopias, may be associated with retrograde trans-synaptic degeneration of the RGC in the corresponding inferior retina. RGC projections in the RNFL respect the horizontal meridian, thus atrophy of RGC axons in the inferior retina may be detected as ppRNFL thinning in the inferior aspect of the ONH. In the manufacturers' summary report for a ppRNFL thickness scan using OCT, RGC in the inferior retina would be most represented in the inferior 90^{o} quadrant. The nasal and temporal 90^{o} quadrants straddle the horizontal meridian and thus will receive projections from both the superior and inferior retina, and the superior quadrant lies superiorly to the horizontal meridian. The trend towards ppRNFL thinning in the inferior 90^{o} quadrant in individuals who had undergone neurosurgery (7/8 of whom had temporal lobe resections), may be related to trans-synaptic retrograde degeneration involving these projections.

7.4.5 Epilepsy type and ppRNFL thinning

ppRNFL thickness changes were also seen in the inferior quadrant in individuals with MTLE wit HS where the ppRNFL was significantly thinner compared to individuals with partial epilepsy of unknown cause. This finding could also be related to pathological changes in the anterior optic radiation and resulting trans-synaptic degeneration of RGGs in the corresponding inferior retina. MTLE is commonly associated with abnormalities of the hippocampus and mesial temporal lobe structures that can be detected using routine MRI. Until recently brain pathology associated with MTLE was thought largely to be confined to these mesial temporal lobe structures.

However, advances in neuroimaging and computerised analysis techniques have demonstrated that in individuals with MTLE, brain atrophy and abnormality extends to involve brain areas outside of the mesial temporal lobe, involving cortical and subcortical grey matter (491;492) and widespread white matter networks (493-495). In addition, a recent pathological study of post mortem brains from individuals with drug-resistant epilepsy and hippocampal sclerosis found widespread neocortical and white matter pathology (496).

Using advanced neuroimaging techniques, including diffusion tensor imaging, voxel-based morphometry and proton magnetic resonance spectroscopy, abnormalities of the temporal (497-499) and extra-temporal white matter (497), have been reported in individuals with MTLE. The abnormalities reported include decreased whole brain white matter volume (500), and decreased white matter volume in the temporal lobe, ipsilateral (499;501;502) and contralateral (502) to the seizure focus. Additionally, features suggestive of abnormal or reduced myelination (297;493-495), and axonoal loss (297;493;498), have been detected in white matter tracts, including the corpus callosum (297;494;495;501-504); cingulum (297;503); external capsule (297;494;495); the fronto-temporal and temporo-occipital projections (493), and the uncinate (505), fronto-occipital and superior longitudinal fasciculus (504).

The pathophysiology and aetiology of white matter abnormalities in individuals with epilepsy are unknown. A number of possible causes have been suggested including direct damage from chronic, recurrent epileptic activity (296;502), disruptions of normal white matter development in individuals with childhood seizures (296;497;502;506) and exposure to AEDs (502). White matter volume reduction was associated with earlier age at seizure onset and longer duration of epilepsy (296)

White matter abnormalities might also be present in the optic radiation, and may be associated with trans-synaptic retrograde degeneration of retinal ganglion cells in the inferior retina. Generalised atrophy involving the optic radiations could result in loss of RGC through trans-synaptic degeneration and account for the decrease in average ppRNFL thickness seen in individuals with epilepsy. More focal atrophy could be related to local pathology, including HS and surgical resection, leading to focal ppRNFL thickness changes that are detectable on analysis of the 90^{o} quadrants or 30^{o} sectors.

7.4.6 White matter abnormalities and cognitive function

Diffuse white matter pathology may also explain differences in ppRNFL thickness seen in individuals with and without learning disability. In this study individuals with learning difficulty were found to have significantly thinner average ppRNFL thickness compared to individuals without learning difficulty ($p=0.015$). An association between cognitive function and ppRNFL thickness has been found in studies of individuals with multiple sclerosis where ppRNFL thinning is associated with cognitive disability (as measured using the Brief Repeatable Battery – Neuropsychology) (293). Similarly in healthy, young individuals ppRNFL thickness was found to be associated with level of cognitive functioning (294). In addition, ppRNFL thinning is found in individuals with Alzheimer's disease (476;477) and mild cognitive impairment (477).

Cognitive impairment is a recognised co-morbidity of chronic epilepsy, adding further to the burden of the disorder (507-510). Much research has focused on factors that may contribute to cognitive dysfunction such as seizure frequency and severity, chronic AED use, age of epilepsy onset and duration of epilepsy (511;512). Recent research has aimed to identify the neural mechanisms of cognitive impairment in epilepsy (511).

Individuals with epilepsy can have impairments in multiple cognitive domains including memory impairment, frontal lobe dysfunction, language deficits and psychomotor slowing (507;510). A "disconnection model" has been suggested to explain this profile of widespread cognitive impairment (493;513). Normal cognitive function depends on the coordinated activity of several brain regions, and disruption of cerebral networks may lead to pervasive cognitive decline (493;511;513).

It is becoming evident that diffuse white matter pathology in individuals with epilepsy may contribute to cognitive impairment (514). Global reduction in white matter volume has been associated with cognitive dysfunction in individuals with epilepsy (515). Similarly, in individuals with TLE widespread white matter abnormalities identified using diffusion tensor imaging, were associated with poor cognitive performance in tasks involving memory (493;505;514), language (514) and executive function (493). The characteristics of the diffusion changes seen using diffusion tensor imaging in individuals with TLE were suggesting of chronic Wallerian degeneration, possibly due to seizure-induced cell damage in the temporal lobe (505). Furthermore it is suggested that abnormalities detected using diffusion tensor imaging can be used to predict cognitive impairment in individuals with TLE (514).

The ppRNFL thinning identified in this study in individuals with learning disability may be associated with the global white matter abnormalities identified in neuroimaging studies of individuals with cognitive impairment. Widespread abnormalities and atrophy of cerebral white matter may result in trans-synaptic changes in RGC, resulting in RGC axon loss and associated RNFL thinning that can be detected by measuring ppRNFL thickness.

7.4.7 Grey matter abnormalities

Neuroimaging studies have demonstrated that individuals with TLE show brain atrophy and abnormality involving cortical and subcortical grey matter (491;492). A review of studies using voxel-based morphometry identified twenty-six grey matter regions that were found to be significantly reduced in volume in individuals with TLE compared to healthy controls (492). The most frequently reported abnormality was in the hippocampus, with abnormalities of the thalamus as the second most reported brain changes in individuals with TLE (492). In individuals with TLE, atrophy of the thalamus has been reported in several recent studies (300;491;516;517). The pattern of abnormal signal detected in the thalamus using diffusion tensor imaging in individuals with MTLE (with and without HS), were consistent with neuronal loss and gliosis (516;518).

The lateral geniculate nucleus is one of the nuclei of the thalamus. More than 80% of RGC axons terminate in the LGN in a highly organised retinotopic pattern, where they make synapses with geniculocalcarine neurones that project to the primary visual cortex. Thalamic atrophy involving the LGN could lead to loss or RGC axons which could be detected using OCT imaging.

7.4.8 Duration of epilepsy

In the present study, longer duration of epilepsy showed a weak association with decreasing average ppRNFL thickness. In individuals with TLE, both grey- (299;300) and white matter (296-298) abnormalities and atrophy have been associated with longer duration of epilepsy, indicating that in some individuals progressive brain atrophy may occur with continuing seizure activity (299). Longer duration of epilepsy is also associated with the development and progression of cognitive impairment which may be associated with progressive neuronal loss (299;507;508). The decreasing ppRNFL

thickness associated with increasing duration of epilepsy seen in this study may be reflecting the progressive cerebral grey- and white matter abnormalities identified using neuroimaging techniques in individuals with TLE. However, both the present study, and those reporting grey and white matter changes associated with duration of epilepsy, have been cross-sectional studies. After controlling for age, duration of epilepsy was not associated with ppRNFL thinning, and thus the correlation seen may reflect age-related loss in ppRNFL thickness, which has been described in healthy individuals (285;390;401;402). However, age was not found to correlate with ppRNFL thickness in this population. Further studies are needed in a larger population to determine the effect of duration of epilepsy and age on ppRNFL thickness.

7.4.9 The utility of OCT in epilepsy

The findings from the present study suggest that OCT ppRNFL imaging may have the potential to become a valuable tool in the evaluation of clinical and prognostic factors in epilepsy. OCT imaging is non-invasive and entails little, if any, discomfort or distress for the subject being examined. It is easily quantifiable and highly repeatable, in addition it is of low cost and has a relatively short examination time (less than 10 minutes) compared to neuroimaging techniques (519).

Of particular interest in the present study is the association between ppRNFL thinning and cognitive impairment and duration of epilepsy. Larger, longitudinal studies are needed to determine whether ppRNFL thinning reflects progressive cognitive decline in association with global or local changes in brain white matter volume in individuals with chronic drug-resistant epilepsy. In the present study the presence of cognitive impairment (or "learning disability") was determined from the clinical notes of each subject. No distinction was made as to the severity or nature of the learning disability, or in some cases whether the individual had undergone formal neuropsychological

assessment. It is possible that in some cases an individual with learning disability may not have been included in the "learning disability" group as there was no record of impairment in the medical notes. Future studies should use more detailed and unambiguous measures of cognitive function, including formal neuropsychological assessments, aiming to determine the relationship between impairment of specific or global cognitive domains and ppRNFL thickness. As cognitive function is reassessed overtime, OCT ppRNFL imaging should also be repeated to determine whether any change in cognitive function is associated with changes in the ppRNFL thickness. If a relationship is present this may suggest a potential for the use of OCT ppRNFL imaging a as a biomarker for disease modifying therapies and for neuroprotective strategies in epilepsy.

Finally, a possible cause of continued seizures following temporal lobectomy for hippocampal sclerosis could be due to more widespread neocortical and white matter pathological changes (496;520;521). If ppRNFL thinning is a marker for widespread neuronal abnormality and loss, it may provide a useful biological marker of surgical outcome in individuals with drug-resistant epilepsy. Further studies should investigate the relationship between ppRNFL thickness measured pre-surgically and post-surgical seizure outcome.

7.5 Conclusion

ppRNFL thinning may be present in up to 22% of individuals with epilepsy not exposed to VGB. ppRNFL thinning may be associated with cognitive impairment, longer duration of epilepsy and specific epilepsy types, in particular MTLE with HS. ppRNFL thinning may occur due to transynaptic degeneration of RGC as a result of white matter

pathology involving the postgeniculate visual pathway. This could entail diffuse axonal loss occurring throughout the CNS or focal lesions involving the visual pathway (484). Alternatively, loss of RGC may result from atrophy of the thalamic nuclei including the lateral geniculate nucleus. Larger longitudinal studies of individuals undergoing detailed neuropsychological assessment, white matter imaging (e.g. using diffusion tensor imaging) and ppRNFL imaging using OCT are needed to fully determine the clinical utility of OCT ppRNFL imaging in epilepsy.

Chapter 8 Conclusions, limitations and future work

8.1 Study limitations

The limitations and weaknesses of the present study must be considered in the interpretation of results and conclusions presented in this thesis, and should be addressed in the development of future work.

8.1.1 General limitations

Study design

A major limitation to the present study is the cross sectional design. The results from this study suggest that ppRNFL thinning and VAVFL progress with continued VGB exposure (Chapter 3, 5 and 6). In addition, it is suggested that in non-exposed individuals, ppRNFL thinning may be associated with longer duration of epilepsy (Chapter 7). These conclusions were inferred from cross sectional data after grouping individuals according to VGB exposure, or by using correlation analysis. Evidently, further prospective studies using OCT in individuals with epilepsy are needed to confirm these finding.

In Chapter 3, the progression of VAVFL with continued VGB exposure was assessed retrospectively by quantifying visual field examinations performed by several examiners over a ten-year period. The limitations of perimetry are discussed in depth in Chapter 3. With regard to the retrospective design of the study, several important issues must be considered. These include inter-examiner sources of variability in the visual field assessment; non-blinded assessments and examiner bias (all examinations were

performed because the individuals were receiving VGB) and missing reports and data (e.g. notes from the examiner on the reliability of the subjects performance).

Small numbers

Although, to my knowledge, this is the largest study to date on ppRNFL thinning in individuals with epilepsy, some of the subgroups included in the analyses were small. For example, in non-exposed individuals there was a non-significant trend for ppRNFL thinning in the inferior quadrant in those who had undergone neurosurgery. However, only eight individuals were included in this group, and the study may have been underpowered to detect a significant effect.

Non-blinded

For the majority of individuals with epilepsy, the VGB exposure status was known by the examiner (L.M.C) prior to assessment and during the quantification and classification of results (i.e. visual fields and ppRNFL thickness). This may have led to bias, particularly in the acquisition of visual field data and the quantification and classification of visual fields, where there is some subjectivity in the measurement (309). In an effort to validate the visual field quantification and classification methods, a second examiner was asked to assess a subset of visual field results. The second examiner was blinded to the VGB exposure status of each individual. The inter-rater reliability was high for both the quantification and classification of the visual fields (Chapter 2), demonstrating that bias from the non-blinded first examiner (L.M.C) probably had little effect on these measures of visual field size. For future studies the examiner should be blinded as to the VGB exposure status of participants. Where this is not possible (e.g. the individuals are known to the examiner), visual field tests should be repeated, preferably by a different examiner. Knowledge of the VGB exposure

status of individuals may also have lead to bias in the selection of OCT scans to use for analysis. Most individuals underwent at least two OCT scans of the right eye. Strict scan selection criteria were utilised to avoid selection bias. For example, if one individual had two right eye scans, both fulfilling the quality control criteria and both with equal signal strength, the most recently acquired scan was selected in all instances. However, because quality control criteria were largely subjective, future studies should be blinded to avoid any selection bias.

Co-existing ophthalmological disease

All participants underwent a screening questionnaire, and examination of colour vision and visual acuity to ensure that individuals who may have had visual field loss and/or retinal pathology related to underlying eye disease were excluded. However, individuals did not undergo formal ophthalmological assessment (i.e. fundus examination and measurement of intra-ocular pressure), and it is possible that some individuals may have had an undiagnosed ophthalmological disease which may have accounted for, or contributed to, visual field loss and/or ppRNFL thinning. Of particular concern may be undiagnosed glaucoma, which manifests with visual field loss (which may be asymptomatic in the early stages) and ppRNFL thinning that can be detected using OCT (252), and has a prevalence of around 1% in the UK in individuals aged 40-89 years (522).

8.1.2 Phenotyping issues

The challenges of phenotyping individuals with epilepsy are well known (427;523). In the present study all clinical, demographic and therapeutic data were obtained retrospectively from the individuals medical records. This method of data collection

assumes that the information provide in the medical notes is correct and complete. However, in many cases, clinical data relies on detailed histories from the patient, family or carers which may not always be accurate.

AED exposure

For all AEDs (excluding VGB), details of the dose and duration of therapy were not considered, similarly the combinations in which the AEDs were used was not recorded. Any individual or combined effect of particular AEDs on ppRNFL thickness may not have been detected. This could be owing to the diverse AED histories of individuals included in the study, and the use of only binary AED exposure data. For example, a group of individuals with a positive history of exposure to a particular AED may include individuals who were exposed for several days and those exposed for several years. To further explore the effects of AEDs (alone, or in combination) on ppRNFL thickness, larger studies are needed with more comprehensive exposure data.

Of particular concern for the present study, data regarding exposure to AEDs may be missing or incomplete, particularly if an individual's AED history is deduced from the patient, family or carers memory. It is possible that some individuals included in the "non-exposed" Group may have been exposed to VGB.

Accurate VGB exposure data

In the present study details of VGB exposure were obtained retrospectively from the medical notes. The issues with accurately quantifying the amount and duration of VGB exposure are outlined in Chapter 2 (see 2.2.2). Although every effort was made to establish an accurate estimation of the amount of VGB exposure, ascertaining detailed AED exposure data retrospectively from clinical notes is challenging and imprecise. Frequently, adequate details of initiation of VGB, dose changes and VGB withdrawal

were not available, resulting in a large number of individuals with missing VGB dose data, decreasing the numbers of individuals available for certain analyses. Future studies should carefully record VGB exposure prospectively, possibly alongside frequent testing of VGB serum levels.

Duration of epilepsy

The duration of epilepsy was determined from the date of epilepsy diagnosis, as outlined in the medical notes; however, it is possible that individuals experienced seizures long before their diagnosis. In these cases, the duration of epilepsy recorded from the medical notes would be shorter than the actual duration of seizures.

Learning disability

Discussed in Chapter 7.

Clinical history

Clinical data obtained from the medical notes often relies on historical accounts from the patient, family or carers which may not always be accurate. To overcome this, strict criteria can be applied for the inclusion of certain historical data. For example, a positive history of febrile seizures may only be included if there is a hospital record of the event, or if a parent or carer can account for the event, thereby minimising the risk of inaccurate data. In the present study, no such criteria were applied, and any record in the medical notes of a particular clinical feature was used to determine a positive history of that variable.

The heterogeneous nature of the group of individuals with epilepsy makes it difficult to determine any individual or combined clinical factors that may be associated with

ppRNFL thinning. Even within a particular clinical variable there may diversity as to the type, severity and frequency of that clinical feature. For example, a history of "status epilepticus" was determined from the medical notes, although details of the type of status epilepticus or the duration of the event were not determined. Similarly, a history of head injury was recorded, but the severity, type and temporal relationship of the head injury to seizure onset was not documented. Whilst "splitting" individuals according to more specific clinical criteria may reduce the heterogeneity of the group, it may result in small, underpowered samples (523). Conversely, "lumping" individual into a broader group may increase the heterogeneity whilst gaining a larger sample size (523).

The heterogeneity of the individuals included in the present study, alongside the broad criteria used to define the presence or absence of a clinical feature, may dilute any effect of discrete clinical, demographic or therapeutic features on ppRNFL thinning. Larger studies with strict, comprehensive phenotype definitions are needed to explore this further.

8.1.3 Limitations of perimetry

The limitations of perimetry have been discussed in Chapter 3. With regards to the methods employed in this study, there are several weaknesses to consider. Each individual underwent only one visual field assessment, although it has been suggested that several repeated assessments should be performed in order to account for a learning effect or other sources of normal variability (107). Furthermore, an assessment of the intra- and inter-examiner reliability in the examination of the visual field using GKP was not performed. Future studies should consider repeating visual field assessments to ensure that the recorded field is a reliable. Although the visual field quantification and

classification methods used in the present study were found to show good intra- and inter-rater reliability (see 2.5.3), errors in the quantification and classification of visual fields may also have occurred.

8.1.4 Limitations of OCT

Manufacturers' normative database

In the present study, measurements of ppRNFL thickness were compared against the manufacturers' normative database, and classified according to the manufacturers' normal distribution percentiles. Details of this normative database are available for the TD-OCT instrument used, including the age ranges, gender and ethnicity of the included subjects (285). Increasing age is known to be associate with ppRNFL thinning (285;390;401;402) and is controlled for in the comparison of each subject to the manufacturers' normative database. However, gender and ethnicity are not considered. Recent studies suggest that there may be ethnic differences in normal ppRNFL thickness (285;358;524-528). Similarly, some studies suggest that there may be gender differences in ppRNFL thickness (385;386). Ethnicity was not considered in the present study, and may have had an effect on the ppRNFL thickness that was not accounted for in the analyses.

Scan circle placement

The location of the scan circle relative to the ONH has an effect on the ppRNFL thickness measurements (see 4.4.2.4) (327). For ppRNFL scans acquired using SD-OCT, inbuilt software automatically centres the scan around the ONH after it has been acquired. In addition, the scan circle can be manually adjusted to optimise its location. The disadvantage of this is that the placement of the scan circle can be subjectively

determined, and the chosen "optimal" position may differ between operators, leading to differences in the measures of ppRNFL thickness. Studies are needed to determine the effect of intra- and inter-examiner reproducibility of scan circle placement and the effect this may have on measures of ppRNFL thickness.

The TD-OCT model used in the present study does not allow manual adjustment of the scan circle after scan acquisition. "Optimal" scan circle placement is subjectively determined by the examiner before the scan is acquired. The fundus image, provided with the tomograph in the manufacturers' summary report, is used to assess the scan circle placement. However, the fundus image showing the scan circle, and the tomograph from which ppRNFL measurements are taken, are not acquired at the same time, and thus the two images do not correspond exactly (529). Because of this, the examiner cannot be certain that that the tomograph was acquired in the optimal location (i.e. centred on the ONH), which may lead to errors in the measurement of ppRNFL thickness due to the misaligned scan (529).

Floor effect

ppRNFL thickness measured using OCT may show a "floor effect" whereby further structural damage cannot be detected whilst functional deterioration (e.g. VAVFL) continues (229;530). In some individuals with no visual perception, due to ischaemic optic neuropathy (530) or advanced glaucoma (531), a residual ppRNFL thickness is maintained, suggesting that even when there are no remaining RGCs ppRNFL thickness measured using OCT will not be reduced to zero (530). Contributions to the residual ppRNFL thickness may be from normal, non-axonal components of the RNFL, including glial cells and blood vessels which are not affected by RGC disease an loss

(530;531). In addition, RGC loss may lead to migration of astrocytes into the RNFL, phagocytosing cellular debris and synthesising new extracellular matrix components (532), and contributing to residual ppRNFL thickness. Lastly, the inbuilt OCT algorithm used to define and measure the ppRNFL may contribute to residual ppRNFL thickness(530), as it attempts to detect RNFL borders from the reflectivity profile, even when there is extremely low reflectivity (284) (i.e. due to a RNFL depleted of RGC axons).

The utility of OCT in individuals with severe VAVFL and ppRNFL thinning needs to be evaluated further. It is possible that in these cases, functional assessment of the visual field may provide a more suitable tool for continued monitoring of VAVFL progression.

64 four-scan segments

In this study a novel summary parameter was created to analyse ppRNFL thickness data; the 64 four-scan segments. Small eye movements during scanning may lead to displacement or distortion of individual A-scans. These may be "smoothed out" during image post-processing, and in the validated summary measures have little effect on the average ppRNFL thickness. However, in the smaller four-scan segments, any distortion of individual A-scans may have a large effect on the average ppRNFL thickness in each segment, giving an inaccurate representation of the true ppRNFL thickness in that ONH area. Analysing ppRNFL thickness data using this method needs validation before it can be more widely applied.

8.2 Conclusions

The aims of this study were to explore the effects of VGB on ppRNFL thickness measured using OCT in a large population of individuals with epilepsy. The findings of

this study have important implications for four areas of concern regarding the use of VGB in individuals with epilepsy.

Firstly, and perhaps most importantly are the issues with assessing the retinotoxic effects of VGB and the associated VAVFL in individuals who are unable to appreciate the demands of perimetry (see 8.2.1).

Secondly, the mechanisms of VGB retinotoxicity have not been identified and the pathological retinal changes leading to VAVFL are unknown. Understanding the mechanisms leading to irreversible VAVFL may lead to more targeted diagnostic and monitoring strategies, and improved ability to identify individuals at risk of VAVFL (see 8.2.2).

Thirdly, the prevalence of VAVFL in VGB-exposed individuals is around 50%, yet currently it is unknown which individuals are most at risk. The identification of risk factors for VAVFL may allow safer prescribing of VGB in some individuals (see 8.2.3).

Lastly, the evolution of VAVFL with continued VGB exposure is uncertain. This adds further apprehension to the use of VGB particularly over long periods of time which may be needed in individuals with drug-resistant complex partial seizures (see 8.2.4).

8.2.1 Using ppRNFL imaging in assessment VGB-exposed individuals

The present study has provided new evidence for the clinical utility of ppRNFL imaging in VGB-exposed individuals. More individuals are able to comply with OCT than perimetry, In addition, ppRNFL imaging is highly repeatable in a VGB-exposed population, particularly when using the latest SD-OCT technology, which has a faster scanning time and allows post image-acquisition scan alignment. In individuals who are unable to perform perimetry average ppRNFL thickness and the pattern of any

ppRNFL thinning can provide a surrogate marker for the integrity of the visual field and enable a judgement to be made about the presence of and severity of VAVFL.

ppRNFL thinning measured using OCT may be detectable before VAVFL is clinically apparent. In the analysis of patterns of ppRNFL thinning the NS sector appears a likely candidate for showing ppRNFL changes associated with early VGB toxicity. Although thinning in the NS sector may occur early after VGB exposure, the ppRNFL thickness measurements may remain within the manufacturers' "normal" boundaries (i.e. $\leq 95^{th}$–$>5^{th}$ percentile), thus baseline measurements before the initiation of VGB are essential, and subsequent examinations should be compared against baseline thickness measurements.

8.2.2 Mechanisms of VGB retinotoxicity

The findings from this study suggest that RGC loss is the pathological mechanism leading to irreversible VAVFL. However, other distinct but interrelated mechanisms may account for reversible and irreversible abnormalities in retinal electrophysiology and defects in colour vision, visual acuity and contrast sensitivity.

8.2.3 Risk factors for VGB retinotoxicity

Risk factors for ppRNFL thinning in VGB-exposed individuals include higher maximum daily VGB dose, higher duration of VGB exposure, male gender and the presence of a homonymous visual field defect related to co-existing visual pathway pathology. These factors explained 31% of the variance in ppRNFL thickness between VGB-exposed individuals indicating that there are yet unknown factors that significantly contribute to the risk of ppRNFL thinning (and VAVFL) after VGB exposure. It is possible that genetic variation could play a role in the development of VAVFL. Genetic variability leading to differences in RGC number, and differences in the expression of proteins involved in GABAergic pathways and GABA metabolism in the retina may be implicated.

8.2.4 The evolution of VGB retinotoxicity

The present study has provided evidence that ppRNFL thinning and VAVFL progress with continued VGB exposure. The progression of the retinotoxic effects of VGB may be subtle and difficult to detect using perimetry. ppRNFL imaging may provide a more sensitive indicator of progression. Prospective longitudinal studies are needed to confirm this.

8.2.5 ppRNFL thinning in individuals with epilepsy

An unexpected finding in this study was the presence of ppRNFL thinning in individuals with epilepsy who had no history of VGB exposure. ppRNFL thinning may

be associated with cognitive impairment, longer duration of epilepsy and specific epilepsy types, in particular MTLE with HS. ppRNFL thinning may occur due to transynaptic degeneration of RGC as a result of white matter pathology involving the postgeniculate visual pathway. This could entail diffuse axonal loss occurring throughout the CNS or focal lesions involving the visual pathway (484). Alternatively, loss of RGC may result from atrophy of the thalamic nuclei including the lateral geniculate nucleus.

8.3 Future work

8.3.1 Prospective longitudinal studies

The findings from this study have provided valuable evidence that ppRNFL imaging using OCT is a useful tool to use in the assessment of VGB-exposed individuals. In addition the findings have made contributions to understanding of the mechanisms of, and possible risk factors for, VAVFL. However, there are limitations to this study, the most apparent being the cross-sectional design of the research. Further prospective longitudinal studies are needed to fully appreciate the utility of ppRNFL imaging in the management of VGB-exposed individuals. Where possible, studies should combine ppRNFL imaging, perimetry and retinal electrodiagnostics alongside careful recording of VGB exposure. Baseline examinations are essential, and careful comparison of repeated assessments should be made. Few adult individuals are newly started on VGB now, creating difficulties in performing this type of study, and cross-centre collaborations will probably be required. There may be particular scope for such prospective studies currently within the United States where the FDA have recently approved VGB.

8.3.2 Genetic association studies

Genetic variation may play a role in the development of ppRNFL thinning and VAVFL. Individual variation in RGC, amacrine and Müller cell number could contribute to differential susceptibility to VGB retinotoxicity. Furthermore, genetic differences in proteins involved in retinal GABAergic pathways and metabolism including GABA-transaminase, GABA-transporters and GABA-receptors may also be associated with differences in response to persistently elevated retinal GABA after VGB exposure. Genetic association studies are needed to determine the presence of genetic risk factors for VGB retinotoxicity. OCT ppRNFL imaging provides a robust phenotype to use in pharmacogenetic studies as it is highly repeatable, objective and easily quantifiable. Identification of genetic risk factors that predispose to VAVFL may allow for safer prescribing of VGB in selected individuals.

8.3.3 Analysis of other retinal layers

The findings in this study implicate RGC axonal loss in the pathogenesis of VAVFL. However, it is not possible to determine whether RGC axons are a primary target of VGB toxicity, or whether RGC axon loss occurs secondary to other retinal cell dysfunction or death. Measurement of other retinal layers may reveal further insights into the mechanisms of VGB retinotoxicity. For example, measurement of ONL thickness may provide evidence as to whether photoreceptor loss is present in VGB-exposed individuals as has been described in VGB-exposed albino rats.

8.3.4 Pathological studies

Only one pathological study of the retina and anterior visual pathway from a VGB-exposed individual has been undertaken. Further pathological studies in humans are needed to confirm the effects of VGB on retinal structure particularly on the RGC and RNFL. Difficulties in obtaining and performing histological analysis of human retina

(250) require alternative methods to be explored. The visual pathways are reitnotopically organised, thus analyses of sections from post mortem samples of optic nerve, optic tract and lateral geniculate nucleus of VGB-exposed individuals may provide pathological evidence of RGC axon loss in addition to providing further evidence as to a retinotopic pattern of RGC atrophy. In the LGN, specific RGC subtypes terminate in defined laminae (533), loss of RGC in specific LGN laminae may indicate susceptibility of classes of RGC to VGB toxicity. For example, if M-cells are particularly susceptible to vigabatrin toxicity, atrophy will be seen preferentially in lamina one and two which contain projections from this RGC subtype.

8.3.4 Large studies of individuals with epilepsy

The finding that individuals with epilepsy not exposed to VGB have thinner ppRNFL than healthy individuals merits further investigation. Larger studies are needed with carefully phenotyped individuals

Larger longitudinal studies of individuals undergoing detailed neuropsychological assessment, white matter imaging (e.g. using diffusion tensor imaging) and ppRNFL imaging using OCT are needed to fully determine the clinical utility of OCT ppRNFL imaging in epilepsy. However, these preliminary findings suggest that potential for OCT ppRNFL imaging a as a biomarker for disease modifying therapies and for neuroprotective strategies in epilepsy.

Appendix 1

Information sheets 1 and 2 and participant consent form.

University College London Hospitals NHS
NHS Foundation Trust

The National Hospital for Neurology and Neurosurgery

Department of Clinical & Experimental Epilepsy
Box 29
Queen Square
London
WC1N 3BG

Version 2, 04th February 2008

PARTICIPANT INFORMATION SHEET (1) FOR STUDY : "ASSESSMENT OF CANDIDATE POLYMORPHISMS FOR VIGABATRIN-INDUCED ADVERSE REACTIONS"

QUESTIONS AND SAMPLE

We would like to invite you to take part in a study at The National Hospital for Neurology & Neurosurgery and Institute of Neurology. Before you decide whether to participate it is important for you to understand why the research is being done and what it will involve. Please take time to read the following information carefully and discuss it with others if you wish. Ask us if there is anything that is not clear or if you would like more information. Take time to decide whether or not you wish to take part.

What is the purpose of the study?

Vigabatrin is an important anti epileptic drug. About 40% of patients who have taken the drug develop an irreversible loss of peripheral vision, such that vigabatrin is now rarely started as treatment in people who have epilepsy. There are some people whose epilepsy was more controlled on vigabatrin, and who remain on vigabatrin, and continue to have eye tests to monitor their visual fields. Vigabatrin is still used for the treatment of some sorts of severe epilepsy in children. If it were possible to identify which patients were more likely to develop visual field loss when given vigabatrin, and which patients might not develop these side effects, then it might be possible to use vigabatrin again. This would be an important achievement, as vigabatrin can be an effective anti epileptic drug for some people with epilepsy.

There is reason to believe that some people are more likely to develop visual field loss when given vigabatrin than other people, and that this vulnerability is at least partly due to people's individual genetic make up. Our research has established that there do appear to be some common genetic variants which increase the risk of developing visual field loss on exposure to vigabatrin. These results were obtained from genetic studies. We now wish to establish whether these gene variants are indeed likely to have an effect that might make some people more vulnerable to the adverse affects of vigabatrin. If our genetic findings are real, we would expect to be able to detect the effects of the genetic variants using specific tests that are described below.

Our findings might lead not only to the chance of using vigabatrin again for some people with epilepsy, but also to the development of new tests that could identify early signs of impending visual field loss in people with epilepsy given vigabatrin.

Why have I been chosen?

You have kindly volunteered to take part in this study. The first part of this study involves taking a sample of blood, to work out whether you have the gene variants in which we are interested. If you do, or if you are taking an antiepileptic drug, you may also be invited to take part in the second part of the study. This is detailed in Participant Information Sheet (2)

Do I have to take part?

It is up to you to decide whether or not to take part. If you do decide to take part you will be given this information sheet to keep and be asked to sign the consent form. Once you have joined the study you will still be free to withdraw at any time and without giving a reason. Your decision whether to take part, or to withdraw at a later point, will not affect any medical care you are receiving.

What is involved in the study?

We will first ask you a series of questions to make sure that you could take part in the second part of the study if you have the appropriate genetic variants, or if you are taking certain antiepileptic drugs. To work out whether you have the appropriate genetic variants, we will take a sample of blood (20ml, about two tablespoons). This will be taking by routine venepuncture. A tourniquet will be tightened around your upper arm. The area over a vein will be cleaned and the blood drawn from this site. Usually this is at the front of the elbow but sometimes another site in the arm may be used. Afterwards the area may be compressed to stop any bleeding and a dressing applied.

Are there any risk involved in taking part?

There are no serious risks involved. Some people may experience discomfort when the blood sample is taken. On some occasions more than one attempt may have to be made to obtain samples. There is a low risk of persistent bleeding from the site, requiring additional compression and dressing. An area of bruising may also be caused at the site. Some people feel light headed during and after the procedure. The amount of blood being taken however is very small and should not cause this.

Will I be asked to do anything else as part of this study?

If you have the appropriate genetic variants, of if you are taking an antiepileptic drug, you may be invited to take part in the second part of the study. The details are given in Participant Information Sheet (2).

What will happen to my blood samples?

The blood samples will be stored at the Institute of Neurology, University College London. The samples will be labelled with a code rather than your real name, for confidentiality purposes. We will then arrange for the blood sample to be tested for the genetic variants of interest. This may take place at the Institute of Neurology, or in a collaborators laboratory in the United States of America. If the sample is transferred to the United States of America, the collaborators there will only receive coded samples, and will not know your identity at any stage.

What will happen to the information from the study?

The information will be processed and stored in the Department of Clinical and Experimental Epilepsy, Institute of Neurology, University College London. The information will be labelled with a code rather

than your real name, for confidentiality purposes. This means that you cannot be identified from the information. The information will be used to address the questions described above.

Professor Sisodiya is the acting custodian of your information. The information will be kept for at least ten years and destroyed if no longer needed in the future. The information remains your property; this means that we will destroy it at an earlier stage if you wish. Information may be used in other research studies, but if this happens it will first be made totally anonymous in order to destroy any links back to you. Any further research using anonymous samples will first be reviewed by a research ethics committee to see if this is appropriate.

What are the possible benefits of taking part?

This study is being done to help establish whether the genetic variants we have identified are likely to have a real role in increasing susceptibility to vigabatrin associated visual field loss. If we do find that the genetic variants are associated with changes in the eye or in the brain that may well increase vulnerability to field loss on exposure to vigabatrin, then it may be that if you have the variants that increase vulnerability it would be best for you not to receive vigabatrin in the future, or to consider coming off vigabatrin if you are taking it currently. This might mean a change to your treatment if you are currently taking vigabatrin. These decisions, however, are complicated and depend on several factors. If the information we obtain is significant, we will pass it back to your treating doctors, to discuss further with you.

What happens if there is a problem?

We would not expect you to suffer any harm or injury because of your participation in this study and every care will be taken to ensure your safety. However, UCL has (insurance) arrangements in place for no-fault compensation in the unlikely event that something unforeseen does go wrong, and on the balance of probabilities, harm is attributed as a result of taking part in the research study

Regardless of this, if you wish to complain or have any concerns about any aspect of the way you have been approached or treated during the course of this study, you can contact the Research Governance Sponsor of this study, University College London. Please write to the Joint UCLH/UCL Biomedical Research Unit, R&D Directorate, Rosenheim Wing, Ground Floor, 25 Grafton Way, London WC1E 5DB quoting reference BRD/07/154. All communication will be dealt in strict confidence.

You can also contact the relevant local Patient Advisory Liaison Service (PALS) if you have any concerns regarding the care you have received, or as an initial point of contact if you have a complaint. For the PALS at UCLH call 020 7380 9975 or email pals@uclh.nhs.uk. You can also visit PALS by asking at any hospital reception.

What information will be held about me?

Some personal details will be held about you including your name, age, clinical history and the type of treatment you are on if you are taking antiepileptic drugs. If the results from the study are published there will be no personal details included. All the information which is collected about you during the course of the research will be kept strictly confidential. If you consent to take part in the research the people conducting the study will abide by the Data Protection Act 1998, and the rights you have under this act.

What will happen to the results of the research study?

This study is being undertaken in part fulfilment of a research student's PhD. The results of the study will be published in a clinical research journal, however, you will not be identified in any reports or publications arising from the study. A copy of the published results will be available through your neurologist.

Who is organising and funding the research?

The study is funded by a grant received from the Tuberous Sclerosis Association. The doctor conducting this research is not being paid for including you, or looking after you, in this study.

Who is reviewing this study?

The National Hospital for Neurology and Neurosurgery and the Institute of Neurology Joint Research Ethics Committee.

Contact for further information

If you wish to take part in this study or if you require any further information, please contact Lisa Clayton by phone on 0203 108 0097 or by email at l.clayton@ion.ucl.ac.uk. You can also contact Professor Sanjay Sisodiya at the Institute of Neurology and The National Hospital for Neurology & Neurosurgery on 0203 108 0125. Please leave a message and you will be contact at the earliest convenience.

Thank you for taking the time to read this information sheet.

University College London Hospitals NHS
NHS Foundation Trust

The National Hospital for Neurology and Neurosurgery

Department of Clinical & Experimental Epilepsy
Box 29
Queen Square
London
WC1N 3BG

Version 3, 15th June 2009

PARTICIPANT INFORMATION SHEET (2) FOR STUDY : "ASSESSMENT OF CANDIDATE POLYMORPHISMS FOR VIGABATRIN-INDUCED ADVERSE REACTIONS"

TMS, OCT AND VISUAL FIELDS

We would like to invite you to take part in a study at The National Hospital for Neurology & Neurosurgery and Institute of Neurology. Before you decide whether to participate it is important for you to understand why the research is being done and what it will involve. Please take time to read the following information carefully and discuss it with others if you wish. Ask us if there is anything that is not clear or if you would like more information. Take time to decide whether or not you wish to take part.

What is the purpose of the study?

Vigabatrin is an important anti epileptic drug. About 40% of patients who have taken the drug develop an irreversible loss of peripheral vision, such that vigabatrin is now rarely started as treatment in people who have epilepsy. There are some people whose epilepsy was more controlled on vigabatrin, and who remain on vigabatrin, and continue to have eye tests to monitor their visual fields. Vigabatrin is still used for the treatment of some sorts of severe epilepsy in children. If it were possible to identify which patients were more likely to develop visual field loss when given vigabatrin, and which patients might not develop these side effects, then it might be possible to use vigabatrin again. This would be an important achievement, as vigabatrin can be an effective anti epileptic drug for some people with epilepsy.

There is reason to believe that some people are more likely to develop visual field loss when given vigabatrin than other people, and that this vulnerability is at least partly due to people's individual genetic make up. Our research has established that there do appear to be some common genetic variants which increase the risk of developing visual field loss on exposure to vigabatrin. These results were obtained from genetic studies. We now wish to establish whether these gene variants are indeed likely to have an effect that might make some people more vulnerable to the adverse affects of vigabatrin. If our genetic

findings are real, we would expect to be able to detect the effects of the genetic variants using specific tests that are described below.

Recent research has suggested that deficiency in the amino acid taurine may be related to the development of visual field loss when taking vigabatrin. Normal levels of taurine are usually easily obtained from our diet; however, some patients taking vigabatrin have been shown to have lower taurine levels than normal. It is possible that low levels of taurine contribute to the development of visual field loss in some people taking vigabatrin, though we still need to establish whether there is a relationship between vigabatrin use, taurine levels and visual field loss.

Our findings might lead not only to the chance of using vigabatrin again for some people with epilepsy, but also to the development of new tests that could identify early signs of impending visual field loss in people with epilepsy given vigabatrin.

Why have I been chosen?

You have been chosen either because the genetic tests you have had show that you have the gene variants we are interested in or you are taking an antiepileptic drug that we are interested in studying. We know this information about you either as a result of the genetic study you have previously helped us with, or as a result of the first part of this study for which you volunteered.

Do I have to take part?

It is up to you to decide whether or not to take part. If you do decide to take part you will be given this information sheet to keep and be asked to sign the consent form. Once you have joined the study you will still be free to withdraw at any time and without giving a reason. Your decision whether to take part, or to withdraw at a later point, will not affect any medical care you are receiving.

What is involved in the study?

There are two sets of tests in this study. In the first set, we will examine your eyes. We will first check your visual acuity, using a test you may have had before at your optician. We will then measure your visual fields, using a test we routinely employ. This involves sitting comfortably, and placing your head on a headrest attached to the device, after which you will be asked to say when you see a light. Lastly, we will look at the thickness of a particular part of your eye, called the retina. You will be given 1% tropicamide eye drops to dilate your pupils so that we can scan your eyes easily. These drops are used routinely in clinical practice and very rarely cause serious side effects. A consultant ophthalmologist will be present in case advice is needed. The drops may sting for a few seconds afterwards and cause some blurring of vision. You are advised not to drive or operate machinery until your vision is clear which could take a few hours. Again you will be seated comfortably at the machine, and asked to place your head on a headrest. You will then be asked to look at a target, and you may have one eye covered briefly with a patch. We will then quickly scan the back of your eye using our special machine. You will see a brief flash of light when we do this. You may temporarily continue to see the light, particularly when you close your eyes, as sometimes happens with flash photography.

The second set of tests will be done in a different building. These tests are called electrophysiological tests, which are tests looking at how brain and nerve cells in your body connect up and communicate with each other. We plan to use the technique called transcranial magnetic stimulation (TMS) to examine the excitability of your brain. This technique has been used for many years to examine the function of the

brain. You will be seated comfortably in an armchair. Three small electrodes will be taped to your hand; these will record activity in your muscle. A small magnetic pulse will be delivered through a coil held close to your head. This is painless but you may feel one or two small taps on your head. You may also feel the muscles in your hand twitch. This will be done around 120 times; each pulse separated by five seconds. There will be chance for breaks throughout and overall it should take about one hour. TMS has been used safely in thousands of individuals around the world. It can be harmful in people who have a pacemaker, an implanted medication pump, a metal plate in the skull, or metal objects inside the eye or skull (for example after brain surgery or a shrapnel wound) or you have a vagal nerve stimulator. Please inform the investigators if you might have any of these. Please do not consume and caffeinated drinks including tea and coffee, or any alcohol on the day of the study as these can affect the results. Since the effects of magnetic stimulation on the foetus are unknown, please also let us know if you think you might be pregnant. During the transcranial magnetic stimulation, you might feel a light tingling on the skin, which fades away very fast.

If you are taking the antiepileptic drugs that we are interested you will be asked to provide some saliva into a special pot so that we can estimate the levels of the drugs in your body. We may also look at your hospital notes to find further information about the drugs you are taking and the diagnostic tests that you have had in the past.

For your participation in this part of the study we will reimburse you with £20 as compensation for your time.

Are there any risk involved in taking part?

There are no serious risks involved. TMS can theoretically cause seizures, which have been rare in practice and difficult to produce on purpose, even in people who have epilepsy. Please note that since the introduction of agreed safety guidelines (which we will implement), there have been no reports of seizures. In the unlikely event of a seizure, you will be given appropriate medical treatment. Besides seizures, the only known risk of TMS is a headache, which has always gone away promptly with non-prescription medication. In the very unlikely event of seizures, the Driving Licence Authority (DVLA) has told us that subjects who suffer seizures during TMS experiments will not be banned from driving if they already have a licence. Please let us know if you are applying for or hold an HGV licence, as we do not intend to perform TMS studies on such people.

What will happen to the information from the study?

The information will be processed and stored in the Department of Clinical and Experimental Epilepsy, Institute of Neurology, University College London. The information will be labelled with a code rather than your real name, for confidentiality purposes. This means that you cannot be identified from the information. The information will be used to address the questions described above.

Professor Sisodiya is the acting custodian of your information. The information will be kept for at least ten years and destroyed if no longer needed in the future. The information remains your property; this means that we will destroy it at an earlier stage if you wish. Information may be used in other research studies, but if this happens it will first be made totally anonymous in order to destroy any links back to you. Any further research using anonymous samples will first be reviewed by a research ethics committee to see if this is appropriate.

What are the possible benefits of taking part?

This study is being done to help establish whether the genetic variants we have identified are likely to have a real role in increasing susceptibility to vigabatrin associated visual field loss. If we do find that the genetic variants are associated with changes in the eye or in the brain that may well increase vulnerability to field loss on exposure to vigabatrin, then it may be that if you have the variants that increase vulnerability it would be best for you not to receive vigabatrin in the future, or to consider coming off vigabatrin if you are taking it currently. This might mean a change to your treatment if you are taking vigabatrin. These decisions, however, are complicated and depend on several factors. If the information we obtain is significant, we will pass it back to your treating doctors, to discuss further with you.

What happens if there is a problem?

We would not expect you to suffer any harm or injury because of your participation in this study and every care will be taken to ensure your safety. However, UCL has (insurance) arrangements in place for no-fault compensation in the unlikely event that something unforeseen does go wrong, and on the balance of probabilities, harm is attributed as a result of taking part in the research study

Regardless of this, if you wish to complain or have any concerns about any aspect of the way you have been approached or treated during the course of this study, you can contact the Research Governance Sponsor of this study, University College London. Please write to the Joint UCLH/UCL Biomedical Research Unit, R&D Directorate, Rosenheim Wing, Ground Floor, 25 Grafton Way, London WC1E 5DB quoting reference BRD/07/154. All communication will be dealt in strict confidence.

You can also contact the relevant local Patient Advisory Liaison Service (PALS) if you have any concerns regarding the care you have received, or as an initial point of contact if you have a complaint. For the PALS at UCLH call 020 7380 9975 or email pals@uclh.nhs.uk. You can also visit PALS by asking at any hospital reception.

What information will be held about me?

Some personal details will be held about you including your name, age, clinical history and the type of treatment you are on. If the results from the study are published there will be no personal details included. All the information which is collected about you during the course of the research will be kept strictly confidential. If you consent to take part in the research the people conducting the study will abide by the Data Protection Act 1998, and the rights you have under this act.

What will happen to the results of the research study?

This study is being undertaken in part fulfilment of a research student's PhD. The results of the study will be published in a clinical research journal; however, you will not be identified in any reports or publications arising from the study. A copy of the published results will be available through your neurologist.

Who is organising and funding the research?

The study is funded by a grant received from the Tuberous Sclerosis Association. The doctor conducting this research is not being paid for including you, or looking after you, in this study.

Who is reviewing this study?

The National Hospital for Neurology and Neurosurgery and the Institute of Neurology Joint Research Ethics Committee.

Contact for further information

If you wish to take part in this study or if you require any further information, please contact Lisa Clayton by phone on 0203 108 0097 or by email at l.clayton@ion.ucl.ac.uk. You can also contact Professor Sanjay Sisodiya at the Institute of Neurology and The National Hospital for Neurology & Neurosurgery on 0203 108 0125. Please leave a message and you will be contact at the earliest convenience.

Thank you for taking the time to read this information sheet.

University College London Hospitals NHS
NHS Foundation Trust

The National Hospital for Neurology and Neurosurgery

Department of Clinical & Experimental Epilepsy
Box 29
Queen Square
London
WC1N 3BG

Version 2, 04th February 2008

Centre Number:

Study Number: 08/0115

Identification Number for this trial:

CONSENT FORM

Title of project: Assessment of candidate polymorphisms for vigabatrin-induced adverse reactions

Name of Researcher: Prof SM Sisodiya

Please tick to confirm

1. I confirm that I have read and understand the information sheet dated 04.02.2008 (version 2) for the above study ☐

2. I have had the opportunity to consider the information, ask questions and have had these answered satisfactorily. ☐

3. I understand that my participation is voluntary and that I am free to withdraw at any time, without giving any reason, without my medical care or legal rights being affected. ☐

4. I understand that sections of any of my medical notes and data collected during the study may be looked at by responsible individuals from regulatory authorities or from the NHS Trust, where it is relevant to my taking part in research. I give permission for these individuals to have access to my records. ☐

5. I understand that any blood taken is given as a gift and may be used in future research. ☐

6. I agree to my GP being informed of my participation in the study. ☐

7. I agree to take part in the above research study. ☐

_____	_____	_____
Name of patient	Date	Signature
_____	_____	_____
Name of Person taking consent (if different from researcher)	Date	Signature
_____	_____	_____
Researcher	Date	Signature

1 copy for patient, 1 copy for Researcher, 1 copy to be kept with hospital notes

If you have any comments or concerns you may discuss these with the Investigator. If you wish to go further and complain about any aspect of the way you have been approached or treated during the course of the study, you should write or get in touch with the Complaints Manager, UCLH. Please quote the UCLH project number at the top of this consent form.

UCL HOSPITALS

UCL Hospitals is an NHS Trust incorporating the Eastman Dental Hospital, the Elizabeth Garrett Anderson & Obstetric Hospital, the Heart Hospital, the Hospital for Tropical Diseases, the Middlesex Hospital, the National Hospital for Neurology & Neurosurgery, The Royal London Homeopathic Hospital and University College Hospital.

Appendix 2

Screening Questionnaire

		Yes or No
Do you currently have any problems with your eyes or vision?		
Are you currently taking any medication for problems with your eyes or vision?		
Have you had any problems with your eyes or vision in the past that you were treated for?		
Have you ever had any surgery to your eyes?		
Do you have diabetes?		
Do you have glaucoma?		
Does anyone in your family have glaucoma?		
Do you wear glasses and/or contact lenses?		

Appendix 3

Translation of instructions for OCT and perimetry into Dutch

Perimetry instructions

- Een oog wordt afgedekt met een lapje. Het is belangrijk dat u niets door het afgedekte oog kunt zien.
- Aan uw rechter kant is ere en belletje, waar u op kunt drukken als u een bewegend lichtjee ziet.
- Leg uw kin op de houder en druk uw voorhoofd tegen de hoofdsteun aan de bovenkant.
- Kijk recht vooruit in het cirkeltje voor u. Lisa zal u dit wijzen.
- Het is erg belangrijk dat u de hele tijd naar dit cirkeltje blijft kijken.
- Een wit lichtje zal bewegen vanuit de buitenkant van uw gezichtsveld, waar u het kunt zien. Op het moment dat u het lichtje ziet drukt u op het belletje.
- Beweeg de ogen niet om het lichtje te zoeken, blijf de hele tijd recht vooruit kijken.

OCT instructions

- De houder voor de kin wordt in de juiste stand gezet
- Leg de kin op de houder aan de kant die Lisa aangeeft
- Leg uw hoord tegen de hoofdsteun
- Kijk recht in de camera lens
- De houder voor de kin wordt voorwaarts bewogen naar de lens. Houdt de kin in de houder en laat het hoofd rusten tegen de hoofdsteun terwijl dit gebeurt. Probeer meet e bewegen met de houder voor de kin.
- Wanneer je dichter bij de lens bent zul je een groene ster zien. Blijf de hele tijd naar de ster kijken.
- Als u wilt kunt u even knipperen met de ogen als dit nodig is, daarna zal Lisa u vragen niet te knipperen (zij zedt: don’t blink) tijdens het maken van de scan.
- Het is erg belangrijk dat wanneer de scan genomen wordt u blijft kijken naar de groene ster, beweeg niet met het hoofd en niet knipperen met de ogen.
- Wanneer één oog gedaan is, zal Lisa vragen de kin op de andere kant van de houder te leggen om het andere oog te kunnen scannen

Appendix 4

Average ppRNFL thickness in the right eye was found to be significantly thickener than average ppRNFL thickness in the left eye in VGB-exposed individuals (from Group 1A) and healthy individuals (Group 3) (Table A1). There was a significant correlation between average ppRNFL thickness in the right eye and average ppRNFL thickness in the left eye ($r = 0.95$, $p<0.001$ and $r = 0.88$, $p<0.001$ for VGB-exposed and healthy individuals, respectively).

Table A1: Average ppRNFL thickness in the right and left eyes in VGB-exposed and healthy individuals

	Right eye average ppRNFL thickness (μm) [SD]	Left eye average ppRNFL thickness (μm) [SD]	P value
VGB-exposed (N= 60)	77.1 (13.1)	74.9 (13.5)	<0.001
Healthy controls (N= 89)	94.0 (9.0)	92.7 (9.6)	0.005

Appendix 5

OCT data from individuals who were unable to perform perimetry were compared against OCT data from individuals from whom visual field data was available to determine whether there was a difference between the two populations.

There was no significant difference in ppRNFL thickness between the two groups ($p>0.05$) (Table A2).

Table A2: Comparison of average ppRNFL thickness between individuals able to perform perimetry and those unable to perform perimetry.

	Able to perform perimetry	Unable to perform perimetry
Average ppRNFL thickness (µm) [range]	79.0 ±12.5 [48-105]	80.6 ±12.0 [49-99]

(1) Schousboe I, Bro B, Schousboe A. Intramitochondrial localization of the 4-aminobutyrate-2-oxoglutarate transaminase from ox brain. Biochem J 1977 Feb 15;162(2):303-7.

(2) Metcalf BW. Inhibitors of GABA metabolism. Biochem Pharmacol 1979 Jun 1;28(11):1705-12.

(3) Meldrum BS. Gamma-aminobutyric acid and the search for new anticonvulsant drugs. Lancet 1978 Aug 5;2(8084):304-6.

(4) McNamara JO. Emerging insights into the genesis of epilepsy. Nature 1999 Jun 24;399(6738 Suppl):A15-A22.

(5) Jung MJ, Lippert B, Metcalf BW, Schechter PJ, Bohlen P, Sjoerdsma A. The effect of 4-amino hex-5-ynoic acid (gamma-acetylenic GABA, gammma-ethynyl GABA) a catalytic inhibitor of GABA transaminase, on brain GABA metabolism in vivo. J Neurochem 1977 Apr;28(4):717-23.

(6) Tunnicliff G. Inhibitors of brain GABA aminotransferase. Comp Biochem Physiol A Comp Physiol 1989;93(1):247-54.

(7) Jung MJ, Metcalf BW. Catalytic inhibition of gamma-aminobutyric acid - alpha-ketoglutarate transaminase of bacterial origin by 4-aminohex-5-ynoic acid, a substrate analog. Biochem Biophys Res Commun 1975 Nov 3;67(1):301-6.

(8) Lippert B, Metcalf BW, Jung MJ, Casara P. 4-amino-hex-5-enoic acid, a selective catalytic inhibitor of 4-aminobutyric-acid aminotransferase in mammalian brain. Eur J Biochem 1977 Apr 15;74(3):441-5.

(9) Schechter PJ, Tranier Y, Jung MJ, Bohlen P. Audiogenic seizure protection by elevated brain GABA concentration in mice: effects of gamma-acetylenic gaba and gamma-vinyl GABA, two irreversible GABA-T inhibitors. Eur J Pharmacol 1977 Oct 15;45(4):319-28.

(10) Jung MJ, Lippert B, Metcalf BW, Bohlen P, Schechter PJ. gamma-Vinyl GABA (4-amino-hex-5-enoic acid), a new selective irreversible inhibitor of GABA-T: effects on brain GABA metabolism in mice. J Neurochem 1977 Nov;29(5):797-802.

(11) French J, Ben-Menachem E. Overview: Antiepileptic drugs. In: Engel J, Pedley TA, editors. Epilepsy a comprehensive textbook. Second ed. Philadelphia: Lippincott Williams & Wilkins; 2008. p. 1431-2.

(12) Wheless JW, Ramsay RE, Collins SD. Vigabatrin. Neurotherapeutics 2007 Jan;4(1):163-72.

(13) Ben-Menachem E. Vigabatrin. In: Levy RH, Mattson RH, Meldrum BS, Perucca E, editors. Antiepileptic Drugs. Fifth Edition ed. Philadelphia: Lippincott Williams & Wiilkins; 2002. p. 855-63.

(14) Neal MJ, Shah MA. Development of tolerance to the effects of vigabatrin (gamma-vinyl-GABA) on GABA release from rat cerebral cortex, spinal cord and retina. Br J Pharmacol 1990 Jun;100(2):324-8.

(15) Sills GJ, Patsalos PN, Butler E, Forrest G, Ratnaraj N, Brodie MJ. Visual field constriction: accumulation of vigabatrin but not tiagabine in the retina. Neurology 2001 Jul 24;57(2):196-200.

(16) Sills GJ, Butler E, Thompson GG, Brodie MJ. Vigabatrin and tiagabine are pharmacologically different drugs. A pre-clinical study. Seizure 1999 Oct;8(7):404-11.

(17) Sills GJ, Butler E, Forrest G, Ratnaraj N, Patsalos PN, Brodie MJ. Vigabatrin, but not gabapentin or topiramate, produces concentration-related effects on enzymes and intermediates of the GABA shunt in rat brain and retina. Epilepsia 2003 Jul;44(7):886-92.

(18) Perry TL, Kish SJ, Hansen S. gamma-Vinyl GABA: effects of chronic administration on the metabolism of GABA and other amino compounds in rat brain. J Neurochem 1979 Jun;32(6):1641-5.

(19) Petroff OA, Rothman DL, Behar KL, Mattson RH. Initial observations on effect of vigabatrin on in vivo 1H spectroscopic measurements of gamma-aminobutyric acid, glutamate, and glutamine in human brain. Epilepsia 1995 May;36(5):457-64.

(20) Gale K, Iadarola MJ. Seizure protection and increased nerve-terminal GABA: delayed effects of GABA transaminase inhibition. Science 1980 Apr 18;208(4441):288-91.

(21) Loscher W. GABA in plasma and cerebrospinal fluid of different species. Effects of gamma-acetylenic GABA, gamma-vinyl GABA and sodium valproate. J Neurochem 1979 May;32(5):1587-91.

(22) Menachem EB, Persson LI, Schechter PJ, Haegele KD, Huebert N, Hardenberg J, et al. Effects of single doses of vigabatrin on CSF concentrations of GABA, homocarnosine, homovanillic acid and 5-hydroxyindoleacetic acid in patients with complex partial epilepsy. Epilepsy Res 1988 Mar;2(2):96-101.

(23) Abdul-Ghani AS, Norris PJ, Smith CC, Bradford HF. Effects of gamma-acetylenic GABA and gamma-vinyl GABA on synaptosomal release and uptake of GABA. Biochem Pharmacol 1981 Jun 1;30(11):1203-9.

(24) Neal MJ, Shah MA. Baclofen and phaclofen modulate GABA release from slices of rat cerebral cortex and spinal cord but not from retina. Br J Pharmacol 1989 Sep;98(1):105-12.

(25) Leach JP, Sills GJ, Majid A, Butler E, Carswell A, Thompson GG, et al. Effects of tiagabine and vigabatrin on GABA uptake into primary cultures of rat cortical astrocytes. Seizure 1996 Sep;5(3):229-34.

(26) Bringmann A, Pannicke T, Biedermann B, Francke M, Iandiev I, Grosche J, et al. Role of retinal glial cells in neurotransmitter uptake and metabolism. Neurochem Int 2009 Mar;54(3-4):143-60.

(27) Loscher W, Frey HH. One to three day dose intervals during subchronic treatment of epileptic gerbils with gamma-vinyl GABA: anticonvulsant efficacy and alterations in regional brain GABA levels. Eur J Pharmacol 1987 Nov 17;143(3):335-42.

(28) Porter TG, Martin DL. Evidence for feedback regulation of glutamate decarboxylase by gamma-aminobutyric acid. J Neurochem 1984 Nov;43(5):1464-7.

(29) Grove J, Tell G, Schechter PJ, Koch-Weser J, Warter JM, Marescaux C, et al. Increased CSF gamma-aminobutyric acid after treatment with gamma-vinyl GABA. Lancet 1980 Sep 20;2(8195 pt 1):647.

(30) Ben-Menachem E, Persson LI, Schechter PJ, Haegele KD, Huebert N, Hardenberg J, et al. The effect of different vigabatrin treatment regimens on CSF biochemistry and seizure control in epileptic patients. Br J Clin Pharmacol 1989;27 Suppl 1:79S-85S.

(31) Grove J, Schechter PJ, Tell G, Koch-Weser J, Sjoerdsma A, Warter JM, et al. Increased gamma-aminobutyric acid (GABA), homocarnosine and beta-alanine in cerebrospinal fluid of patients treated with gamma-vinyl GABA (4-amino-hex-5-enoic acid). Life Sci 1981 May 21;28(21):2431-9.

(32) Schechter PJ, Hanke NF, Grove J, Huebert N, Sjoerdsma A. Biochemical and clinical effects of gamma-vinyl GABA in patients with epilepsy. Neurology 1984 Feb;34(2):182-6.

(33) Ben-Menachem E, Hamberger A, Mumford J. Effect of long-term vigabatrin therapy on GABA and other amino acid concentrations in the central nervous system--a case study. Epilepsy Res 1993 Dec;16(3):241-3.

(34) Kendall DA, Fox DA, Enna SJ. Effect of gamma-vinyl GABA on bicuculline-induced seizures. Neuropharmacology 1981 Apr;20(4):351-5.

(35) Meldrum B, Horton R. Blockade of epileptic responses in the photosensitive baboon, Papio papio, by two irreversible inhibitors of GABA-transaminase, gamma-acetylenic GABA (4-amino-hex-5-ynoic acid) and gamma-vinyl GABA (4-amino-hex-5-enoic acid). Psychopharmacology (Berl) 1978 Sep 15;59(1):47-50.

(36) Stevens JR, Phillips I, de BR. gamma-Vinyl GABA in endopiriform area suppresses kindled amygdala seizures. Epilepsia 1988 Jul;29(4):404-11.

(37) Rimmer EM, Richens A. Double-blind study of gamma-vinyl GABA in patients with refractory epilepsy. Lancet 1984 Jan 28;1(8370):189-90.

(38) Browne TR, Mattson RH, Penry JK, Smith DB, Treiman DM, Wilder BJ, et al. Vigabatrin for refractory complex partial seizures: multicenter single-blind study with long-term follow-up. Neurology 1987 Feb;37(2):184-9.

(39) Gram L, Lyon BB, Dam M. Gamma-vinyl-GABA: a single-blind trial in patients with epilepsy. Acta Neurol Scand 1983 Jul;68(1):34-9.

(40) Gram L, Klosterskov P, Dam M. gamma-Vinyl GABA: a double-blind placebo-controlled trial in partial epilepsy. Ann Neurol 1985 Mar;17(3):262-6.

(41) Loiseau P, Hardenberg JP, Pestre M, Guyot M, Schechter PJ, Tell GP. Double-blind, placebo-controlled study of vigabatrin (gamma-vinyl GABA) in drug-resistant epilepsy. Epilepsia 1986 Mar;27(2):115-20.

(42) Tartara A, Manni R, Galimberti CA, Hardenberg J, Orwin J, Perucca E. Vigabatrin in the treatment of epilepsy: a double-blind, placebo-controlled study. Epilepsia 1986 Nov;27(6):717-23.

(43) Tassinari CA, Michelucci R, Ambrosetto G, Salvi F. Double-blind study of vigabatrin in the treatment of drug-resistant epilepsy. Arch Neurol 1987 Sep;44(9):907-10.

(44) French JA, Mosier M, Walker S, Sommerville K, Sussman N. A double-blind, placebo-controlled study of vigabatrin three g/day in patients with uncontrolled complex partial seizures. Vigabatrin Protocol 024 Investigative Cohort. Neurology 1996 Jan;46(1):54-61.

(45) Dean C, Mosier M, Penry K. Dose-Response Study of Vigabatrin as add-on therapy in patients with uncontrolled complex partial seizures. Epilepsia 1999 Jan;40(1):74-82.

(46) Bruni J, Guberman A, Vachon L, Desforges C. Vigabatrin as add-on therapy for adult complex partial seizures: a double-blind, placebo-controlled multicentre study. The Canadian Vigabatrin Study Group. Seizure 2000 Apr;9(3):224-32.

(47) Hemming K, Maguire MJ, Hutton JL, Marson AG. Vigabatrin for refractory partial epilepsy. Cochrane Database Syst Rev 2008;(3):CD007302.

(48) Hancock EC, Osborne JP, Edwards SW. Treatment of infantile spasms. Cochrane Database Syst Rev 2008;(4):CD001770.

(49) Wong M, Trevathan E. Infantile spasms. Pediatr Neurol 2001 Feb;24(2):89-98.

(50) Pellock JM, Hrachovy R, Shinnar S, Baram TZ, Bettis D, Dlugos DJ, et al. Infantile spasms: a U.S. consensus report. Epilepsia 2010 Oct;51(10):2175-89.

(51) Chiron C, Dulac O, Beaumont D, Palacios L, Pajot N, Mumford J. Therapeutic trial of vigabatrin in refractory infantile spasms. J Child Neurol 1991;Suppl 2:S52-S59.

(52) Appleton RE, Montiel-Viesca F. Vigabatrin in infantile spasms--why add on? Lancet 1993 Apr 10;341(8850):962.

(53) Vigevano F, Cilio MR. Vigabatrin versus ACTH as first-line treatment for infantile spasms: a randomized, prospective study. Epilepsia 1997 Dec;38(12):1270-4.

(54) Granstrom ML, Gaily E, Liukkonen E. Treatment of infantile spasms: results of a population-based study with vigabatrin as the first drug for spasms. Epilepsia 1999 Jul;40(7):950-7.

(55) Elterman RD, Shields WD, Mansfield KA, Nakagawa J. Randomized trial of vigabatrin in patients with infantile spasms. Neurology 2001 Oct 23;57(8):1416-21.

(56) Elterman RD, Shields WD, Bittman RM, Torri SA, Sagar SM, Collins SD. Vigabatrin for the Treatment of Infantile Spasms: Final Report of a Randomized Trial. J Child Neurol 2010 Apr 19.

(57) Appleton RE, Peters AC, Mumford JP, Shaw DE. Randomised, placebo-controlled study of vigabatrin as first-line treatment of infantile spasms. Epilepsia 1999 Nov;40(11):1627-33.

(58) Lux AL, Edwards SW, Hancock E, Johnson AL, Kennedy CR, Newton RW, et al. The United Kingdom Infantile Spasms Study (UKISS) comparing hormone treatment with vigabatrin on developmental and epilepsy outcomes to age 14 months: a multicentre randomised trial. Lancet Neurol 2005 Nov;4(11):712-7.

(59) Askalan R, Mackay M, Brian J, Otsubo H, McDermott C, Bryson S, et al. Prospective preliminary analysis of the development of autism and epilepsy in children with infantile spasms. J Child Neurol 2003 Mar;18(3):165-70.

(60) Chiron C, Dumas C, Jambaque I, Mumford J, Dulac O. Randomized trial comparing vigabatrin and hydrocortisone in infantile spasms due to tuberous sclerosis. Epilepsy Res 1997 Jan;26(2):389-95.

(61) Aicardi J, Mumford JP, Dumas C, Wood S. Vigabatrin as initial therapy for infantile spasms: a European retrospective survey. Sabril IS Investigator and Peer Review Groups. Epilepsia 1996 Jul;37(7):638-42.

(62) Sander JW, Hart YM. Vigabatrin and behaviour disturbances. Lancet 1990 Jan 6;335(8680):57.

(63) Gibson JP, Yarrington JT, Loudy DE, Gerbig CG, Hurst GH, Newberne JW. Chronic toxicity studies with vigabatrin, a GABA-transaminase inhibitor. Toxicol Pathol 1990;18(2):225-38.

(64) Butler WH, Ford GP, Newberne JW. A study of the effects of vigabatrin on the central nervous system and retina of Sprague Dawley and Lister-Hooded rats. Toxicol Pathol 1987;15(2):143-8.

(65) Graham D. Neuropathology of vigabatrin. Br J Clin Pharmacol 1989;27 Suppl 1:43S-5S.

(66) Pedersen B, Hojgaard K, Dam M. Vigabatrin: no microvacuoles in a human brain. Epilepsy Res 1987 Jan;1(1):74-6.

(67) Agosti R, Yasargil G, Egli M, Wieser HG, Wiestler OD. Neuropathology of a human hippocampus following long-term treatment with vigabatrin: lack of microvacuoles. Epilepsy Res 1990 Jul;6(2):166-70.

(68) Sivenius J, Paljarvi L, Vapalahti M, Nousiainen U, Riekkinen PJ. Vigabatrin (gamma-vinyl-GABA): neuropathologic evaluation in five patients. Epilepsia 1993 Jan;34(1):193-6.

(69) Hammond EJ, Ballinger WE, Jr., Lu L, Wilder BJ, Uthman BM, Reid SA. Absence of cortical white matter changes in three patients undergoing long-term vigabatrin therapy. Epilepsy Res 1992 Sep;12(3):261-5.

(70) Horton M, Rafay M, Del Bigio MR. Pathological evidence of vacuolar myelinopathy in a child following vigabatrin administration. J Child Neurol 2009 Dec;24(12):1543-6.

(71) Schroeder CE, Gibson JP, Yarrington J, Heydorn WE, Sussman NM, Arezzo JC. Effects of high-dose gamma-vinyl GABA (vigabatrin) administration on visual and somatosensory evoked potentials in dogs. Epilepsia 1992;33 Suppl 5:S13-S25.

(72) Cosi V, Callieco R, Galimberti CA, Manni R, Tartara A, Mumford J, et al. Effects of vigabatrin on evoked potentials in epileptic patients. Br J Clin Pharmacol 1989;27 Suppl 1:61S-8S.

(73) Hammond EJ, Wilder BJ. Effect of gamma-vinyl GABA on human pattern evoked visual potentials. Neurology 1985 Dec;35(12):1801-3.

(74) Mauguiere F, Chauvel P, Dewailly J, Dousse N. No effect of long-term vigabatrin treatment on central nervous system conduction in patients with refractory epilepsy: results of a multicenter study of somatosensory and visual evoked potentials. PMS Study Multicenter Group. Epilepsia 1997 Mar;38(3):301-8.

(75) Liegeois-Chauvel C, Marquis P, Gisselbrecht D, Pantieri R, Beaumont D, Chauvel P. Effects of long term vigabatrin on somatosensory evoked potentials in epileptic patients. Br J Clin Pharmacol 1989;27 Suppl 1:69S-72S.

(76) Levinson DF, Devinsky O. Psychiatric adverse events during vigabatrin therapy. Neurology 1999 Oct 22;53(7):1503-11.

(77) Sander JW, Hart YM, Trimble MR, Shorvon SD. Vigabatrin and psychosis. J Neurol Neurosurg Psychiatry 1991 May;54(5):435-9.

(78) Eke T, Talbot JF, Lawden MC. Severe persistent visual field constriction associated with vigabatrin. BMJ 1997 Jan 18;314(7075):180-1.

(79) Wilson EA, Brodie MJ. Severe persistent visual field constriction associated with vigabatrin. Chronic refractory epilepsy may have role in causing these unusual lesions. BMJ 1997 Jun 7;314(7095):1693.

(80) Harding GF. Severe persistent visual field constriction associated with vigabatrin. Four possible explanations exist. BMJ 1997 Jun 7;314(7095):1694.

(81) Lawden MC, Eke T, Degg C, Harding GF, Wild JM. Visual field defects associated with vigabatrin therapy. J Neurol Neurosurg Psychiatry 1999 Dec;67(6):716-22.

(82) Wong IC, Mawer GE, Sander JW. Severe persistent visual field constriction associated with vigabatrin. Reaction might be dose dependent. BMJ 1997 Jun 7;314(7095):1693-4.

(83) Blackwell N, Hayllar J, Kelly G. Severe persistent visual field constriction associated with vigabatrin. Patients taking vigabatrin should have regular visual field testing. BMJ 1997 Jun 7;314(7095):1694.

(84) Harding GF. Severe persistent visual field constriction associated with vigabatrin. Benefit: risk ratio must be calculated for individual patients. BMJ 1998 Jan 17;316(7126):232-3.

(85) Mackenzie R, Klistorner A. Severe persistent visual field constriction associated with vigabatrin. Asymptomatic as well as symptomatic defects occur with vigabatrin. BMJ 1998 Jan 17;316(7126):233.

(86) Backstrom JT, Hinkle RL, Flicker MR. Severe persistent visual field constriction associated with vigabatrin. Manufacturers have started several studies. BMJ 1997 Jun 7;314(7095):1694-5.

(87) Wilton LV, Stephens MD, Mann RD. Visual field defect associated with vigabatrin: observational cohort study. BMJ 1999 Oct 30;319(7218):1165-6.

(88) Comaish IF, Gorman C, Galloway NR. Visual field defect associated with vigabatrin. Many more patients may be affected than were found in study. BMJ 2000 May 20;320(7246):1403.

(89) Midelfart A. Visual field defect associated with vigabatrin. Means of selecting patients was misleading. BMJ 2000 May 20;320(7246):1404.

(90) Manuchehri K. Visual field defect associated with vigabatrin. Method of estimating prevalence was inappropriate. BMJ 2000 May 20;320(7246):1403-4.

(91) Maguire MJ, Hemming K, Wild JM, Hutton JL, Marson AG. Prevalence of visual field loss following exposure to vigabatrin therapy: A systematic review. Epilepsia 2010 Nov 10.

(92) Wild JM, Chiron C, Ahn H, Baulac M, Bursztyn J, Gandolfo E, et al. Visual field loss in patients with refractory partial epilepsy treated with vigabatrin: final results from an open-label, observational, multicentre study. CNS Drugs 2009 Nov 1;23(11):965-82.

(93) Sergott RC, Bittman RM, Christen EM, Sagar SM. Vigabatrin-induced peripheral visual field defects in patients with refractory partial epilepsy. Epilepsy Res 2010 Oct 14.

(94) Hardus P, Verduin WM, Postma G, Stilma JS, Berendschot TT, van Veelen CW. Concentric contraction of the visual field in patients with temporal lobe epilepsy and its association with the use of vigabatrin medication. Epilepsia 2000 May;41(5):581-7.

(95) Newman WD, Tocher K, Acheson JF. Vigabatrin associated visual field loss: a clinical audit to study prevalence, drug history and effects of drug withdrawal. Eye (Lond) 2002 Sep;16(5):567-71.

(96) Malmgren K, Ben-Menachem E, Frisen L. Vigabatrin visual toxicity: evolution and dose dependence. Epilepsia 2001 May;42(5):609-15.

(97) Wild JM, Martinez C, Reinshagen G, Harding GF. Characteristics of a unique visual field defect attributed to vigabatrin. Epilepsia 1999 Dec;40(12):1784-94.

(98) Nicolson A, Leach JP, Chadwick DW, Smith DF. The legacy of vigabatrin in a regional epilepsy clinic. J Neurol Neurosurg Psychiatry 2002 Sep;73(3):327-9.

(99) Kinirons P, Cavalleri GL, O'Rourke D, Doherty CP, Reid I, Logan P, et al. Vigabatrin retinopathy in an Irish cohort: lack of correlation with dose. Epilepsia 2006 Feb;47(2):311-7.

(100) Nousiainen I, Mantyjarvi M, Kalviainen R. No reversion in vigabatrin-associated visual field defects. Neurology 2001 Nov 27;57(10):1916-7.

(101) Daneshvar H, Racette L, Coupland SG, Kertes PJ, Guberman A, Zackon D. Symptomatic and asymptomatic visual loss in patients taking vigabatrin. Ophthalmology 1999 Sep;106(9):1792-8.

(102) Tseng YL, Lan MY, Lai SL, Huang FC, Tsai JJ. Vigabatrin-attributable visual field defects in patients with intractable partial epilepsy. Acta Neurol Taiwan 2006 Dec;15(4):244-50.

(103) McDonagh J, Stephen LJ, Dolan FM, Parks S, Dutton GN, Kelly K, et al. Peripheral retinal dysfunction in patients taking vigabatrin. Neurology 2003 Dec 23;61(12):1690-4.

(104) Kalviainen R, Nousiainen I, Mantyjarvi M, Nikoskelainen E, Partanen J, Partanen K, et al. Vigabatrin, a gabaergic antiepileptic drug, causes concentric visual field defects. Neurology 1999 Sep 22;53(5):922-6.

(105) Krauss GL, Johnson MA, Sheth S, Miller NR. A controlled study comparing visual function in patients treated with vigabatrin and tiagabine. J Neurol Neurosurg Psychiatry 2003 Mar;74(3):339-43.

(106) Miller NR, Johnson MA, Paul SR, Girkin CA, Perry JD, Endres M, et al. Visual dysfunction in patients receiving vigabatrin: clinical and electrophysiologic findings. Neurology 1999 Dec 10;53(9):2082-7.

(107) Conway M, Cubbidge RP, Hosking SL. Visual field severity indices demonstrate dose-dependent visual loss from vigabatrin therapy. Epilepsia 2008 Jan;49(1):108-16.

(108) Schmitz B, Schmidt T, Jokiel B, Pfeiffer S, Tiel-Wilck K, Ruther K. Visual field constriction in epilepsy patients treated with vigabatrin and other antiepileptic drugs: a prospective study. J Neurol 2002 Apr;249(4):469-75.

(109) van der TK, Graniewski-Wijnands HS, Polak BC. Visual field and electrophysiological abnormalities due to vigabatrin. Doc Ophthalmol 2002 Mar;104(2):181-8.

(110) Fledelius HC. Vigabatrin-associated visual field constriction in a longitudinal series. Reversibility suggested after drug withdrawal. Acta Ophthalmol Scand 2003 Feb;81(1):41-6.

(111) Paul SR, Krauss GL, Miller NR, Medura MT, Miller TA, Johnson MA. Visual function is stable in patients who continue long-term vigabatrin therapy: implications for clinical decision making. Epilepsia 2001 Apr;42(4):525-30.

(112) Besch D, Kurtenbach A, pfelstedt-Sylla E, Sadowski B, Dennig D, Asenbauer C, et al. Visual field constriction and electrophysiological changes associated with vigabatrin. Doc Ophthalmol 2002 Mar;104(2):151-70.

(113) Manuchehri K, Goodman S, Siviter L, Nightingale S. A controlled study of vigabatrin and visual abnormalities. Br J Ophthalmol 2000 May;84(5):499-505.

(114) Arndt CF, Derambure P, foort-Dhellemmes S, Hache JC. Outer retinal dysfunction in patients treated with vigabatrin. Neurology 1999 Apr 12;52(6):1201-5.

(115) Hui AC, Liu DT, Wong KK, Man BL, Leung T, Lam PT, et al. Vigabatrin-induced visual dysfunction in Chinese patients with refractory epilepsy. Eur J Ophthalmol 2008 Jul;18(4):624-7.

(116) Midelfart A, Midelfart E, Brodtkorb E. Visual field defects in patients taking vigabatrin. Acta Ophthalmol Scand 2000 Oct;78(5):580-4.

(117) Moreno MC, Giagante B, Saidon P, Kochen S, Benozzi J, Rosenstein RE. Visual defects associated with vigabatrin: a study of epileptic argentine patients. Can J Neurol Sci 2005 Nov;32(4):459-64.

(118) Toggweiler S, Wieser HG. Concentric visual field restriction under vigabatrin therapy: extent depends on the duration of drug intake. Seizure 2001 Sep;10(6):420-3.

(119) Ardagil AA, Gokceer S, Erbil HH, Isik N, Ozdoker L, Salar S, et al. Detecting retinal vigabatrin toxicity in patients with partial symptomatic or cryptogenic epilepsy. Eur J Ophthalmol 2010 Feb 8;20(4):763-9.

(120) Ponjavic V, Andreasson S. Multifocal ERG and full-field ERG in patients on long-term vigabatrin medication. Doc Ophthalmol 2001 Jan;102(1):63-72.

(121) Jensen H, Sjo O, Uldall P, Gram L. Vigabatrin and retinal changes. Doc Ophthalmol 2002 Mar;104(2):171-80.

(122) Vanhatalo S, Nousiainen I, Eriksson K, Rantala H, Vainionpaa L, Mustonen K, et al. Visual field constriction in 91 Finnish children treated with vigabatrin. Epilepsia 2002 Jul;43(7):748-56.

(123) You SJ, Ahn H, Ko TS. Vigabatrin and visual field defects in pediatric epilepsy patients. J Korean Med Sci 2006 Aug;21(4):728-32.

(124) Werth R, Schadler G. Visual field loss in young children and mentally handicapped adolescents receiving vigabatrin. Invest Ophthalmol Vis Sci 2006 Jul;47(7):3028-35.

(125) Agrawal S, Mayer DL, Hansen RM, Fulton AB. Visual fields in young children treated with vigabatrin. Optom Vis Sci 2009 Jun;86(6):767-73.

(126) Gross-Tsur V, Banin E, Shahar E, Shalev RS, Lahat E. Visual impairment in children with epilepsy treated with vigabatrin. Ann Neurol 2000 Jul;48(1):60-4.

(127) Gaily E, Jonsson H, Lappi M. Visual fields at school-age in children treated with vigabatrin in infancy. Epilepsia 2009 Feb;50(2):206-16.

(128) Ascaso FJ, Lopez MJ, Mauri JA, Cristobal JA. Visual field defects in pediatric patients on vigabatrin monotherapy. Doc Ophthalmol 2003 Sep;107(2):127-30.

(129) Wohlrab G, Boltshauser E, Schmitt B, Schriever S, Landau K. Visual field constriction is not limited to children treated with vigabatrin. Neuropediatrics 1999 Jun;30(3):130-2.

(130) Iannetti P, Spalice A, Perla FM, Conicella E, Raucci U, Bizzarri B. Visual field constriction in children with epilepsy on vigabatrin treatment. Pediatrics 2000 Oct;106(4):838-42.

(131) Spencer EL, Harding GF. Examining visual field defects in the paediatric population exposed to vigabatrin. Doc Ophthalmol 2003 Nov;107(3):281-7.

(132) Rebolleda G, Munoz-Negrete FJ, Gutierrez C. Screening of patients taking vigabatrin. Ophthalmology 2000 Jul;107(7):1219-20.

(133) Luchetti A, Amadi A, Gobbi G. Visual field defects associated with vigabratin monotherapy in children. J Neurol Neurosurg Psychiatry 2000 Oct;69(4):566.

(134) Harding GF, Wild JM, Robertson KA, Lawden MC, Betts TA, Barber C, et al. Electro-oculography, electroretinography, visual evoked potentials, and multifocal electroretinography in patients with vigabatrin-attributed visual field constriction. Epilepsia 2000 Nov;41(11):1420-31.

(135) Comaish IF, Gorman C, Brimlow GM, Barber C, Orr GM, Galloway NR. The effects of vigabatrin on electrophysiology and visual fields in epileptics: a controlled study with a discussion of possible mechanisms. Doc Ophthalmol 2002 Mar;104(2):195-212.

(136) Hardus P, Verduin WM, Berendschot TT, Kamermans M, Postma G, Stilma JS, et al. The value of electrophysiology results in patients with epilepsy and vigabatrin associated visual field loss. Acta Ophthalmol Scand 2001 Apr;79(2):169-74.

(137) Hardus P, Verduin WM, Engelsman M, Edelbroek PM, Segers JP, Berendschot TT, et al. Visual field loss associated with vigabatrin: quantification and relation to dosage. Epilepsia 2001 Feb;42(2):262-7.

(138) Krauss GL, Johnson MA, Miller NR. Vigabatrin-associated retinal cone system dysfunction: electroretinogram and ophthalmologic findings. Neurology 1998 Mar;50(3):614-8.

(139) Clayton LM, Duncan JS, Sisodiya SM, Acheson JF. Delayed, rapid visual field loss in a patient after ten years of vigabatrin therapy. Eye (Lond) 2010 Jan;24(1):185-6.

(140) Wild JM, Ahn HS, Baulac M, Bursztyn J, Chiron C, Gandolfo E, et al. Vigabatrin and epilepsy: lessons learned. Epilepsia 2007 Jul;48(7):1318-27.

(141) Ophthalmic findings in VGB-exposed adults. US Food and Drug Administration . 1-7-2009. 12-10-2010.

Ref Type: Internet Communication

(142) Fechtner RD, Khouri AS, Figueroa E, Ramirez M, Federico M, Dewey SL, et al. Short-term treatment of cocaine and/or methamphetamine abuse with vigabatrin: ocular safety pilot results. Arch Ophthalmol 2006 Sep;124(9):1257-62.

(143) Kiratli H, Turkcuoglu P. Rapid development of visual field defects associated with vigabatrin therapy. Eye (Lond) 2001 Oct;15(Pt 5):672-4.

(144) Morong S, Westall CA, Nobile R, Buncic JR, Logan WJ, Panton CM, et al. Longitudinal changes in photopic OPs occurring with vigabatrin treatment. Doc Ophthalmol 2003 Nov;107(3):289-97.

(145) Harding GF, Robertson KA, Edson AS, Barnes P, Wild J. Visual electrophysiological effect of a GABA transaminase blocker. Doc Ophthalmol 1998;97(2):179-88.

(146) Ruether K, Pung T, Kellner U, Schmitz B, Hartmann C, Seeliger M. Electrophysiologic evaluation of a patient with peripheral visual field contraction associated with vigabatrin. Arch Ophthalmol 1998 Jun;116(6):817-9.

(147) Frisen L, Malmgren K. Characterization of vigabatrin-associated optic atrophy. Acta Ophthalmol Scand 2003 Oct;81(5):466-73.

(148) Best JL, Acheson JF. The natural history of Vigabatrin associated visual field defects in patients electing to continue their medication. Eye (Lond) 2005 Jan;19(1):41-4.

(149) Schmidt T, Ruther K, Jokiel B, Pfeiffer S, Tiel-Wilck K, Schmitz B. Is visual field constriction in epilepsy patients treated with vigabatrin reversible? J Neurol 2002 Aug;249(8):1066-71.

(150) Graniewski-Wijnands HS, van der TK. Electro-ophthalmological recovery after withdrawal from vigabatrin. Doc Ophthalmol 2002 Mar;104(2):189-94.

(151) Hardus P, Verduin W, Berendschot T, Postma G, Stilma J, van VC. Vigabatrin: longterm follow-up of electrophysiology and visual field examinations. Acta Ophthalmol Scand 2003 Oct;81(5):459-65.

(152) Hardus P, Verduin WM, Postma G, Stilma JS, Berendschot TT, van Veelen CW. Long term changes in the visual fields of patients with temporal lobe epilepsy using vigabatrin. Br J Ophthalmol 2000 Jul;84(7):788-90.

(153) Johnson MA, Krauss GL, Miller NR, Medura M, Paul SR. Visual function loss from vigabatrin: effect of stopping the drug. Neurology 2000 Jul 12;55(1):40-5.

(154) Kjellstrom U, Lovestam-Adrian M, Andreasson S, Ponjavic V. Full-field ERG and visual fields in patients 5 years after discontinuing vigabatrin therapy. Doc Ophthalmol 2008 Sep;117(2):93-101.

(155) Vanhatalo S, Alen R, Riikonen R, Rantala H, Aine MR, Mustonen K, et al. Reversed visual field constrictions in children after vigabatrin withdrawal--true retinal recovery or improved test performance only? Seizure 2001 Oct;10(7):508-11.

(156) Krakow K, Polizzi G, Riordan-Eva P, Holder G, MacLeod WN, Fish DR. Recovery of visual field constriction following discontinuation of vigabatrin. Seizure 2000 Jun;9(4):287-90.

(157) Giordano L, Valseriati D, Vignoli A, Morescalchi F, Gandolfo E. Another case of reversibility of visual-field defect induced by vigabatrin monotherapy: is young age a favorable factor? Neurol Sci 2000 Jun;21(3):185-6.

(158) Versino M, Veggiotti P. Reversibility of vigabratin-induced visual-field defect. Lancet 1999 Aug 7;354(9177):486.

(159) Wild JM, gler-Harles M, Searle AE, O'Neill EC, Crews SJ. The influence of the learning effect on automated perimetry in patients with suspected glaucoma. Acta Ophthalmol (Copenh) 1989 Oct;67(5):537-45.

(160) Heijl A, Lindgren G, Olsson J. The effect of perimetric experience in normal subjects. Arch Ophthalmol 1989 Jan;107(1):81-6.

(161) Olson JA, Purdie AT, Coleman RJ. Tangent screens are still useful in the assessment of vigabatrin induced visual field defects. Br J Ophthalmol 2002 Aug;86(8):931-2.

(162) Ravindran J, Blumbergs P, Crompton J, Pietris G, Waddy H. Visual field loss associated with vigabatrin: pathological correlations. J Neurol Neurosurg Psychiatry 2001 Jun;70(6):787-9.

(163) Frisen L. Vigabatrin-associated loss of vision: rarebit perimetry illuminates the dose-damage relationship. Acta Ophthalmol Scand 2004 Feb;82(1):54-8.

(164) Arndt CF, Salle M, Derambure PH, foort-Dhellemmes S, Hache JC. The effect on vision of associated treatments in patients taking vigabatrin: carbamazepine versus valproate. Epilepsia 2002 Aug;43(8):812-7.

(165) Harding GF, Wild JM, Robertson KA, Rietbrock S, Martinez C. Separating the retinal electrophysiologic effects of vigabatrin: treatment versus field loss. Neurology 2000 Aug 8;55(3):347-52.

(166) Franciotta D, Kwan P, Perucca E. Genetic basis for idiosyncratic reactions to antiepileptic drugs. Curr Opin Neurol 2009 Apr;22(2):144-9.

(167) Durbin S, Mirabella G, Buncic JR, Westall CA. Reduced grating acuity associated with retinal toxicity in children with infantile spasms on vigabatrin therapy. Invest Ophthalmol Vis Sci 2009 Aug;50(8):4011-6.

(168) Kinirons P, Cavalleri GL, Singh R, Shahwan A, Acheson JF, Wood NW, et al. A pharmacogenetic exploration of vigabatrin-induced visual field constriction. Epilepsy Res 2006 Aug;70(2-3):144-52.

(169) Hisama FM, Mattson RH, Lee HH, Felice K, Petroff OA. GABA and the ornithine delta-aminotransferase gene in vigabatrin-associated visual field defects. Seizure 2001 Oct;10(7):505-7.

(170) Roubertie A, Bellet H, Echenne B. Vigabatrin-associated retinal cone system dysfunction. Neurology 1998 Dec;51(6):1779-81.

(171) Daune G, Seiler N. Interrelationships between ornithine, glutamate, and GABA. II. Consequences of inhibition of GABA-T and ornithine aminotransferase in brain. Neurochem Res 1988 Jan;13(1):69-75.

(172) Sorri I, Brigell MG, Malyusz M, Mahlamaki E, de MC, Kalviainen R. Is reduced ornithine-delta-aminotransferase activity the cause of vigabatrin-associated visual field defects? Epilepsy Res 2010 Sep 15.

(173) Rao GP, Fat FA, Kyle G, Leach JP, Chadwick DW, Batterbury M. Study is needed of visual field defects associated with any long term antiepileptic drug. BMJ 1998 Jul 18;317(7152):206.

(174) Schmidt T, Ruther K, Schmitz B. Are vigabatrin-associated visual field constrictions asymptomatic? J Neurol 2004 Jul;251(7):887-8.

(175) Verrotti A, Manco R, Matricardi S, Franzoni E, Chiarelli F. Antiepileptic drugs and visual function. Pediatr Neurol 2007 Jun;36(6):353-60.

(176) Hilton EJ, Hosking SL, Betts T. The effect of antiepileptic drugs on visual performance. Seizure 2004 Mar;13(2):113-28.

(177) Szlyk JP, Seiple W, Fishman GA, Alexander KR, Grover S, Mahler CL. Perceived and actual performance of daily tasks: relationship to visual function tests in individuals with retinitis pigmentosa. Ophthalmology 2001 Jan;108(1):65-75.

(178) Hawker MJ, Astbury NJ. The ocular side effects of vigabatrin (Sabril): information and guidance for screening. Eye (Lond) 2008 Sep;22(9):1097-8.

(179) Ray A, Pathak-Ray V, Walters R, Hatfield R. Driving after epilepsy surgery: effects of visual field defects and epilepsy control. Br J Neurosurg 2002 Oct;16(5):456-60.

(180) Acheson JF. Vigabatrin associated visual field constriction. J Neurol Neurosurg Psychiatry 1999 Dec;67(6):707-8.

(181) Nousiainen I, Kalviainen R, Mantyjarvi M. Contrast and glare sensitivity in epilepsy patients treated with vigabatrin or carbamazepine monotherapy compared with healthy volunteers. Br J Ophthalmol 2000 Jun;84(6):622-5.

(182) Beck RW. Vigabatrin-associated retinal cone system dysfunction. Neurology 1998 Dec;51(6):1778-9.

(183) Buncic JR, Westall CA, Panton CM, Munn JR, MacKeen LD, Logan WJ. Characteristic retinal atrophy with secondary "inverse" optic atrophy identifies vigabatrin toxicity in children. Ophthalmology 2004 Oct;111(10):1935-42.

(184) Nousiainen I, Kalviainen R, Mantyjarvi M. Color vision in epilepsy patients treated with vigabatrin or carbamazepine monotherapy. Ophthalmology 2000 May;107(5):884-8.

(185) Hilton EJ, Cubbidge RP, Hosking SL, Betts T, Comaish IF. Patients treated with vigabatrin exhibit central visual function loss. Epilepsia 2002 Nov;43(11):1351-9.

(186) Steinhoff BJ, Freudenthaler N, Paulus W. The influence of established and new antiepileptic drugs on visual perception. II. A controlled study in patients with epilepsy under long-term antiepileptic medication. Epilepsy Res 1997 Dec;29(1):49-58.

(187) Mecarelli O, Rinalduzzi S, Accornero N. Changes in color vision after a single dose of vigabatrin or carbamazepine in healthy volunteers. Clin Neuropharmacol 2001 Jan;24(1):23-6.

(188) Steinhoff BJ, Freudenthaler N, Paulus W. The influence of established and new antiepileptic drugs on visual perception. 1. A placebo-controlled, double-blind, single-dose study in healthy volunteers. Epilepsy Res 1997 Dec;29(1):35-47.

(189) Paulus W, Schwarz G, Steinhoff BJ. The effect of anti-epileptic drugs on visual perception in patients with epilepsy. Brain 1996 Apr;119 (Pt 2):539-49.

(190) Bayer AU, Thiel HJ, Zrenner E, Dichgans J, Kuehn M, Paulus W, et al. Color vision tests for early detection of antiepileptic drug toxicity. Neurology 1997 May;48(5):1394-7.

(191) Verrotti A, Lobefalo L, Priolo T, Rapinese M, Trotta D, Morgese G, et al. Color vision in epileptic adolescents treated with valproate and carbamazepine. Seizure 2004 Sep;13(6):411-7.

(192) Nousiainen I, Mantyjarvi M, Kalviainen R. Visual function in patients treated with GABAergic anticonvulsant drug tiagabine. Clinical Drug Investigation 2000;20:393-400.

(193) Lopez L, Thomson A, Rabinowicz AL. Assessment of colour vision in epileptic patients exposed to single-drug therapy. Eur Neurol 1999;41(4):201-5.

(194) Tiel-Wilck K, Jokiel B, Zinser P, Heine Fr, Pfeiffer S, Wilck B, et al. Afferent visual function after single dose application of -vinyl GABA. Neuro-ophthamology 1995;15(6):305-10.

(195) Sartucci F, Massetani R, Galli R, Bonanni E, Tognoni G, Milani S, et al. Visual contrast sensitivity in carbamazepine-resistant epileptic patients receiving vigabatrin as add-on therapy. J Epilepsy 1997;10(1):7-11.

(196) Banin E, Shalev RS, Obolensky A, Neis R, Chowers I, Gross-Tsur V. Retinal function abnormalities in patients treated with vigabatrin. Arch Ophthalmol 2003 Jun;121(6):811-6.

(197) Koul R, Chacko A, Ganesh A, Bulusu S, Al RK. Vigabatrin associated retinal dysfunction in children with epilepsy. Arch Dis Child 2001 Dec;85(6):469-73.

(198) Choi HJ, Kim DM. Visual field constriction associated with vigabatrin: retinal nerve fiber layer photographic correlation. J Neurol Neurosurg Psychiatry 2004 Oct;75(10):1395.

(199) Wall M, Johnson CA. Principles and techniques of the examination of the visual sensory system. In: Miller NR, Newman NJ, editors. Walsh and Hoyt's Clinical Neuro-Ophthalmology. Sixth edition ed. Philadelphia: Lippincott Williams and Wilkins; 2005. p. 83-150.

(200) Holder GE, Gale RP, Acheson JF, Robson AG. Electrodiagnostic assessment in optic nerve disease. Curr Opin Neurol 2009 Feb;22(1):3-10.

(201) Odom JV, Bach M, Brigell M, Holder GE, McCulloch DL, Tormene AP, et al. ISCEV standard for clinical visual evoked potentials (2009 update). Doc Ophthalmol 2010 Feb;120(1):111-9.

(202) Brown M, Marmor M, Vaegan, Zrenner E, Brigell M, Bach M. ISCEV Standard for Clinical Electro-oculography (EOG) 2006. Doc Ophthalmol 2006 Nov;113(3):205-12.

(203) Arden GB, Constable PA. The electro-oculogram. Prog Retin Eye Res 2006 Mar;25(2):207-48.

(204) ARMINGTON JC, JOHNSON EP, RIGGS LA. The scotopic A-wave in the electrical response of the human retina. J Physiol 1952 Nov;118(3):289-98.

(205) Plant GT. Recent advances in the electrophysiology of visual disorders. Curr Opin Ophthalmol 1995 Dec;6(6):54-9.

(206) Wachtmeister L. Oscillatory potentials in the retina: what do they reveal. Prog Retin Eye Res 1998 Oct;17(4):485-521.

(207) Marmor MF, Fulton AB, Holder GE, Miyake Y, Brigell M, Bach M. ISCEV Standard for full-field clinical electroretinography (2008 update). Doc Ophthalmol 2009 Feb;118(1):69-77.

(208) Verma R, Pianta MJ. The contribution of human cone photoreceptors to the photopic flicker electroretinogram. J Vis 2009;9(3):9-12.

(209) Ventura LM, Porciatti V. Pattern electroretinogram in glaucoma. Curr Opin Ophthalmol 2006 Apr;17(2):196-202.

(210) RIGGS LA, JOHNSON EP, Schick AM. Electrical Responses of the Human Eye to Moving Stimulus Patterns. Science 1964 May 1;144(3618):567.

(211) Holder GE. Pattern electroretinography (PERG) and an integrated approach to visual pathway diagnosis. Prog Retin Eye Res 2001 Jul;20(4):531-61.

(212) Hood DC, Bach M, Brigell M, Keating D, Kondo M, Lyons JS, et al. ISCEV Guidelines for clinical multifocal electroretinography (2007). 2007.

(213) Duckett T, Brigell MG, Ruckh S. Electroretinographic changes are not associated with loss of visual function in paediatric patients following treatment with vigabatrin. Invest Ophthalmol Vis Sci 39, S973. 1998.
Ref Type: Abstract

(214) Brigell MG. Vigabatrin-associated retinal cone system dysfunction. Neurology 1998 Dec;51(6):1779-81.

(215) Holder GE, Brigell MG, Hawlina M, Meigen T, Vaegan, Bach M. ISCEV standard for clinical pattern electroretinography--2007 update. Doc Ophthalmol 2007 May;114(3):111-6.

(216) Coupland SG, Zackon DH, Leonard BC, Ross TM. Vigabatrin effect on inner retinal function. Ophthalmology 2001 Aug;108(8):1493-6.

(217) Westall CA, Logan WJ, Smith K, Buncic JR, Panton CM, Abdolell M. The Hospital for Sick Children, Toronto, Longitudinal ERG study of children on vigabatrin. Doc Ophthalmol 2002 Mar;104(2):133-49.

(218) Bayer AU, Zrenner E, Reid SA, Schmidt D. Psychophysical and electrophysiological findings in patients with epilepsy. Invest Ophthalmol Vis Sci 31, 427. 1990.
Ref Type: Abstract

(219) Verrotti A, Trotta D, Cutarella R, Pascarella R, Morgese G, Chiarelli F. Effects of antiepileptic drugs on evoked potentials in epileptic children. Pediatr Neurol 2000 Nov;23(5):397-402.

(220) Thakral A, Shenoy R, Deleu D. Acute visual dysfunction following phenytoin-induced toxicity. Acta Neurol Belg 2003 Dec;103(4):218-20.

(221) Arndt CF, Husson J, Derambure P, Hache JC, Arnaud B, Defoort-Dhellemmes S. Retinal electrophysiological results in patients receiving lamotrigine monotherapy. Epilepsia 2005 Jul;46(7):1055-60.

(222) Westall CA, Nobile R, Morong S, Buncic JR, Logan WJ, Panton CM. Changes in the electroretinogram resulting from discontinuation of vigabatrin in children. Doc Ophthalmol 2003 Nov;107(3):299-309.

(223) Harding GF, Robertson K, Spencer EL, Holliday I. Vigabatrin; its effect on the electrophysiology of vision. Doc Ophthalmol 2002 Mar;104(2):213-29.

(224) Harding GF, Jones AL, Tipper VJ, Betts TA, Mumford JP. Electroretinogram, pattern electroretinogram and visual evoked potential assessment in patients receiving vigabatrin. Brain Nerve 36[Suppl 3], S108. 1995.
Ref Type: Abstract

(225) Lukasiewicz PD, Eggers ED, Sagdullaev BT, McCall MA. GABAC receptor-mediated inhibition in the retina. Vision Res 2004 Dec;44(28):3289-96.

(226) Kapousta-Bruneau NV. Opposite effects of GABA(A) and GABA(C) receptor antagonists on the b-wave of ERG recorded from the isolated rat retina. Vision Res 2000;40(13):1653-65.

(227) Feigenspan A, Bormann J. Differential pharmacology of GABAA and GABAC receptors on rat retinal bipolar cells. Eur J Pharmacol 1994 Dec 15;288(1):97-104.

(228) Shields CR, Tran MN, Wong RO, Lukasiewicz PD. Distinct ionotropic GABA receptors mediate presynaptic and postsynaptic inhibition in retinal bipolar cells. J Neurosci 2000 Apr 1;20(7):2673-82.

(229) Wild JM, Robson CR, Jones AL, Cunliffe IA, Smith PE. Detecting vigabatrin toxicity by imaging of the retinal nerve fiber layer. Invest Ophthalmol Vis Sci 2006 Mar;47(3):917-24.

(230) Rizzo JF. Embryology, anatomy, and physiology of the afferent visual pathway. In: Miller NR, Newman NJ, editors. Walsh and Hoyt's Clinical Neuro-Ophthalmology. Sixth Edition ed. Philadelphia: Lippincott Williams & Wilkins; 2005. p. 3-82.

(231) Kolb H, Fernandez E, Nelson R. Webvision The organization of the retina and visual system. 2011. 6-12-2010.
Ref Type: Online Source

(232) Johnson J, Chen TK, Rickman DW, Evans C, Brecha NC. Multiple gamma-Aminobutyric acid plasma membrane transporters (GAT-1, GAT-2, GAT-3) in the rat retina. J Comp Neurol 1996 Nov 11;375(2):212-24.

(233) Biedermann B, Bringmann A, Reichenbach A. High-affinity GABA uptake in retinal glial (Muller) cells of the guinea pig: electrophysiological characterization, immunohistochemical localization, and modeling of efficiency. Glia 2002 Sep;39(3):217-28.

(234) Neal MJ, Cunningham JR, Shah MA, Yazulla S. Immunocytochemical evidence that vigabatrin in rats causes GABA accumulation in glial cells of the retina. Neurosci Lett 1989 Mar 13;98(1):29-32.

(235) Cubells JF, Blanchard JS, Smith DM, Makman MH. In vivo action of enzyme-activated irreversible inhibitors of glutamic acid decarboxylase and gamma-aminobutyric acid transaminase in retina vs. brain. J Pharmacol Exp Ther 1986 Aug;238(2):508-14.

(236) Ponjavic V, Granse L, Kjellstrom S, Andreasson S, Bruun A. Alterations in electroretinograms and retinal morphology in rabbits treated with vigabatrin. Doc Ophthalmol 2004 Mar;108(2):125-33.

(237) Hyde JC, Robinson N. Localisation of sites of GABA catabolism in the rat retina. Nature 1974 Mar 29;248(447):432-3.

(238) Duboc A, Hanoteau N, Simonutti M, Rudolf G, Nehlig A, Sahel JA, et al. Vigabatrin, the GABA-transaminase inhibitor, damages cone photoreceptors in rats. Ann Neurol 2004 May;55(5):695-705.

(239) Izumi Y, Ishikawa M, Benz AM, Izumi M, Zorumski CF, Thio LL. Acute vigabatrin retinotoxicity in albino rats depends on light but not GABA. Epilepsia 2004 Sep;45(9):1043-8.

(240) Wang QP, Jammoul F, Duboc A, Gong J, Simonutti M, Dubus E, et al. Treatment of epilepsy: the GABA-transaminase inhibitor, vigabatrin, induces neuronal plasticity in the mouse retina. Eur J Neurosci 2008 Apr;27(8):2177-87.

(241) Jammoul F, Wang Q, Nabbout R, Coriat C, Duboc A, Simonutti M, et al. Taurine deficiency is a cause of vigabatrin-induced retinal phototoxicity. Ann Neurol 2009 Jan;65(1):98-107.

(242) Jammoul F, Degardin J, Pain D, Gondouin P, Simonutti M, Dubus E, et al. Taurine deficiency damages photoreceptors and retinal ganglion cells in vigabatrin-treated neonatal rats. Mol Cell Neurosci 2010 Apr;43(4):414-21.

(243) Kjellstrom U, Bruun A, Ghosh F, Andreasson S, Ponjavic V. Dose-related changes in retinal function and PKC-alpha expression in rabbits on vigabatrin medication. Effect of vigabatrin in the rabbit eye. Graefes Arch Clin Exp Ophthalmol 2009 Aug;247(8):1057-67.

(244) Kjellstrom U, Kjellstrom S, Bruun A, Andreasson S, Ponjavic V. Retinal function in rabbits does not improve 4-5 months after terminating treatment with vigabatrin. Doc Ophthalmol 2006 Jan;112(1):35-41.

(245) Ogden TE. Nerve fiber layer of the macaque retina: retinotopic organization. Invest Ophthalmol Vis Sci 1983 Jan;24(1):85-98.

(246) Pollock SC, Miller NR. The retinal nerve fiber layer. Int Ophthalmol Clin 1986;26(4):201-21.

(247) Radius RL, Anderson DR. The course of axons through the retina and optic nerve head. Arch Ophthalmol 1979 Jun;97(6):1154-8.

(248) Plant GT, Perry VH. The anatomical basis of the caecocentral scotoma. New observations and a review. Brain 1990 Oct;113 (Pt 5):1441-57.

(249) Naito J. Retinogeniculate projection fibers in the monkey optic nerve: a demonstration of the fiber pathways by retrograde axonal transport of WGA-HRP. J Comp Neurol 1989 Jun 8;284(2):174-86.

(250) Frenkel S, Morgan JE, Blumenthal EZ. Histological measurement of retinal nerve fibre layer thickness. Eye (Lond) 2005 May;19(5):491-8.

(251) Cohen MJ, Kaliner E, Frenkel S, Kogan M, Miron H, Blumenthal EZ. Morphometric analysis of human peripapillary retinal nerve fiber layer thickness. Invest Ophthalmol Vis Sci 2008 Mar;49(3):941-4.

(252) Townsend KA, Wollstein G, Schuman JS. Imaging of the retinal nerve fibre layer for glaucoma. Br J Ophthalmol 2009 Feb;93(2):139-43.

(253) Vessani RM, Moritz R, Batis L, Zagui RB, Bernardoni S, Susanna R. Comparison of quantitative imaging devices and subjective optic nerve head assessment by general ophthalmologists to differentiate normal from glaucomatous eyes. J Glaucoma 2009 Mar;18(3):253-61.

(254) Deleon-Ortega JE, Arthur SN, McGwin G, Jr., Xie A, Monheit BE, Girkin CA. Discrimination between glaucomatous and nonglaucomatous eyes using quantitative imaging devices and subjective optic nerve head assessment. Invest Ophthalmol Vis Sci 2006 Aug;47(8):3374-80.

(255) Medeiros FA, Zangwill LM, Bowd C, Weinreb RN. Comparison of the GDx VCC scanning laser polarimeter, HRT II confocal scanning laser ophthalmoscope, and stratus OCT optical coherence tomograph for the detection of glaucoma. Arch Ophthalmol 2004 Jun;122(6):827-37.

(256) Lawthom C, Smith PE, Wild JM. Nasal retinal nerve fiber layer attenuation: a biomarker for vigabatrin toxicity. Ophthalmology 2009 Mar;116(3):565-71.

(257) Durnian JM, Clearkin LG. Retinal nerve fibre layer characteristics with vigabatrin-associated visual field loss--could scanning laser polarimetry aid diagnosis? Eye (Lond) 2008 Apr;22(4):559-63.

(258) Moseng L, Saeter M, Morch-Johnsen GH, Hoff JM, Gajda A, Brodtkorb E, et al. Retinal nerve fibre layer attenuation: clinical indicator for vigabatrin toxicity. Acta Ophthalmol 2011 Jan 21.

(259) Clayton LM, Devile M, Punte T, Kallis C, de Haan G, Sander JW, et al. Retinal nerve fibre layer thickness in vigabatrin exposed patients. Ann Neurol 2010;In Press.

(260) Lobefalo L, Rapinese M, Altobelli E, Di MR, Lattanzi D, Gallenga PE, et al. Retinal nerve fiber layer and macular thickness in adolescents with epilepsy treated with valproate and carbamazepine. Epilepsia 2006 Apr;47(4):717-9.

(261) Sabril ophthalmic assessment form. 2011. Lundbeck S.H.A.R.E.
Ref Type: Online Source

(262) Sergott RC. Recommendations for visual evaluations of patients treated with vigabatrin. Curr Opin Ophthalmol 2010 Sep 1.

(263) Peripheral and Central Nervous System Advisory Committee Briefing Document. US Food and Drug Administration . 2010. 1-11-2010.
Ref Type: Internet Communication

(264) Huang D, Swanson EA, Lin CP, Schuman JS, Stinson WG, Chang W, et al. Optical coherence tomography. Science 1991 Nov 22;254(5035):1178-81.

(265) Fujimoto JG, Brezinski ME, Tearney GJ, Boppart SA, Bouma B, Hee MR, et al. Optical biopsy and imaging using optical coherence tomography. Nat Med 1995 Sep;1(9):970-2.

(266) Costa RA, Skaf M, Melo LA, Jr., Calucci D, Cardillo JA, Castro JC, et al. Retinal assessment using optical coherence tomography. Prog Retin Eye Res 2006 May;25(3):325-53.

(267) Drexler W, Fujimoto JG. State-of-the-art retinal optical coherence tomography. Prog Retin Eye Res 2008 Jan;27(1):45-88.

(268) Toth CA, Narayan DG, Boppart SA, Hee MR, Fujimoto JG, Birngruber R, et al. A comparison of retinal morphology viewed by optical coherence tomography and by light microscopy. Arch Ophthalmol 1997 Nov;115(11):1425-8.

(269) Drexler W, Fujimoto JG. Introduction to optical coherence tomography. In: Drexler W, Fujimoto JG, editors. Optical coherence tomography technology and applications. Springer; 2008. p. 45.

(270) Hee MR, Izatt JA, Swanson EA, Huang D, Schuman JS, Lin CP, et al. Optical coherence tomography of the human retina. Arch Ophthalmol 1995 Mar;113(3):325-32.

(271) Geitzenauer W, Hitzenberger CK, Schmidt-Erfurth UM. Retinal optical coherence tomography: past, present and future perspectives. Br J Ophthalmol 2010 Jul 31.

(272) Thomas D, Duguid G. Optical coherence tomography--a review of the principles and contemporary uses in retinal investigation. Eye (Lond) 2004 Jun;18(6):561-70.

(273) Izatt JA, Choma MA. Theory of optical coherence tomography. In: Drexler W, Fujimoto JG, editors. Optical coherence tomography technology and applications. Springer; 2008. p. 47-63.

(274) Drexler W, Sattmann H, Hermann B, Ko TH, Stur M, Unterhuber A, et al. Enhanced visualization of macular pathology with the use of ultrahigh-resolution optical coherence tomography. Arch Ophthalmol 2003 May;121(5):695-706.

(275) Chen TC, Cense B, Pierce MC, Nassif N, Park BH, Yun SH, et al. Spectral domain optical coherence tomography: ultra-high speed, ultra-high resolution ophthalmic imaging. Arch Ophthalmol 2005 Dec;123(12):1715-20.

(276) Sakata LM, Deleon-Ortega J, Sakata V, Girkin CA. Optical coherence tomography of the retina and optic nerve - a review. Clin Experiment Ophthalmol 2009 Jan;37(1):90-9.

(277) van Velthoven ME, Faber DJ, Verbraak FD, van Leeuwen TG, de Smet MD. Recent developments in optical coherence tomography for imaging the retina. Prog Retin Eye Res 2007 Jan;26(1):57-77.

(278) de Boer JF. Spectral/Fourier Domain Optical Coherence Tomography. In: Drexler W, Fujimoto JG, editors. Optical coherence tomography technology and applications. Springer; 2008. p. 147-75.

(279) Wojtkowski M, Leitgeb R, Kowalczyk A, Bajraszewski T, Fercher AF. In vivo human retinal imaging by Fourier domain optical coherence tomography. J Biomed Opt 2002 Jul;7(3):457-63.

(280) Huang Y, Cideciyan AV, Papastergiou GI, Banin E, Semple-Rowland SL, Milam AH, et al. Relation of optical coherence tomography to microanatomy in normal and rd chickens. Invest Ophthalmol Vis Sci 1998 Nov;39(12):2405-16.

(281) Chen TC, Cense B, Miller JW, Rubin PA, Deschler DG, Gragoudas ES, et al. Histologic correlation of in vivo optical coherence tomography images of the human retina. Am J Ophthalmol 2006 Jun;141(6):1165-8.

(282) Anger EM, Unterhuber A, Hermann B, Sattmann H, Schubert C, Morgan JE, et al. Ultrahigh resolution optical coherence tomography of the monkey fovea. Identification of retinal sublayers by correlation with semithin histology sections. Exp Eye Res 2004 Jun;78(6):1117-25.

(283) Schuman JS, Hee MR, Puliafito CA, Wong C, Pedut-Kloizman T, Lin CP, et al. Quantification of nerve fiber layer thickness in normal and glaucomatous eyes using optical coherence tomography. Arch Ophthalmol 1995 May;113(5):586-96.

(284) Ishikawa H, Piette S, Liebmann JM, Ritch R. Detecting the inner and outer borders of the retinal nerve fiber layer using optical coherence tomography. Graefes Arch Clin Exp Ophthalmol 2002 May;240(5):362-71.

(285) Budenz DL, Anderson DR, Varma R, Schuman J, Cantor L, Savell J, et al. Determinants of normal retinal nerve fiber layer thickness measured by Stratus OCT. Ophthalmology 2007 Jun;114(6):1046-52.

(286) The Ocular Side-Effects of Vigabatin (Sabril) Information and Guidance for Screening. Royal College of Ophthalmologists, London, 2008, pp 5-6. 2010. 25-10-2010.
Ref Type: Internet Communication

(287) Harding GF, Spencer EL, Wild JM, Conway M, Bohn RL. Field-specific visual-evoked potentials: identifying field defects in vigabatrin-treated children. Neurology 2002 Apr 23;58(8):1261-5.

(288) Kim MJ, Lee EJ, Kim TW. Peripapillary retinal nerve fibre layer thickness profile in subjects with myopia measured using the Stratus optical coherence tomography. Br J Ophthalmol 2010 Jan;94(1):115-20.

(289) Kasperaviciute D, Catarino CB, Heinzen EL, Depondt C, Cavalleri GL, Caboclo LO, et al. Common genetic variation and susceptibility to partial epilepsies: a genome-wide association study. Brain 2010 Jul;133(Pt 7):2136-47.

(290) Berg AT, Berkovic SF, Brodie MJ, Buchhalter J, Cross JH, van Emde BW, et al. Revised terminology and concepts for organization of seizures and epilepsies: report of the ILAE Commission on Classification and Terminology, 2005-2009. Epilepsia 2010 Apr;51(4):676-85.

(291) Kwan P, Arzimanoglou A, Berg AT, Brodie MJ, Allen HW, Mathern G, et al. Definition of drug resistant epilepsy: consensus proposal by the ad hoc Task Force of the ILAE Commission on Therapeutic Strategies. Epilepsia 2010 Jun;51(6):1069-77.

(292) Kee C, Hwang JM. Optical coherence tomography in a patient with tobacco-alcohol amblyopia. Eye (Lond) 2008 Mar;22(3):469-70.

(293) Toledo J, Sepulcre J, Salinas-Alaman A, Garcia-Layana A, Murie-Fernandez M, Bejarano B, et al. Retinal nerve fiber layer atrophy is associated with physical and cognitive disability in multiple sclerosis. Mult Scler 2008 Aug;14(7):906-12.

(294) van Koolwijk LM, Despriet DD, Van Duijn CM, Oostra BA, van Swieten JC, de K, I, et al. Association of cognitive functioning with retinal nerve fiber layer thickness. Invest Ophthalmol Vis Sci 2009 Oct;50(10):4576-80.

(295) Jindahra P, Petrie A, Plant GT. Retrograde trans-synaptic retinal ganglion cell loss identified by optical coherence tomography. Brain 2009 Mar;132(Pt 3):628-34.

(296) Seidenberg M, Kelly KG, Parrish J, Geary E, Dow C, Rutecki P, et al. Ipsilateral and contralateral MRI volumetric abnormalities in chronic unilateral temporal lobe epilepsy and their clinical correlates. Epilepsia 2005 Mar;46(3):420-30.

(297) Concha L, Beaulieu C, Collins DL, Gross DW. White-matter diffusion abnormalities in temporal-lobe epilepsy with and without mesial temporal sclerosis. J Neurol Neurosurg Psychiatry 2009 Mar;80(3):312-9.

(298) Meng L, Xiang J, Kotecha R, Rose D, Zhao H, Zhao D, et al. White matter abnormalities in children and adolescents with temporal lobe epilepsy. Magn Reson Imaging 2010 Nov;28(9):1290-8.

(299) Bonilha L, Rorden C, Appenzeller S, Coan AC, Cendes F, Li LM. Gray matter atrophy associated with duration of temporal lobe epilepsy. Neuroimage 2006 Sep;32(3):1070-9.

(300) Natsume J, Bernasconi N, Andermann F, Bernasconi A. MRI volumetry of the thalamus in temporal, extratemporal, and idiopathic generalized epilepsy. Neurology 2003 Apr 22;60(8):1296-300.

(301) Fujikawa DG. Prolonged seizures and cellular injury: understanding the connection. Epilepsy Behav 2005 Dec;7 Suppl 3:S3-11.

(302) Toth Z, Yan XX, Haftoglou S, Ribak CE, Baram TZ. Seizure-induced neuronal injury: vulnerability to febrile seizures in an immature rat model. J Neurosci 1998 Jun 1;18(11):4285-94.

(303) Gennarelli TA, Thibault LE, Adams JH, Graham DI, Thompson CJ, Marcincin RP. Diffuse axonal injury and traumatic coma in the primate. Ann Neurol 1982 Dec;12(6):564-74.

(304) Nowomiejska K, Vonthein R, Paetzold J, Zagorski Z, Kardon R, Schiefer U. Comparison between semiautomated kinetic perimetry and conventional Goldmann manual kinetic perimetry in advanced visual field loss. Ophthalmology 2005 Aug;112(8):1343-54.

(305) Ramirez AM, Chaya CJ, Gordon LK, Giaconi JA. A comparison of semiautomated versus manual Goldmann kinetic perimetry in patients with visually significant glaucoma. J Glaucoma 2008 Mar;17(2):111-7.

(306) Kolling GH, Wabbels B. Kinetic perimetry in neuroophthalmological practice. Strabismus 2000 Sep;8(3):215.

(307) Trobe JD, Acosta PC, Shuster JJ, Krischer JP. An evaluation of the accuracy of community-based perimetry. Am J Ophthalmol 1980 Nov;90(5):654-60.

(308) Beck RW, Bergstrom TJ, Lichter PR. A clinical comparison of visual field testing with a new automated perimeter, the Humphrey Field Analyzer, and the Goldmann perimeter. Ophthalmology 1985 Jan;92(1):77-82.

(309) Day SJ, Altman DG. Statistics notes: blinding in clinical trials and other studies. BMJ 2000 Aug 19;321(7259):504.

(310) Manji H, Plant GT. Epilepsy surgery, visual fields, and driving: a study of the visual field criteria for driving in patients after temporal lobe epilepsy surgery with a comparison of Goldmann and Esterman perimetry. J Neurol Neurosurg Psychiatry 2000 Jan;68(1):80-2.

(311) Johnson CA, Keltner JL. Optimal rates of movement for kinetic perimetry. Arch Ophthalmol 1987 Jan;105(1):73-5.

(312) Haag-Streit International. Original Goldmann Perimeter 940 Instructions for use. 1950. Switzerland, Haag-Streit International.
Ref Type: Pamphlet

(313) Greve EL, Groothuyse MT, Verduin WM. Automation of perimetry. Doc Ophthalmol 1976 Mar 31;40(2):243-54.

(314) Cooper SA, Metcalfe RA. Assess and interpret the visual fields at the bedside. Pract Neurol 2009 Dec;9(6):324-34.

(315) Ohkubo H. Visual field in hysteria-reliability of visual field by Goldmann perimetry. Doc Ophthalmol 1989 Jan;71(1):61-7.

(316) Sorri I. Effects of antiepileptic drugs on visual function, with special reference to Vigabatrin. Acta Ophthalmol Scand 2002 Jun;80(3):343-4.

(317) Shrout PE, Fleiss JL. Intraclass correlations: uses in assessing rater reliability. Psychol Bull 1979 Mar;86(2):420-8.

(318) Viera AJ, Garrett JM. Understanding interobserver agreement: the kappa statistic. Fam Med 2005 May;37(5):360-3.

(319) Petrie A, Sabin C. Medical Statistics at a Glance. Second ed. 2005.

(320) Wolfs RC, Grobbee DE, Hofman A, de Jong PT. Risk of acute angle-closure glaucoma after diagnostic mydriasis in nonselected subjects: the Rotterdam Study. Invest Ophthalmol Vis Sci 1997 Nov;38(12):2683-7.

(321) Savini G, Carbonelli M, Parisi V, Barboni P. Effect of pupil dilation on retinal nerve fibre layer thickness measurements and their repeatability with Cirrus HD-OCT. Eye (Lond) 2010 Sep;24(9):1503-8.

(322) Zafar S, Gurses-Ozden R, Vessani R, Makornwattana M, Liebmann JM, Tello C, et al. Effect of pupillary dilation on retinal nerve fiber layer thickness measurements using optical coherence tomography. J Glaucoma 2004 Feb;13(1):34-7.

(323) Savini G, Zanini M, Barboni P. Influence of pupil size and cataract on retinal nerve fiber layer thickness measurements by Stratus OCT. J Glaucoma 2006 Aug;15(4):336-40.

(324) Schuman JS, Pedut-Kloizman T, Hertzmark E, Hee MR, Wilkins JR, Coker JG, et al. Reproducibility of nerve fiber layer thickness measurements using optical coherence tomography. Ophthalmology 1996 Nov;103(11):1889-98.

(325) Carpineto P, Ciancaglini M, Zuppardi E, Falconio G, Doronzo E, Mastropasqua L. Reliability of nerve fiber layer thickness measurements using optical coherence tomography in normal and glaucomatous eyes. Ophthalmology 2003 Jan;110(1):190-5.

(326) Cense B, Chen TC, Park BH, Pierce MC, de Boer JF. Thickness and birefringence of healthy retinal nerve fiber layer tissue measured with polarization-sensitive optical coherence tomography. Invest Ophthalmol Vis Sci 2004 Aug;45(8):2606-12.

(327) Gabriele ML, Ishikawa H, Wollstein G, Bilonick RA, Townsend KA, Kagemann L, et al. Optical coherence tomography scan circle location and mean retinal nerve fiber layer measurement variability. Invest Ophthalmol Vis Sci 2008 Jun;49(6):2315-21.

(328) Stein DM, Ishikawa H, Hariprasad R, Wollstein G, Noecker RJ, Fujimoto JG, et al. A new quality assessment parameter for optical coherence tomography. Br J Ophthalmol 2006 Feb;90(2):186-90.

(329) Samarawickrama C, Pai A, Huynh SC, Burlutsky G, Wong TY, Mitchell P. Influence of OCT signal strength on macular, optic nerve head, and retinal nerve fiber layer parameters. Invest Ophthalmol Vis Sci 2010 Sep;51(9):4471-5.

(330) Cheung CY, Leung CK, Lin D, Pang CP, Lam DS. Relationship between retinal nerve fiber layer measurement and signal strength in optical coherence tomography. Ophthalmology 2008 Aug;115(8):1347-51, 1351.

(331) Lumbroso B, Rispoli M. Guide toInterpreting Spectral Domain Optical Coherence Tomography. 2011.

Ref Type: Online Source

(332) Krivoy D, Harizman N, Tello C, Liebmann J. Clinical Applications of Optical Coherence Tomography in Glaucoma. In: Arevalo JF, editor. Retinal Angiography and Optical Coherence Tomography.New York: Springer Science and Business Media, LLC; 2009. p. 311-36.

(333) Ray WA, O'Day DM. Statistical analysis of multi-eye data in ophthalmic research. Invest Ophthalmol Vis Sci 1985 Aug;26(8):1186-8.

(334) Murdoch IE, Morris SS, Cousens SN. People and eyes: statistical approaches in ophthalmology. Br J Ophthalmol 1998 Aug;82(8):971-3.

(335) Mwanza JC, Durbin MK, Budenz DL. Interocular Symmetry in Peripapillary Retinal Nerve Fiber Layer Thickness Measured with the Cirrus HD-OCT in Healthy Eyes. Am J Ophthalmol 2011 Jan 12.

(336) Knight OJ, Chang RT, Feuer WJ, Budenz DL. Comparison of retinal nerve fiber layer measurements using time domain and spectral domain optical coherent tomography. Ophthalmology 2009 Jul;116(7):1271-7.

(337) Parrish RK, Schiffman J, Anderson DR. Static and kinetic visual field testing. Reproducibility in normal volunteers. Arch Ophthalmol 1984 Oct;102(10):1497-502.

(338) Wild JM, Searle AE, Dengler-Harles M, O'Neill EC. Long-term follow-up of baseline learning and fatigue effects in the automated perimetry of glaucoma and ocular hypertensive patients. Acta Ophthalmol (Copenh) 1991 Apr;69(2):210-6.

(339) Becker ST, Vonthein R, Volpe NJ, Schiefer U. Factors influencing reaction time during automated kinetic perimetry on the Tubingen computer campimeter. Invest Ophthalmol Vis Sci 2005 Jul;46(7):2633-8.

(340) Kutzko KE, Brito CF, Wall M. Effect of instructions on conventional automated perimetry. Invest Ophthalmol Vis Sci 2000 Jun;41(7):2006-13.

(341) Ross DF, Fishman GA, Gilbert LD, Anderson RJ. Variability of visual field measurements in normal subjects and patients with retinitis pigmentosa. Arch Ophthalmol 1984 Jul;102(7):1004-10.

(342) Hessen E, Lossius MI, Reinvang I, Gjerstad L. Influence of major antiepileptic drugs on attention, reaction time, and speed of information processing: results from a randomized, double-blind, placebo-controlled withdrawal study of seizure-free epilepsy patients receiving monotherapy. Epilepsia 2006 Dec;47(12):2038-45.

(343) Aldenkamp AP. Effects of antiepileptic drugs on cognition. Epilepsia 2001;42 Suppl 1:46-9, discussion.

(344) Meador KJ. Cognitive outcomes and predictive factors in epilepsy. Neurology 2002 Apr 23;58(8 Suppl 5):S21-S26.

(345) Berry V, Drance SM, Wiggins RL. An evaluation of differences between two observers plotting and measuring visual fields. Can J Ophthalmol 1966 Oct;1(4):297-300.

(346) Vizzeri G, Weinreb RN, Gonzalez-Garcia AO, Bowd C, Medeiros FA, Sample PA, et al. Agreement between spectral-domain and time-domain OCT for measuring RNFL thickness. Br J Ophthalmol 2009 Jun;93(6):775-81.

(347) Budenz DL, Fredette MJ, Feuer WJ, Anderson DR. Reproducibility of peripapillary retinal nerve fiber thickness measurements with stratus OCT in glaucomatous eyes. Ophthalmology 2008 Apr;115(4):661-6.

(348) Hood DC, Kardon RH. A framework for comparing structural and functional measures of glaucomatous damage. Prog Retin Eye Res 2007 Nov;26(6):688-710.

(349) Harwerth RS, Vilupuru AS, Rangaswamy NV, Smith EL, III. The relationship between nerve fiber layer and perimetry measurements. Invest Ophthalmol Vis Sci 2007 Feb;48(2):763-73.

(350) Yoo C, Suh IH, Kim YY. The influence of eccentric scanning of optical coherence tomography on retinal nerve fiber layer analysis in normal subjects. Ophthalmologica 2009;223(5):326-32.

(351) Wall M, Woodward KR, Brito CF. The effect of attention on conventional automated perimetry and luminance size threshold perimetry. Invest Ophthalmol Vis Sci 2004 Jan;45(1):342-50.

(352) Wallace DK, El-Dairi M, Freedman SF. Technological advances in pediatric eye care. Arch Ophthalmol 2009 Jun;127(6):805-6.

(353) Yeh EA, Weinstock-Guttman B, Lincoff N, Reynolds J, Weinstock A, Madurai N, et al. Retinal nerve fiber thickness in inflammatory demyelinating diseases of childhood onset. Mult Scler 2009 Jul;15(7):802-10.

(354) El-Dairi MA, Holgado S, Asrani SG, Enyedi LB, Freedman SF. Correlation between optical coherence tomography and glaucomatous optic nerve head damage in children. Br J Ophthalmol 2009 Oct;93(10):1325-30.

(355) Chavala SH, Farsiu S, Maldonado R, Wallace DK, Freedman SF, Toth CA. Insights into advanced retinopathy of prematurity using handheld spectral domain optical coherence tomography imaging. Ophthalmology 2009 Dec;116(12):2448-56.

(356) Vinekar A, Sivakumar M, Shetty R, Mahendradas P, Krishnan N, Mallipatna A, et al. A novel technique using spectral-domain optical coherence tomography (Spectralis, SD-OCT+HRA) to image supine non-anaesthetized infants: utility demonstrated in aggressive posterior retinopathy of prematurity. Eye (Lond) 2010 Feb;24(2):379-82.

(357) Scott AW, Farsiu S, Enyedi LB, Wallace DK, Toth CA. Imaging the infant retina with a hand-held spectral-domain optical coherence tomography device. Am J Ophthalmol 2009 Feb;147(2):364-73.

(358) El-Dairi MA, Asrani SG, Enyedi LB, Freedman SF. Optical coherence tomography in the eyes of normal children. Arch Ophthalmol 2009 Jan;127(1):50-8.

(359) Willmore LJ, Abelson MB, Ben-Menachem E, Pellock JM, Shields WD. Vigabatrin: 2008 update. Epilepsia 2009 Feb;50(2):163-73.

(360) Pantcheva MB, Wollstein G, Ishikawa H, Noecker RJ, Schuman JS. Optical coherence tomography algorithm failure to detect nerve fibre layer defects: report of two cases. Br J Ophthalmol 2009 Sep;93(9):1141-2, 1185.

(361) Vizzeri G, Bowd C, Medeiros FA, Weinreb RN, Zangwill LM. Effect of improper scan alignment on retinal nerve fiber layer thickness measurements using Stratus optical coherence tomograph. J Glaucoma 2008 Aug;17(5):341-9.

(362) Varma R, Skaf M, Barron E. Retinal nerve fiber layer thickness in normal human eyes. Ophthalmology 1996 Dec;103(12):2114-9.

(363) Leung CK, Cheung CY, Weinreb RN, Qiu Q, Liu S, Li H, et al. Retinal nerve fiber layer imaging with spectral-domain optical coherence tomography: a variability and diagnostic performance study. Ophthalmology 2009 Jul;116(7):1257-63, 1263.

(364) Hood DC, Anderson SC, Wall M, Kardon RH. Structure versus function in glaucoma: an application of a linear model. Invest Ophthalmol Vis Sci 2007 Aug;48(8):3662-8.

(365) Ito Y, Nakamura M, Yamakoshi T, Lin J, Yatsuya H, Terasaki H. Reduction of inner retinal thickness in patients with autosomal dominant optic atrophy associated with OPA1 mutations. Invest Ophthalmol Vis Sci 2007 Sep;48(9):4079-86.

(366) Deleon-Ortega J, Carroll KE, Arthur SN, Girkin CA. Correlations between retinal nerve fiber layer and visual field in eyes with nonarteritic anterior ischemic optic neuropathy. Am J Ophthalmol 2007 Feb;143(2):288-94.

(367) Trip SA, Schlottmann PG, Jones SJ, Altmann DR, Garway-Heath DF, Thompson AJ, et al. Retinal nerve fiber layer axonal loss and visual dysfunction in optic neuritis. Ann Neurol 2005 Sep;58(3):383-91.

(368) Costello F, Coupland S, Hodge W, Lorello GR, Koroluk J, Pan YI, et al. Quantifying axonal loss after optic neuritis with optical coherence tomography. Ann Neurol 2006 Jun;59(6):963-9.

(369) Petzold A, de Boer JF, Schippling S, Vermersch P, Kardon R, Green A, et al. Optical coherence tomography in multiple sclerosis: a systematic review and meta-analysis. Lancet Neurol 2010 Sep;9(9):921-32.

(370) Levin LA, Gordon LK. Retinal ganglion cell disorders: types and treatments. Prog Retin Eye Res 2002 Sep;21(5):465-84.

(371) Newman NM, Stevens RA, Heckenlively JR. Nerve fibre layer loss in diseases of the outer retinal layer. Br J Ophthalmol 1987 Jan;71(1):21-6.

(372) Stone JL, Barlow WE, Humayun MS, de Juan E Jr, Milam AH. Morphometric analysis of macular photoreceptors and ganglion cells in retinas with retinitis pigmentosa. Arch Ophthalmol 1992 Nov;110(11):1634-9.

(373) Marshall J, Heckenlively JR. Pathologic findings and putative mechanisms in retinitis pigmentosa. In: Heckenlively JR, editor. Retinitis Pigmentosa.Philadelphia: JB Lippincott; 1988. p. 37-67.

(374) Oishi A, Otani A, Sasahara M, Kurimoto M, Nakamura H, Kojima H, et al. Retinal nerve fiber layer thickness in patients with retinitis pigmentosa. Eye (Lond) 2009 Mar;23(3):561-6.

(375) Walia S, Fishman GA, Edward DP, Lindeman M. Retinal nerve fiber layer defects in RP patients. Invest Ophthalmol Vis Sci 2007 Oct;48(10):4748-52.

(376) Walia S, Fishman GA. Retinal nerve fiber layer analysis in RP patients using Fourier-domain OCT. Invest Ophthalmol Vis Sci 2008 Aug;49(8):3525-8.

(377) Pasadhika S, Fishman GA, Allikmets R, Stone EM. Peripapillary retinal nerve fiber layer thinning in patients with autosomal recessive cone-rod dystrophy. Am J Ophthalmol 2009 Aug;148(2):260-5.

(378) Barnes EM, Jr. Use-dependent regulation of GABAA receptors. Int Rev Neurobiol 1996;39:53-76.

(379) Pallant J. SPSS Survival Manual. Third ed. London: Open University Press; 2007.

(380) Osborne JW, Overbay A. The power of outliers (any why researchers should always check for them). Practical Assessment, Research and Evaluation 2004;9(6).

(381) Faught E, Duh MS, Weiner JR, Guerin A, Cunnington MC. Nonadherence to antiepileptic drugs and increased mortality: findings from the RANSOM Study. Neurology 2008 Nov 11;71(20):1572-8.

(382) Song WK, Lee SC, Lee ES, Kim CY, Kim SS. Macular thickness variations with sex, age, and axial length in healthy subjects: a spectral domain-optical coherence tomography study. Invest Ophthalmol Vis Sci 2010;51(8):3913-8.

(383) Wong AC, Chan CW, Hui SP. Relationship of gender, body mass index, and axial length with central retinal thickness using optical coherence tomography. Eye (Lond) 2005;19(3):292-7.

(384) Wagner-Schuman M, Dubis AM, Nordgren RN, Lei Y, Odell D, Chiao H, et al. Race- and sex-related differences in retinal thickness and foveal pit morphology. Invest Ophthalmol Vis Sci 2011;52(1):625-34.

(385) Kilic A, Altintas O, Yuksel N, Altintas L, Celik M, Caglar Y. Optical coherence tomography measurment of retinal nerve fibre layer, optic nerve head and macula in normal subjects. Neuro-ophthamology 2010;34(1):36-44.

(386) Varma R, Bazzaz S, Lai M. Optical tomography-measured retinal nerve fiber layer thickness in normal latinos. Invest Ophthalmol Vis Sci 2003 Aug;44(8):3369-73.

(387) Sony P, Sihota R, Tewari HK, Venkatesh P, Singh R. Quantification of the retinal nerve fibre layer thickness in normal Indian eyes with optical coherence tomography. Indian J Ophthalmol 2004 Dec;52(4):303-9.

(388) Bowd C, Zangwill LM, Blumenthal EZ, Vasile C, Boehm AG, Gokhale PA, et al. Imaging of the optic disc and retinal nerve fiber layer: the effects of age, optic disc area, refractive error, and gender. J Opt Soc Am A Opt Image Sci Vis 2002 Jan;19(1):197-207.

(389) Kanno M, Nagasawa M, Suzuki M, Yamashita H. Peripapillary retinal nerve fiber layer thickness in normal Japanese eyes measured with optical coherence tomography. Jpn J Ophthalmol 2010 Jan;54(1):36-42.

(390) Parikh RS, Parikh SR, Sekhar GC, Prabakaran S, Babu JG, Thomas R. Normal age-related decay of retinal nerve fiber layer thickness. Ophthalmology 2007 May;114(5):921-6.

(391) Guedes V, Schuman JS, Hertzmark E, Wollstein G, Correnti A, Mancini R, et al. Optical coherence tomography measurement of macular and nerve fiber layer thickness in normal and glaucomatous human eyes. Ophthalmology 2003 Jan;110(1):177-89.

(392) Bendschneider D, Tornow RP, Horn FK, Laemmer R, Roessler CW, Juenemann AG, et al. Retinal nerve fiber layer thickness in normals measured by spectral domain OCT. J Glaucoma 2010 Sep;19(7):475-82.

(393) Hougaard JL, Kessel L, Sander B, Kyvik KO, Sorensen TI, Larsen M. Evaluation of heredity as a determinant of retinal nerve fiber layer thickness as measured by optical coherence tomography. Invest Ophthalmol Vis Sci 2003 Jul;44(7):3011-6.

(394) Ravizza T, Friedman LK, Moshe SL, Veliskova J. Sex differences in GABA(A)ergic system in rat substantia nigra pars reticulata. Int J Dev Neurosci 2003 Aug;21(5):245-54.

(395) Frankfurt M, Fuchs E, Wuttke W. Sex differences in gamma-aminobutyric acid and glutamate concentrations in discrete rat brain nuclei. Neurosci Lett 1984 Sep 7;50(1-3):245-50.

(396) Manev H, Pericic D. Sex difference in the turnover of GABA in the rat substantia nigra. J Neural Transm 1987;70(3-4):321-8.

(397) Chudomel O, Herman H, Nair K, Moshe SL, Galanopoulou AS. Age- and gender-related differences in GABAA receptor-mediated postsynaptic currents in GABAergic neurons of the substantia nigra reticulata in the rat. Neuroscience 2009 Sep 29;163(1):155-67.

(398) Quigley HA, Dunkelberger GR, Green WR. Retinal ganglion cell atrophy correlated with automated perimetry in human eyes with glaucoma. Am J Ophthalmol 1989 May 15;107(5):453-64.

(399) Balazsi AG, Rootman J, Drance SM, Schulzer M, Douglas GR. The effect of age on the nerve fiber population of the human optic nerve. Am J Ophthalmol 1984 Jun;97(6):760-6.

(400) Dolman CL, McCormick AQ, Drance SM. Aging of the optic nerve. Arch Ophthalmol 1980 Nov;98(11):2053-8.

(401) Alamouti B, Funk J. Retinal thickness decreases with age: an OCT study. Br J Ophthalmol 2003 Jul;87(7):899-901.

(402) Sung KR, Wollstein G, Bilonick RA, Townsend KA, Ishikawa H, Kagemann L, et al. Effects of age on optical coherence tomography measurements of healthy retinal nerve fiber layer, macula, and optic nerve head. Ophthalmology 2009 Jun;116(6):1119-24.

(403) Hirsch E. Outer retinal dysfunction in patients treated with vigabatrin. Neurology 2000 Mar 28;54(6):1396.

(404) Sorri I, Rissanen E, Mantyjarvi M, Kalviainen R. Visual function in epilepsy patients treated with initial valproate monotherapy. Seizure 2005 Sep;14(6):367-70.

(405) Ozkul Y, Gurler B, Uckardes A, Bozlar S. Visual functions in epilepsy patients on valproate monotherapy. J Clin Neurosci 2002 May;9(3):247-50.

(406) Nau H, Loscher W. Valproic acid: brain and plasma levels of the drug and its metabolites, anticonvulsant effects and gamma-aminobutyric acid (GABA) metabolism in the mouse. J Pharmacol Exp Ther 1982 Mar;220(3):654-9.

(407) Johannessen CU. Mechanisms of action of valproate: a commentatory. Neurochem Int 2000 Aug;37(2-3):103-10.

(408) Jeelani NU, Jindahra P, Tamber MS, Poon TL, Kabasele P, James-Galton M, et al. 'Hemispherical asymmetry in the Meyer's Loop': a prospective study of visual-field deficits in 105 cases undergoing anterior temporal lobe resection for epilepsy. J Neurol Neurosurg Psychiatry 2010 Sep;81(9):985-91.

(409) van Baarsen KM, Porro GL, Wittebol-Post D. Epilepsy surgery provides new insights in retinotopic organization of optic radiations. A systematic review. Curr Opin Ophthalmol 2009 Nov;20(6):490-4.

(410) Bridge H, Jindahra P, Barbur JL, Plant G. Imaging reveals optic tract degeneration in hemianopia. Invest Ophthalmol Vis Sci 2010 Aug 25.

(411) Frisen L. Quadruple sectoranopia and sectorial optic atrophy: a syndrome of the distal anterior choroidal artery. J Neurol Neurosurg Psychiatry 1979 Jul;42(7):590-4.

(412) Miller NR, Newman SA. Transsynaptic degeneration. Arch Ophthalmol 1981 Sep;99(9):1654.

(413) Sachdev MS, Kumar H, Jain AK, Goulatia RK, Misra NK. Transsynaptic neuronal degeneration of optic nerves associated with bilateral occipital lesions. Indian J Ophthalmol 1990 Oct;38(4):151-2.

(414) Beatty RM, Sadun AA, Smith L, Vonsattel JP, Richardson EP, Jr. Direct demonstration of transsynaptic degeneration in the human visual system: a comparison of retrograde and anterograde changes. J Neurol Neurosurg Psychiatry 1982 Feb;45(2):143-6.

(415) HADDOCK JN, BERLIN L. Transsynaptic degeneration in the visual system; report of a case. Arch Neurol Psychiatry 1950 Jul;64(1):66-73.

(416) Fletcher WA, Hoyt WF, Narahara MH. Congenital quadrantanopia with occipital lobe ganglioglioma. Neurology 1988 Dec;38(12):1892-4.

(417) VANBUREN JM. TRANS-SYNAPTIC RETROGRADE DEGENERATION IN THE VISUAL SYSTEM OF PRIMATES. J Neurol Neurosurg Psychiatry 1963 Oct;26:402-9.

(418) Cowey A, Stoerig P, Williams C. Variance in transneuronal retrograde ganglion cell degeneration in monkeys after removal of striate cortex: effects of size of the cortical lesion. Vision Res 1999 Oct;39(21):3642-52.

(419) Johnson H, Cowey A. Transneuronal retrograde degeneration of retinal ganglion cells following restricted lesions of striate cortex in the monkey. Exp Brain Res 2000 May;132(2):269-75.

(420) Mehta JS, Plant GT. Optical coherence tomography (OCT) findings in congenital/long-standing homonymous hemianopia. Am J Ophthalmol 2005 Oct;140(4):727-9.

(421) Jindahra P, Plant GT, Petrie A. Demonstration of the time course of retrograde trans-synaptic degeneration in the visual system using optical coherence tomography. J.Neurol.Neurosurg.Psychiatry 81, 23-24. 2010.
Ref Type: Abstract

(422) van Koolwijk LM, Despriet DD, Van Duijn CM, Pardo Cortes LM, Vingerling JR, Aulchenko YS, et al. Genetic contributions to glaucoma: heritability of intraocular pressure, retinal nerve fiber layer thickness, and optic disc morphology. Invest Ophthalmol Vis Sci 2007 Aug;48(8):3669-76.

(423) Curcio CA, Allen KA. Topography of ganglion cells in human retina. J Comp Neurol 1990 Oct 1;300(1):5-25.

(424) Johnson BM, Miao M, Sadun AA. Age-related decline of human optic nerve axon populations. Age 1987;10(1):5-9.

(425) Repka MX, Quigley HA. The effect of age on normal human optic nerve fiber number and diameter. Ophthalmology 1989 Jan;96(1):26-32.

(426) Hood DC, Anderson SC, Wall M, Raza AS, Kardon RH. A test of a linear model of glaucomatous structure-function loss reveals sources of variability in retinal nerve fiber and visual field measurements. Invest Ophthalmol Vis Sci 2009 Sep;50(9):4254-66.

(427) Schulze TG, McMahon FJ. Defining the phenotype in human genetic studies: forward genetics and reverse phenotyping. Hum Hered 2004;58(3-4):131-8.

(428) Craddock N, Kendler K, Neale M, Nurnberger J, Purcell S, Rietschel M, et al. Dissecting the phenotype in genome-wide association studies of psychiatric illness. Br J Psychiatry 2009 Aug;195(2):97-9.

(429) Lundbeck; Support, Help and Resources for Epilepsy (SHARE). http://www lundbeckshare com/ 2010 [cited 2010 Aug 1];

(430) Quigley HA, Addicks EM. Quantitative studies of retinal nerve fiber layer defects. Arch Ophthalmol 1982 May;100(5):807-14.

(431) Sommer A, Quigley HA, Robin AL, Miller NR, Katz J, Arkell S. Evaluation of nerve fiber layer assessment. Arch Ophthalmol 1984 Dec;102(12):1766-71.

(432) Hoyt WF, Frisen L, Newman NM. Fundoscopy of nerve fiber layer defects in glaucoma. Invest Ophthalmol 1973;12(11):814-29.

(433) United States Food and Drug Administration 2009. http://www fda gov/NewsEvents/Newsroom/PressAnnouncements/ucm179855 htm 2009 [cited 2009 Oct 5];

(434) Leung CK, Choi N, Weinreb RN, Liu S, Ye C, Liu L, et al. Retinal nerve fiber layer imaging with spectral-domain optical coherence tomography: pattern of RNFL defects in glaucoma. Ophthalmology 2010 Dec;117(12):2337-44.

(435) Radius RL, Anderson DR. The histology of retinal nerve fiber layer bundles and bundle defects. Arch Ophthalmol 1979 May;97(5):948-50.

(436) Stone J, Johnston E. The topography of primate retina: a study of the human, bushbaby, and new- and old-world monkeys. J Comp Neurol 1981 Feb 20;196(2):205-23.

(437) Hebel R, Hollander H. Size and distribution of ganglion cells in the human retina. Anat Embryol (Berl) 1983;168(1):125-36.

(438) Bunt AH, Hendrickson AE, Lund JS, Lund RD, Fuchs AF. Monkey retinal ganglion cells: morphometric analysis and tracing of axonal projections, with a consideration of the peroxidase technique. J Comp Neurol 1975 Dec 1;164(3):265-85.

(439) Dacey DM, Petersen MR. Dendritic field size and morphology of midget and parasol ganglion cells of the human retina. Proc Natl Acad Sci U S A 1992 Oct 15;89(20):9666-70.

(440) Rodieck RW, Binmoeller KF, Dineen J. Parasol and midget ganglion cells of the human retina. J Comp Neurol 1985 Mar 1;233(1):115-32.

(441) Ivanov D, Dvoriantchikova G, Barakat DJ, Nathanson L, Shestopalov VI. Differential gene expression profiling of large and small retinal ganglion cells. J Neurosci Methods 2008 Sep 15;174(1):10-7.

(442) Glovinsky Y, Quigley HA, Dunkelberger GR. Retinal ganglion cell loss is size dependent in experimental glaucoma. Invest Ophthalmol Vis Sci 1991 Mar;32(3):484-91.

(443) Glovinsky Y, Quigley HA, Pease ME. Foveal ganglion cell loss is size dependent in experimental glaucoma. Invest Ophthalmol Vis Sci 1993 Feb;34(2):395-400.

(444) Morgan JE, Uchida H, Caprioli J. Retinal ganglion cell death in experimental glaucoma. Br J Ophthalmol 2000 Mar;84(3):303-10.

(445) Luo XG, Chiu K, Lau FH, Lee VW, Yung KK, So KF. The selective vulnerability of retinal ganglion cells in rat chronic ocular hypertension model at early phase. Cell Mol Neurobiol 2009 Dec;29(8):1143-51.

(446) Dreyer EB, Pan ZH, Storm S, Lipton SA. Greater sensitivity of larger retinal ganglion cells to NMDA-mediated cell death. Neuroreport 1994 Jan 31;5(5):629-31.

(447) Vorwerk CK, Kreutz MR, Bockers TM, Brosz M, Dreyer EB, Sabel BA. Susceptibility of retinal ganglion cells to excitotoxicity depends on soma size and retinal eccentricity. Curr Eye Res 1999 Jul;19(1):59-65.

(448) Dandona L, Hendrickson A, Quigley HA. Selective effects of experimental glaucoma on axonal transport by retinal ganglion cells to the dorsal lateral geniculate nucleus. Invest Ophthalmol Vis Sci 1991 Apr;32(5):1593-9.

(449) Hanitzsch R, Kuppers L. The effects of GABA and vigabatrin on horizontal cell responses to light and the effect of vigabatrin on the electroretinogram. Doc Ophthalmol 2002 Nov;105(3):313-26.

(450) Sarthy PV, Lam DM. Biochemical studies of isolated glial (Muller) cells from the turtle retina. J Cell Biol 1978 Sep;78(3):675-84.

(451) Pow DV. Differences in cellular sites of accumulation of vigabatrin in central versus peripheral primate retina. 2000.

(452) Reichenbach A, Robinson SR. Phylogenetic constraintson retinal organisation and development. Prog Retin Eye Res 1995;15(1):139-71.

(453) Distler C, Dreher Z. Glia cells of the monkey retina--II. Muller cells. Vision Res 1996 Aug;36(16):2381-94.

(454) Bringmann A, Pannicke T, Grosche J, Francke M, Wiedemann P, Skatchkov SN, et al. Muller cells in the healthy and diseased retina. Prog Retin Eye Res 2006 Jul;25(4):397-424.

(455) Distler C, Kopatz K. Macroglia cells of the macaque monkey retina. Rev Bras Biol 1996 Dec;56 Su 1 Pt 1:53-67.

(456) Izumi Y, Kirby CO, Benz AM, Olney JW, Zorumski CF. Muller cell swelling, glutamate uptake, and excitotoxic neurodegeneration in the isolated rat retina. Glia 1999 Feb 15;25(4):379-89.

(457) Kawasaki A, Otori Y, Barnstable CJ. Muller cell protection of rat retinal ganglion cells from glutamate and nitric oxide neurotoxicity. Invest Ophthalmol Vis Sci 2000 Oct;41(11):3444-50.

(458) Heidinger V, Hicks D, Sahel J, Dreyfus H. Ability of retinal Muller glial cells to protect neurons against excitotoxicity in vitro depends upon maturation and neuron-glial interactions. Glia 1999 Feb 1;25(3):229-39.

(459) Kitano S, Morgan J, Caprioli J. Hypoxic and excitotoxic damage to cultured rat retinal ganglion cells. Exp Eye Res 1996 Jul;63(1):105-12.

(460) van Adel BA, Arnold JM, Phipps J, Doering LC, Ball AK. Ciliary neurotrophic factor protects retinal ganglion cells from axotomy-induced apoptosis via modulation of retinal glia in vivo. J Neurobiol 2005 Jun;63(3):215-34.

(461) Newman E, Reichenbach A. The Muller cell: a functional element of the retina. Trends Neurosci 1996 Aug;19(8):307-12.

(462) Izumi Y, Shimamoto K, Benz AM, Hammerman SB, Olney JW, Zorumski CF. Glutamate transporters and retinal excitotoxicity. Glia 2002 Jul;39(1):58-68.

(463) Dreyer EB. A proposed role for excitotoxicity in glaucoma. J Glaucoma 1998 Feb;7(1):62-7.

(464) Osborne NN, Wood JP, Chidlow G, Bae JH, Melena J, Nash MS. Ganglion cell death in glaucoma: what do we really know? Br J Ophthalmol 1999 Aug;83(8):980-6.

(465) Ullian EM, Barkis WB, Chen S, Diamond JS, Barres BA. Invulnerability of retinal ganglion cells to NMDA excitotoxicity. Mol Cell Neurosci 2004 Aug;26(4):544-57.

(466) Lotery AJ. Glutamate excitotoxicity in glaucoma: truth or fiction? Eye (Lond) 2005 Apr;19(4):369-70.

(467) Tezel G, Wax MB. Increased production of tumor necrosis factor-alpha by glial cells exposed to simulated ischemia or elevated hydrostatic pressure induces apoptosis in cocultured retinal ganglion cells. J Neurosci 2000 Dec 1;20(23):8693-700.

(468) Kashiwagi K, Iizuka Y, Araie M, Suzuki Y, Tsukahara S. Effects of retinal glial cells on isolated rat retinal ganglion cells. Invest Ophthalmol Vis Sci 2001 Oct;42(11):2686-94.

(469) Calabresi PA, Balcer LJ, Frohman EM. Retinal pathology in multiple sclerosis: insight into the mechanisms of neuronal pathology. Brain 2010 Jun;133(Pt 6):1575-7.

(470) Miller N, Drachman DA. The optic nerve: a window into diseases of the brain? Neurology 2006 Nov 28;67(10):1742-3.

(471) Eye test that spots Alzheimer's 20 years before symptoms: Middle-aged could be screened at routine optician's visit. The Daily Mail . 2010. 10-11-2010.
Ref Type: Internet Communication

(472) Liu B, Rasool S, Yang Z, Glabe CG, Schreiber SS, Ge J, et al. Amyloid-peptide vaccinations reduce {beta}-amyloid plaques but exacerbate vascular deposition and inflammation in the retina of Alzheimer's transgenic mice. Am J Pathol 2009 Nov;175(5):2099-110.

(473) Blanks JC, Hinton DR, Sadun AA, Miller CA. Retinal ganglion cell degeneration in Alzheimer's disease. Brain Res 1989 Nov 6;501(2):364-72.

(474) Jindahra P, Hedges TR, Mendoza-Santiesteban CE, Plant GT. Optical coherence tomography of the retina: applications in neurology. Curr Opin Neurol 2010 Feb;23(1):16-23.

(475) Greenberg BM, Frohman E. Optical coherence tomography as a potential readout in clinical trials. Ther Adv Neurol Disord 2010 May;3(3):153-60.

(476) Lu Y, Li Z, Zhang X, Ming B, Jia J, Wang R, et al. Retinal nerve fiber layer structure abnormalities in early Alzheimer's disease: evidence in optical coherence tomography. Neurosci Lett 2010 Aug 9;480(1):69-72.

(477) Paquet C, Boissonnot M, Roger F, Dighiero P, Gil R, Hugon J. Abnormal retinal thickness in patients with mild cognitive impairment and Alzheimer's disease. Neurosci Lett 2007 Jun 13;420(2):97-9.

(478) Inzelberg R, Ramirez JA, Nisipeanu P, Ophir A. Retinal nerve fiber layer thinning in Parkinson disease. Vision Res 2004 Nov;44(24):2793-7.

(479) Fortuna F, Barboni P, Liguori R, Valentino ML, Savini G, Gellera C, et al. Visual system involvement in patients with Friedreich's ataxia. Brain 2009 Jan;132(Pt 1):116-23.

(480) Martinez A, Proupim N, Sanchez M. Retinal nerve fibre layer thickness measurements using optical coherence tomography in migraine patients. Br J Ophthalmol 2008 Aug;92(8):1069-75.

(481) Rufa A, Pretegiani E, Frezzotti P, De SN, Cevenini G, Dotti MT, et al. Retinal nerve fiber layer thinning in CADASIL: an optical coherence tomography and MRI study. Cerebrovasc Dis 2011;31(1):77-82.

(482) Henderson AP, Trip SA, Schlottmann PG, Altmann DR, Garway-Heath DF, Plant GT, et al. A preliminary longitudinal study of the retinal nerve fiber layer in progressive multiple sclerosis. J Neurol 2010 Jul;257(7):1083-91.

(483) Sepulcre J, Murie-Fernandez M, Salinas-Alaman A, Garcia-Layana A, Bejarano B, Villoslada P. Diagnostic accuracy of retinal abnormalities in predicting disease activity in MS. Neurology 2007 May 1;68(18):1488-94.

(484) Serbecic N, Aboul-Enein F, Beutelspacher SC, Graf M, Kircher K, Geitzenauer W, et al. Heterogeneous pattern of retinal nerve fiber layer in multiple sclerosis. High resolution optical coherence tomography: potential and limitations. PLoS One 2010;5(11):e13877.

(485) Bernhard MK, Glaser A, Ulrich K, Merkenschlager A. Is there a need for ophthalmological examinations after a first seizure in paediatric patients? Eur J Pediatr 2010 Jan;169(1):31-3.

(486) Beran RG, Currie J, Sandbach J, Plunkett M. Visual field restriction with new antiepileptic medication. Brain Nerve 39[Suppl 2], 6. 1998.
Ref Type: Abstract

(487) Kaufman KR, Lepore FE, Keyser BJ. Visual fields and tiagabine: a quandary. Seizure 2001 Oct;10(7):525-9.

(488) Suzdak PD, Jansen JA. A review of the preclinical pharmacology of tiagabine: a potent and selective anticonvulsant GABA uptake inhibitor. Epilepsia 1995 Jun;36(6):612-26.

(489) Lawden MC. Vigabatrin, tiagabine, and visual fields. J Neurol Neurosurg Psychiatry 2003 Mar;74(3):286.

(490) Crooks J, Kolb H. Localization of GABA, glycine, glutamate and tyrosine hydroxylase in the human retina. J Comp Neurol 1992;315(3):287-302.

(491) Bonilha L, Elm JJ, Edwards JC, Morgan PS, Hicks C, Lozar C, et al. How common is brain atrophy in patients with medial temporal lobe epilepsy? Epilepsia 2010 Sep;51(9):1774-9.

(492) Keller SS, Roberts N. Voxel-based morphometry of temporal lobe epilepsy: an introduction and review of the literature. Epilepsia 2008 May;49(5):741-57.

(493) Riley JD, Franklin DL, Choi V, Kim RC, Binder DK, Cramer SC, et al. Altered white matter integrity in temporal lobe epilepsy: association with cognitive and clinical profiles. Epilepsia 2010 Apr;51(4):536-45.

(494) Arfanakis K, Hermann BP, Rogers BP, Carew JD, Seidenberg M, Meyerand ME. Diffusion tensor MRI in temporal lobe epilepsy. Magn Reson Imaging 2002 Sep;20(7):511-9.

(495) Gross DW, Concha L, Beaulieu C. Extratemporal white matter abnormalities in mesial temporal lobe epilepsy demonstrated with diffusion tensor imaging. Epilepsia 2006 Aug;47(8):1360-3.

(496) Blanc F, Martinian L, Liagkouras I, Catarino C, Sisodiya SM, Thom M. Investigation of widespread neocortical pathology associated with hippocampal sclerosis in epilepsy: a postmortem study. Epilepsia 2011 Jan;52(1):10-21.

(497) McMillan AB, Hermann BP, Johnson SC, Hansen RR, Seidenberg M, Meyerand ME. Voxel-based morphometry of unilateral temporal lobe epilepsy reveals abnormalities in cerebral white matter. Neuroimage 2004 Sep;23(1):167-74.

(498) Meiners LC, van der GJ, van Rijen PC, Springorum R, de Kort GA, Jansen GH. Proton magnetic resonance spectroscopy of temporal lobe white matter in patients with histologically proven hippocampal sclerosis. J Magn Reson Imaging 2000 Jan;11(1):25-31.

(499) Coste S, Ryvlin P, Hermier M, Ostrowsky K, Adeleine P, Froment JC, et al. Temporopolar changes in temporal lobe epilepsy: a quantitative MRI-based study. Neurology 2002 Sep 24;59(6):855-61.

(500) Oyegbile TO, Bhattacharya A, Seidenberg M, Hermann BP. Quantitative MRI biomarkers of cognitive morbidity in temporal lobe epilepsy. Epilepsia 2006 Jan;47(1):143-52.

(501) Bernasconi N, Duchesne S, Janke A, Lerch J, Collins DL, Bernasconi A. Whole-brain voxel-based statistical analysis of gray matter and white matter in temporal lobe epilepsy. Neuroimage 2004 Oct;23(2):717-23.

(502) Yu A, Li K, Li L, Shan B, Wang Y, Xue S. Whole-brain voxel-based morphometry of white matter in medial temporal lobe epilepsy. Eur J Radiol 2008 Jan;65(1):86-90.

(503) Thivard L, Lehericy S, Krainik A, Adam C, Dormont D, Chiras J, et al. Diffusion tensor imaging in medial temporal lobe epilepsy with hippocampal sclerosis. Neuroimage 2005 Nov 15;28(3):682-90.

(504) Schoene-Bake JC, Faber J, Trautner P, Kaaden S, Tittgemeyer M, Elger CE, et al. Widespread affections of large fiber tracts in postoperative temporal lobe epilepsy. Neuroimage 2009 Jul 1;46(3):569-76.

(505) Diehl B, Busch RM, Duncan JS, Piao Z, Tkach J, Luders HO. Abnormalities in diffusion tensor imaging of the uncinate fasciculus relate to reduced memory in temporal lobe epilepsy. Epilepsia 2008 Aug;49(8):1409-18.

(506) Hermann BP, Seidenberg M, Bell B. The neurodevelopmental impact of childhood onset temporal lobe epilepsy on brain structure and function and the risk of progressive cognitive effects. Prog Brain Res 2002;135:429-38.

(507) Seidenberg M, Pulsipher DT, Hermann B. Cognitive progression in epilepsy. Neuropsychol Rev 2007 Dec;17(4):445-54.

(508) Dodrill CB. Neuropsychological effects of seizures. Epilepsy Behav 2004 Feb;5 Suppl 1:S21-S24.

(509) Thompson PJ, Duncan JS. Cognitive decline in severe intractable epilepsy. Epilepsia 2005 Nov;46(11):1780-7.

(510) Oyegbile TO, Dow C, Jones J, Bell B, Rutecki P, Sheth R, et al. The nature and course of neuropsychological morbidity in chronic temporal lobe epilepsy. Neurology 2004 May 25;62(10):1736-42.

(511) Vlooswijk MC, Jansen JF, de Krom MC, Majoie HM, Hofman PA, Backes WH, et al. Functional MRI in chronic epilepsy: associations with cognitive impairment. Lancet Neurol 2010 Oct;9(10):1018-27.

(512) Hermann BP, Lin JJ, Jones JE, Seidenberg M. The emerging architecture of neuropsychological impairment in epilepsy. Neurol Clin 2009 Nov;27(4):881-907.

(513) Catani M, ffytche DH. The rises and falls of disconnection syndromes. Brain 2005 Oct;128(Pt 10):2224-39.

(514) McDonald CR, Ahmadi ME, Hagler DJ, Tecoma ES, Iragui VJ, Gharapetian L, et al. Diffusion tensor imaging correlates of memory and language impairments in temporal lobe epilepsy. Neurology 2008 Dec 2;71(23):1869-76.

(515) Hermann B, Seidenberg M, Bell B, Rutecki P, Sheth RD, Wendt G, et al. Extratemporal quantitative MR volumetrics and neuropsychological status in temporal lobe epilepsy. J Int Neuropsychol Soc 2003 Mar;9(3):353-62.

(516) Kim CH, Koo BB, Chung CK, Lee JM, Kim JS, Lee SK. Thalamic changes in temporal lobe epilepsy with and without hippocampal sclerosis: a diffusion tensor imaging study. Epilepsy Res 2010 Jun;90(1-2):21-7.

(517) Dreifuss S, Vingerhoets FJ, Lazeyras F, Andino SG, Spinelli L, Delavelle J, et al. Volumetric measurements of subcortical nuclei in patients with temporal lobe epilepsy. Neurology 2001 Nov 13;57(9):1636-41.

(518) Focke NK, Yogarajah M, Bonelli SB, Bartlett PA, Symms MR, Duncan JS. Voxel-based diffusion tensor imaging in patients with mesial temporal lobe epilepsy and hippocampal sclerosis. Neuroimage 2008 Apr 1;40(2):728-37.

(519) Sergott RC, Frohman E, Glanzman R, Al-Sabbagh A. The role of optical coherence tomography in multiple sclerosis: expert panel consensus. J Neurol Sci 2007 Dec 15;263(1-2):3-14.

(520) Bertram EH. Temporal lobe epilepsy: where do the seizures really begin? Epilepsy Behav 2009 Jan;14 Suppl 1:32-7.

(521) Yasuda CL, Valise C, Saude AV, Pereira AR, Pereira FR, Ferreira Costa AL, et al. Dynamic changes in white and gray matter volume are associated with outcome of surgical treatment in temporal lobe epilepsy. Neuroimage 2010 Jan 1;49(1):71-9.

(522) Kroese M, Burton H, Vardy S, Rimmer T, McCarter D. Prevalence of primary open angle glaucoma in general ophthalmic practice in the United Kingdom. Br J Ophthalmol 2002 Sep;86(9):978-80.

(523) Winawer MR. Phenotype definition in epilepsy. Epilepsy Behav 2006 May;8(3):462-76.

(524) Samarawickrama C, Wang JJ, Huynh SC, Pai A, Burlutsky G, Rose KA, et al. Ethnic differences in optic nerve head and retinal nerve fibre layer thickness parameters in children. Br J Ophthalmol 2010 Jul;94(7):871-6.

(525) Huynh SC, Wang XY, Rochtchina E, Mitchell P. Peripapillary retinal nerve fiber layer thickness in a population of 6-year-old children: findings by optical coherence tomography. Ophthalmology 2006 Sep;113(9):1583-92.

(526) Racette L, Boden C, Kleinhandler SL, Girkin CA, Liebmann JM, Zangwill LM, et al. Differences in visual function and optic nerve structure between healthy eyes of blacks and whites. Arch Ophthalmol 2005 Nov;123(11):1547-53.

(527) Poinoosawmy D, Fontana L, Wu JX, Fitzke FW, Hitchings RA. Variation of nerve fibre layer thickness measurements with age and ethnicity by scanning laser polarimetry. Br J Ophthalmol 1997 May;81(5):350-4.

(528) Sinai MJ, Garway-Heath DF, Fingeret M, Varma R, Liggan B, Greenfield DS, et al. The Role of Ethnicity on the Retinal Nerve Fiber Layer and Optic Disc Area Measured With Fourier Domain Optical Coherence Tomography. Invest Ophthalmol.Vis.Sci. 50, 4785. 2009.

Ref Type: Abstract

(529) Ishikawa H, Gabriele ML, Wollstein G, Ferguson RD, Hammer DX, Paunescu LA, et al. Retinal nerve fiber layer assessment using optical coherence tomography with active optic nerve head tracking. Invest Ophthalmol Vis Sci 2006 Mar;47(3):964-7.

(530) Hood DC, Anderson S, Rouleau J, Wenick AS, Grover LK, Behrens MM, et al. Retinal nerve fiber structure versus visual field function in patients with ischemic optic neuropathy. A test of a linear model. Ophthalmology 2008 May;115(5):904-10.

(531) Sihota R, Sony P, Gupta V, Dada T, Singh R. Diagnostic capability of optical coherence tomography in evaluating the degree of glaucomatous retinal nerve fiber damage. Invest Ophthalmol Vis Sci 2006 May;47(5):2006-10.

(532) Quigley HA, Addicks EM, Green WR, Maumenee AE. Optic nerve damage in human glaucoma. II. The site of injury and susceptibility to damage. Arch Ophthalmol 1981 Apr;99(4):635-49.

(533) Le Gros Clark WE, Penman GG. The Projection of the Retina in the Lateral Geniculate Body. Proceedings of the Royal Society of London Series B, Containing Papers of a Biological Character 1934;114(788):291-313.